ORGANOPHOTOREDOX CATALYSIS

MULTICATALYTIC METAL-FREE BOND FORMATIONS WITH VISIBLE LIGHT

Dissertation

zur Erlangung des Doktorgrades der Naturwissenschaften
Dr. rer. nat.
an der Fakultät für Chemie und Pharmazie
der Universität Regensburg

vorgelegt von
Matthias Neumann
aus Reuth b. Erbendorf

Regensburg 2012

Der experimentelle Teil dieser Arbeit wurde in der Zeit zwischen März 2009 und Juni 2012 unter Anleitung von Prof. Dr. Kirsten Zeitler am Lehrstuhl für Organische Chemie der Universität Regensburg angefertigt. Meiner Betreuerin danke ich herzlich für die Überlassung dieses faszinierenden Projektes sowie für die hervorragende Betreuung und Unterstützung.

Die Arbeit wurde angeleitet von:		Prof. Dr. Kirsten Zeitler
Promotionsgesuch eingereicht am:		08.10.2012
Promotionskolloquium am:		26.10.2012
Prüfungsausschuss:	Vorsitz	Prof. Dr. Axel Jacobi von Wangelin
	Erstgutachter	Prof. Dr. Kirsten Zeitler
	Zweitgutachter	Prof. Dr. Oliver Reiser
	Dritter Prüfer	Prof. Dr. Arno Pfitzner

„Mehr Licht!”
(Johann Wolfgang von Goethe)

Table of Contents

1 Visible Light Photoredox Multicatalysis ... 1

  1.1 Introduction ... 1

    1.1.1 Sequential Catalysis ... 3

    1.1.2 Cooperative Catalysis ... 4

    1.1.3 Synergistic Catalysis ... 8

    1.1.4 Domino Reactions ... 17

    1.1.5 Summary and Outlook ... 18

    1.1.6 References ... 19

  1.2 Metal-Free, Visible Light Cooperative Asymmetric Organophotoredox Catalysis ... 22

    1.2.1 Introduction ... 23

    1.2.2 Results and Discussion ... 24

    1.2.3 Conclusion ... 29

    1.2.4 Experimental Section ... 29

    1.2.5 References ... 55

  1.3 Visible light Promoted Stereoselective Alkylation by Combining Heterogeneous Photocatalysis with Organocatalysis ... 57

    1.3.1 Introduction ... 58

    1.3.2 Results and Discussion ... 58

    1.3.3 Conclusion ... 63

    1.3.4 Experimental Section ... 64

    1.3.5 References ... 79

  1.4 Application of Microflow Conditions to Visible Light Photoredox Catalysis ... 82

    1.4.1 Introduction ... 83

    1.4.2 Results and discussion ... 83

    1.4.3 Experimental section ... 89

    References ... 97

  1.5 A Cooperative Hydrogen Bond Promoted Organophotoredox Catalysis Strategy for Highly Diastereoselective, Reductive Enone Cyclizations ... 99

    1.5.1 Introduction ... 99

    1.5.2 Results and Discussion ... 100

    1.5.3 Conclusion ... 107

    1.5.4 Experimental section ... 108

    1.5.5 References ... 160

2 List of Abbreviations 162
3 Summary 163
4 Zusammenfassung 165
5 Curriculum Vitae 167
6 Acknowledgments 170

1 Visible Light Photoredox Multicatalysis

1.1 Introduction[i]

After pioneering examples in the 1980s[1] and 1990s[2] visible light photoredox chemistry somehow was left unexploited for about two decades till key publications by Yoon[3] and MacMillan[4] triggered off an enormous renaissance of this field.[5] The use of sunlight or light from simple household bulbs, ambient reaction temperature and without the need for specialized equipment has made this approach already a mild and operationally simple alternative for several catalytic transformations and even more important photoredox catalysis has become a superior candidate for merging with other catalytic activation modes.

In contrast to traditional (UV-)photochemistry, where molecules are excited direct or *via* energy transfer of appropriate sensitizers, photoredox chemistry uses single electron transfer (SET) reactions from an excited photocatalyst, also termed photoelectron transfer (PET). In general terms, an excited photocatalyst can either be quenched reductively or by oxidation *via* SET in the presence of a (sacrificial) substrate. The resulting intermediate catalyst species then typically possesses high oxidative or reductive power depending on the nature of the prior quenching process and is – ideally – capable of performing a further SET to a different substrate or will undergo regeneration with a sacrificial electron acceptor or donor, respectively. After stepwise oxidation or reduction, the photocatalyst mediates electron transfer reactions between different substrates or, if required, sacrificial agents within a photoredox catalytic cycle. Widely used photocatalysts are transition metal based polypyridine complexes[5c], organic[6] or inorganic[7] semiconductors, metal organic frameworks (MOF)[8] as well as organic dyes[9] that can be excited by visible light, posses sufficient redox potentials and life time in their excited state and furthermore do not suffer from decomposition.
Numerous examples base on the photocatalytic generation of radical or cationic electrophiles such as α-carbonyl radicals or iminium ions which are further reacted with mostly superstoichiometric (pro-) nucleophiles or in intramolecular reactions. To achieve an even broader range of substrates, different other catalytic activation modes were utilized to generate reactive intermediates for “in situ” coupling with photoredox intermediates in a variety of multicatalytic reactions either in single or multistep procedures.

---

[i] This manuscript has been prepared as a *Concept Paper* on invitation by *Chemistry - A European Journal* and will be submitted as soon as possible.

Up to now, despite the great potential of this approach, multistep procedures like domino[10], tandem[11] or cascade[12] reactions as well as sequential catalysis are playing a minor role and only few examples have been reported yet. This fact might be attributed to the short life time of most photoredox derived intermediates that do not allow any later step follow up chemistry.

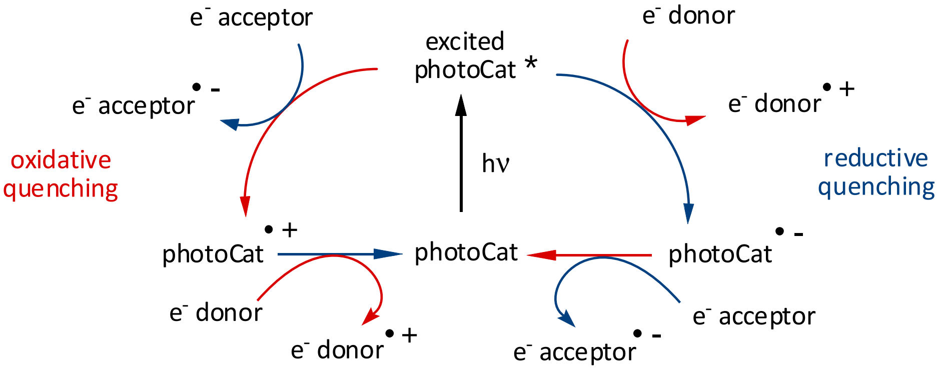
e⁻ acceptor
excited photoCat *
e⁻ donor
e⁻ acceptor•-
e⁻ donor•+
oxidative quenching
hν
reductive quenching
photoCat•+
photoCat
photoCat•-
e⁻ donor
e⁻ donor•+
e⁻ acceptor
e⁻ acceptor•-

Scheme 1. Quenching modes in photoredox catalysis

In “singlestep” multicatalysis various modes of activation are possible and a differentiation in the following three distinct classes according to the nature of the catalysts interplay in product formation might be useful: cooperative catalysis, synergistic catalysis or reactions with multifunctional catalysts.[13] In cooperative catalysis and reactions with multifunctional catalysts, all catalytic sites, either located on the same catalyst or not, enable product formation by activation of *one* substrate in a single catalytic cycle. In contrast, in synergistic catalysis (often also referred to dual catalysis) *two* distinct catalysts simultaneously generate in different, but *directly coupled catalytic* cycles each a distinct reactive intermediate, a nucleophile or electrophile species.[14]

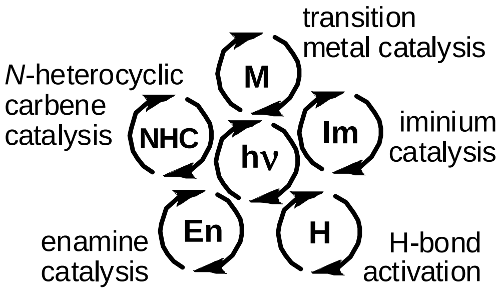
transition metal catalysis
M
N-heterocyclic carbene catalysis
NHC
hν
Im
iminium catalysis
enamine catalysis
En
H
H-bond activation

Scheme 2. Modes of activation combined with photoredox catalysis.

For successful merger with other activation modes, whether in single or multistep procedures, a second catalyst should not suffer from undesired redox reactions (self-quenching), but should offer substrate selectivity and, ideally, regio and stereocontrol of the reaction. This article aims to point out challenges and opportunities which result from merging single electron transfer photoredox catalysis with transition metal as well as organocatalytic activation modes in multicatalytic reactions.

1.1.1 Sequential Catalysis

hν Cu

Tertiary amines are attractive sacrificial agents in photoredox chemistry as they are inexpensive and easily oxidized. Moreover, their good quenching performance also can be used to activate them for nucleophilic attack adjacent to nitrogen *via* iminium ion formation[15] or in α-amino radical generation[16], which is not involved in multicatalytic processes so far. The main class of amines used in iminium based coupling reactions are *N*-aryl-1,2,3,4-tetrahydroisoquinoline derivatives (THIQ), which show unique reactivity as well as regioselectivity for C-H activation. Building on seminal results from metal mediated oxidative C-H-functionalizations by stoichiometric oxidants and subsequent C-C[17] and C-P[18] coupling reactions, Stephenson et al. recently were able to develop photocatalytic conditions for the generation of benchstable THIQ iminium salts[19] by the use of stoichiometric terminal oxidant bromotrichloromethane.[20] Prior photocatalytic protocols for C-H activation of THIQs based on atmospheric oxygen could not deliver isolable intermediates,[21] which are essential for sequential approaches. The initial step of the iminium formation is the reductive quenching of an excited photocatalyst by a THIQ derivative **1**, followed by the reoxidation of the reduced photocatalyst by the terminal oxidant bromotrichloromethane to close the photoredox cycle. The resulting trichloromethane radical **2** can further act as a hydrogen radical acceptor oxidizing the THIQ radical cation **3** to its iminium species **4**, which is stabilized by salt formation with bromide stemming from the bromotrichloromethane reduction.

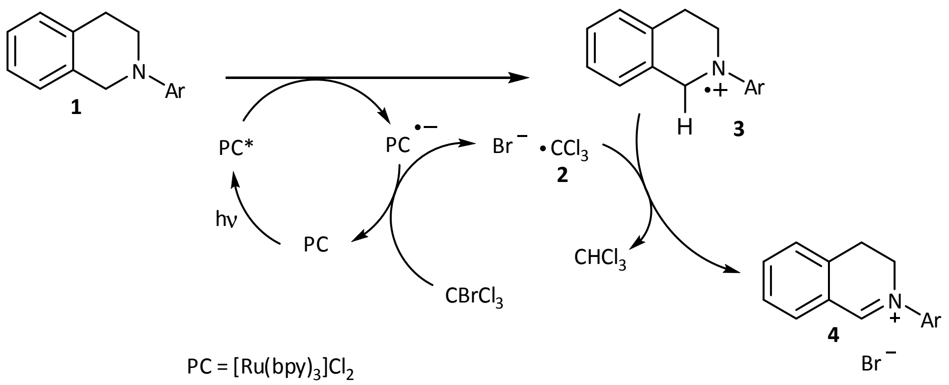
1
PC*
hν
PC
PC•−
Br− •CCl3
2
CBrCl3
CHCl3
3
4
Br−
PC = [Ru(bpy)3]Cl2

Scheme 3. Proposed mechanism for photooxidative iminium bromide generation.

After having established best conditions for THIQ bromide generation, the authors tested several (pro-)nucleophiles for bond formation with the iminium. The excess nucleophiles were added in excess, after full conversion of the starting THIQ amine with additional excess of triethylamine in a “dark reaction”.[20] Besides, it was shown that THIQ bromides also react in sequential copper(I) catalyzed alkynylation reactions.[ii]

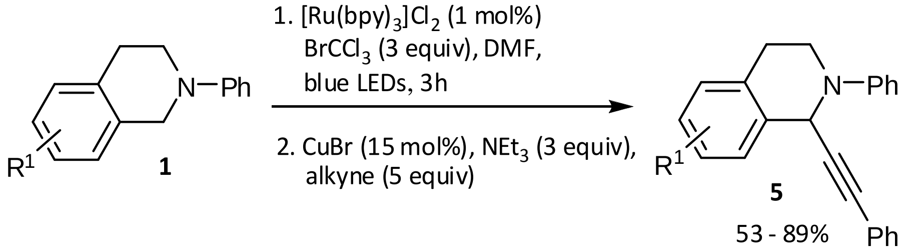
1
1. [Ru(bpy)3]Cl2 (1 mol%)
BrCCl3 (3 equiv), DMF,
blue LEDs, 3h
2. CuBr (15 mol%), NEt3 (3 equiv),
alkyne (5 equiv)
5
53 - 89%

Scheme 4. Sequential photooxidative copper catalyzed alkynylation.

Up to now, this alkynylation approach is the only sequential catalysis involving photoredox activation. Due to its operational simplicity and the stable intermediates, it will surely inspire future approaches to merge photocatalytic iminium salt formation with other catalytic modes for nucleophile generation whether organo- or transitionmetal catalyzed.

1.1.2 Cooperative Catalysis

Polypyridine complexes of ruthenium, especially the prominent $[Ru(bpy)_3]^{2+}$, are well understood and broadly studied photoactive systems in the realm of solar energy conversion.[22] Depending on the quenching mode, the oxidized or reduced species are potent reducing or oxidizing agents. These quenchers are typically used in superstoichiometric amounts and are consumed within the course of reaction. Among oxidative quenching agents, nitro compounds, quinones and viologen species proved to be suitable substrates. Methylviologen (MV) **6**, which upon its reduction by an excited photocatalyst can easily be reoxidized, for instance by atmospheric oxygen, represents a useful alternative to stoichiometric terminal oxidants and was first used in a synthetic application in intra and intermolecular cycloadditions by Yoon *et al.*[23] In this cooperative catalysis the excited $[Ru(bpy)_3]^{2+}$ photocatalyst is oxidatively quenched by MV, providing the catalytic active Ru(III) species (+1.29V in MeCN vs. SCE)[22], capable of one electron oxidation of electron rich styrenes **7**.[iii]

[ii] Photoredox alkynylations also are possible via synergistic approaches see chapter 1.1.3.1

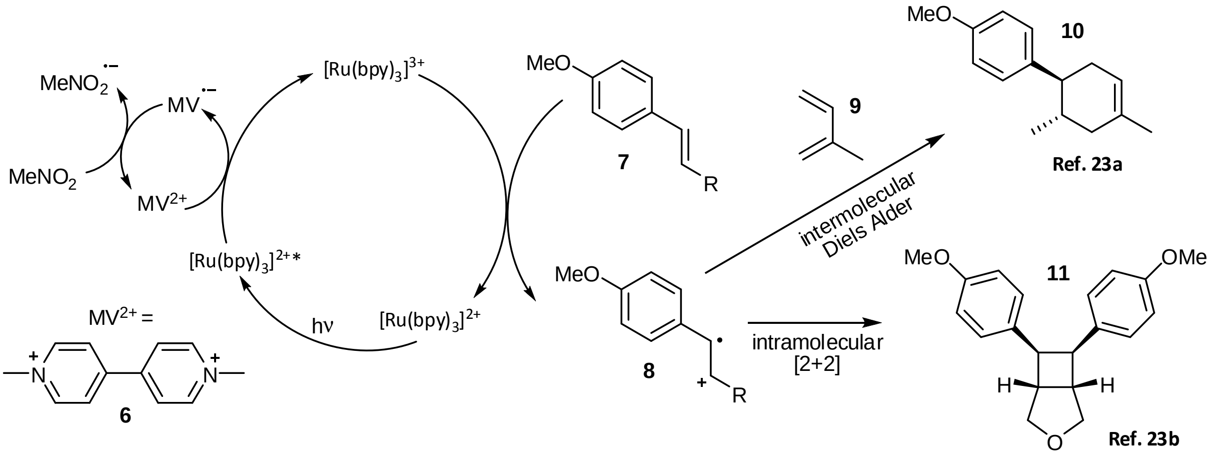

Scheme 5. Cooperative oxidation of electron rich styrenes.

The resulting radical cations **8** were proven to perform cycloaddition with excess dienophiles or intramolecular alkenes in formal Diels Alder[23a] or [2+2][23b] reactions respectively. Reduced MV **6** is subsequently reoxidized by the solvent nitromethane and re-enters the catalytic cycle.

A rather unique cooperative combination of covalent organocatalysis with photoredox chemistry recently was presented by Jiao and coworkers in a sunlight mediated oxidation of benzyl halides with pyridine catalysts and $[Ru(bpy)_3]^{2+}$ photocatalysis.[24]

[iii] In intensive studies the Yoon group later on was able to broaden the scope to inactivated styrenes *via* energy transfer catalysts, see: Z. Lu, T. P. Yoon, *Angew. Chem., Int. Ed.* **2012**, *51*, 10329

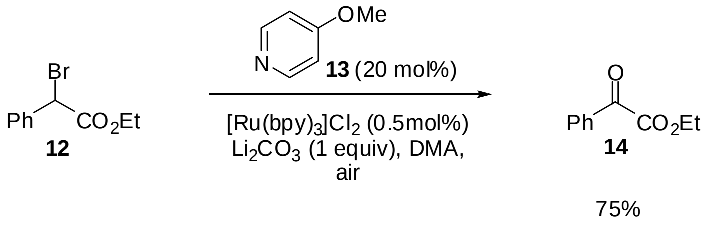
Br
Ph
CO2Et
12
OMe
N
13 (20 mol%)
[Ru(bpy)3]Cl2 (0.5mol%)
Li2CO3 (1 equiv), DMA,
air
O
Ph
CO2Et
14
75%

Scheme 6. Aerobic oxidation of benzyl halides

Here, the authors utilized the strong reduction potential of reductively quenched $[Ru(bpy)_3]^+$ (-1.33 V vs. SCE)[25] for single electron reduction of pyridinium salts **15** which are in situ formed from benzyl halides **12** and the 4-methoxypyridine **13** as cocatalyst. The resulting dihydropyridine radical **15** is assumed todisproportionates to 4-methoxypyridine **13** and a benzylic radical, which subsequently is oxidized by atmospheric oxygen generating hydrobromic acid and a superoxide radical which further reacts as reductive photocatalyst quencher. In order to prevent the pyridine catalyst **13** from deactivation *via* protonation with HBr, the reaction mixture is buffered with lithium carbonate. Without the presence of a pyridine species no oxidation product was observable, as shown in a series of test reactions, proofing the need of a cooperative interaction of both catalysts.

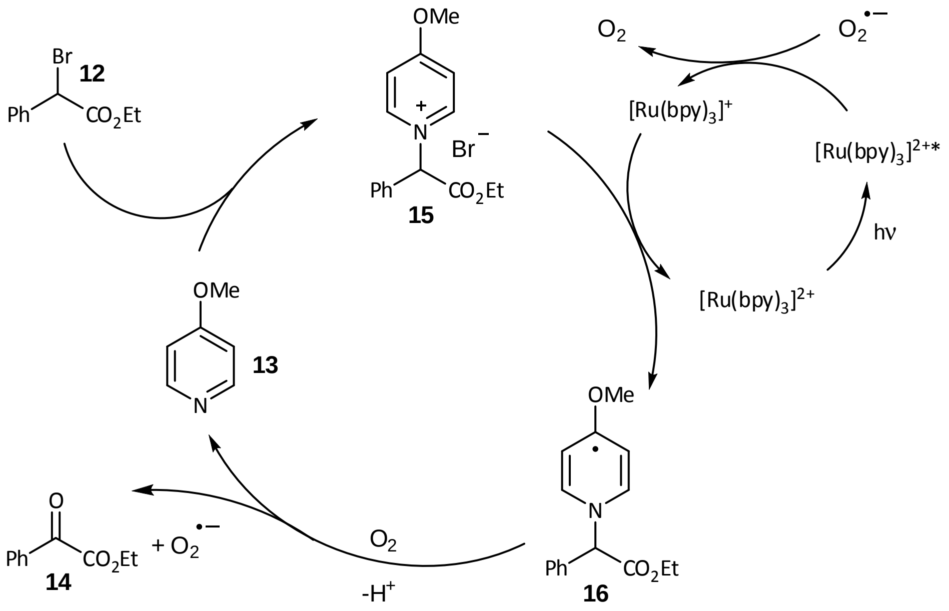
Br
12
Ph
CO2Et
OMe
+
N
Br−
Ph
CO2Et
15
O2
O2•−
[Ru(bpy)3]+
[Ru(bpy)3]2+*
hν
[Ru(bpy)3]2+
OMe
N
13
OMe
N
Ph
CO2Et
16
O
Ph
CO2Et
14
+ O2•−
O2
-H+

Scheme 7. Mechanistic proposal for visible light aerobic oxidation of benzyl halides.

The biomimetic Lewis acid like activation of carbonyls by hydrogen bond donors represents an important column of organocatalysis and hence, a variety of catalytic transformations either in single or multicatalysis are known.[26] Very recently, Zeitler et al. presented the first catalytic reductive cyclization of bisenone systems in the context of a new type of cooperative organophotoredox transformation. Lewis acid like activation of enones with Schreiner – thiourea **17**[27] enables electron transfer from the reductively quenched photocatalyst Eosin Y radical anion, triggering a *trans*-selective 5-*exo*-trig cyclization. The resulting α-carbonyl radical **20** further is probably reduced by formal hydrogen radical transfer from oxidized Hantzsch ester **23** that prior acted as reductive quencher for the excited photocatalyst. With this new protocol a series of symmetrical and unsymetrical enone systems **18** as well as non Michael-type acceptors like styrenes could be cyclized in good excellent yields in a mild and benign fashion compared to prior presented harsh condition approaches without[28] or with superstoichiometric lewis/brønsted acid activation[29] of the enones.

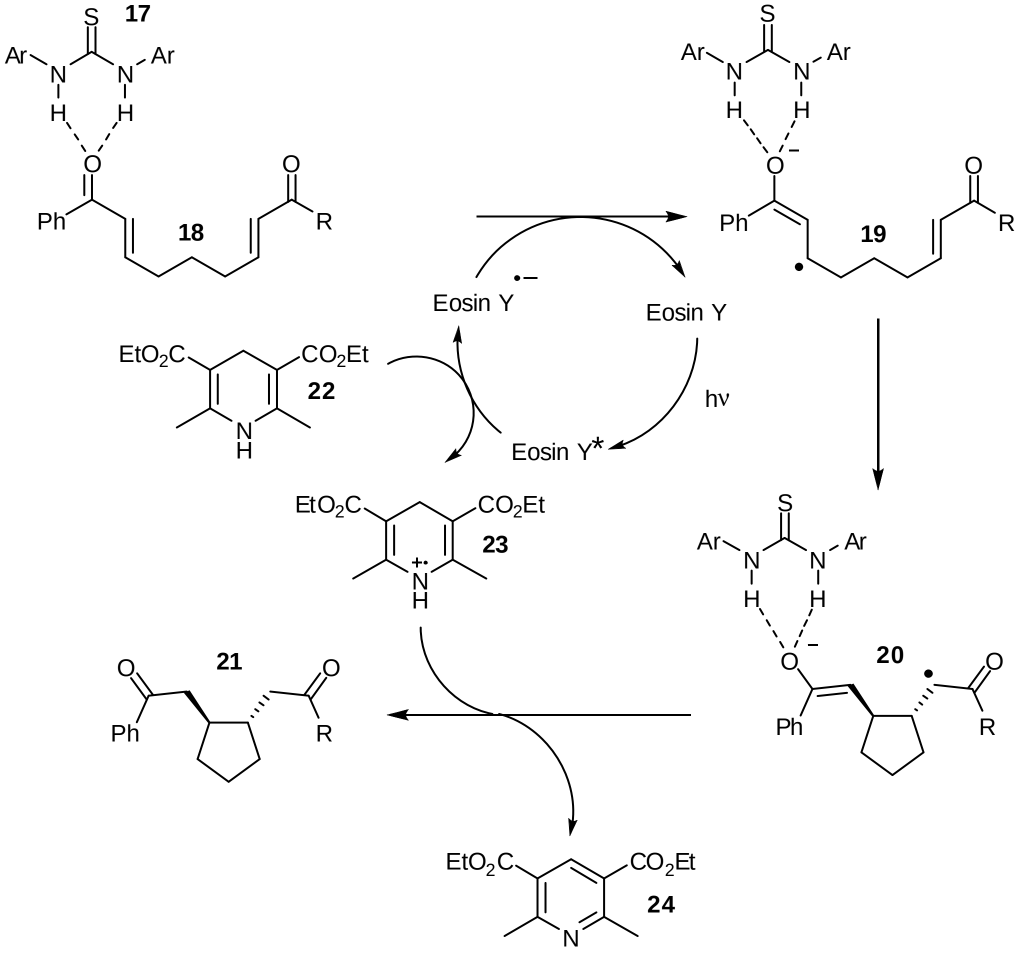

Scheme 8. Mechanistic picture of cooperative reductive bisenon cyclisation (Ar = 3,5-bis(trifluoromethyl)benzene).

1.1.3 Synergistic Catalysis

At this stage the majority of all multicatalytic visible light photoredox processes is represented by Synergistic catalysis. Nevertheless, only two types of photoredox intermediates are involved: stabilized iminium ions derived from oxidation of tertiary amines and electron deficient carbon centered radicals via photoreductive (pseudo-)dehalogenation of electron deficient alkyl and aryl compounds.

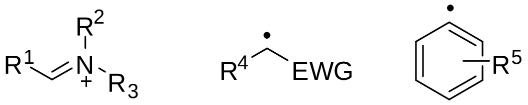

Scheme 9. Photoredox intermediates involved in synergistic catalysis (EWG = electron withdrawing group).

Both intermediates are electronically stabilized by an appropriate substitution pattern in combination with additional stabilization by polar solvents to guarantee a sufficient life time of these intermediates for reaction with an organo- or transition-metal catalysis derived intermediary nucleophile. Unlike to cooperative and sequential approaches more than one substrate needs to be activated for reaction, which affords an elaborate balancing of reaction rates of all involved catalysis modes by tuning catalyst loadings, light intensity, concentration, temperature and other reaction parameters.

1.1.3.1 Stabilized Iminium Ions

Along with the iminium formation by stoichiometric terminal oxidants in sequential photoredox approaches (*vide supra*), also non stabilized intermediates are utilized in bond formation with strong nucleophiles or *via* synergistic catalysis. Again reductive quenching of an excited photocatalyst by *N*-aryl-1,2,3,4-tetrahydroisoquinoline (THIQ) derivative **1**, resulting in the formation of the amine´s corresponding radical cation **3** and the reduced photocatalyst species, is the initial step. The reduced photocatalyst species is capable of reducing atmospheric oxygen in solution returning to its ground state. The hereby formed superoxide radical can subsequently oxidize and deprotonate the amino radical cation **3** to the electrophilic iminium ion **4**[30] which then can be trapped by a variety of (pro-)nucleophiles such as cyanides,[9a, 31] TMS-trifluoromethane,[31a] dialkyl malonates,[9a, 9b] phosphonates[9a, 32] or alcohols and amines.[33] This proposed mechanism later was partly confirmed by EPR detection of the intermediary superoxide radical by Wu and co-workers in the context of an Eosin-catalyzed reaction.[9b] In the last few years several variations of this reaction have been developed and besides using diverse (pro-)nucleophiles, photocatalytically generated iminium ions have also served as precursors for 1,3-dipoles and their subsequent cycloaddition reactions;[34] moreover the application of different photocatalysts, such as organic dyes,[9a, 9b, 9d, 31a] organic[35] and inorganic semiconductors[7a, 7b, 36] or MOFs[8] has been reported.

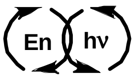

Rueping *et al.* initially showed a synergistic combination of the photooxidative THIQ iminium generation with enamine catalysis.[37] In this Mannich-type reaction the authors obtained best yields if the iminium ion had access to a sufficient concentration of nucleophile, whereas undesired side reactions like amide formation lower the product yield if the rate of iminium generation is too high. In order to find the best balance between photooxidation and enamine concentration the authors tested a number of light sources of different intensity and wavelength. Rather modest light of a 5W fluorescent light bulb proved to be superior to, for instance, high power LEDs, assuring low iminium concentration compared to intermediary enamine and hence allowing for pseudo first order reaction conditions. The scope of this transformation is limited to simple ketones including cycloalkanones with predominant formation of the kinetic product in case of unsymmetric ketones. Reactions proceed best if ketone is used as solvent or at least in 10-fold excess.

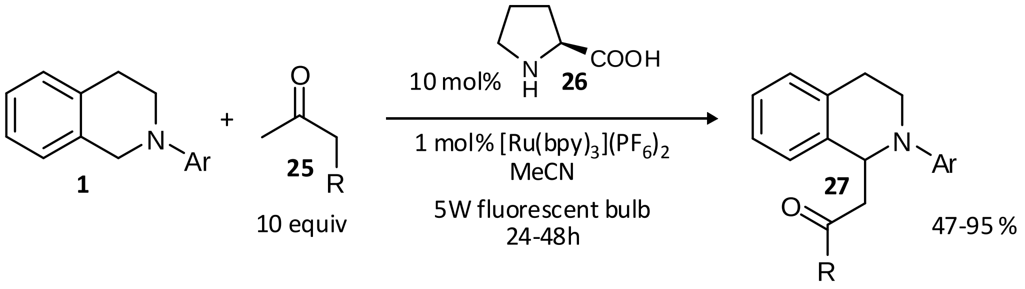

Scheme 10. Organocatalyzed photooxidative Mannich reaction

In a later publication the same group following to their prior results also could show the synergistic merger of photooxidative iminium generation with coinage metal catalyzed alkynilations.[38] As both the nucleophilic intermediate **4** and the transition metal catalyst **28** are sensitive to reductive and/or oxidative conditions the appropriate tuning of the photocatalytic cycle proved essential. Lowering the light intensity again turned out to be beneficial for clean conversion as described above.

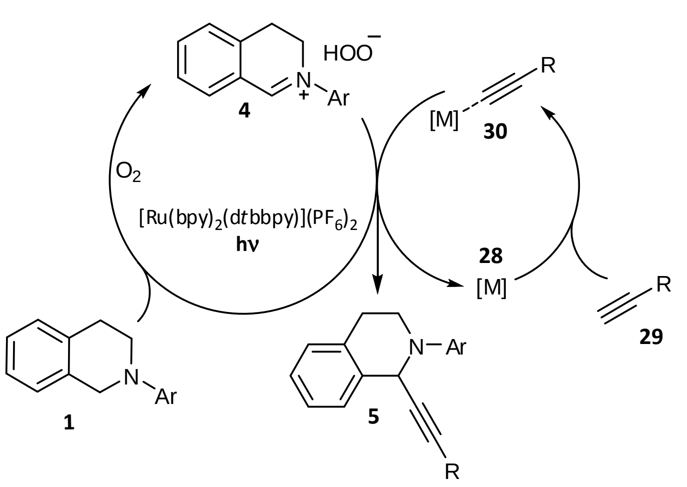
4
HOO⁻
Ar
O2
[Ru(bpy)2(dtbbpy)](PF6)2
hν
[M]
R
30
28
[M]
R
29
1
N
Ar
5
N–Ar
R

Scheme 11. Photooxidative copper catalyzed alkynylation.

Having established best conditions the authors were able to demonstrate the scope of this reaction with a variety of terminal aryl and alkyl alkynes. A large series of tested alkynes and THIQ derivatives afforded the cross dehydrogenative coupling (CDC) products in moderate to very good yields, except for *p*-(*t*-butyl)phenyl alkyne **29a**. Here, only replacement of the metal catalyst from copper(I) complex to a silver salt allowed the alkyne **29a** to be coupled to THIQ **1**, illustrating the modular character of this synergistic catalysis in which each catalytic cycle can be adapted to the substrates´ demands.

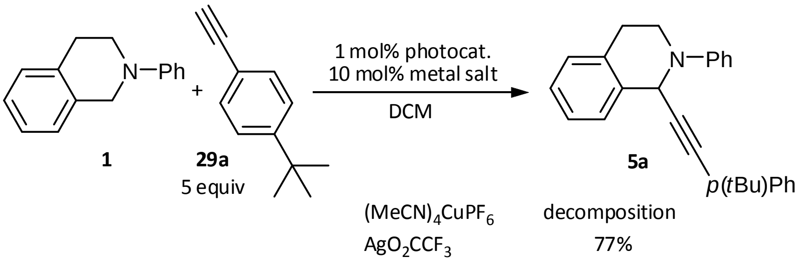
N–Ph
+
1
29a
5 equiv
1 mol% photocat.
10 mol% metal salt
DCM
N–Ph
5a
p(tBu)Ph
(MeCN)4CuPF6
AgO2CCF3
decomposition
77%

Scheme 12. Limitation in scope and change of metal catalyst to adjust the dual catalytic cycle.

The concept of umpolung[39] (i. e. polarity reversal) allows for various non-traditional C-X and C-C bond formations. In this context the use of aldehydes as so-called “acylanion equivalents” such as for common C-C coupling reactions (e.g. benzoin or Stetter-type reactions[40] etc.) is well established. For catalytic umpolung transformations *N*-heterocyclic carbenes (NHCs) are most frequently applied as catalysts to generate the intermediary Breslow intermediate (enaminol) which then serves as a nucleophile.[41]

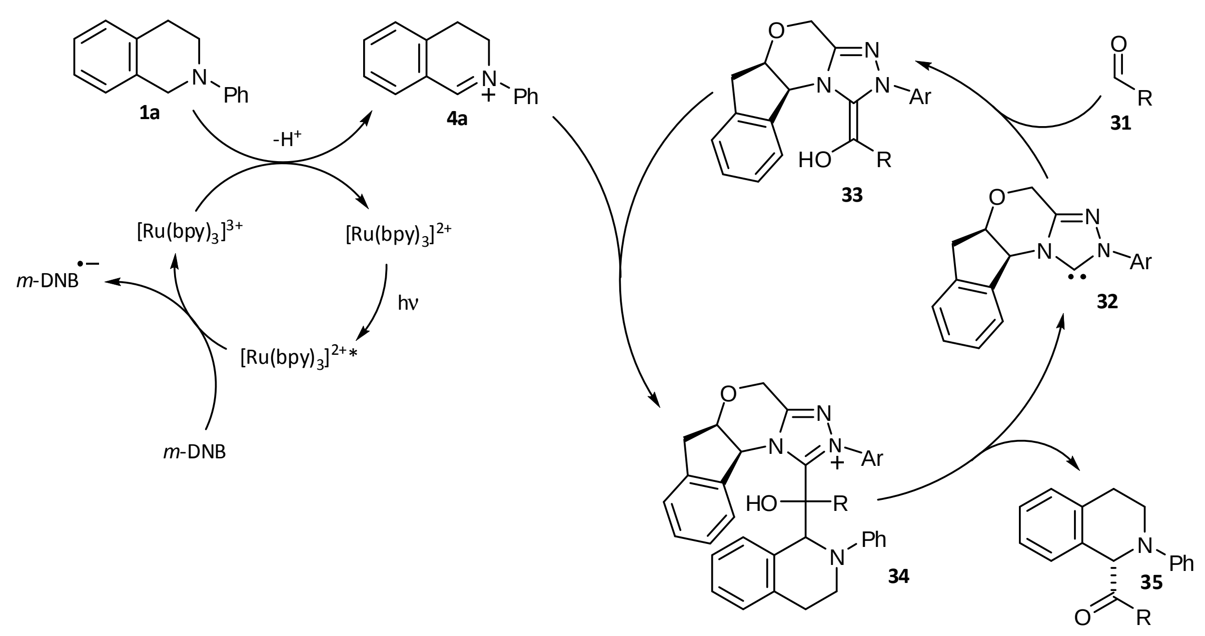

Scheme 13. Mechanistc proposal for α-acylation of THIQs. m-DNB: m-dinitronenzene.

Apart from a number of NHC-catalysed domino transformations[42] as well as cooperative combinations with Lewis acids[43] or with enamine respectively iminium catalysis,[44] a first successful fusion of photocatalytic iminium ion generation with NHC-catalyzed umpolung resulting in an acylation of THIQs has been published very recently by the Rovis group.[45] Unlike to the aforementioned iminium generation using $[Ru(bpy)_3]^{2+}$ as photocatalyst the Rovis group suggested an oxidatively quenched photoredox cycle mediated by *meta*-dinitrobenzene which either can be recycled by atmospheric oxygen or act as terminal oxidant under anaerobic conditions. The strongly oxidative Ru(III) species is capable of iminium formation from THIQ **1a** which can then be attacked by a Breslow intermediate **33** generated *in situ* from the chiral NHC catalyst **32** and the aldehyde **31**. Having established the best catalysts and best conditions the authors could apply this transformation for the synthesis of a variety of enantioenriched acylation products from THIQs and different aliphatic aldehydes.

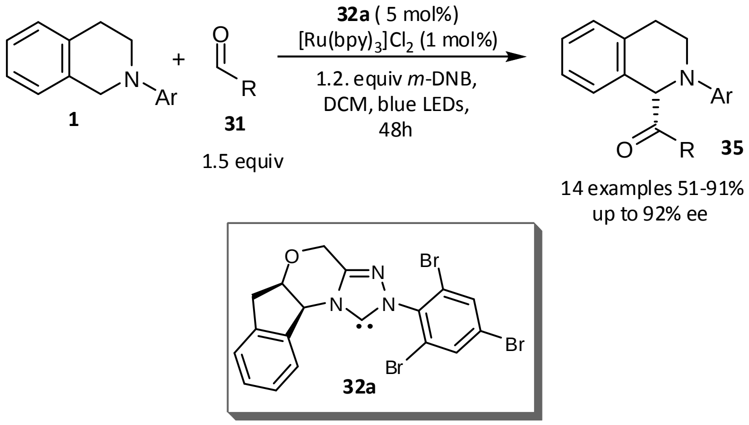

Scheme 14. Synergistic NHC catalyzed asymmetric α-acylation of THIQs.

1.1.3.2 Electrophilic Carbon Centered Radicals

Seminal examples from the 1980s have demonstrated the possibility of carbon-halogen bond[1d-i] as well as related pseudo halogen type such as carbon-diazo bond cleavage[1a-c] if these are adjacent to either carbonyl groups or electron poor aromatic systems which are capable of accepting one electron from any common photocatalyst. The resulting, carbon centred radicals either were trapped in intramolecular cyclization reactions or by hydride donors. With beginning of the photoredox renaissance many groups entered the field and mainly focused their work on follow-up chemistry of α-carbonyl halides derived electrophilic radicals for C-C bond formations in intra- and intermolecular reactions.[5]

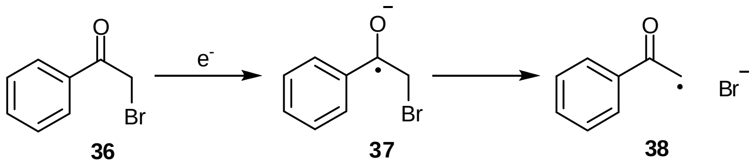

Scheme 15. Radical generation form bromo acetopenone via SET.

The first problem to be solved by means of synergistic photoredox catalysis was the catalytic asymmetric functionalization of the α-position of aldehydes by alkylation that has been a very challenging task for a long time, especially in the context of organocatalysis.[46] In 2007 the MacMillan group was able to present a first asymmetric α-allylation of aldehydes, introducing the concept of single occupied molecular orbital (SOMO) catalysis.[47] In this approach the intermediary enamines are oxidized by a stoichiometric amount of oxidant (e. g. cer ammonium nitrate (CAN)) to an electrophilic amine radical cation which can be trapped by nucleophilic SOMOphiles, such as allylsilanes followed by a second oxidation to yield the alkylation products. Later, the same group transfered this strategy to the very first synergistic visible light photoredox catalysis.[4]

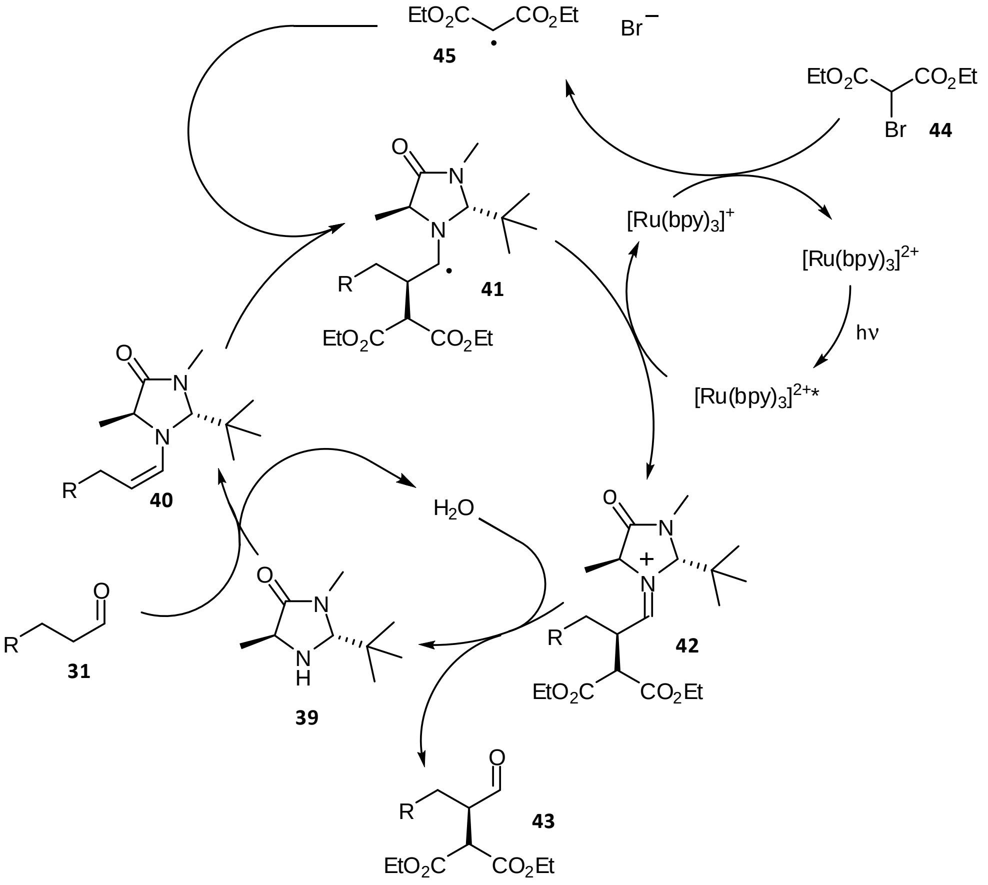

Scheme 16. Asymmetric photoredox α-alkylation of aldehydes with bromo diethylmalonate.

In this asymmetric secondary amine catalysis the intermediary enamine **40** is attacked by the electrophilic radical **45** stemming from photoreductive cleavage of the bromoalkyl derivative **44**. The resulting α-aminoradical **41** is oxidized subsequent by the excited photocatalyst to an iminum ion **42** that readily releases the alkylated product **43** in high yields and high enantioselevtivity upon regeneration of the imidazolidinoncatalyst **39**. Remarkably, this synergistic approach does not require any additional sacrificial agent or electron shuffle auxillary. With this powerful concept in hands the MacMillan group expanded the scope of this asymmetric alkylation to benzylations[48] and perfluoroalkylations as well as trifluoromethylations[49] of a broad range of (enolizable) aldehydes. In the case of α-benzylation reactions a oxidative quenching photocycle based on *fac*-Ir(ppy)$_3$ is proposed. This Ir-complex, which typically is used as a green emitter in OLED applications[50] possesses a high reduction potential ($E_{1/2}$ Ir^{3+*} = -1.73 V vs. SCE in CH_3CN) in its excited state.[51] Hence, in contrast to the prior described mechanism, here the excited photocatalyst generates the carbon centered radical and is then re-oxidized by the intermediary α-amine radical **41.**

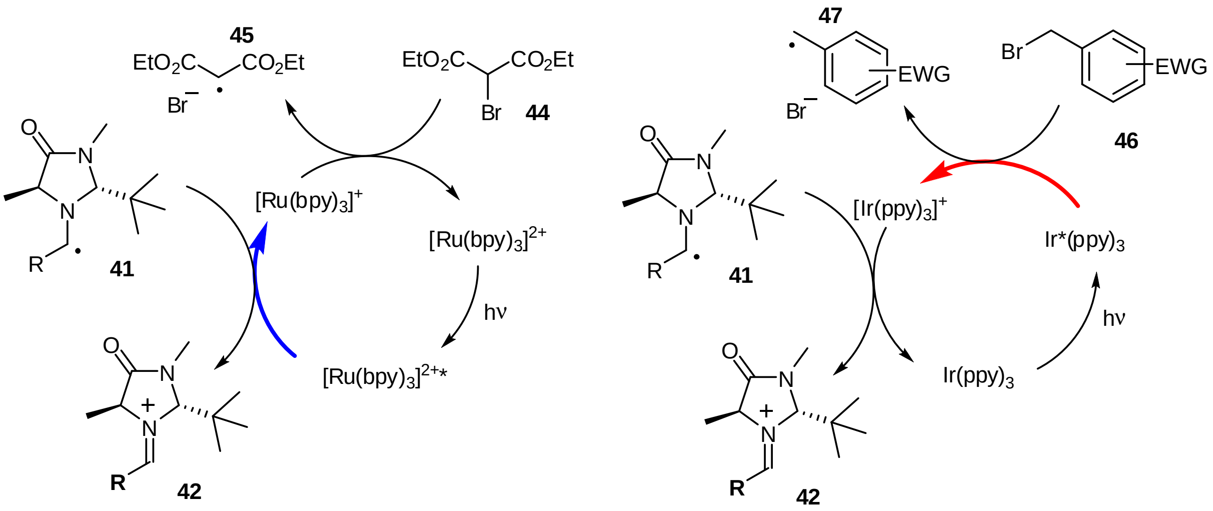

Scheme 17. Comparison of reductive and oxidative quenching modes in α-alkylation reactions.

A transition metal free alternative to common Iridium and Ruthenium based catalysts recently was presented by Zeitler and coworkers using simple, inexpensive organic dyes.[52] With development of a fast screening reaction the group was able to identify Eosin Y, from the xanthene dye family, as most promising candidate. Besides reductive dehalogenations also enantioselective, metal-free, synergistic photoredox catalysis based on the asymmetric α-alkylation reactions described above could be realized in comparable yield and enantioselectivity.

In a subsequent recent study the same group has demonstrated the beneficial effects of microflow conditions on the performance of visible light synergistic photoredox chemistry.[53] They were able to show a drastic rate acceleration[54] in reactions with excess nucleophiles in aza-Henry reactions if performed in a commercially available microstructured flow reactor (100 µl internal volume). Furthermore, the productivity (mmol/h) of the synergistic enantioselective photoredox α-alkylations can be increased by at least two orders of magnitude if conducted in a simple, self-made FEP (fluorinated ethylene propylene copolymer)-tubing reactor Remarkably, similar conditions as in the batch approach could be used without observing any significant loss in enantioselectivity.[53]

Transition metal catalyzed C-H activation for C-C and C-X bond formation is of major interest in current organic synthesis. But besides recent advancements in functional group tolerance and substrate scope typical protocols still require elevated temperatures (> 80° C),[55] hence room temperature protocols for C-H arylations are still very desirable. Recently, the Sanford group presented a synergistic visible light palladium-catalyzed arylation of a series of phenylpyridines and other activated aryl-moieties.[56]

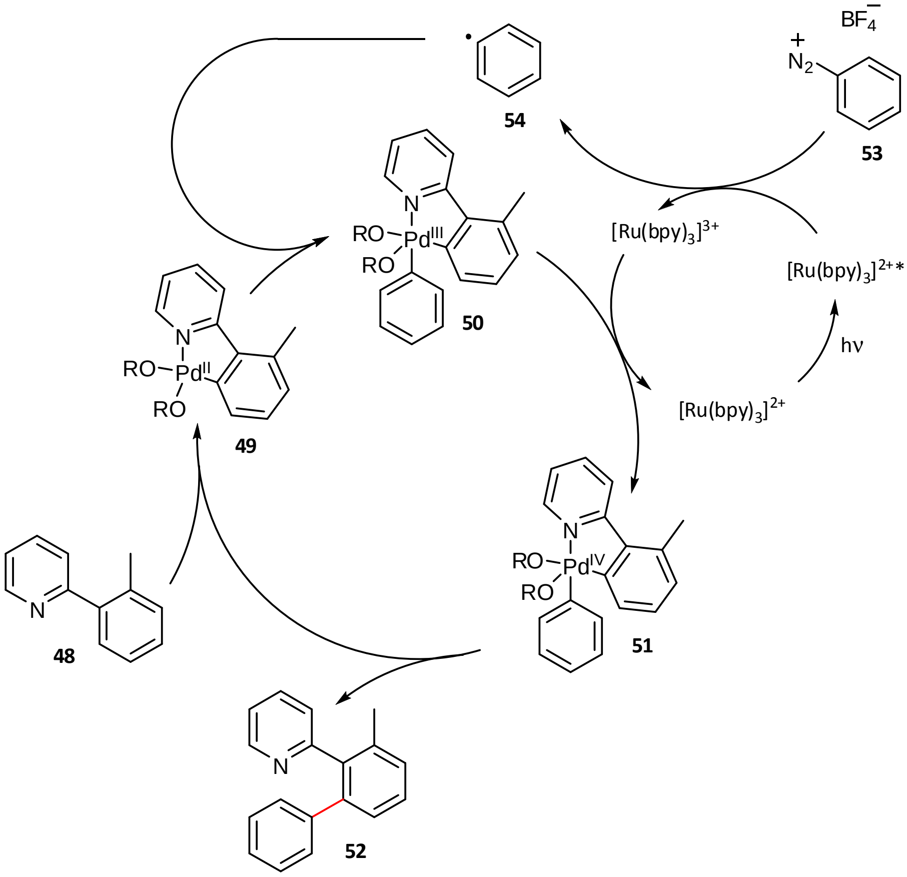

Scheme 18. Mechanistic proposal for the combination of Pd-catalyzed C-H arylation and photocatalytic electrophile generation.

This successful merger of the both known concepts of visible light photoredox catalytic access to phenyl radicals from diazonium salts[1a-c] and ligand-directed C-H arylation[57] now offers an easy to perform room temperature protocol. Oxidative addition of a photogenerated phenyl radical **54** to palladacycle **49** results in formation of palladium(III) complex **50** which is assumed further to be oxidized to a palladium(IV) species **51** capable of reductive elimination to afford the desired biaryl product **52**. Based on established best conditions the extension of the scope of the reaction was examined. In addition to the original 2-pyridyl substrates also amides, pyrazoles, pyrimidines and oxime ethers could be successfully employed to provide the corresponding regioselective arylation products in moderate to good yields.

Fluorinated compounds and especially trifluoromethyl groups, a bioisoster of chlorine, bromine and methyl is highly demanded in the synthesis of pharmaceuticals.[58] Hence several protocols for direct trifluoromethylations have been developed, typically by Pd- and Cu-catalysis, but up to now they often suffer from several limitations such as expensive trifluoromethyl sources, and harsh reaction conditions. An approach for the Cu-catalyzed cross coupling of inexpensive CF_3I with commercially available aryl boronic acids at 60°C was recently reported by Sanford et al.[59]

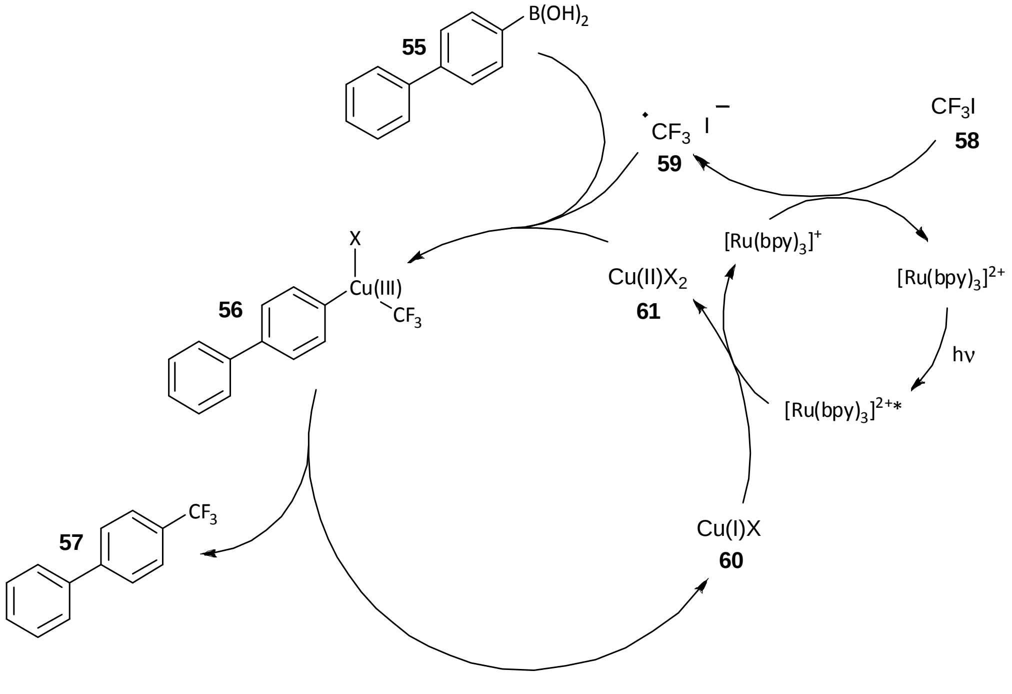

Scheme 19. Mechanistic proposal for Cu-catalyzed trifluoromethylation.

The authors assume a copper(III) species **56** as the key intermediate of this synergistic catalysis which after reductive elimination forms the product **57** and regenerates the copper(I) species of the catalyst. The order of oxidative addition of trifluoromethyl radical and transmetalation of boron to copper resulting in intermediate **56** remains unclear.

To investigate the full scope of this transformation several aryl boronic acids were tested examining electronic effects of substituents and functional group tolerance.

1.1.4 Domino Reactions

The oxyamination of (intermediary) enamines with TEMPO ((2,2,6,6-tetramethylpiperidin-1-yl)oxyl)either by oxidation with inorganic oxidants[60] or by photoredox catalysis[61] represents a synthetical useful access to α-hydroxy aldehydes. Jang *et al* extended this approach in a Michael addition photooxyamination domino reaction[62] of unsaturated aldehydes and stable TEMPO radical. Iminium ions **64** form Joergensen-Hayashi organocatalyst **63** and an α,β-unsaturated aldehyde is alkylated at the β-position by malonate **65** producing a enamine intermediated **66** which is subsequently photooxidized to a SOMO activated amine radical cation by excited $[Ru(byp)_3]^{2+*}$ catalyst. Radical recombination of stabile TEMPO radical **68** and the SOMO species **67** forms iminium ion 69 which upon hydrolysis closes the domino sequence releasing the organocatalyst **63** and the double funtionalized product **70** in high yields, regio- and enantioselectivity.

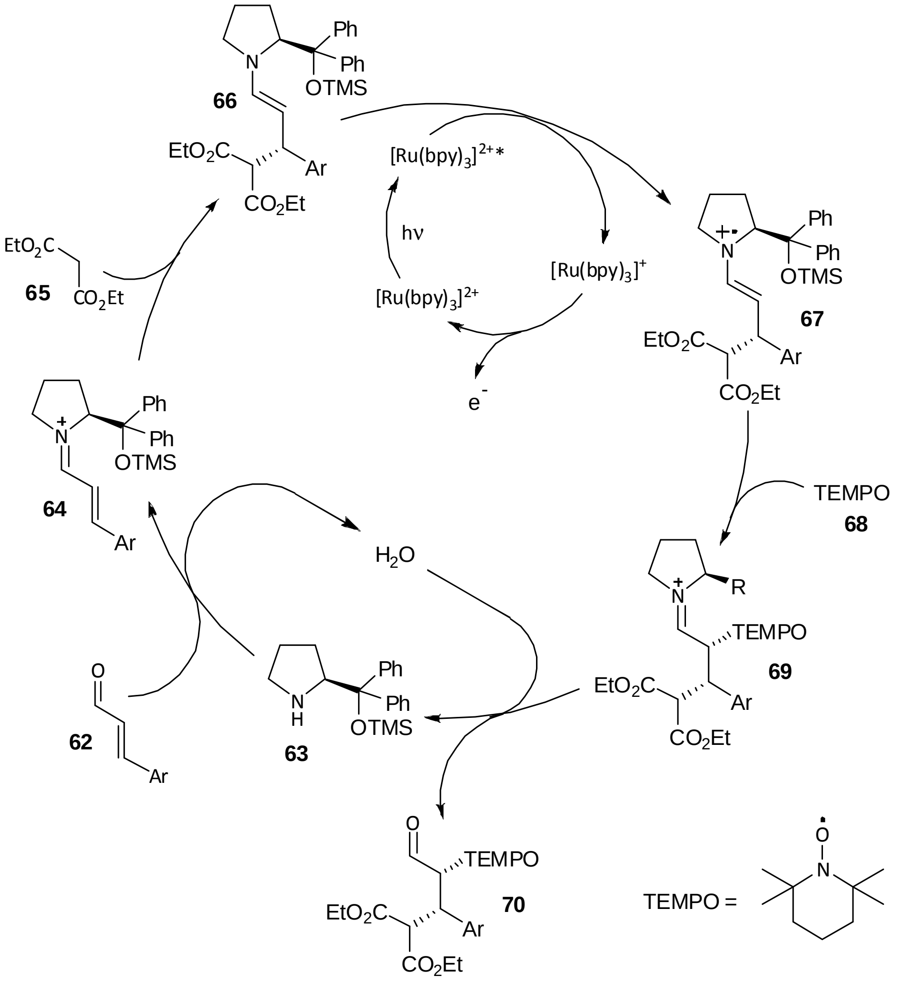

Scheme 20. Mechanistic proposal for domino alkylation, photooxidation, oxyamination reaction.

The applied photocatalyst in this sequence is a commercial material often used in dye sensitized solar cell (DSSC) substrate which consists of a ruthenium polypyridine isothiocyanate complex (N719) immobiliszed on TiO_2; this is the first example for its use in asymmetric catalysis. Remarkably, both DSSC components, the dye and the inorganic semiconductor, could yield the desired product individually, but only the combination of both allowed for high yields. The reduced Ru(I) photocatalyst species needs to get rid of an electron which the authors argue might be transferred to atmospheric oxygen or excess TEMPO radical within the reaction mixture. The use of acid additives furthermore accelerates the initial iminium formation from amine and aldehyde and assures high concentration of iminium species for Michael addition of malonate.

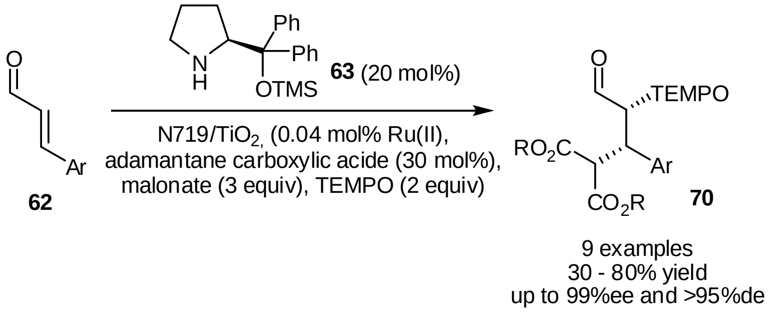
Ph
Ph
N
H
OTMS
63 (20 mol%)
O
Ar
62
N719/TiO2, (0.04 mol% Ru(II),
adamantane carboxylic acide (30 mol%),
malonate (3 equiv), TEMPO (2 equiv)
O
TEMPO
RO2C
Ar
CO2R
70
9 examples
30 - 80% yield
up to 99%ee and >95%de

Scheme 21. Tandem Michael addition oxyamination reaction.

1.1.5 Summary and Outlook

Although seminal examples of visible light photoredox catalysis were already date back to the 1980s this fascinating field only scarcely developed compared to the closely related photovoltaics. Nevertheless its renaissance was a fortiori story of success and thanks to its operational simplicity and robustness the synthetic organic chemistry community quickly recognized the unique qualification for merger with additional catalytic activation modes to gain access to an even broader pool of transformations. Within only three years several multicatalytic transformations combining metal-based and metal-free photoredox catalysis with either organocatalysis or transition metal catalysis have been developed. The sharp limitation to stabilized photoredox derived electrophiles hitherto somehow renders the scope of potential substrates. In order to broaden the scope, future investigations should aim at the identification of new classes of photoredox derived reactive intermediates and reaction conditions that prolong life time of charged species present. Also the utilization of modern reaction techniques like, for instance microflow reactors, should be taken into account, as their beneficial effects have already been shown independently by several groups. Hence, the combination of visible light photoredox catalysis with other catalytic activation modes may be perceived as considerably challenging the examples presented here should illustrate the benefits of this novel approach. Beyond a doubt, this powerful strategy will certainly continue to grow enabling new transformations, not accessible by single catalyst methods so far.

1.1.6 References

[1] a)H. Cano-Yelo, A. Deronzier, *J. Chem. Soc., Perkin Trans. 2* **1984**, 1093; b)H. Cano-Yelo, A. Deronzier, *Tetrahedron Lett.* **1984**, *25*, 5517; c)H. Cano-Yelo, A. Deronzier, *New J. Chem.* **1987**, *11*, 479; d)S. Fukuzumi, S. Mochizuki, T. Tanaka, *J. Phys. Chem.* **1990**, *94*, 722; e)Z. Goren, I. Willner, *J. Am. Chem. Soc.* **1983**, *105*, 7764; f)K. Hironaka, S. Fukuzumi, T. Tanaka, *J. Chem. Soc., Perkin Trans. 2* **1984**, 1705; g)R. Maidan, Z. Goren, J. Y. Becker, I. Willner, *J. Am. Chem. Soc.* **1984**, *106*, 6217; h)S. H. Mashraqui, R. M. Kellogg, *Tetrahedron Lett.* **1985**, *26*, 1453; i)I. Willner, T. Tsfania, Y. Eichen, *J. Org. Chem* **1990**, *55*, 2656.

[2] G. Pandey, M. K. Ghoria, S. Hajra, *Pure Appl. Chem.* **1996**, *68*, 653.

[3] M. A. Ischay, M. E. Anzovino, J. Du, T. P. Yoon, *J. Am. Chem. Soc.* **2008**, *130*, 12886.

[4] D. A. Nicewicz, D. W. C. MacMillan, *Science* **2008**, *322*, 77.

[5] a)J. M. R. Narayanam, C. R. J. Stephenson, *Chem. Soc. Rev.* **2011**, *40*, 102; b)F. Teplý, *Collect. Czech. Chem. Commun.* **2011**, *76*, 859; c)J. W. Tucker, C. R. J. Stephenson, *J. Org. Chem* **2012**, *77*, 1617; d)J. Xuan, W.-J. Xiao, *Angew. Chem. Int. Ed.* **2012**, *51*, 6828; e)T. P. Yoon, M. A. Ischay, J. Du, *Nat Chem* **2010**, *2*, 527; f)K. Zeitler, *Angew. Chem. Int. Ed.* **2009**, *48*, 9785.

[6] L. Möhlmann, M. Baar, J. Rieß, M. Antonietti, X. Wang, S. Blechert, *Adv. Synth. Catal.* **2012**, DOI: 10.1002/adsc.201100894.

[7] a)M. Cherevatskaya, M. Neumann, S. Füldner, C. Harlander, S. Kümmel, S. Dankesreiter, A. Pfitzner, K. Zeitler, B. König, *Angewandte Chemie, International Edition* **2012**, *51*, 4062; b)T. Mitkina, C. Stanglmair, W. Setzer, M. Gruber, H. Kisch, B. König, *Org. Biomol. Chem.* **2012**, *10*, 3556; c)M. Rueping, J. Zoller, D. C. Fabry, K. Poscharny, R. M. Koenigs, T. E. Weirich, J. Mayer, *Chem. Eur. J.* **2012**, *18*, 3478.

[8] a)C. Wang, Z. Xie, K. E. deKrafft, W. Lin, *J. Am. Chem. Soc.* **2011**, *133*, 13445; b)Z. Xie, C. Wang, K. E. deKrafft, W. Lin, *J. Am. Chem. Soc.* **2011**, *133*, 2056.

[9] a)D. P. Hari, B. König, *Org. Lett.* **2011**, *13*, 3852; b)Q. Liu, Y.-N. Li, H.-H. Zhang, B. Chen, C.-H. Tung, L.-Z. Wu, *Chem.- Eur. J.* **2012**, *18*, 620; c)M. Neumann, S. Füldner, B. König, K. Zeitler, *Angew. Chem., Int. Ed.* **2011**, *50*, 951; d)Y. Pan, C. W. Kee, L. Chen, C.-H. Tan, *Green Chem.* **2011**, *13*, 2682.

[10] L. F. Tietze, G. Brasche, K. M. Gericke, in *Domino Reactions in Organic Synthesis*, Wiley-VCH Verlag GmbH & Co. KGaA, **2006**.

[11] D. E. Fogg, E. N. dos Santos, *Coord. Chem. Rev.* **2004**, *248*, 2365.

[12] A. M. Walji, D. W. C. MacMillan, *Synlett* **2007**, 1477.

[13] R. C. Wende, P. Schreiner, *Green Chem.* **2012**, *14*, 1821.

[14] A. E. Allen, D. W. C. MacMillan, *Chem. Sci* **2012**, *3*, 633.

[15] L. Shi, W. Xia, *Chem. Soc. Rev.* **2012**.

[16] a)P. Kohls, D. Jadhav, G. Pandey, O. Reiser, *Org. Lett.* **2012**, *14*, 672; b)A. McNally, C. K. Prier, D. W. C. MacMillan, *Science* **2011**, *334*, 1114; c)Y. Miyake, Y. Ashida, K. Nakajima, Y. Nishibayashi, *Chem. Commun.* **2012**, *48*, 6966; d)Y. Miyake, K. Nakajima, Y. Nishibayashi, *J. Am. Chem. Soc.* **2012**, *134*, 3338.

[17] Z. Li, D. S. Bohle, C.-J. Li, *Proc. Natl. Acad. Sci.* **2006**, *103*, 8928.

[18] O. Basle, C.-J. Li, *Chem. Commun.* **2009**, 4124.

[19] D. Beke, M. Bárczai-Beke, L. Föcze, *Chem. Ber.* **1962**, *95*, 1054.

[20] D. B. Freeman, L. Furst, A. G. Condie, C. R. J. Stephenson, *Org. Lett.* **2011**, *14*, 94.

[21] A. G. Condie, J. C. González-Gómez, C. R. J. Stephenson, *J. Am. Chem. Soc.* **2010**, *132*, 1464.

[22] K. Kalyanasundaram, *Coord. Chem. Rev.* **1982**, *46*, 159.

[23] a)S. Lin, M. A. Ischay, C. G. Fry, T. P. Yoon, *J. Am. Chem. Soc.* **2011**, *133*, 19350; b)M. A. Ischay, Z. Lu, T. P. Yoon, *J. Am. Chem. Soc.* **2010**, *132*, 8572.

[24] Y. Su, L. Zhang, N. Jiao, *Org. Lett.* **2011**, *13*, 2168.

[25] C. R. Bock, J. A. Connor, A. R. Gutierrez, T. J. Meyer, D. G. Whitten, B. P. Sullivan, J. K. Nagle, *J. Am. Chem. Soc.* **1979**, *101*, 4815.

[26] a)A. G. Doyle, E. N. Jacobsen, *Chem. Rev.* **2007**, *107*, 5713; b)P. M. Pihko, *Angew. Chem., Int. Ed.* **2004**, *43*, 2062; c)P. R. Schreiner, *Chem. Soc. Rev.* **2003**, *32*, 289; d)P. R. Schreiner, A. Wittkopp, *Org. Lett.* **2002**, *4*, 217; e)M. S. Taylor, E. N. Jacobsen, *Angew. Chem., Int. Ed.* **2006**, *45*, 1520.

[27] A. Wittkopp, P. R. Schreiner, *Chem.- Eur. J.* **2003**, *9*, 407.

[28] a)T.-G. Baik, A. L. Luis, L.-C. Wang, M. J. Krische, *J. Am. Chem. Soc.* **2001**, *123*, 6716; b)E. J. Enholm, K. S. Kinter, *J. Am. Chem. Soc.* **1991**, *113*, 7784; c)G. Pandey, S. Hajra, *Angew. Chem., Int. Ed.* **1994**, *33*, 1169; d)G. Pandey, S. Hajra, M. K. Ghorai, *Tetrahedron Lett.* **1994**, *35*, 7837; e)G. Pandey, S. Hajra, M. K. Ghorai, K. R. Kumar, *J. Am. Chem. Soc.* **1997**, *119*, 8777; f)Y. Roh, H.-Y. Jang, V. Lynch, N. L. Bauld, M. J. Krische, *Org. Lett.* **2002**, *4*, 611.

[29] J. Du, L. R. Espelt, I. A. Guzei, T. P. Yoon, *Chem. Sci* **2011**, *2*, 2115.

[30] H. Mayr, B. Kempf, A. R. Ofial, *Acc. Chem. Res.* **2002**, *36*, 66.

[31] a)Y. Pan, S. Wang, C. W. Kee, E. Dubuisson, Y. Yang, K. P. Loh, C.-H. Tan, *Green Chem.* **2011**, *13*, 3341; b)M. Rueping, S. Zhu, R. M. Koenigs, *Chem. Commun.* **2011**, *47*, 12709.

[32] M. Rueping, S. Zhu, R. M. Koenigs, *Chem. Commun.* **2011**, *47*, 8679.

[33] a)J. Xuan, Z.-J. Feng, S.-W. Duan, W.-J. Xiao, *RSC Adv.* **2012**, *2*, 4065; b)J. Xuan, Y. Cheng, J. An, L.-Q. Lu, X.-X. Zhang, W.-J. Xiao, *Chem. Commun.* **2011**, *47*, 8337.

[34] a)M. Rueping, D. Leonori, T. Poisson, *Chem. Commun.* **2011**, *47*, 9615; b)Y.-Q. Zou, L.-Q. Lu, L. Fu, N.-J. Chang, J. Rong, J.-R. Chen, W.-J. Xiao, *Angew. Chem. Int. Ed.* **2011**, *50*, 7171.

[35] L. Möhlmann, M. Baar, J. Rieß, M. Antonietti, X. Wang, S. Blechert, *Adv. Synth. Catal.* **2012**, *354*, 1909.

[36] M. Rueping, J. Zoller, D. C. Fabry, K. Poscharny, R. M. Koenigs, T. E. Weirich, J. Mayer, *Chem.- Eur. J.* **2012**, 3478.

[37] M. Rueping, C. Vila, R. M. Koenigs, K. Poscharny, D. C. Fabry, *Chem. Commun.* **2011**, *47*, 2360.

[38] M. Rueping, R. M. Koenigs, K. Poscharny, D. C. Fabry, D. Leonori, C. Vila, *Chem.- Eur. J.* **2012**, *18*, 5170.

[39] a)X. Bugaut, F. Glorius, *Chem. Soc. Rev.* **2012**, *41*, 3511; b)D. Seebach, *Angew. Chem. Int. Ed.* **1979**, *18*, 239.

[40] D. A. DiRocco, T. Rovis, *Science of Synthesis* **2011**, 835

[41] a)K. Zeitler, *Angew. Chem. Int. Ed.* **2005**, *44*, 7506; b)D. Enders, O. Niemeier, A. Henseler, *Chem. Rev.* **2007**, *107*, 5606; c)A. T. Biju, N. Kuhl, F. Glorius, *Acc. Chem. Res.* **2011**, *44*, 1182.

[42] A. Grossmann, D. Enders, *Angew. Chem. Int. Ed.* **2012**, *51*, 314.

[43] D. T. Cohen, K. A. Scheidt, *Chem. Sci* **2012**, *3*, 53.

[44] a)K. E. Ozboya, T. Rovis, *Chem. Sci* **2011**, *2*, 1835; b)S. P. Lathrop, T. Rovis, *J. Am. Chem. Soc.* **2009**, *131*, 13628.

[45] D. A. DiRocco, T. Rovis, *J. Am. Chem. Soc.* **2012**, *134*, 8094.

[46] A.-N. Alba, M. Viciano, R. Rios, *ChemCatChem* **2009**, *1*, 437.

[47] T. D. Beeson, A. Mastracchio, J.-B. Hong, K. Ashton, D. W. C. MacMillan, *Science* **2007**, *316*, 582.

[48] H.-W. Shih, M. N. Vander Wal, R. L. Grange, D. W. C. MacMillan, *J. Am. Chem. Soc.* **2010**, *132*, 13600.

[49] D. A. Nagib, M. E. Scott, D. W. C. MacMillan, *J. Am. Chem. Soc.* **2009**, *131*, 10875.

[50] A. Rausch, H. Homeier, H. Yersin, *Top. Organomet. Chem.* **2010**, *29*, 193.

[51] L. Flamigni, A. Barbieri, C. Sabatini, B. Ventura, F. Barigelletti, *Top. Curr. Chem.* **2007**, *281*, 143.

[52] M. Neumann, S. Füldner, B. König, K. Zeitler, *Angew. Chem. Int. Ed.* **2011**, *50*, 951.

[53] M. Neumann, K. Zeitler, *Org. Lett.* **2012**, *14*, 2658.

[54] a)F. R. Bou-Hamdan, P. H. Seeberger, *Chem. Sci.* **2012**, *3*, 1612; b)R. S. Andrews, J. J. Becker, M. R. Gagné, *Angew. Chem., Int. Ed.* **2012**, *51*, 4140; c)J. W. Tucker, Y. Zhang, T. F. Jamison, C. R. J. Stephenson, *Angew. Chem., Int. Ed.* **2012**, *51*, 4144.

[55] a)G. P. Chiusoli, M. Catellani, M. Costa, E. Motti, N. Della Ca', G. Maestri, *Coord. Chem. Rev.* **2010**, *254*, 456; b)O. Daugulis, *Top. Curr. Chem.* **2010**, *292*, 57; c)T. W. Lyons, M. S. Sanford, *Chem. Rev.* **2010**, *110*, 1147.

[56] D. Kalyani, K. B. McMurtrey, S. R. Neufeldt, M. S. Sanford, *J. Am. Chem. Soc.* **2011**, *133*, 18566.

[57] W.-Y. Yu, W. N. Sit, Z. Zhou, A. S. C. Chan, *Org. Lett.* **2009**, *11*, 3174.

[58] I. Ojima, *Fluorine in Medicinical Chemistry and Chemical Biology*, Wiley-Blackwell, Chichester, U.K, **2009**.

[59] Y. Ye, M. S. Sanford, *J. Am. Chem. Soc.* **2012**, *134*, 9034.

[60] a)M. P. Sibi, M. Hasegawa, *J. Am. Chem. Soc.* **2007**, *129*, 4124; b)J. F. Van Humbeck, S. P. Simonovich, R. R. Knowles, D. W. C. MacMillan, *J. Am. Chem. Soc.* **2010**, *132*, 10012.

[61] T. Koike, M. Akita, *Chem. Lett.* **2009**, *38*, 166.

[62] H.-S. Yoon, X.-H. Ho, J. Jang, H.-J. Lee, S.-J. Kim, H.-Y. Jang, *Org. Lett.* **2012**.

[63] M. Kotke, P. R. Schreiner, *Tetrahedron* **2006**, *62*, 434.

1.2 Metal-Free, Visible Light Cooperative[i] Asymmetric Organophotoredox Catalysis[ii]

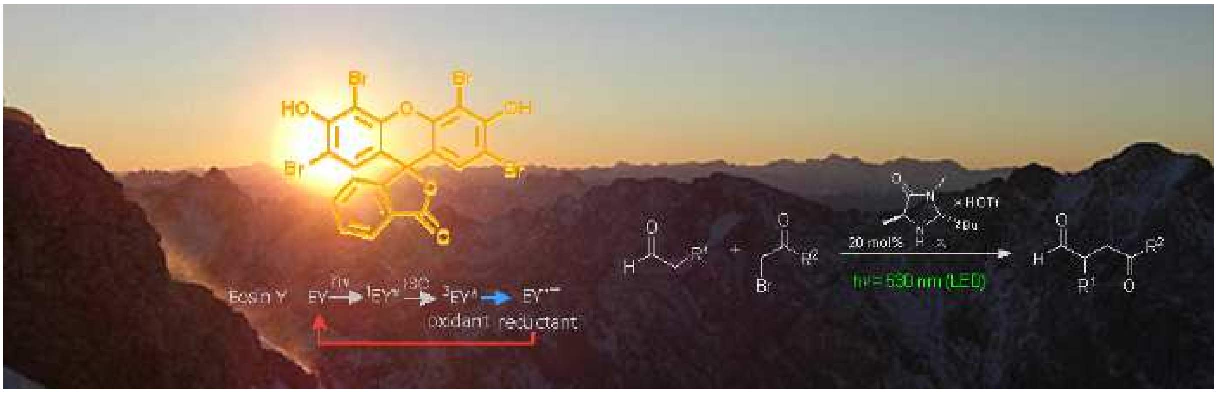
Br
Br
HO
OH
O
Br
Br
O
O
Eosin Y
EY
hν
¹EY*
ISC
³EY*
EY•−
oxidant
reductant
O
H
R¹
+
O
R²
Br
O
N
× HOTf
ᵗBu
N
H
20 mol%
hν = 530 nm (LED)
O
H
R¹
R²
O

The dawn of old stars: Classic xanthene dyes like eosin Y (gr. εος=goddess of dawn) and green-light irradiation can replace precious metal complexes for the organocatalytic asymmetric α-alkylation of aldehydes, thus rendering the process purely organic.[iii]

---

[i] According to a later published definition the term cooperative should be changed to synergistic.

[ii] Reproduced with permission from: M. Neumann, S. Füldner, B. König, K. Zeitler, *Angew. Chem. Int. Ed*. **2011**, 50, 951. Copyright 2011 Wiley-VCH

[iii] Determination of quantum yield was performed in cooperation with S. Füldner. All other experiments were performed by M. Neumann

1.2.1 Introduction

In the last decade organocatalysis has developed into an essential third branch of asymmetric catalysis that now complements the fields of metal and enzyme catalysis and allows for widely applicable methods for efficient organic synthesis.[1, 2] Especially the combination and integration in cooperative catalysis such as domino reactions[3] or the recent efforts for combining organocatalysis with metal activation[4] demonstrate its still not fully uncovered potential for the development of new activation modes in selective organic synthesis. Moreover, photocatalysis with visible light[5] is undoubtedly part of the emerging strategies to meet the increasing demand for more sustainable chemical processes. Building on seminal results employing photoinduced electron transfer processes[6] which often required UV light, recently a number of powerful methods applying organometallic complexes such as $[Ru(bpy)_3]^{2+}$ or $[Ir(ppy)_2(dtb\text{-}bpy)]^+$ as photocatalysts have been developed,[5, 7] culminating in a cooperative combination with an organocatalytic cycle[8] offering one of the rare catalytic methods for the enantioselective α-alkylation of aldehydes.[9, 10]

However, the high cost and potential toxicity of the ruthenium and iridium salts as well as their future limited availability render these metal-based methods somewhat disadvantageous. Stimulated by the attractiveness of using green light as the most abundant part of solar light, we speculated that a number of red to orange dyes could also successfully be used in photoredox catalysis and the choice of appropriate reaction conditions would additionally allow for cooperative merging with asymmetric organocatalysis.

Herein, we present a versatile metal-free, purely organic visible light photoredox catalysis. As a first example of our strategy we demonstrate the successful application of simple, inexpensive organic dyes as effective photocatalysts for the cooperative organocatalytic asymmetric intermolecular α-alkylation of aldehydes.[11] Initial studies began with the screening of a number of red and orange dyes (Scheme 1) for the photocatalytic reductive dehalogenation of α-bromoacetophenone (E^0 = -0.49 V *vs.* SCE)[12] as a test reaction (Table 1).[6c, 13] Following the observation that classic organic dyes show striking similarities to the widely employed organometallic ruthenium and iridium containing photosensitizers we chose our test candidates based on their λ_{max}, their redox potential E^0 and their precedent use as photosensitizers for semiconductor based photocatalysis or dye solar cells.[14, 15]

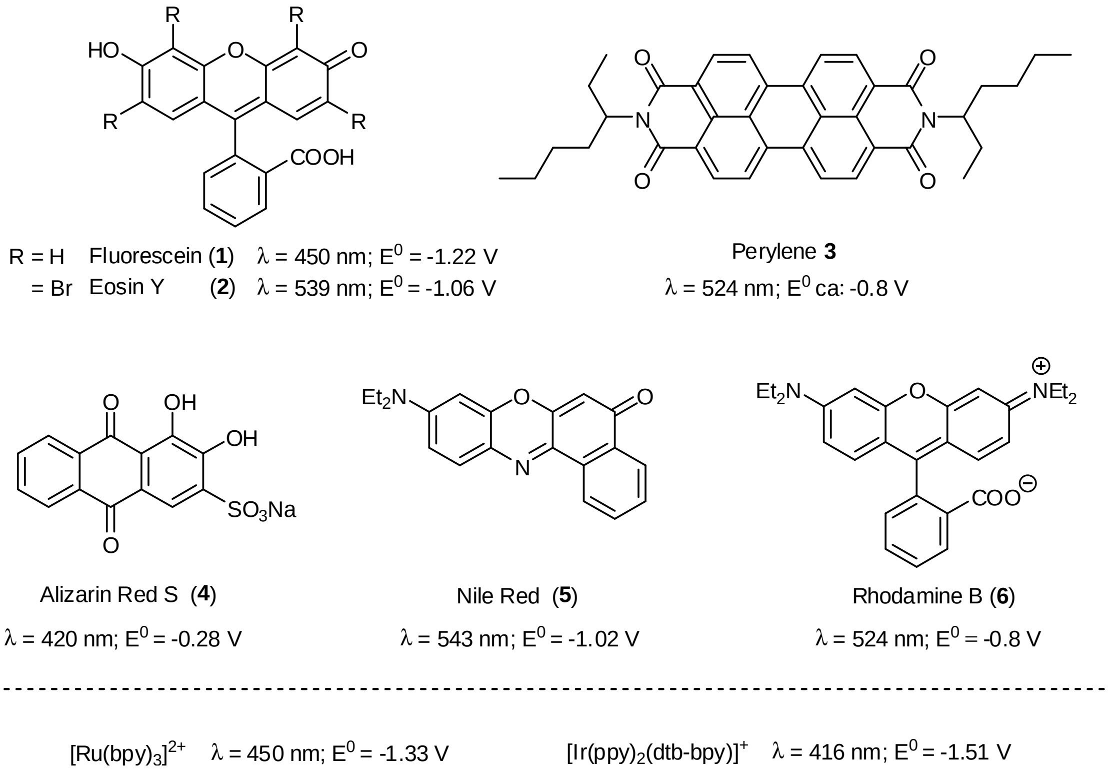
R = H Fluorescein (1) λ = 450 nm; E0 = -1.22 V
= Br Eosin Y (2) λ = 539 nm; E0 = -1.06 V
Perylene 3
λ = 524 nm; E0 ca: -0.8 V
Alizarin Red S (4)
λ = 420 nm; E0 = -0.28 V
Nile Red (5)
λ = 543 nm; E0 = -1.02 V
Rhodamine B (6)
λ = 524 nm; E0 = -0.8 V
[Ru(bpy)3]2+ λ = 450 nm; E0 = -1.33 V
[Ir(ppy)2(dtb-bpy)]+ λ = 416 nm; E0 = -1.51 V

Scheme 1. Absorption and redox properties of red and orange organic dyes used as photoredox catalysts (□$_{max}$ (CH_3CN) in nm; **3** in CH_2Cl_2; E^0 (Dye/Dye$^{•\,□}$) in V *vs.* SCE)[16] in comparison with common organometallic photocatalysts. SCE: saturated calomel electrode.

1.2.2 Results and Discussion

To achieve this desired transformation we investigated conditions reported by Stephenson and co-workers in the photocatalytic dehalogenation of activated benzylic halides in the presence of $[Ru(bpy)_3]^{2+}$. In accordance with their results we noticed that also for our α-carbonyl bromide substrate conditions employing 1.1 equiv of Hantzsch ester **7** as a hydride source was beneficial in order to avoid potential side reactions. While under these conditions a slow background reaction also renders detectable amounts of the debrominated product (Table 1, entry 1) most of the simple organic dyes were effective for this transformation under optimized conditions, albeit with different yields. Whereas light proved essential for this transformation (entry 8) the reaction can be conducted using different light sources. Fast conversion is observed in ambient sunlight (entry 9), however with a slight decrease in product yield, potentially due to side reactions that may occur at the higher reaction temperature and the UV portion of the solar spectrum. Upon irradiation with green light[17] from high power LEDs with an emission of approx. λ ≈ 530 nm bleaching of the dyes was minimized, but still observable for alizarin (**4**), nile red (**5**) and rhodamine B (**6**) indicating the slow destruction of the photosensitizer.

Table 1. Dehalogenation of α-bromoacetophenone.

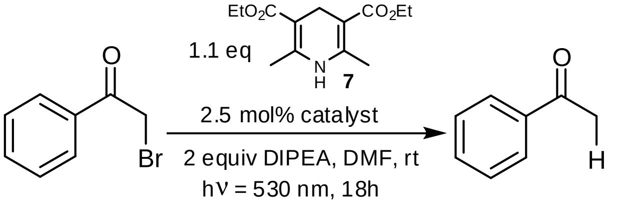

Entry[a]	Dye Catalyst	Yield [%][b]
1	none	40
2	Ru(bpy)$_3^{2+}$ (**8**)[c]	100
3	Alizarin S (**4**)	36
4	Perylene **3**	100
5	Nile Red (**5**)	100
6	Fluorescein (**1**)	100
7	Eosin Y (**2**)	100
8	Eosin Y (**2**)	3[d]
9	Eosin Y (**2**)	80[e]
10	Rhodamine B (**6**)	80

[a] Standard conditions as depicted above. [b] GC yield determined using a calibrated internal standard. [c] A blue high power LED (λ ≈ 455 nm) was used instead. [d] Reaction was performed in the dark. [e] Reaction was conducted in sunlight; full conversion was reached after 1h of irradiation.

However, perylene **3** and the xanthene-based dyes **1** and especially Eosin Y (**2**) proved to be sufficiently stable under the reaction conditions. Using eosin **2** as photocatalyst affords the defunctionalized product in a very clean, high yielding reaction as determined by both GC and NMR studies using appropriate internal standards.[18] Due to its simplicity and favorable redox and photochemical properties Eosin Y (**2**) was selected as photocatalyst for our subsequent studies.[19]

A number of dehalogenations (Table 2) under our optimized conditions showed that the reaction is also tolerant to aromatic residues with electron-withdrawing substituents (entry 2). Polar functional groups such as esters are tolerated and exclusive chemoselectivity for α-activated substrates over aryl halides was observed for the defunctionalization (entries 3 and 4). In all cases the obtained isolated yields are equal or better than for the reported transition metal based catalytic counterpart[13] proving the effectiveness of our operational simple, inexpensive conditions.[20]

It also should be noted that the irradiation power of the employed LEDs and therefore the applied energy to the reaction system is drastically reduced as compared to sunlight or typically applied fluorescent household bulbs.[17]

Table 2. Photocatalytic reductive dehalogenation with Eosin Y using Hantzsch ester as reduction equivalent.

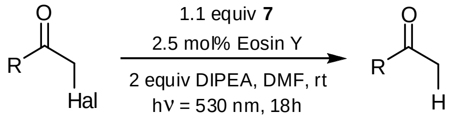

Entry	Halogenide	Product	Yield [%][a]
1	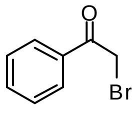 **9**	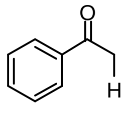 **10**	100[b]
2	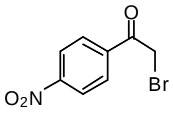 **11**	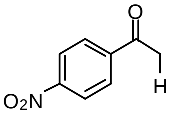 **12**	83
3	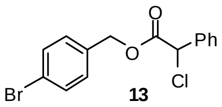 **13**	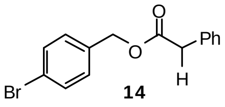 **14**	78 (78)[c]
4	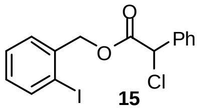 **15**	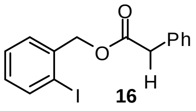 **16**	89 (88)[c]

[a] Isolated yields. [b] Yield determined by GC and NMR using appropriate calibrated internal standards. [c] Yields in brackets as reported in ref. 13.

Next we turned our attention to the application of organic dyes as photoredox catalysts in asymmetric organocatalytic C–C bond formations developed by MacMillan.[8] As highlighted in Table 3 the transformations were found to be both high yielding and enantioselective applying a combination of Eosin Y (**2**) and MacMillan´s imidazolidinone catalyst **17**. Even if our organic dye sensitized conditions require somewhat longer reaction times[21] we did not observe product racemization over the indicated reaction times further illustrating the previously elucidated strict differentiation of the *trans*–substituted catalyst between α-methylene aldehydes and α-substituted products.[22] The enantioselectivity depends on the reaction temperature (entries 1, 4 and 5) and –5 °C was found to be optimal. Performing the reaction under direct sunlight led to faster conversion, albeit with a slight erosion in enantioselectivity presumably due to the thereby increased reaction temperature (ca. 30 °C). Our methodology is also compatible with the stereospecific incorporation of polyfluorinated alkyl substituents (Table 3, compound **21**), which are important elements in drug design to modulate the specific properties.[23]

Table 3. Purely organocatalytic enantioselective α-alkylation/ perfluoroalkylation of aliphatic aldehydes.

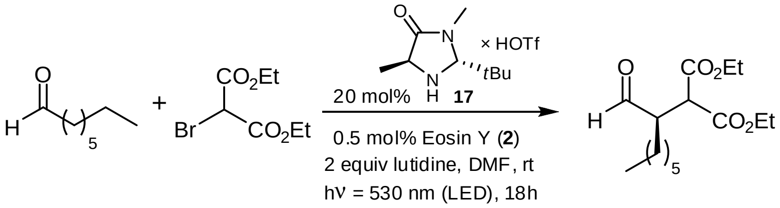

Entry	Variation from the standard conditions[a]	Yield [%][b]	ee [%][c]
1	none	63	77
2	23W fluorescent bulb instead of LED	78	80
3	23W fluorescent bulb instead of LED **and** [Ru(bpy)$_3$]Cl$_2$ (**8**)	75	76
4	T = 0 °C	70	81
5	T = – 5 °C	85	88
6	sunlight (T≈ 30 °C)[d]	77	76

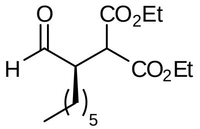

18 85%
88% ee

[e

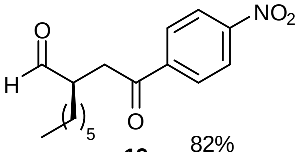

19 82%
95% ee

[f]

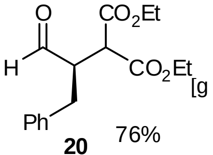

[g

20 76%
86% ee

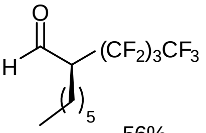

21 56%
96% ee

[a] Standard conditions as depicted above. [b] Isolated yields. [c] Enantiomeric excess was determined as reported in ref. 8a. [d] Full conversion is already reached after approx. 4h. [e] Reaction was performed at + 5 °C; *p*-NO$_2$-phenacyl bromide was used. [f] Phenylpropionaldehyde was used instead of octanal. [g] Reaction was performed at –15 °C; 1-Iodo-perfluorobutane was used instead of diethyl bromomalonate.

At present, the mechanistic picture of this reaction is not complete. It is evident, however, that Eosin Y acts as a photoredox catalyst after its excitation with visible light and population of its more stable triplet state finally enabling single electron transfer (SET).[24] Similar to the chemistry of Ru^{2+*} both reductive and oxidative quenching are known for excited Eosin Y ^{3}**EY***.[25] Due to comparable results with the previous work of MacMillan we presume that Eosin Y acts a reductant – relying on the sacrificial oxidation of a catalytic amount of the enamine as initial electron reservoir[26] – to furnish the electron-deficient alkyl radical via SET with an alkyl halide. Addition of this radical to the electron-rich olefin of the enamine that is simultaneously generated within the organocatalytic cycle merges both activation pathways. In the catalytic cycle the subsequent oxidation of the amino radical to the iminium species provides the electron for the reductive quenching of the dye´s excited state **^{3}EY***.[27]

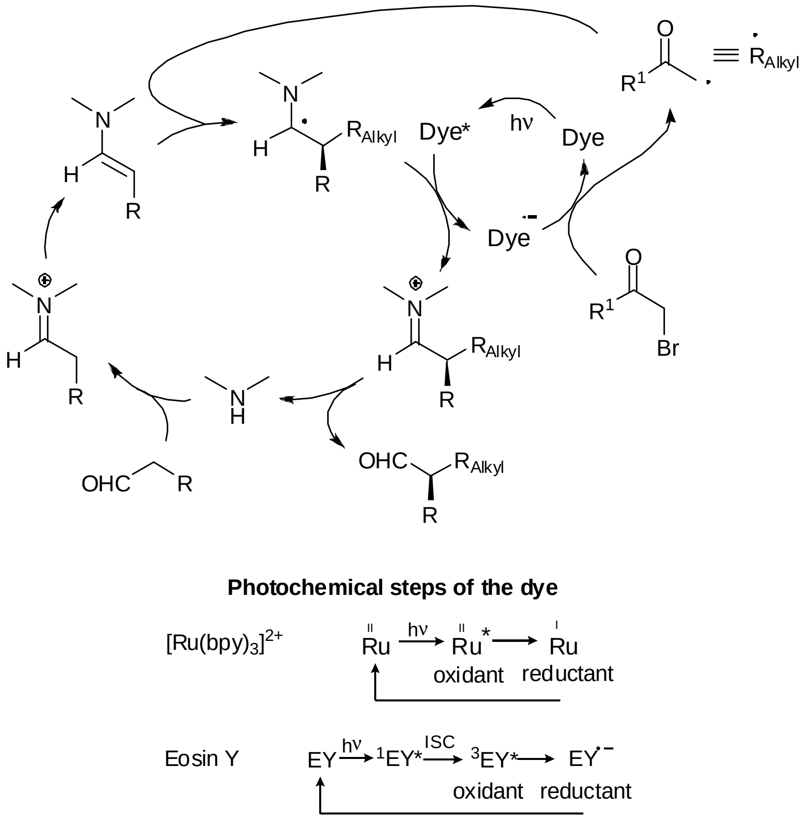
R1
O
≡ RAlkyl
N
H
R
RAlkyl
Dye*
hν
Dye
Dye·−
Br
OHC
Photochemical steps of the dye
[Ru(bpy)3]2+
Ru II → hν Ru II* → Ru I
oxidant
reductant
Eosin Y
EY → hν 1EY* → ISC 3EY* → EY·−
oxidant
reductant

Scheme 2. Proposed mechanism and comparison of Ru^{II} and Eosin Y photoredox cycle.

Having successfully demonstrated the versatility of simple organic dyes for photoredox catalysis we directed our efforts to the determination of the quantum yield of the reaction to gain further information on its efficiency.[28] We reproducibly found values in the range of 6 to 9% indicating a more complex reaction course than the proposed simplified mechanistic platform. To further prove this presumption we conducted an additional GC-based yield determination after keeping the initially irradiated sample in the dark for 3h and respectively 6h. Here we found a significant increase of the yield which might stem from the involvement of an amplifying “dark reaction”.

1.2.3 Conclusion

In summary, we have developed a metal-free method using inexpensive Eosin Y as a powerful photocatalyst for various photoredox transformations allowing for an equal performance as compared to noble metal catalysts. The discovery of a purely organic asymmetric cooperative photoredox organocatalysis will facilitate applications of these useful reactions in organic synthesis significantly as xanthene dyes are readily accessible, cheap and less toxic compared to transition metal complexes. This extension of highly versatile photoredox catalysis to classic organic dyes is expected to be broadly useful across many related applications.

1.2.4 Experimental Section

1.2.4.1 General Methods

Unless otherwise noted, all commercially available compounds were used as provided without further purification.

NMR spectra were recorded on a Bruker Avance 300 (300.13 MHz), 400 MHz (400.13 MHz) or a Bruker Avance 600 (600.13 MHz) and using the solvent peak as internal reference ($CDCl_3$: δ H 7.26; δ C 77.0 and DMSO-d_6: δ H 2.51; δ C 39.5). Multiplicities are indicated, s (singlet), d (doublet), t (triplet), q (quartet), quint (quintet), sept (septet), m (multiplet)); coupling constants (J) are in Hertz (Hz). All reactions were monitored by thin-layer chromatography using Merck silica gel plates 60 F_{254}; visualization was accomplished with UV light and/or staining with appropriate stains (anisaldehyde or phosphomolybdic acid). Standard flash chromatography procedures were followed (particle size 40−63 µm). Optical rotation measurements were made on Krüss optotronic P8000-T polarimeter at 589 nm and are quoted in degree; concentration c is given in g/mL.

HPLC analysis was performed on a Varian LC920 using a Daicel OD-H (6.6 mm x 25 cm) column. Gas chromatographic analysis was performed on a Fisons Instrument GC 8130 equipped with a capillary column J&W Scientific DB-1 (30 m x 0.25 mm / 0.25 µm film).

UV VIS spectra were recorded on a Varian Cary 50 BIO spectrometer using 1cm cuvettes.

All reactions were carried out under a protective atmosphere of dry nitrogen or argon using oven-dried glassware unless otherwise stated.

Imidazolidinone catalyst **17** was prepared according to a procedure described by Hruby *et al.* [vii]

[vii] W. M. Kazmierski, Z. Urbanczyk-Lipkowska, V. J. Hruby, *J. Org. Chem.* **1994**, *59*, 1789-1795.

Irradiation with green light was performed using high-power LEDs Philips LUXEON® Rebel (1W, λ = 530±10 nm, 145 lm @700mA); blue light irradiation was performed with Philips LUXEON® Rebel LED (1W, λ = 455±10 nm, 425 mW @700mA).

Irradiation with a "daylight" source was conducted using a household fluorescent bulb (OSRAM®, 23 W, 6500 K, 1470 lm).

1.2.4.2 General Procedures

General Procedure 1: (Reductive Dehalogenation of α-Halogenated Carbonyl Compounds)

In a 5 mL snap cap vial equipped with a magnetic stirring bar and fitted with a septum the α-halogen carbonyl derivative (1 eq), diethyl 2,6-dimethyl-1,4-dihydropyridine-3,5-dicarboxylate (7) (1.1 eq) and Eosin Y (2) (0.025 eq) were dissolved in DMF (c=0.25 mmol/ml). DIPEA (2 eq) was added and the mixture was degassed by "pump-freeze-thaw" cycles (×3) *via* a syringe needle. The vial was irradiated through the vial´s plane bottom side using LEDs fixed to a heat sink (Philips Luxeon® Rebel, 1 W, 530 nm, 80 lm)[viii] for the indicated time. After the reaction was completed (as judged by GC) the mixture was transferred to a separation funnel, diluted with diethyl ether and washed with water. The aqueous phase was extracted three times with diethyl ether. The combined organic layers were dried over $MgSO_4$, filtered and concentrated in vacuum. Purification of the crude product was achieved by silica gel column chromatography.

General Procedure 2 (α-Alkylation of Aldehydes)

In a 5 mL snap cap vial equipped with a magnetic stirring bar and fitted with a septum (2*R*,5*S*)-2-*tert*-butyl-3,5-dimethylimidazolidin-4-one×TfOH (17) (25 mg, 78 µmol, 0.2 eq) and Eosin Y (2) (1.3 mg, 2 µmol, 0.005 eq) were dissolved in DMF (0.8 mL). Aldehyde (0.8 mmol, 2 eq), α-bromo carbonyl compound (0.4 mmol, 1 eq) and 2,6-lutidine (91 µl, 0.8 mmol, 2 eq) were added. The solution was degassed by "pump-freeze-thaw" cycles (×3) *via* a syringe needle. The vial was then irradiated by a single LED (Philips Luxeon® Rebel, 1 Watt, 530 nm, 145 lm) for the time indicated through the bottom of the vial which was immerged into a cooling bath. After the reaction was completed (as judged by GC) the mixture was transferred to a separation funnel, diluted with 8 mL diethyl ether and washed with 8 mL water. The aqueous phase was extracted three times with 8 mL diethyl ether. The combined organic layers were successively washed with each 8 mL of saturated solutions of NH_4Cl, $NaHCO_3$ and NaCl. The organic layer was dried over $MgSO_4$, filtered and concentrated in vacuum. Purification of the crude product was achieved by silica gel column chromatography.

[viii] If the LEDs are run at lower current (here: 350 mA) as the indicated maximum current of 700 mA, the corresponding luminous flux/radiometric power is accordingly lower.

1.2.4.3 Sensitizer Screening

General Procedure

For the screening of potential metal-free organic dyes the photoreductive dehalogenation of activated α–halogenated carbonyl compounds was selected.[ix] The following protocol (using trichloroethylene as calibrated internal standard) was applied to 2-bromoacetophenone. An exemplary procedure and spectral data are shown for the use of Eosin Y (2).

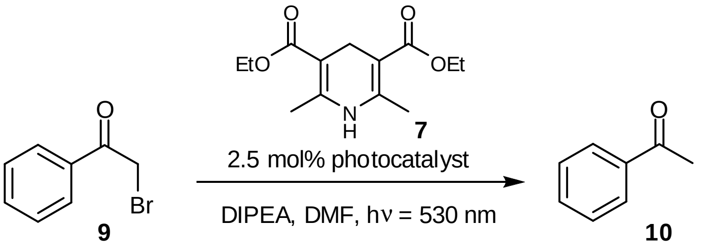

In a 5 mL snap cap vial equipped with a magnetic stirring bar and fitted with a septum bromoacetophenone (9) (40 mg, 0.2 mmol, 1 eq), Eosin Y (2) (3.5 mg, 5 µmol, 0.025 eq) and diethyl-2,6-dimethyl-1,4-dihydropyridine-3,5-dicarboxylate ("Hantzsch ester") (7) (56 mg, 0.22 mmol 1.1 eq) were dissolved in d^7-DMF (0.75 mL). To the solution was added DIPEA (70 µl, 0.4 mmol, 2 eq) and trichloroethylene (36 µl, 0.4 mmol, 2 eq, as internal standard). The mixture was degassed by "pump-freeze-thaw" cycles (×3) *via* a syringe needle and was subsequently transferred to a NMR sample tube under Argon atmosphere. The vial was placed beside an array of LEDs (5x Luxeon Rebel, 1 Watt, 530 nm, 80 lm) in approximately 5 mm distance and irradiated for the indicated time.

GC (40 °C, 1 min, 15.0 °C/min, 250°C): Originally present reduction equivalent Hantzsch ester 7 could not been detected by our GC analysis.

^{1}H NMR (300 MHz, d^7-DMF): δ: = 7.46 ppm (s, 1H, trichloroethylene), 5.12 ppm (s, 2H, C(O)-CH_2-Br, starting material), 2.80 ppm (s, 3H, C(O)-CH_3, product)

[ix] J. M. R. Narayanam, J. W. Tucker, C. R. J. Stephenson, *J. Am. Chem. Soc.* **2009**, *131*, 8756.

GC and NMR Spectra for Screening with Internal Standard (trichloroethylene)

GC

Reaction mixture of the reductive dehalogenation of 2-bromoacetophenone for dye screening before irradiation.

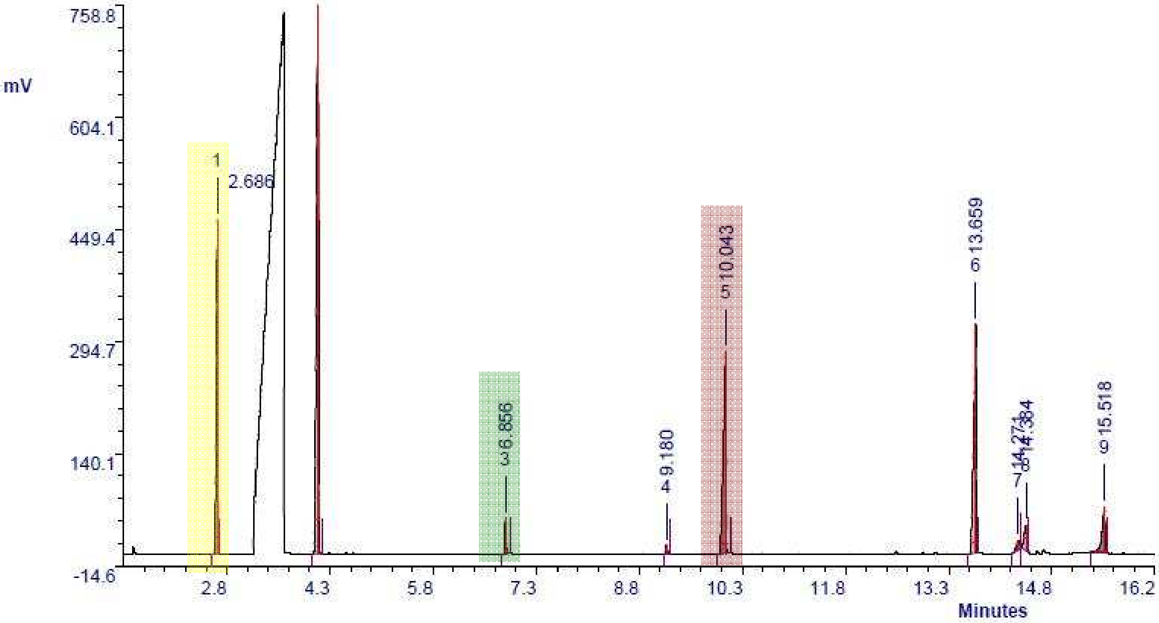

2.7 min (trichloroethylene) standard
4.2 min (DIPEA),
6.9 min (acetophenone (**10**)) product
10.5 min (2-bromoacetophenone (**9**)) starting. material
13.7 min (diethyl 2,6-dimethylpyridine-3,5-dicarboxylate).

After complete reaction

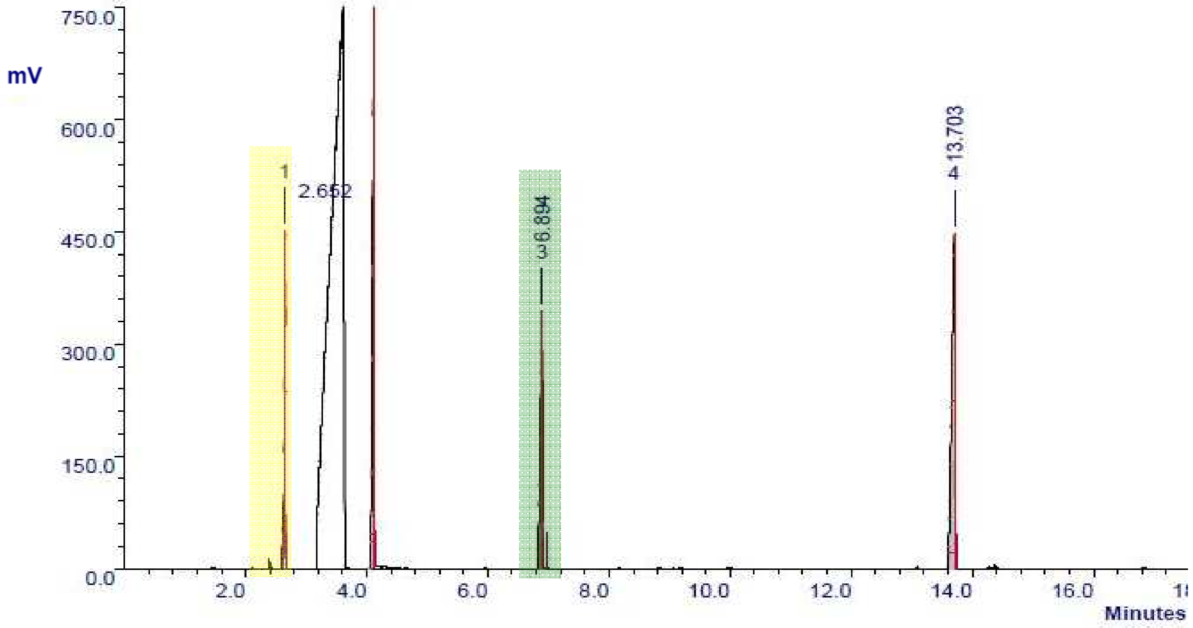

Figure 1) Determination of the response factor for the reductive dehalogenation of 2-bromoacetophenone using trichloroethylene as internal standard

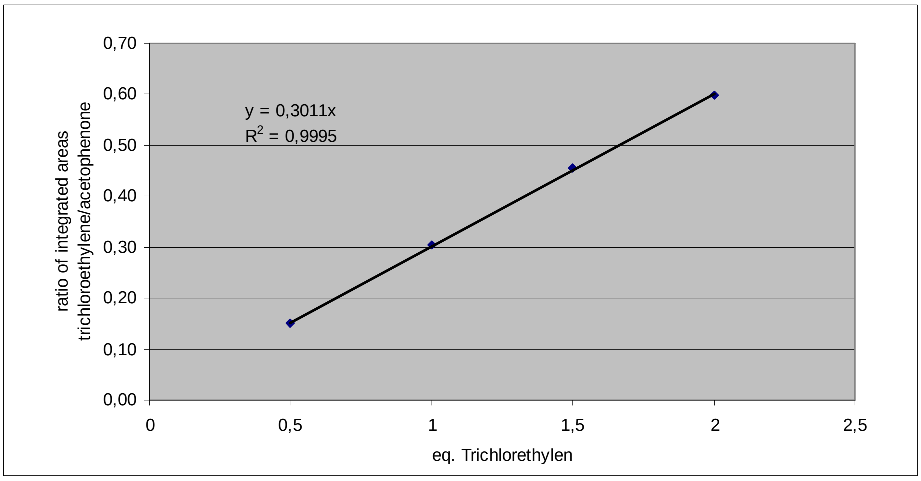

NMR

Reaction mixture of the reductive dehalogenation of 2-bromoacetophenone for dye screening before irradiation

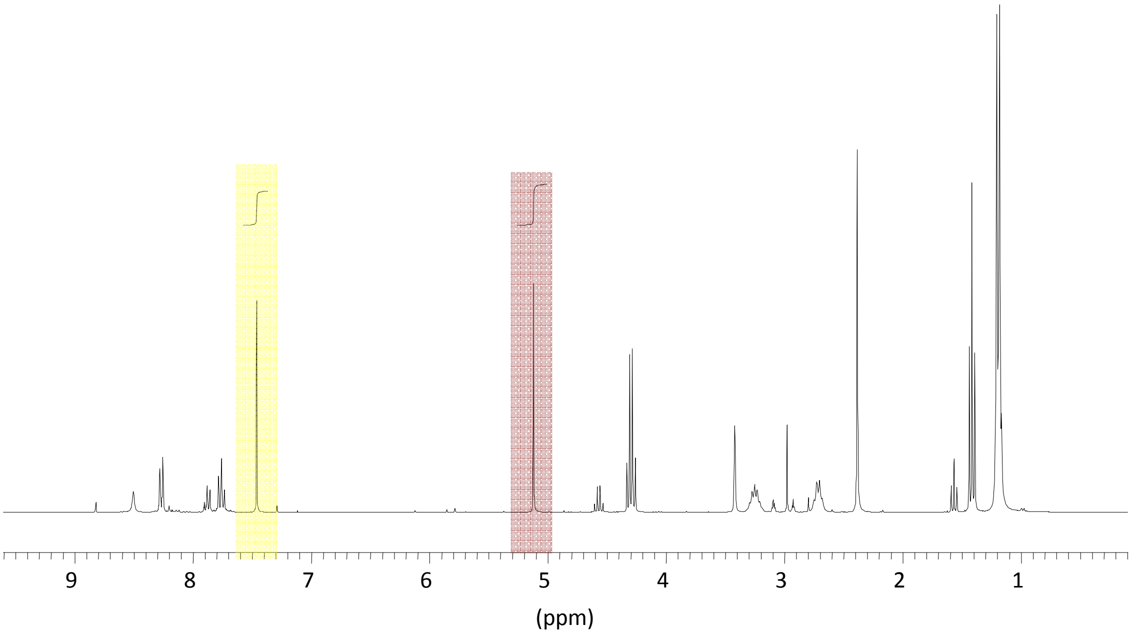

δ: = 7.46 ppm (s, 1H, trichloroethylene), 5.12 ppm (s, 2H, C(O)-C**H**$_2$-Br, starting material), 2.80 ppm (s, 3H, C(O)-C**H**$_3$, product)

After 8 h irradiation

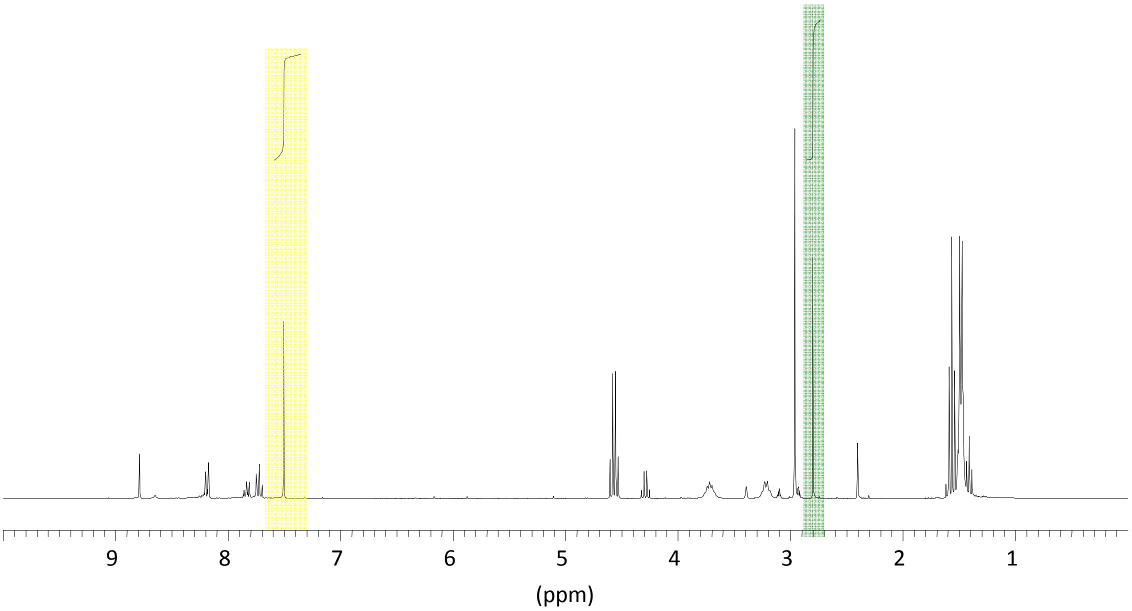

1.2.4.4 Experimental Data for Reductive Dehalogenation Reactions

4-Nitroacetophenone (12, table 2, entry 2)

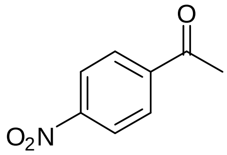

$C_8H_7NO_3$
165.15 g/mol

according to general procedure 1: 2-bromo-1-(4-nitrophenyl)ethanone (11) (162 mg, 631 µmol), 2,6-dimethyl-1,4-dihydropyridine-3,5-dicarboxylate (7) (176 mg, 694 µmol), Eosin Y (2) (11 mg, 16 µmol), DIPEA (22 µL, 364 µmol) in 1.5 mL DMF afforded 86 mg 12 after purification by SiO_2 column chromatography (hexanes/Et_2O 4/1) as a colorless solid. 83% yield. R_f (hexanes/Et_2O 4/1) = 0.29.

^{1}H NMR (300 MHz, $CDCl_3$): δ 8.30 (m, 2H, ArH), 8.10 (m, 2H, ArH), 2.67 (s, 3H, CH_3). ^{13}C NMR (75.5 MHz, CDCl3) δ 196.3, 150.4, 14.4, 129.3, 213.9, 27.0; GC (40 °C 1 min, 15.0 °C/min, 200 °C): t_R (product) = 10.8 min, t_R (starting material) = 12.8 min.

4-Bromobenzyl 2-phenylacetate (14, table 2, entry 3)

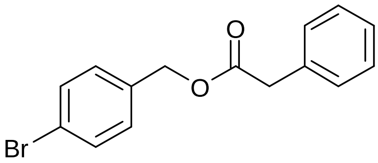

$C_{15}H_{13}BrO_2$
305.17 g/mol

according to **general procedure 1**: 4-bromobenzyl 2-chloro-2-phenylacetate (**13**) (78 mg, 215 µmol), 2,6-dimethyl-1,4-dihydropyridine-3,5-dicarboxylate (**7**) (60 mg, 237 µmol), Eosin Y (**2**) (3.75 mg, 5.4 µmol), DIPEA (94 µL, 537 µmol) in 0.8 mL DMF afforded 51 mg **14** after purification by SiO_2 column chromatography (hexanes/EtOAc 9/1) as a colorless oil. 78% yield. R_f (hexanes/EtOAc 9/1) = 0.38.

^{1}H NMR (300 MHz, $CDCl_3$): δ 7.49-7.11 (m, 9H, ArH), 5.08 (s, 2H, Ar-C**H₂**-O), 3.67 (s, 2H, C(O)-C**H₂**-Ph). ^{13}C NMR (75.5 MHz, CDCl3) δ 171.3, 135.5, 134.8, 131.8, 129.8, 129.3, 128.7, 128.0, 127.3, 122.3, 65.8, 41.3. GC (40 °C 1 min, 15.0 °C/min, 300 °C): t_R (product) = 16.0 min, t_R (starting material) = 17.1 min

2-Iodobenzyl 2-phenylacetate (16, table 2, entry 4)

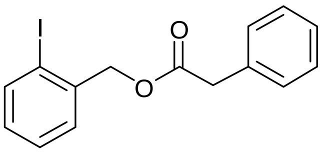

$C_{15}H_{13}IO_2$
352.17 g/mol

according to **general procedure 1**: 2-iodobenzyl 2-chloro-2-phenylacetate (**15**) (89 mg, 239 µmol), 2,6-dimethyl-1,4-dihydropyridine-3,5-dicarboxylate (**7**) (64 mg, 253 µmol), Eosin Y (**2**) (4 mg, 5.8 µmol), DIPEA (80 µL, 460 µmol) in 0.8 mL DMF afforded 51 mg **16** after purification by SiO_2 column chromatography (hexanes/EtOAc

9/1) as a colorless oil. 89% yield. R_f (hexanes/EtOAc 9/1) = 0.41.

^{1}H NMR (300 MHz, $CDCl_3$): δ 7.85 (d, *J* =7.7 Hz, 1H, Ar**H**), 7.37-7.27 (m, 7H, Ar**H**), 7.02 (m, 1H, Ar**H**), 5.15 (s, 2H, Ar-C**H_2**-O), 3.72 (s, 2H, C(O)-C**H_2**-Ph). ^{13}C NMR (75.5 MHz, CDCl3) δ: 171.1, 139.5, 138.2, 133.8, 129.9, 129.4, 128.6, 128.3, 127.2, 98.3, 70.4, 41.3. GC (40 °C 1 min, 15.0 °C/min, 300 °C): t_R (product) = 16.8 min, t_R (starting material) = 17.7 min.

Experimental Data for the α-Alkylation of Aldehydes

(*R*)-Diethyl 2-(1-oxooctan-2-yl)malonate (18)

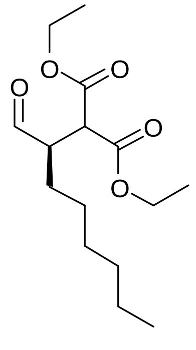

$C_{15}H_{26}O_5$
286.36 g/mol

according to **general procedure 2**: After 15 h irradiation at -5 °C the reaction mixture was subjected to the workup protocol and further purified by column chromatography (hexanes/ Et_2O 6/1). 85% yield, 88% ee as a colorless oil. R_f (hexanes/Et_2O 4/1) = 0.30 stain: anisaldehyde (yellow spot).

^{1}H NMR (300 MHz, $CDCl_3$): δ 9.74 (d, *J* = 1.2 Hz, 1H, C**H**O), 4.25-4.17 (m, 4H, 2 × CO_2C**H_2**CH_3), 3.71 (d, *J* = 8.8 Hz, 1H, C**H**($CO_2Et)_2$), 3.12-3.05 (m, 1H, HCOC**H**), 1.75-1.45 (m, 2H, C**H_2**($CH_2)_4CH_3$), 1.44-1.22 (m, 14H, CH_2(C**H_2**)$_4CH_3$, 2 × CO_2CH_2C**H_3**), 0.87 (m, 3H, $CH_2(CH_2)_4C$**H_3**); ^{13}C NMR (75.5 MHz, CDCl3) δ 201.6, 168.1, 168.0, 61.9, 61.8, 51.7, 50.2, 31.4, 29.3, 27.0, 26.4, 22.5, 14.1, 14.0, 14.0; GC (40 °C 1 min, 15.0 °C/min, 250 °C): t_R (product) = 13.8 min, t_R (starting material) = 9.0 min. Enantiomeric excess was determined after acetalization of the aldehyde with (2*S*, 4*S*)-(+)-2,4-pentanediol *via* integration of ^{1}H NMR signals of the diastereomeric acetals ($CDCl_3$, both doublets) at 3.63 ppm (minor) and 3.59 ppm (major).[x]

(*R*)-2-(2-(4-Nitrophenyl)-2-oxoethyl)octanal (19)

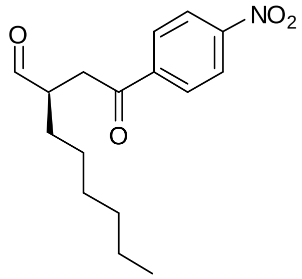

$C_{16}H_{21}NO_4$
291.34 g/mol

according to **general procedure 2**: After 16 h irradiation at +5 °C the reaction mixture was subjected to the workup protocol and further purified by column chromatography (hexanes/Et_2O 1/0 to 6/1) 82% yield, 96% ee, yellowish solid. R_f (hexanes/Et_2O 6/1) = 0.34 stain: anisaldehyde (purple spot).

^{1}H NMR (300 MHz, $CDCl_3$): δ 9.80 (s, 1H, C**H**O), 8.33-8.31 (m, 2H, Ar**H**), 8.15-8.11 (m, 2H, Ar**H**), 3.51 (dd, *J* = 8.5, 18.0 Hz, 1H, C**H_2**COAr), 3.22-3.13 (m, 1H, HCOC**H**), 2.96 (dd, *J* = 4.2, 18.0 Hz, 1H, C**H_2**COAr), 1.86-1.75 (m, 1H, C**H_2**($CH_2)_4CH_3$), 1.62-1.53 (m, 1H, C**H_2**($CH_2)_4CH_3$), 1.45-1.23 (m, 8H,

---

[x] D. A. Nicewicz, D. W. C. MacMillan, *Science* **2008**, *322*, 77.

$CH_2(C\mathbf{H}_2)_4CH_3$), 0.88 (t, *J* = 6.9 Hz, 3H, $CH_2(CH_2)_4C\mathbf{H}_3$); $[\alpha_{D}^{23}]$ = 43.3 (c = 0.94, CH_2Cl_2). GC (40°C 1min, 15.0 °C/min, 250°C): t_R (product) = 15.9 min, t_R (starting material) = 12.8 min. Enantiomeric excess was determined by comparison of optical rotation to literature values (lit.: $[\alpha_{D}^{23}]$ = +43.6 (c = 0.94, CH_2Cl_2)).[x]

(*R*)-Diethyl 2-(1-oxo-3-phenylpropan-2-yl)malonate (20)

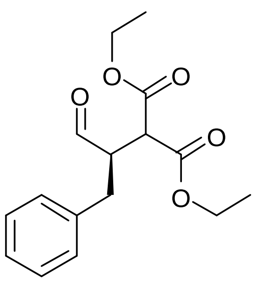

$C_{16}H_{20}O_5$
292.33 g/mol

according to **general procedure 2**: After 18 h irradiation at -2 °C the reaction mixture was subjected to the workup protocol and further purified by column chromatography (hexanes/Et_2O 1/0 to 6/1) 76% yield, 86% ee, colorless oil. R_f (hexanes/Et_2O 6/1) = 0.28 stain: anisaldehyde (yellow spot).

^1H NMR (300 MHz, $CDCl_3$): δ 9.73 (s, 1H, C**H**O), 7.29 – 7.12 (5H, Ar**H**), 4.19-4.11 (m, 4H, 2 × $CO_2C\mathbf{H}_2CH_3$), 3.62 (d, *J* = 7.1 Hz, 1H, C**H**$(CO_2Et)_2$), 3.37-3.30 (m, 1H, HCOC**H**), 3.09 (dd, *J* = 7.5, 14.2 Hz, 1H, $C\mathbf{H}_2Ph$), 2.78 (dd, *J* = 7.3, 14.2 Hz, 1H, $C\mathbf{H}_2Ph$), 1.22 (t, *J* = 7.1 Hz, 6H, 2 × $CO_2CH_2C\mathbf{H}_3$); GC (40 °C 1 min, 15.0 °C/min, 250 °C): t_R (product) = 15.0 min, t_R (starting material) = 9.0 min. Enantiomeric excess was determined after acetalization of the aldehyde with (2*S*, 4*S*)-(+)-2,4-pentanediol *via* integration of ^1H-NMR signals of the diastereomeric acetals ($CDCl_3$, both doublets) at 4.93 ppm (major) and 4.82 ppm (minor).[x]

(*S*)-2-(Perfluorobutyl)octanal (21)

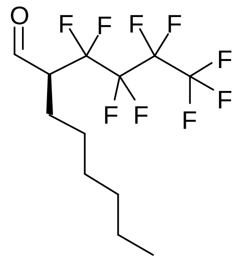

$C_{12}H_{15}F_9O$
346.23 g/mol

Closely related to **general procedure 2:** In a 5 mL snap cap vial equipped with a magnetic stirring bar and fitted with a septum (2*R*, 5*S*)-2-*tert*-butyl-3,5-dimethylimidazolidin-4-one hydrochloride (**17×HCl**) (21.2 mg, 0.102 mmol, 0.2 eq) and Eosin Y (**2**) (1.3 mg, 2 µmol, 0.005 eq) were dissolved in DMF (0.8 mL). Octanal (80 µl, 0.51 mmol, 1 eq), 1-iodononafluorobutane (727 µL, 4.1 mmol, 8 eq) and 2,6-lutidine (84 µL, 0.72 mmol, 1.4 eq)) were added. The solution was degassed by "pump-freeze-thaw" cycles (×3) *via* a syringe needle. The vial was then irradiated through the bottom of the vial which was immerged into a cooling bath at -15 °C. After the reaction was completed, as judged by GC (usually 18 h), the reaction mixture was transferred to a pre-cooled 50 mL round bottom flask. Remaining solids were washed out with 10 mL pre-cooled CH_2Cl_2. To the cooled solution was added sodium borohydride (202 mg, 5.1 mmol) and the resulting suspension was stirred for 30 min. Pre-cooled methanol (10 mL) was added and after 1 h additional stirring the reaction was quenched by addition of saturated NH_4Cl solution (15 mL). The mixture was warmed to room temperature and subsequently transferred to a separation funnel. The aqueous phase was extracted three times with diethyl ether (8 mL each). Combined organic phases were washed twice with saturated $NaHCO_3$ solution (15mL each), dried over $MgSO_4$, filtered and concentrated in vacuum. The crude product was purified by column chromatography (hexanes/Et_2O 6/1). 56% yield, 96% ee colorless oil. R_f (hexanes/Et_2O 4/1) = 0.31 stain: phosphomolybdic acid (green spot).

^1H NMR (300 MHz, $CDCl_3$): δ 3.89 (m, 2H, HO–C**H₂**), 2.28 (m, 1H, C**H**CF_2), 1.60–1.23 (m, 10H, -C**H₂**–), 0.89 (m, 3H,–C**H₃**); ^{13}C NMR (75.5 MHz, $CDCl_3$) δ 131.1, 58.9, 43.8, 31.6, 29.3, 26.9, 23.8, 22.5, 13.9; ^{19}F NMR (282 MHz, $CDCl_3$) δ -81.5 (tt, 3F, *J* =9.6, 2.8 Hz, –C**F₃**), -114.6 (m, 2F, -CHC**F₂**-), -122.5 (dd, 2F, *J* = 15.4, 10.4 Hz, –C**F₂**–), -126.6 (m, 2F, –C**F₂**–). Enantiomeric excess was determined by HPLC after derivatization of the alcohol as its 2-naphthoyl ester (OD-H, heptane/*iso*-propanol 97/3, 0.5mL/min, 254 nm) 8.6 min (major), 10.8 min (minor).[xi]

1.2.4.5 Quantum Yield Determination

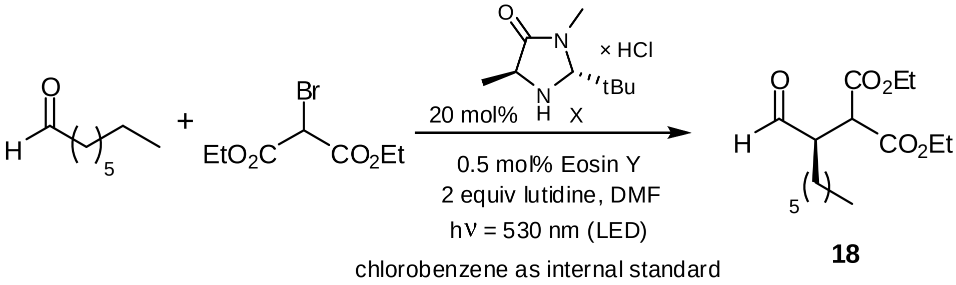

18

A standard fluorescence cuvette was evacuated and set under an atmosphere of nitrogen. (2R,5S)-2-tert-butyl-3,5-dimethylimidazolidin-4-one hydrochloride (17×HCl) (41 mg, 0.197 mmol, 0.2 eq), Eosin Y (2) (3.2 mg, 0.5 µmol, 0.005 eq), diethyl bromomalonate (168 µL, 0.985 mmol, 1 eq), 2,6-lutidine (229 µL, 1.97 mmol, 2 eq), octanal (307 µL, 1.97 mmol, 2 eq), chlorobenzene (103 µL, 0.985 mmol, 1 eq) and 2 mL dry DMF (degassed by "pump-freeze-thaw" cycles prior to use) were mixed in the cuvette under nitrogen atmosphere and light exclusion. The mixture was stirred for 1 minute, 50 µL were taken by a syringe and diluted with 950 µL of dry DMF. A 1 µL sample of this diluted mixture was subjected to GC analysis. The cuvette was irradiated with a LED (Luxeon® Rebel, 1W, 530 nm, 145 lm), the absorbed optical power was measured to Pabs = 21 mW and after 6 h another sample was taken and analyzed by GC as described before. The mixture was stirred for further 6 h under light exclusion and another sample was taken and subjected to GC analysis (vide intra). The yield of 18 after 6 h irradiation was determined as 19%, which corresponds to a quantum yield (Q.Y.) of 9% in correlation to the absorbed optical power.[xii] Under light exclusion a further rise in yield to 21% (+2%) within 6 h was observable.

[xi] D. A. Nagib, M. E. Scott, D. W. C. MacMillan, *J. Am. Chem. Soc.* **2009**, *131*, 10875.

GC (40 °C 1 min, 15.0 °C/min, 250 °C) t_R : = 4.4 min (chlorobenzene), 4.8 min (2,6-lutidine), 6.2 min (octanal), 9.0 min (diethyl bromomalonate), 13.8 min (product)

QY determination: GC of the reaction mixture at before irradiation

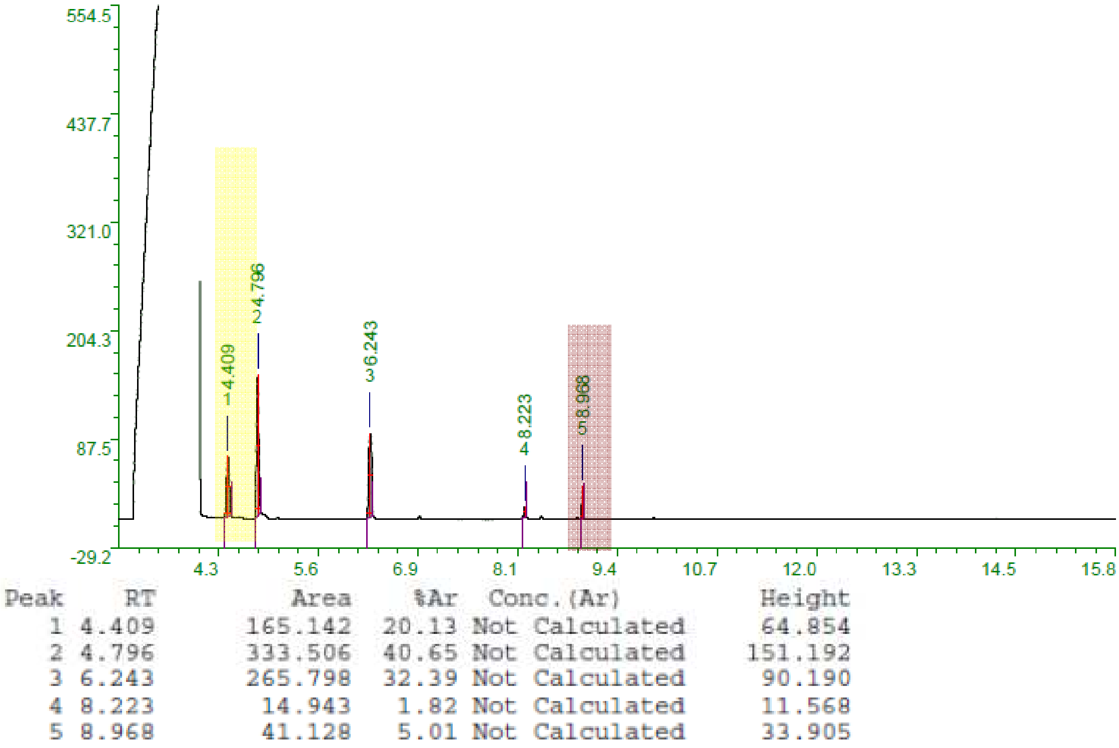

Peak	RT	Area	%Ar	Conc.(Ar)	Height
1	4.409	165.142	20.13	Not Calculated	64.854
2	4.796	333.506	40.65	Not Calculated	151.192
3	6.243	265.798	32.39	Not Calculated	90.190
4	8.223	14.943	1.82	Not Calculated	11.568
5	8.968	41.128	5.01	Not Calculated	33.905

GC (40 °C 1 min, 15.0 °C/min, 250 °C) t_R : = 4.4 min (chlorobenzene, standard), 4.8 min (2,6-lutidine), 6.2 min (octanal), 9.0 min (diethyl bromomalonate), 13.8 min (product)

QY determination: GC of the reaction mixture after 6 h irradiation

---

[xii] Q. Y. = $\frac{n_{product}}{n_{photons_{abs.}}}$, with $n_{photons} = P_{abs} \cdot \Delta t \cdot \lambda$ (here: Δt = 6 h and λ = 530 nm).

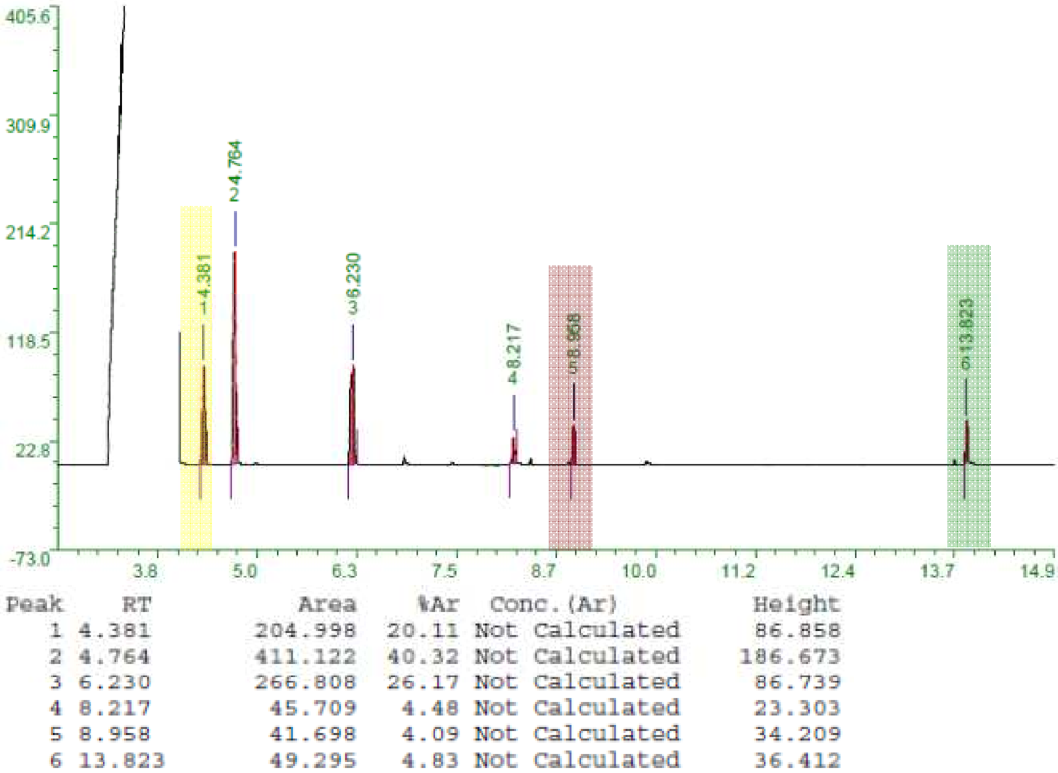

```
Peak    RT          Area    %Ar   Conc.(Ar)          Height
   1 4.381       204.998  20.11 Not Calculated       86.858
   2 4.764       411.122  40.32 Not Calculated      186.673
   3 6.230       266.808  26.17 Not Calculated       86.739
   4 8.217        45.709   4.48 Not Calculated       23.303
   5 8.958        41.698   4.09 Not Calculated       34.209
   6 13.823       49.295   4.83 Not Calculated       36.412
```

Figure 2) Determination of the response factor for the quantum yield determination reaction using chlorobenzene as internal standard (generation of diethyl 2-(1-oxooctan-2-yl)malonate)

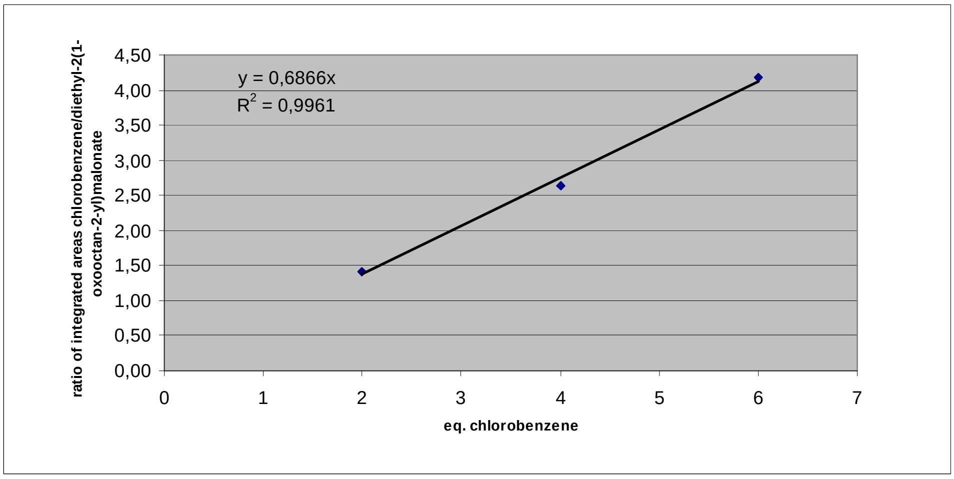

1.2.4.6 UV/VIS Spectra of the Organic Dyes

All spectra were recorded in CH_3CN at a concentration of c = 0.02 mM (with exception of perylene **3**: solvent: CH_2Cl_2, c = 0.002 mM).

Figure 3) UV/VIS spectra of red and orange dyes used as photocatalysts.

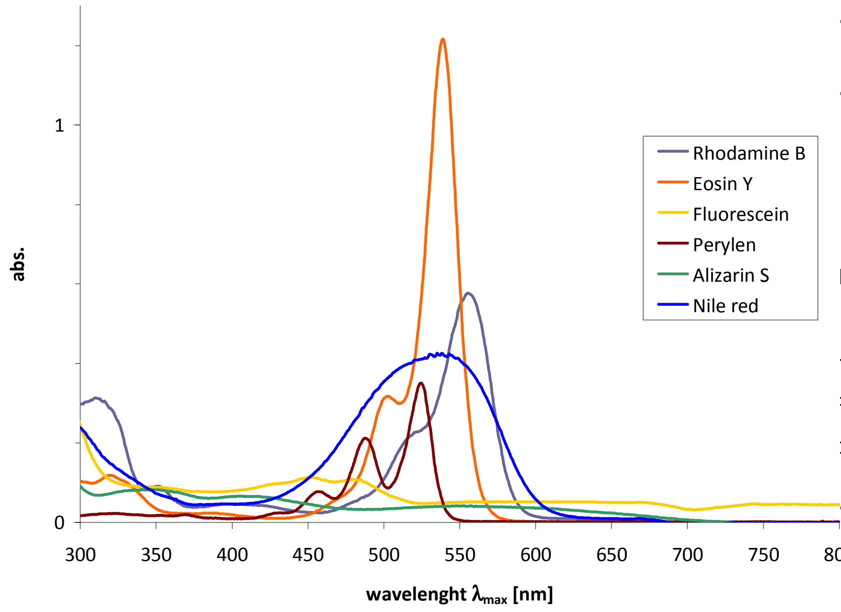

Dye	λ_{max} (nm)	ε ($M^{-1}cm^{-1}$)
luorescein	450	5665
Eosin	539	60803
Perylene	524	175049
lizarin Red	420	3282
Nile Red	543	21298
hodamine B	555	28817
Ru(bpy)$_3$]$^{2+}$	450	25996
py)$_2$(dtb-bpy)]$^+$	416	4920

Figure 4) UV/VIS spectra of Eosin Y (**2**) in comparison with Ru and Ir photocatalysts..

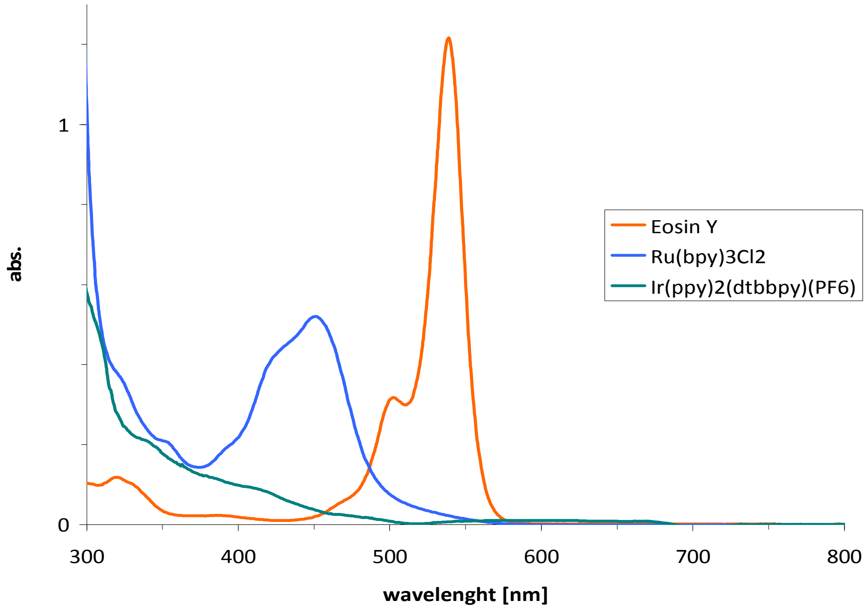

1.2.4.7 Redox Properties of the Photocatalysts and Substrates – Mechanistic Considerations

A postulated mechanism – analog as for $Ru(bpy)_3^{2+}$ – is anticipated to follow two steps where photoexcited Eosin Y first is reductively quenched by a sacrificial amount of enamine (E^0_{ox} = 0.74 V *vs*. SCE; original: E^0_{ox} = 0.72 V *vs.* Ag/Ag$^+$)[xiii], [xiv] resp. an amino radical (E^0 = -0.92 to -1.12 V *vs*. SCE)[xv, xvi]; to furnish the reduced dye species (STEP 1) that now can subsequently react as a strong reductant to allow for the reductive C–Hal bond cleavage of activated halogen derivatives, e.g. *a*-bromo acetophenone (E^0 = -0.49 V *vs.* SCE; ; original: -0.78 V *vs*.- Ag/Ag$^+$ClO$_4^-$)[xvii] or CF$_3$I (E^0 = -1.22 V *vs.* SCE)[xi, xviii] (STEP 2).

Table S1

Dye	E^0(Dye/Dye$^{\bullet\text{⍰}}$) in V *vs.* SCE	E^0(Dye/Dye$^{\bullet\text{⍰}}$) original[a] and ref.
Fluorescein	-1.22	-1.22[S1]
Eosin	-1.06	-1.06[S1]
Perylene	ca. -0.85	-0.6 (NHE)[S2]
Alizarin Red	-0.28	-0.26 (Ag/AgCl)[S3]
Nile Red	-1.02	-1.02[S4]
Rhodamine B	-0.8	-0.8[S5]
$[Ru(bpy)_3]^{2+}$	-1.33	-1.33[S6]
$[Ir(ppy)_2(dtb\text{-}bpy)]^+$	-1.51	-1.51(SCE) [S7a]/-1.89(Fc/Fc$^+$) [S7b]

[a] For a better comparison all values are reported in reference to the SCE electrode. If necessary the original values were converted according to: V. V. Pavlishchuk, A. W. Addison, *Inorg. Chim. Acta* **2000**, *298*, 97-102.

[xiii] N.-N. Bui, X.-H.Ho, S.-i. Mho, H.-Y. Jang, *Eur. J. Chem.* **2009**, 5309-5312.

[xiv] *Note added in proof*: MacMillan *et al.* report a E^0_{ox} = 0.58 V (vs. SCE – original: 0.6 V Ag/AgCl) for the oxidation of an imidazolidinone derived enamine: J. F. Van Humbeck, S. P. Simonovich, R. R. Knowles, D. W. C. MacMillan, *J. Am. Chem. Soc.* **2010**, doi: 10.1021/ja1043006

[xv] D. D. M. Wayner, J. J. Dannenberg, D. Griller, *Chem. Phys. Lett.* **1986**, *131*, 189-191.

[xvi] Alternative data: reduction potential of an pyrrolidine derived iminium ion: E^0= -1.04 V *vs.* SCE (original: E^0= -1.42 V *vs.* Fc/Fc$^+$)*:* A. P. Shaw, B. L. Ryland, M. J. Franklin, J. R. Norton, J. Y.-C. Chen, M. Lynn Hall, *J. Org. Chem.* **2008**, *73*, 9668–9674.

[xvii] D. D. Tanner, H. K. Singh, *J. Org. Chem.* **1986**, *51*, 5182-5186.

[xviii] Y. Y. Volodin, A. A. Stepanov, L. I. Denisovich, V. A. Grinberg, *Russ. J. Electrochem.* **2000**, *36*, 1160-1162.

S1 T. Lazarides, T. McCormick, P. Du, G. Luo, B. Lindley, R. Eisenberg, *J. Am. Chem. Soc.* **2009**, *131*, 9192-9194.

S2 C. Wagner, Doctoral Thesis, TU München **2006**.

S3 H.-P.Dai, K.-K. Shiu, *Electrochim. Acta* **1998**, *43*, 2709-2715.

S4 N. A. Kuznetsova, V. I. Alekseeva,O. L. Kaliya, A. A. Engovatov, E. A. Luk'yanets, L. E. Marinina,T. I. Maksakova, *J. Appl. Spectroscopy Engl.* **1980**, *32*, 333-337.

S5 a) G. Pelzer, E. De Pauw, D. Viet Dung, J. Marient, *J. Phys. Chem.***1984**, *88*, 5065-5068; b) N. O. Mchedlov-Petrossyan, V. I. Kukhtik, V. D. Bezugliyz, *J. Phys. Org. Chem.* **2003**, *16*, 380-397.

S6 a) in CH_3CN: C. R. Bock, J. A. Connor, A. R. Gutierrez, T. J. Meyer, D. G. Whitten, B. P. Sullivan, J. K. Nagle, *J. Am. Chem. Soc.* **1979**, *101*, 4815-4824; b) in H_2O: S. Campagna, F. Puntoriero, F. Nastasi, G. Bergamini, V. Balzani, *Top. Curr. Chem.* **2007**, *280*, 117-214.

S7 a) D. A. Nagib, M. E. Scott, D. W. C. MacMillan, *J. Am. Chem. Soc.* **2009**, *131*, 10875-10877; b) A. B. Tamayo, S. Garon, T. Sajoto, P. I. Djurovich, I. M. Tsyba, R. T. Bau, M. E. Thompson, *Inorg. Chem.* **2005**, *44*, 8723-8732.

For a very rough estimation of redox potential e. g. the oxidative power of the dye´s excited states, its E_{00} energy also needs to be considered, following this equation:

$$E^0(D^*/D^{\bullet -}) = E^0(D/D^{\bullet -}) + E_{00}$$

The following scheme shows the comparative redox values for photoexcited Ru^{2+} ($E_{00}(Ru^{2+})$ = 2.12 eV)[S6] and Eosin Y (E_{00} (^3EY) = 1.89 eV)[xix] in modified Latimer diagrams.

Scheme 1: Comparison of redox properties in CH_3CN

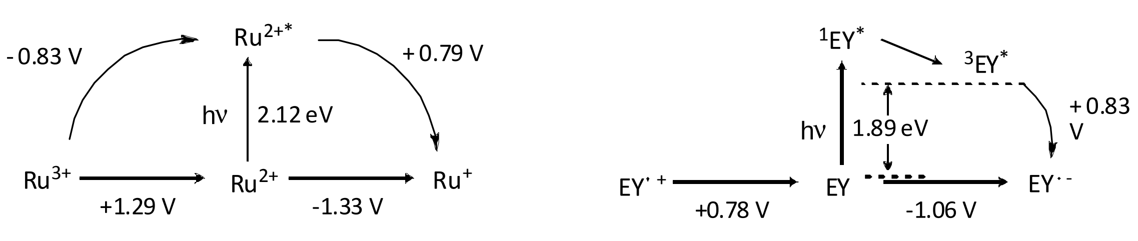

$[Ru(bpy)_3]^{2+}$ Eosin Y

[xix] A. W.-H. Mau, O. Johansen, O. Sasse, *Photochem. Photobiol.* **1985**, *41*, 503-509.

1.2.4.8 ^{1}H, ^{13}C and ^{19}F NMR Spectra of Products

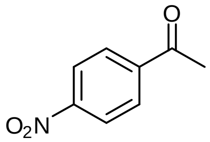

12

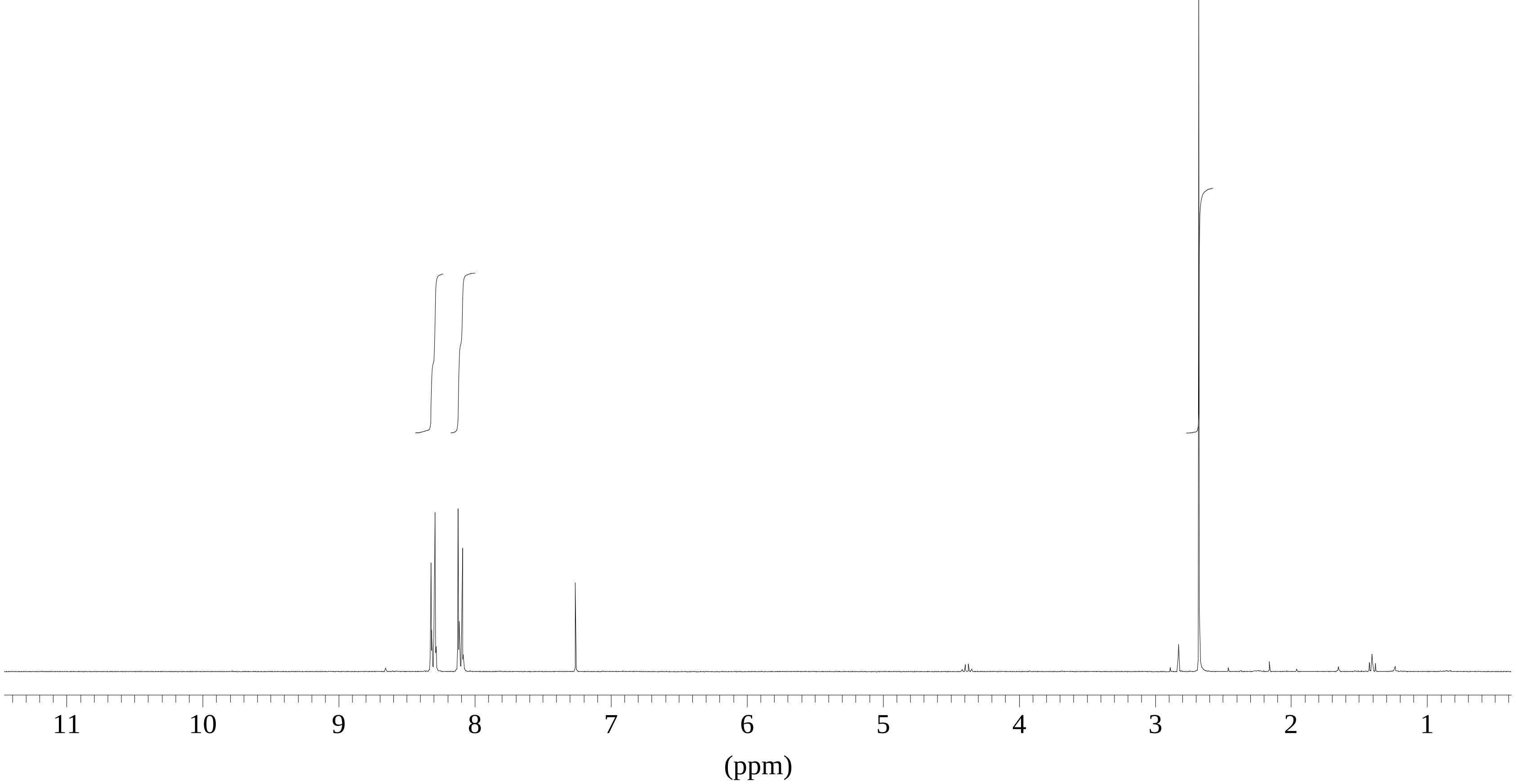

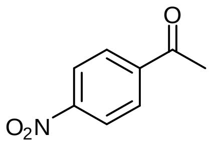

12

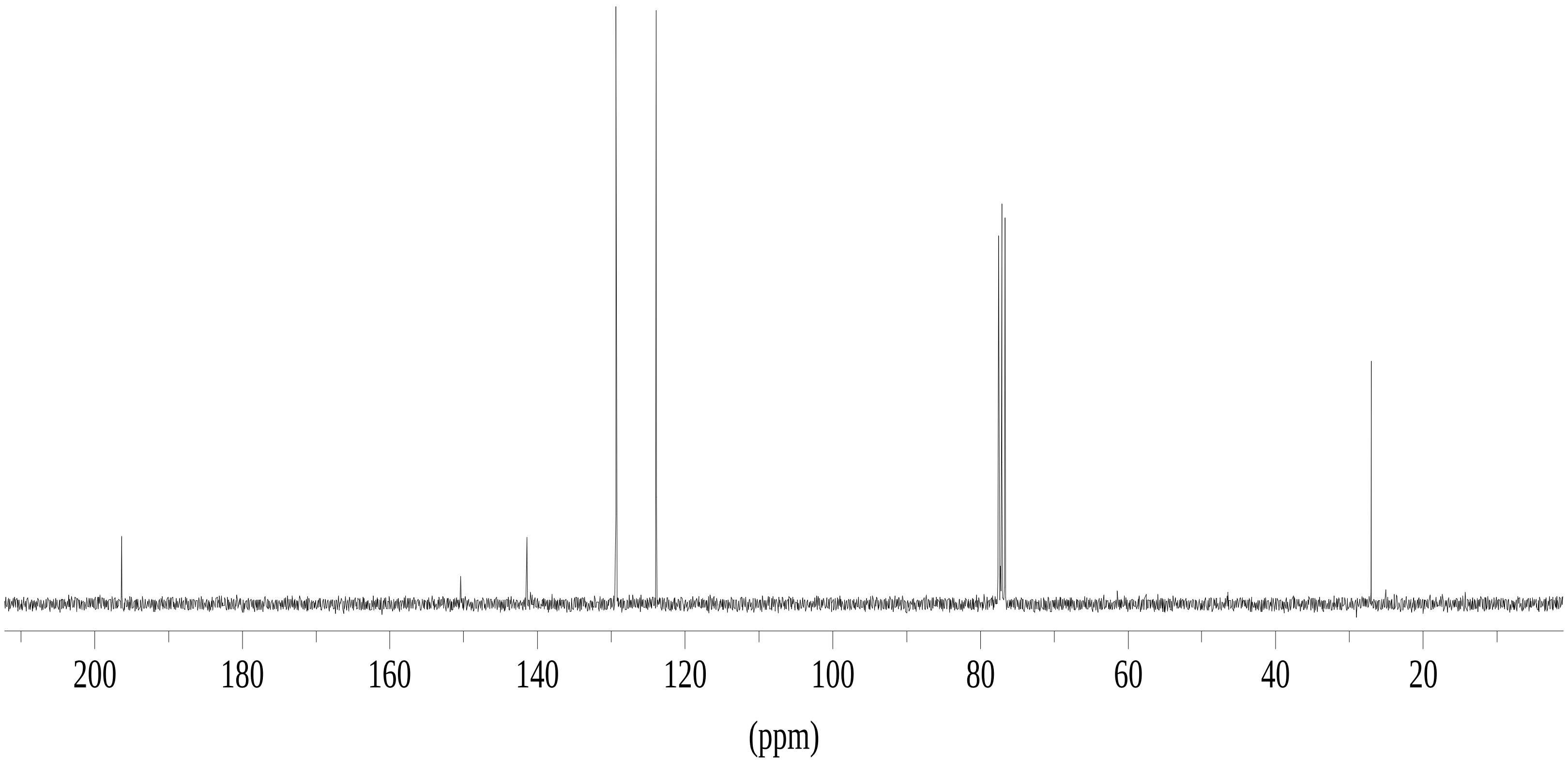

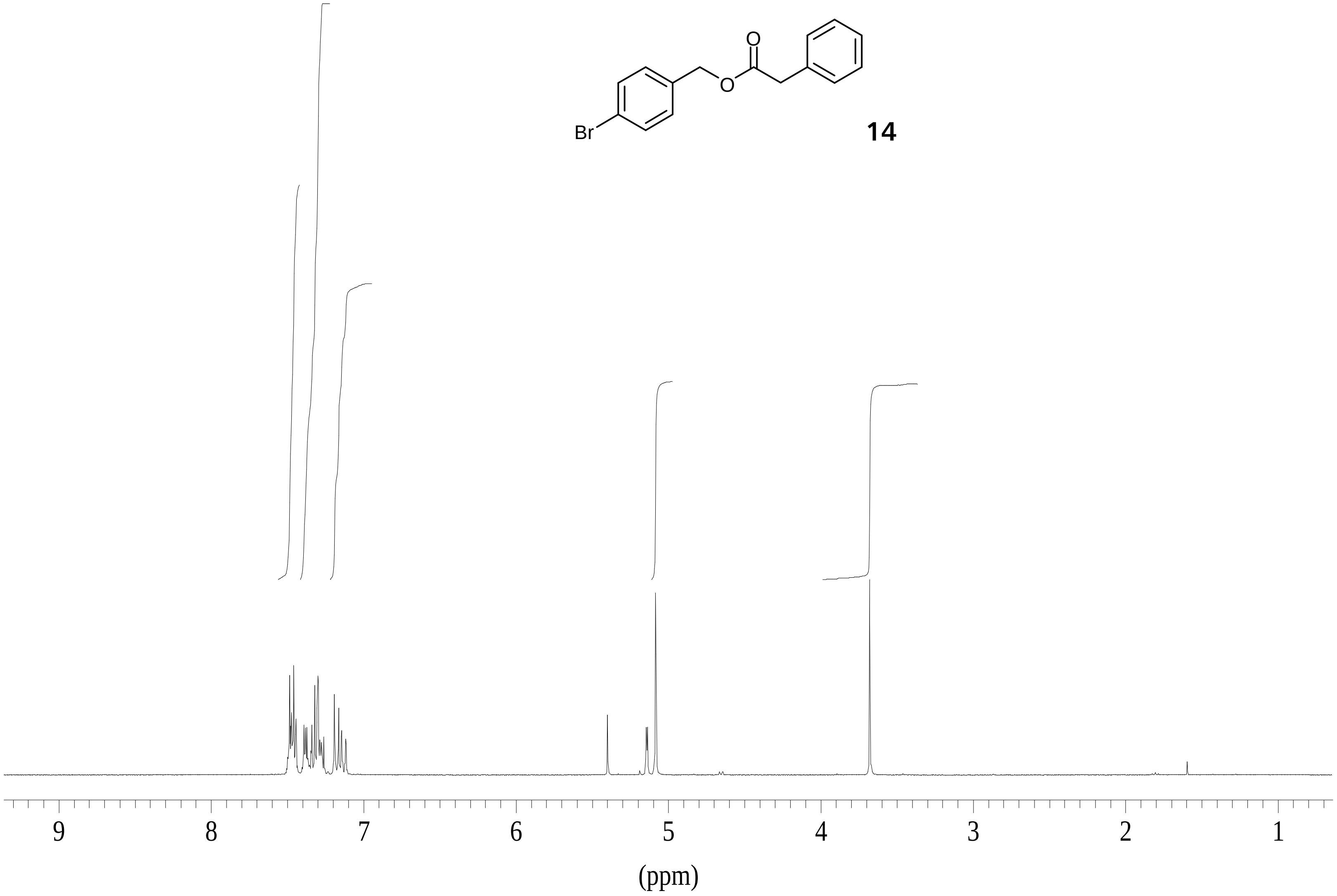

14

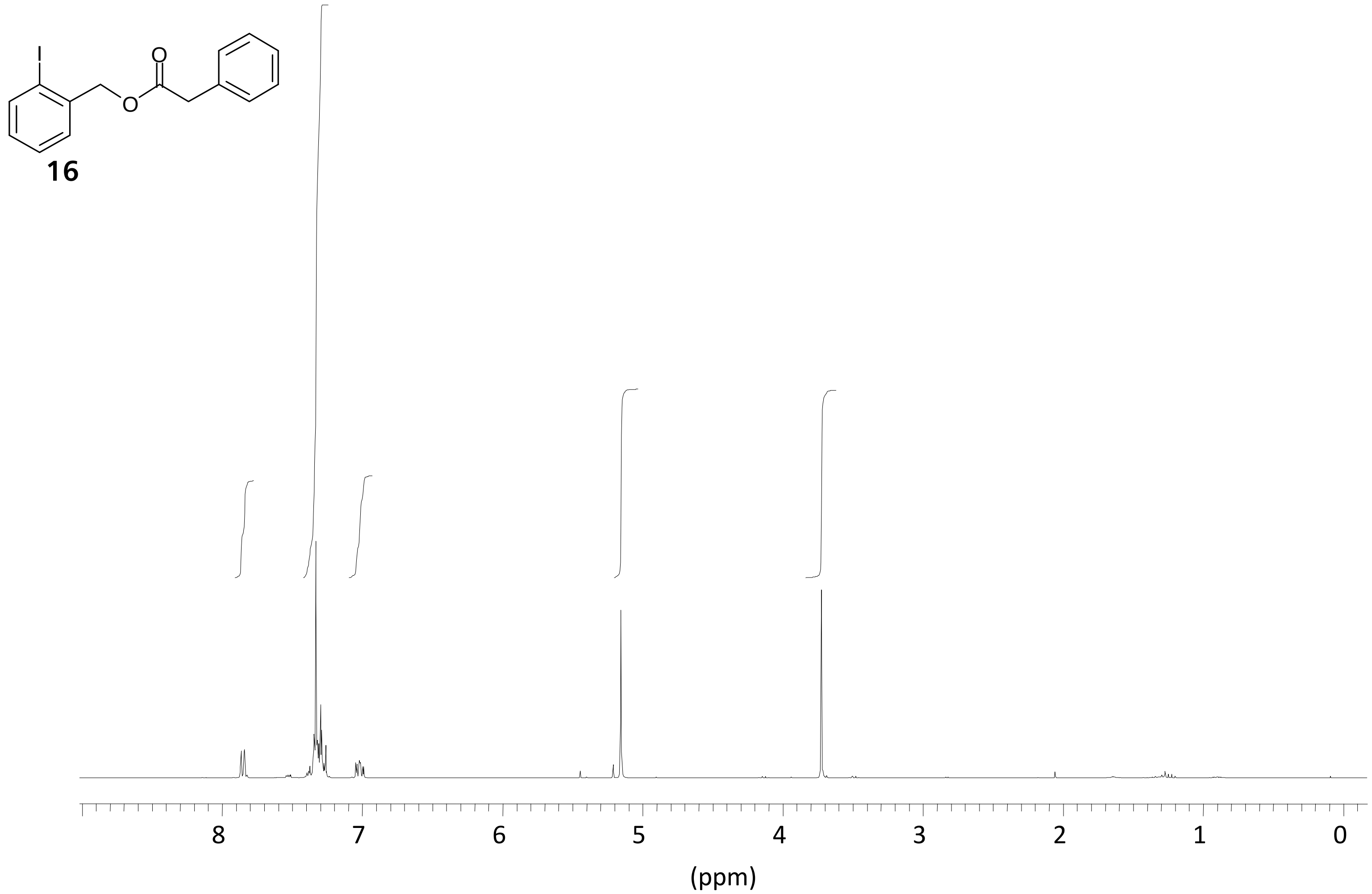

16

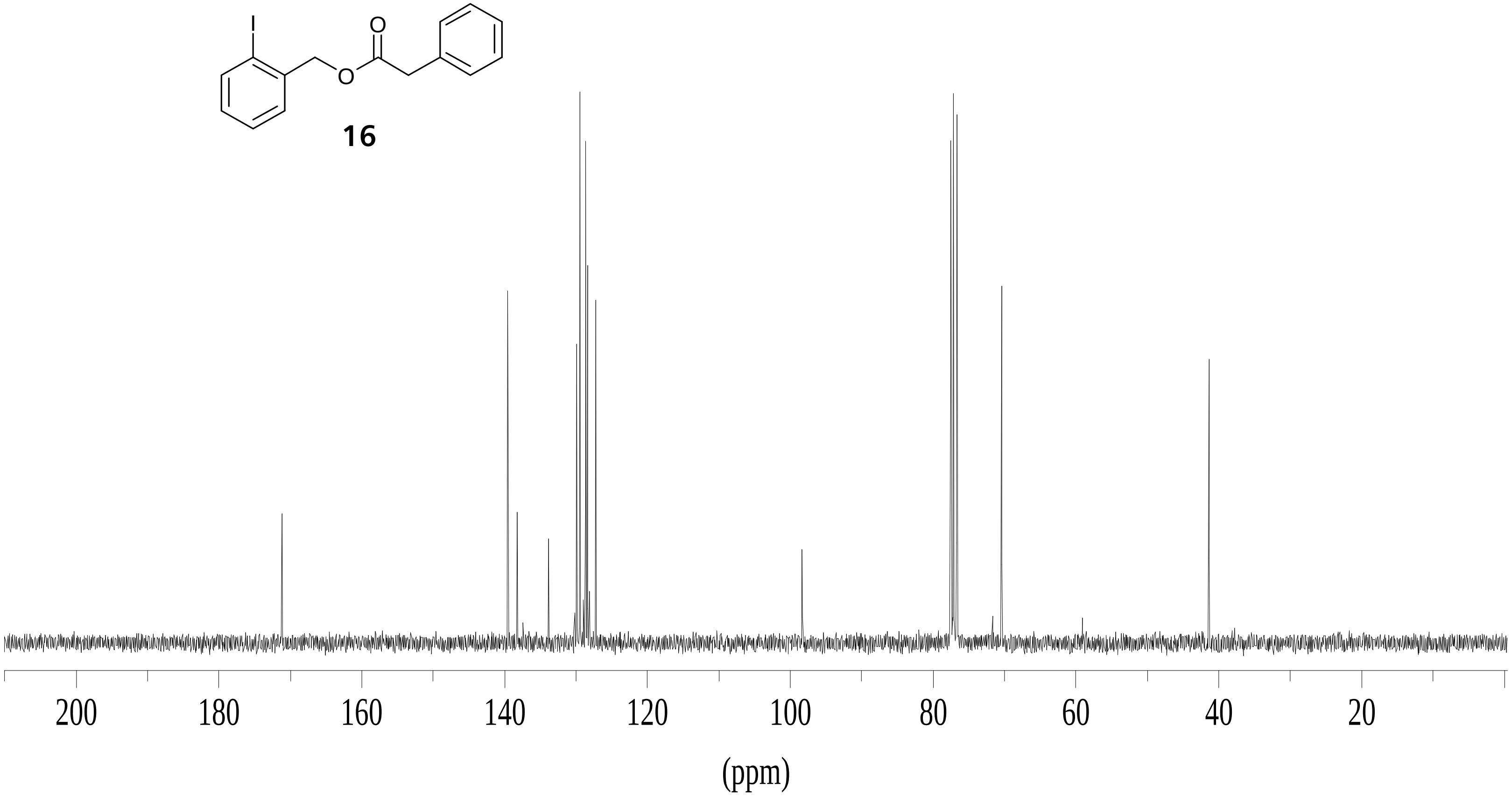

16

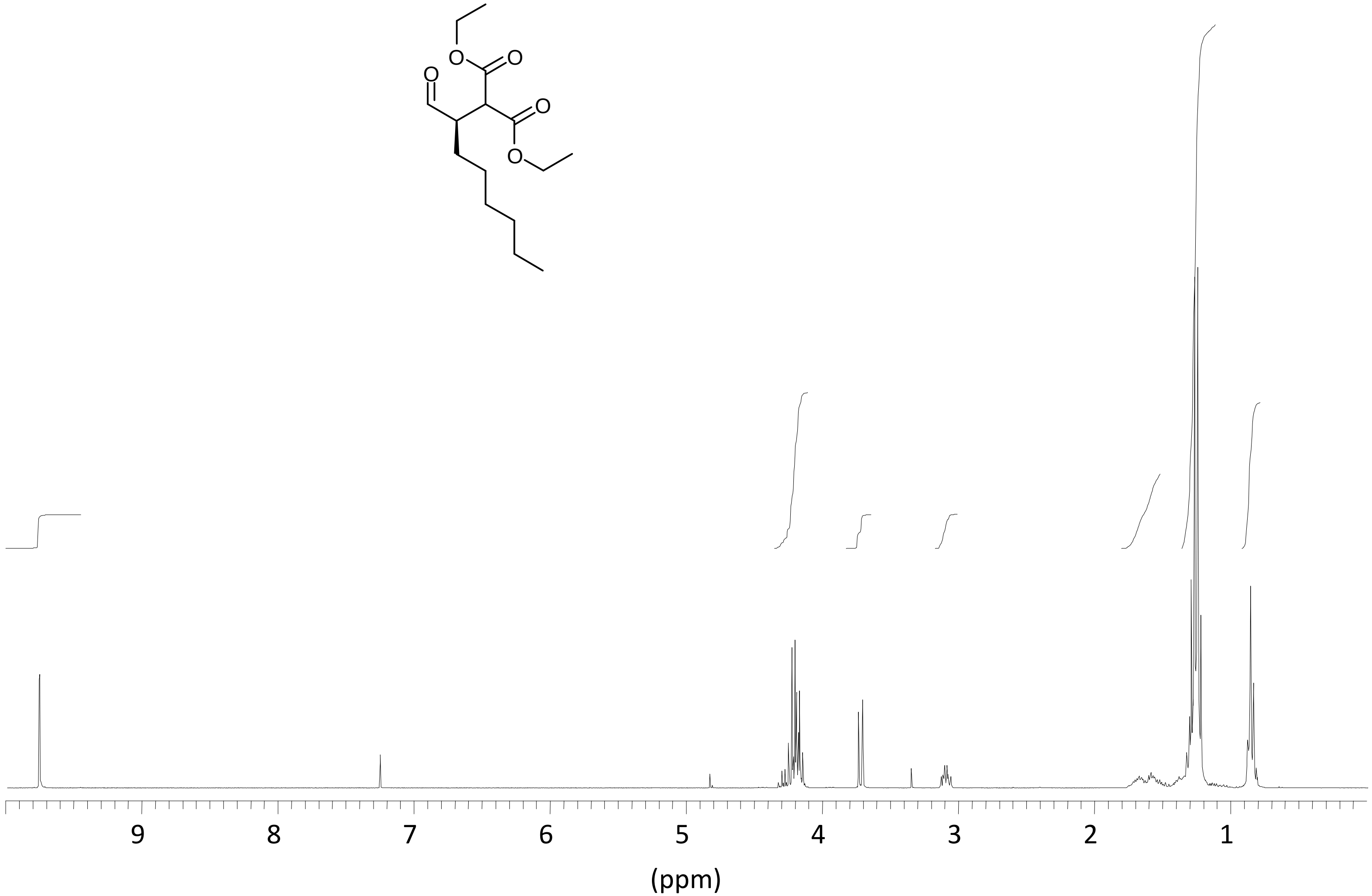
O
O
O
O
O
O
9
8
7
6
5
4
3
2
1
(ppm)

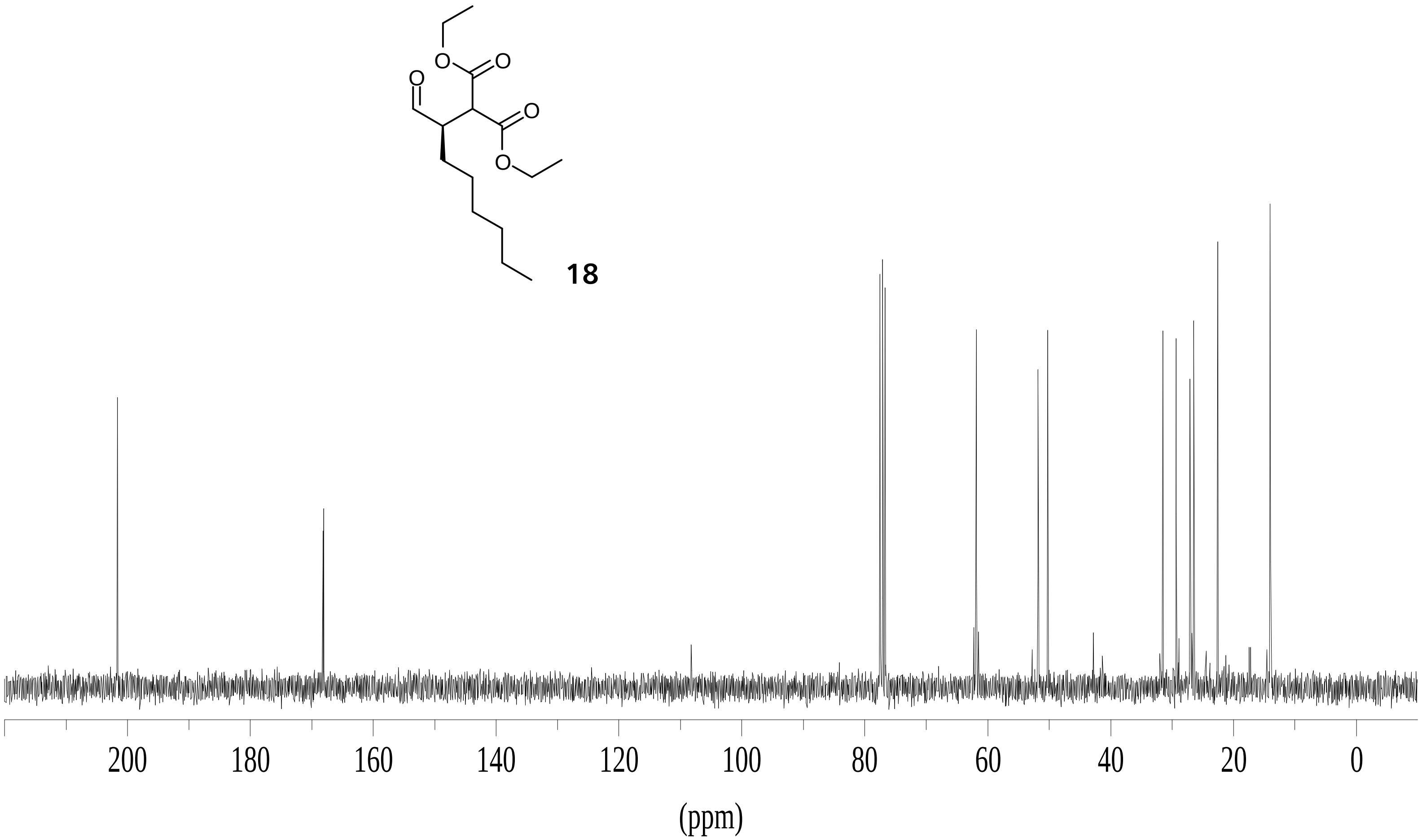

18

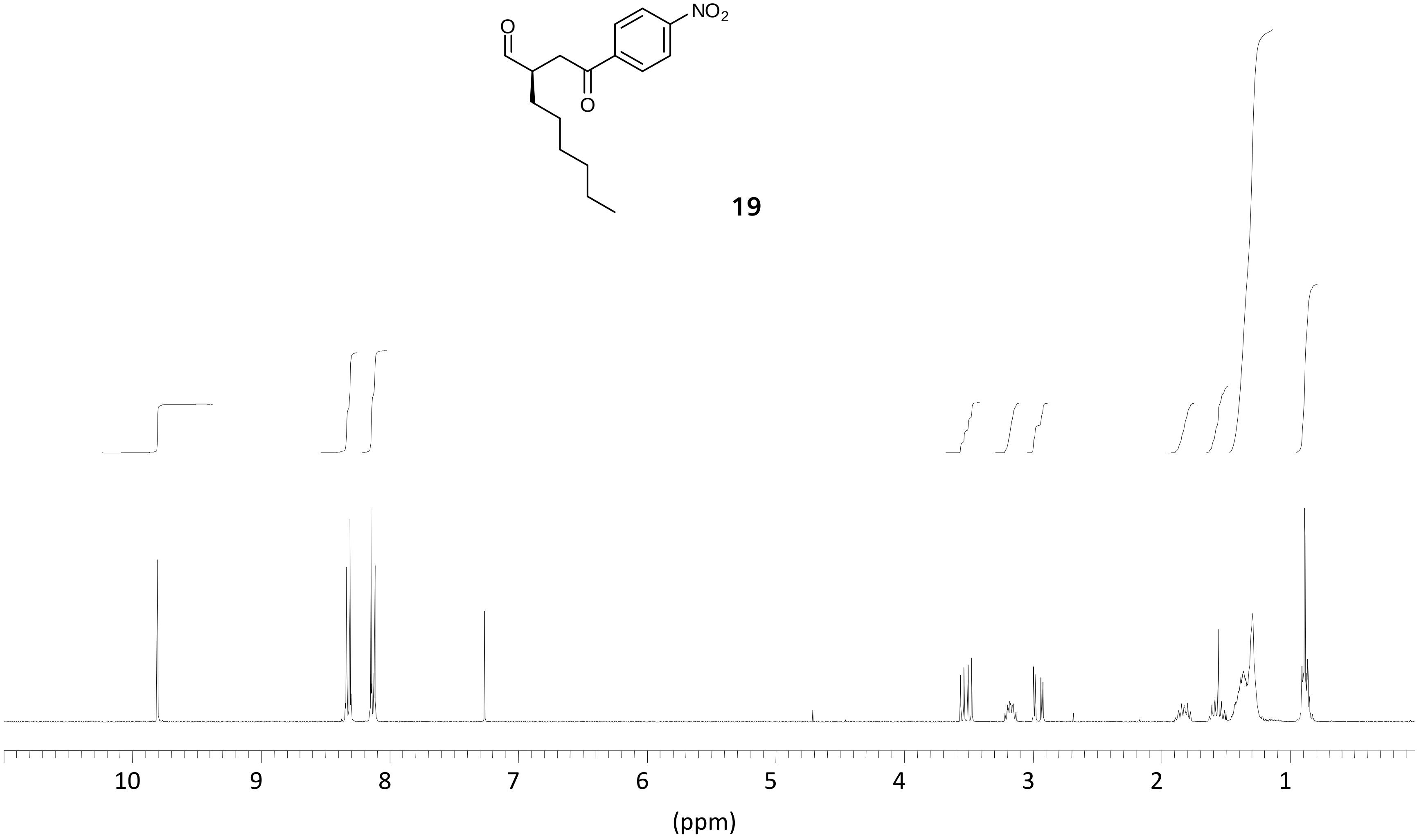

19

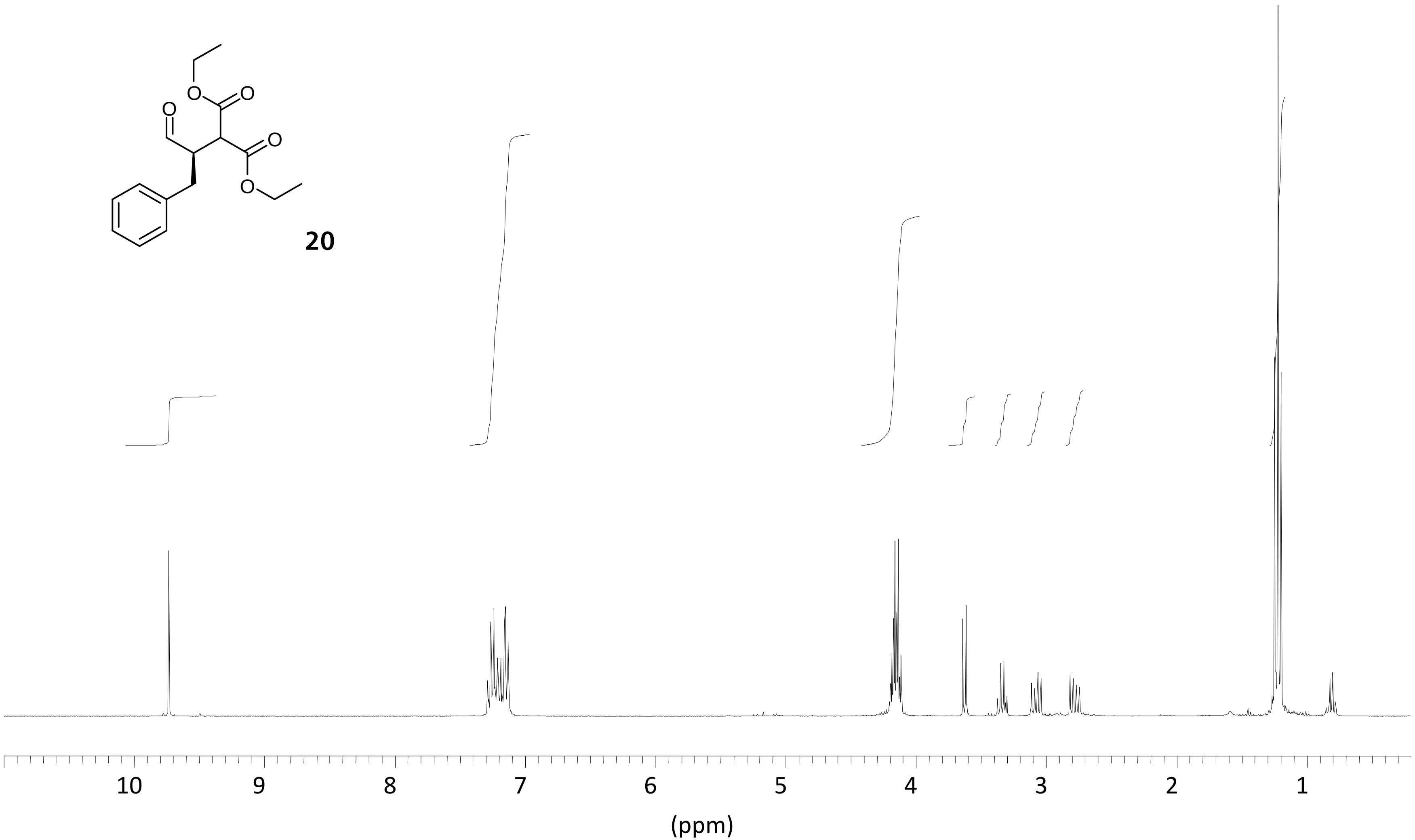
20
10
9
8
7
6
5
4
3
2
1
(ppm)

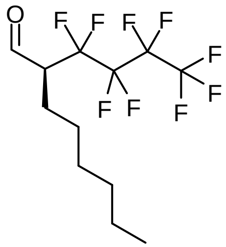
O
F
F
F
F
F
F
F
F
F

21

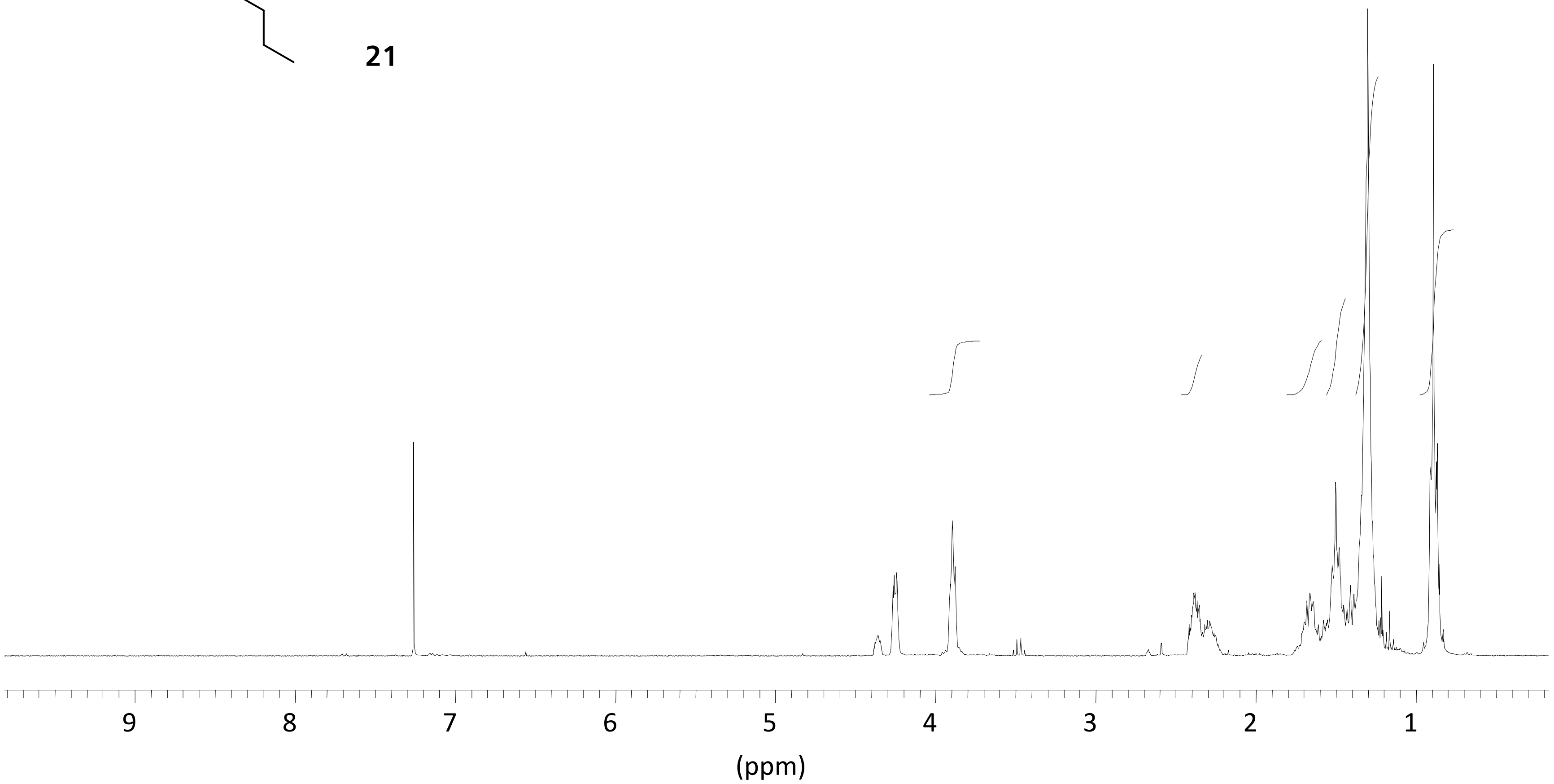

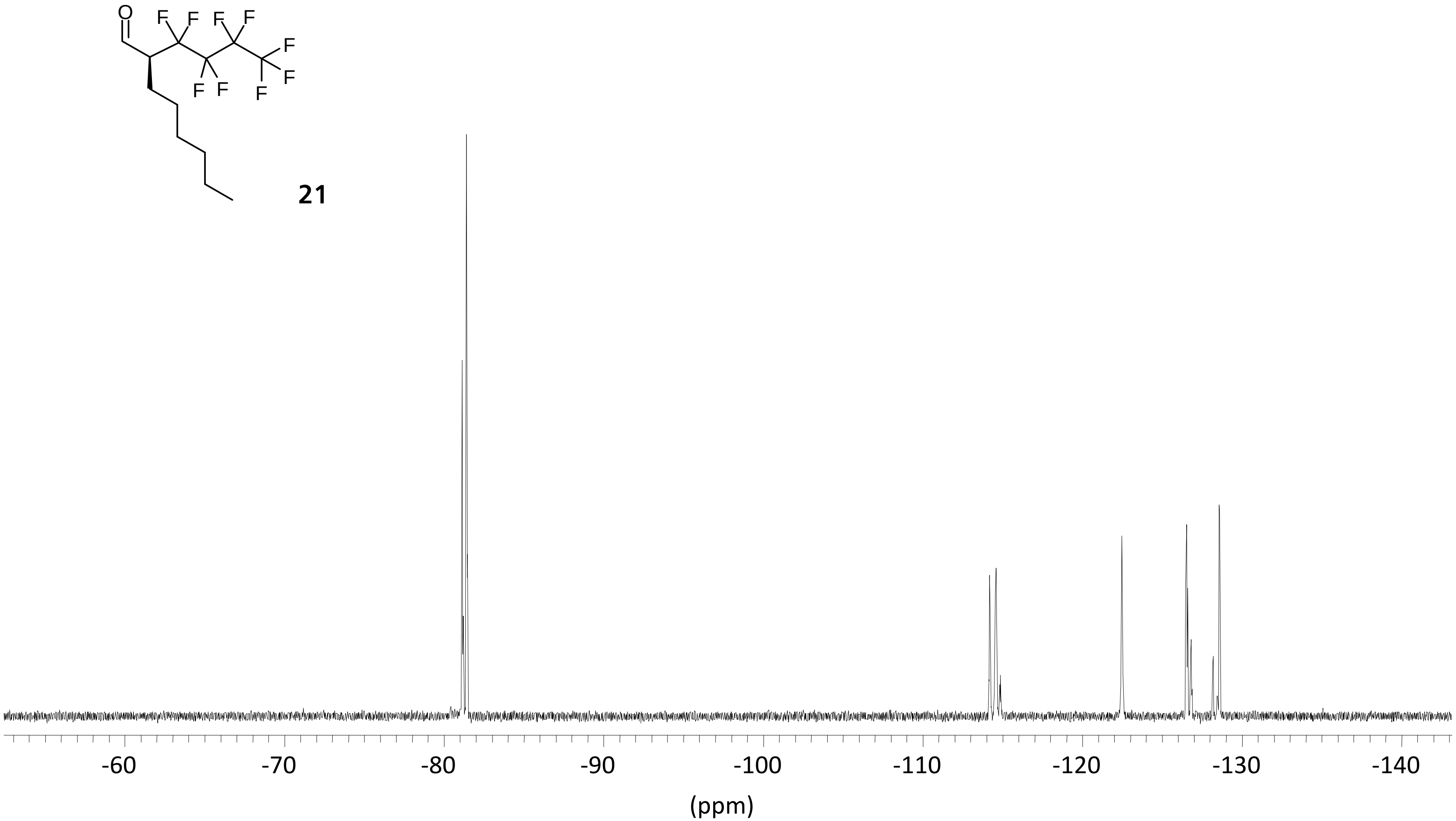

21

1.2.5 References

[1] For recent reviews on organocatalysis, see: a) A. Dondoni, A. Massi, *Angew. Chem.* **2008**, *120*, 4716-4739; *Angew. Chem. Int. Ed.* **2008**, *47*, 4638-4660; b) D. W. C. MacMillan, *Nature* **2008**, *455*, 304-308; c) special issue on organocatalysis: *Chem. Rev.* **2007**, *107* (12), 5413-5883; d) special issue on organocatalysis: *Acc. Chem. Res.* **2004**, *37* (8), 487-631; e) special issue on organocatalysis: *Adv. Synth. Catal.* **2004,** *346* (9/10), 1007-1249; f) J. Seayad, B. List, *Org. Biomol. Chem.* **2005**, *3*, 719-724; g) A. Berkessel, H. Gröger, *Asymmetric Organocatalysis*, WILEY-VCH, Weinheim, **2005**; h) P. I. Dalko, *Enantioselective Organocatalysis*, WILEY-VCH, Weinheim, **2007**.

[2] For some selected recent applications, see: a) H. Ishikawa, T. Suzuki, Y. Hayashi, *Angew. Chem.* **2009**, *121*, 1330-1333; *Angew. Chem. Int. Ed.* **2009**, *48*, 1304-1307; b) B.-C. Hong, P. Kotame, C.-W. Tsai, J.-H. Liao, *Org. Lett.* **2010**, *12*, 776-779; c) P. Jakubec, D. M. Cockfield, D. J. Dixon, *J. Am. Chem. Soc.* **2009**, *131*, 16632-16633; d) Review: R. M. de Figueiredo, M. Christmann, *Eur. J. Org.Chem.* **2007**, 2575-2600.

[3] a) C. Grondal, M. Jeanty, D. Enders, *Nature Chem.* **2010**, *2*, 167-178; b) D. Enders, C. Grondal, M. R. M. Hüttl, *Angew. Chem.* **2007**, *119*, 1590-1601; *Angew. Chem. Int. Ed.* **2007**, *46*, 1570-1581; c) L. F. Tietze, G. Brasche, K. Gerike, *Domino Reactions in Organic Chemistry*, Wiley-VCH, Weinheim, **2006**.

[4] a) J. Zhou, *Chem. Asian J.* **2010**, *5*, 422-434; b) C. Zhong, X. Shi, *Eur. J. Org. Chem.* **2010**, doi: 10.1002/ejoc.201000004; c) Z. Shao, H. Zhang, *Chem. Soc. Rev.* **2009**, *38* 2745-2755.

[5] a) K. Zeitler, *Angew. Chem.* **2009**, *121*, 9969-9974; *Angew. Chem. Int. Ed.* **2009**, *48*, 9785-9789; b) D. Ravelli, D. Dondi, M. Fagnoni, A. Albini, *Chem. Soc. Rev.* **2009**, *38*, 1999-2011.

[6] a) M. Ishikawa, S. Fukuzumi, *J. Am. Chem. Soc.* **1990**, *112*, 8864-8870; b) S. Fukuzumi, S. Mochizuki, T. Tanaka, *J. Chem. Soc. Perkin 2* **1989**, 1583-1589; c) S. Fukuzumi, S. Mochizuki, T. Tanaka, *J. Phys. Chem.* **1990**, *94*, 122-126; d) G. Pandey, S. Hajra, *Angew. Chem.* **1994**, *106*, 1217-1218; *Angew. Chem. Int. Ed.* **1994**, *33*, 1169-1171; e) G. Pandey, M. K. Ghorai, S. Hajra, *Pure Appl. Chem*. **1996**, *68*, 653-658.

[7] a) A. G. Condie, J. C. González-Gómez, C. R. J. Stephenson, *J. Am. Chem. Soc.* **2010**, *132*, 1464-1465; b) J. W. Tucker, J. M. R. Narayanam, S. W. Krabbe, C. R. J. Stephenson, *Org. Lett.* **2010**, *12*, 368–371; c) J. Du, T. P. Yoon, *J. Am. Chem. Soc.* **2009**, *131*, 14604-14605; d) M. A. Ischay, M. E. Anzovino, J. Du, T. P. Yoon, *J. Am. Chem. Soc.* **2008**, *130*, 12886-12887; e) T. Koike, M. Akita, *Chem. Lett.* **2009**, *38*, 166-167.

[8] a) D. A. Nicewicz, D. W. C. MacMillan, *Science* **2008**, *322*, 77-80; b) D. A. Nagib, M. E. Scott, D. W. C. MacMillan, *J. Am. Chem. Soc.* **2009**, *131*, 10875-10877.

[9] For a pioneering example in intramolecular organocatalytic asymmetric alkylation: a) N. Vignola, B. List, *J. Am. Chem. Soc.* **2004**, *126*, 450-451; for intramolecular examples within domino processes, see: b) D. Enders, C. Wang, J. W. Bats, *Angew. Chem.* **2008**, *120*, 7649-7653; *Angew. Chem. Int. Ed.* **2008**, *47*, 7539-7542; c) H. Xie, L. Zu, H. Li, J. Wang, W. Wang, *J. Am. Chem. Soc.* **2007**, *129*, 10886-10894; d) R. Rios, H. Sundén, J. Vesely, G.-L. Zhao, P. Dziedzic, A. Córdova, *Adv. Synth. Catal.* **2007**, *34**9***, 1028-1032.

[10] For recent examples relying on the use of stabilized carbocations as compatible electrophiles: a) R. R. Shaikh, A. Mazzanti, M. Petrini, G. Bartoli, P. Melchiorre, *Angew. Chem.* **2008**, *120*, 8835-8838; *Angew. Chem. Int. Ed.* **2008**, *47*, 8707-8710; b) P. G. Cozzi, F. Benfatti, L. Zoli, *Angew. Chem.* **2009**, *121*, 1339-1342; *Angew. Chem. Int. Ed.* **2009**, *48*, 1313-1316; c) L. Zhang, L. Cui, X. Li, J. Li, S. Luo, J.-P. Cheng, *Chem. Eur. J.* **2010**, *16*, 2045-2049.

[11] For a recent review on catalytic asymmetric α-alkylations, see: A.-N. Alba, M. Viciano, R. Rios, *ChemCatChem* **2009**, *1*, 437-439.

[12] Considering a reductive quenching of the dyes´s photoexcited state **Dye*** to **Dye**$^{\bullet ▯}$ by an available electron donating species (*vide infra*) all the displayed dyes apart from Alizarin Red

S (**4**) have been shown to be potent reductants (c. f. redox potentials E^0) that should allow for cleaving the C–Hal bond to furnish the electron deficient radical by SET to the activated ⍰-bromocarbonyl compound.

[13] J. M. R. Narayanam, J. W. Tucker, C. R. J. Stephenson, *J. Am. Chem. Soc.* **2009**, *131*, 8756-8757.

[14] M. Zhang, C. Chen, W. Ma, J. Zhao, *Angew. Chem.* **2008**, *120*, 9876-9879; *Angew. Chem. Int. Ed.* **2008**, *47*, 9730-9733.

[15] a) J. Moser, M. Grätzel, *J. Am. Chem. Soc.* **1984**, *106*, 6557-6564; for recent reviews, see: b) Y. Ooyama, Y. Harima, *Eur. J. Org. Chem.* **2009**, 2903-2934; c) A. Mishra, M. K. R. Fischer, P. Bäuerle, *Angew. Chem.* **2009**, *121*, 2510-2536; *Angew. Chem. Int. Ed.* **2009**, *48*, 2474-2499.

[16] For a better comparison all values are reported in reference to the SCE electrode. If necessary the orginal values were converted according to: V. V. Pavlishchuk, A. W. Addison, *Inorg. Chim. Acta* **2000**, *298*, 97-102; see Supporting information for details and references.

[17] The reaction can also be conducted under the light of a 23 W fluorescent bulb; see also ref 21. High power LEDs applied for photocatalysis (e.g. Philips LUXEON® Rebel 1W) show high color fidelity (λ = 530±10 nm) and a radiometric power of ca. 145 lm.

[18] See Supporting information for details.

[19] In a number of comparative studies using xanthene dyes as photoinitiators Eosin Y has demonstrated to counterbalance high reactivity with sufficient stability. For selected examples, see: a) T. Lazarides, T. McCormick, P. Du, G. Luo, B. Lindley, R. Eisenberg, *J. Am. Chem. Soc.* **2009**, *131*, 9192-9194; b) M. V. Encinas, A. M. Rufs, S. G. Bertolotti, C. M. Previtali, *Polymer* **2009**, *50***,** 2762-2767; c) S. H. Lee, D. H. Nam, C. B. Park, *Adv. Synth. Cat.* **2009**, *351*, 2589-2594.

[20] Price per mmol and molecular weight of different photocatalysts: $[Ru(bpy)_3]Cl_2\times6H_2O$ (MW = 748.62 gmmol^{-1}): \$62.50; $[Ir(ppy)_2(dtb\text{-}bpy)]PF_6$ (MW = 1072.09 gmmol^{-1}): ca. \$630 (single step synthesis from commercial $[Ir(ppy)_2Cl]_2$ with 2 eq dtb-bpy); Eosin Y (MW = 647.89 gmmol^{-1}): \$2.66 (based on Sigma-Aldrich resp. Acros pricing for 2010).

[21] In our hands using in Germany available household fluorescent bulbs (e. g. OSRAM®, 23 W, 6500 K, 1470 lm) we also could not reach full conversion in the time span reported by MacMillan and co-workers[8a] using their optimized $[Ru(bpy)_3]^{2+}$ conditions (see Table 3, entry 3).

[22] M. Amatore, T. D. Beeson, S. P. Brown, D. W. C. MacMillan, *Angew. Chem.* **2009**, *121*, 5223-5226; *Angew. Chem. Int. Ed.* **2009**, *48*, 5121-5124.

[23] For the seminal report on enantioselective trifluormethylation of aldehydes via photoredox catalysis see ref. 8b. A mechanistically different non-photolytic (closed-shell) approach merging organocatalysis with iodonium salts was published only recently: A. E. Allen, D. W. C. MacMillan, *J. Am. Chem. Soc.* **2010**, *132*, 4986-4987.

[24] The efficient formation of long-lived triplet states following photoexcitation *via* ISC is facilitated by the heavy atom effect (increased spin-orbit-mixing; Br substituents): a) T. Shimidzu, T. Iyoda, Y. Koide, *J. Am. Chem. Soc.* **1985**, *107*, 35-41; b) D. C. Neckers, O. M. Valdes-Aguilera, *Adv. Photochem.* **1993**, *18*, 315-394.

[25] For a discussion on reductive vs. oxidative properties of the excited $^3EY^*$, see ref. 19a. For selected recent examples on reductive resp. oxidative quenching, see: a) F. Labat, I. Ciofini, H. P. Hratchian, M. Frisch, K. Raghavachari, C. Adamo, *J. Am. Chem. Soc.* **2009**, *131*, 14290–14298; b) M. A. Jhonsi, A. Kathiravan, R. Renganathan, *J. Mol. Struct.* **2009**, *921*, 279–284.

[26] The high energy intermediate of Eosin Y $\mathbf{^3EY^*}$ can function as an oxidant, showing similar redox properties as for photoexcited $[Ru(bpy)_3]^{2+*}$: cf. $E^0(^3EY^*/EY^{\bullet}$⍰$)$ = +0.83 V *vs*. $E^0(Ru^{2+*}/Ru^+)$ = +0.79 V *vs* . SCE; see Supporting information for details.

[27] Remarkably, in contrast to the majority of other photocatalytic processes the system of MacMillan does not require any sacrificial oxidant or reductant by its design; both oxidation and reduction step are productive and lead to the formation of the desired product.

[28] For a recent discussion on the normalization of photocatalytic reactions, see: T. Maschmeyer, M. Che, *Angew. Chem.* **2010**, *122*, 1578-1582; *Angew. Chem. Int. Ed.* **2010**, *49*, 1536-1539.

1.3 Visible light Promoted Stereoselective Alkylation by Combining Heterogeneous Photocatalysis with Organocatalysis[i]

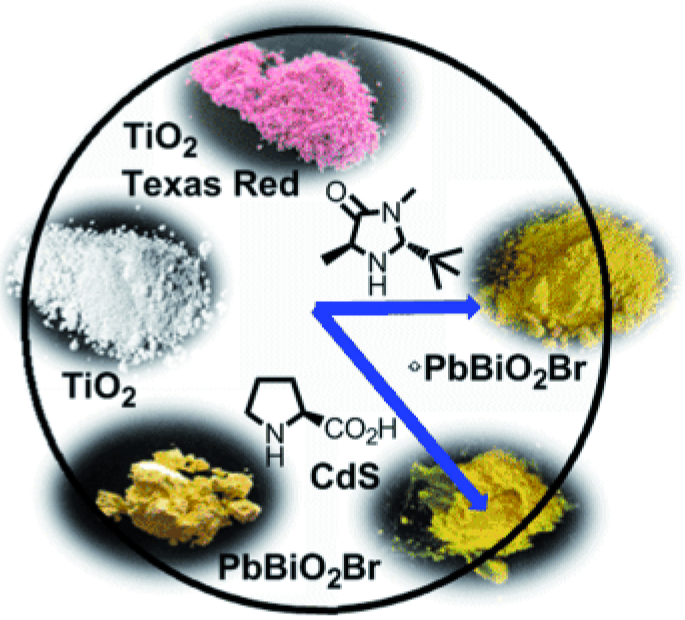

Dream team: Heterogeneous inorganic semiconductors and chiral organocatalysts team up for the stereoselective photocatalytic formation of carbon–carbon bonds. However, the connection between the organic and inorganic catalysts should not be too tight: Covalent immobilization inactivates the system.[ii]

---

[i] Reproduced with permission from: M. Cherevatskaya,M. Neumann, S. Füldner, C. Harlander, S. Kümmel, S. Dankesreiter, A. Pfitzner, K. Zeitler, B. König, *Angew. Chem. Int. Ed*. **2012**, 51, 4062. Copyright 2012 Wiley-VCH

[ii] The synthesis of azide-functionalized Imidazolidinone catalyst and all catalytic Mannich reactions were performed by M.Neumann

1.3.1 Introduction

The application of sensitizers to utilize visible light for chemical reactions is known for long.[1] Several recent publications[2] have impressively demonstrated the versatile use of visible light for various transformations, such as the conversion of alcohols to alkyl halides,[3] [2+2],[4] [3+2][5] and [4+2][6]-cycloadditions or carbon-carbon[7] and carbon-heteroatom bond formations.[8] The cooperative merger of organocatalysis with visible light photoredox catalysis using ruthenium- or iridium metal complexes[9] or organic dyes[9d] as photocatalysts allows for an expansion to enantioselective reactions.[10] Although organic semiconductors, such as titanium dioxide, have been widely used in the photocatalytic degradation of organic waste,[11] the number of examples in which they photocatalyze bond formation in organic synthesis is still limited.[12] Kisch[13] explored CdS mediated bond formations and oxidative C-C coupling reactions with titanium dioxide[14] are known. However, bond formations on heterogeneous photocatalysts typically proceed without control of the stereochemistry and mixtures of isomers are obtained.[15,16] We demonstrate in this work that the combination of stereoselective organocatalysis with visible light heterogeneous photoredox catalysis allows for the stereoselective formation of carbon-carbon bonds in good selectivity and yield. The approach combines the advantages of heterogeneous catalysis, as robust, simple and easy to separate catalyst material, with the stereoselectivity achieved in homogeneous organocatalysis.[17,18]

1.3.2 Results and Discussion

The enantioselective α-alkylation of aldehydes developed by MacMillan *et al.*[9a] was selected as a test reaction to apply inorganic heterogeneous photocatalysts (Table 1). Five semiconductors were used: Commercially available white TiO_2 (**1**),[19] the same material covalently surface modified with a Phos-Texas Red dye increasing the visible light absorption (Phos-Texas-Red-TiO_2, **2**), yellow $PbBiO_2Br$, which absorbs blue light, as *bulk* material (**3**) and in nano-crystalline form (**4**). TiO_2 (**1**) with an average particle size of 21 nm is a stable and inexpensive semiconductor with a band gap of 3.2 eV, but the unmodified powder absorbs only weakly up to 405 nm due to defects and surface deposits.[20] Its absorption range can be extended into the visible range by structure modification[21] or dye surface modification.[22,23] The Texas Red derived dye **10**,[24], was covalently anchored on TiO_2 yielding **2**, which absorbs at 560 nm (see Supporting Information for the synthesis of **10** and the characterization of **2**). $PbBiO_2Br$ **3** and **4** were prepared by different synthetic routes leading to different particle sizes of the semiconductors: $PbBiO_2Br$ bulk material **3** with 2.47 eV band gap was prepared by high temperature solid phase synthesis,[25] while the nanocrystalline material **4** was obtained from aqueous solution synthesis leading to an average calculated particle size of 28 ± 6 nm and an optical band gap of 2.56 eV. Yellow CdS (**5**) has a band gap of 2.4 eV and was prepared as previously reported.[26]

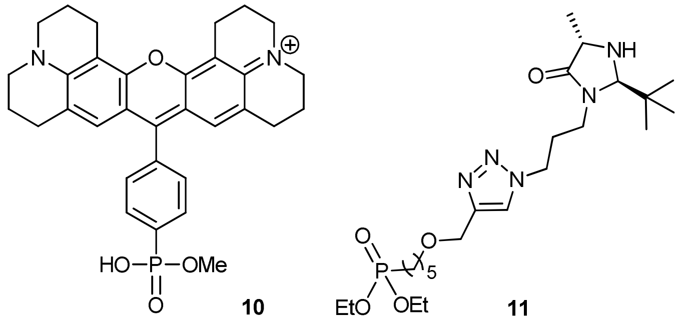

Scheme 1. Compounds for covalent surface immobilization on TiO_2. Phos-Texas-Red **10;** chiral organocatalyst **11.**

The α-alkylation of aldehyde **7** in the presence of 20 mol% of secondary amine **8** as chiral catalyst and unmodified TiO_2 affords product **9** in moderate yield and good enantioselectivity after extended irradiation time (entry 1), as only a small fraction of the visible light at 440 nm is absorbed. TiO_2 can be reused giving similar results (entry 2). With higher light intensity in a microreactor set up (entry 3) the reaction time can be reduced to 3 h. Lowering the reaction temperature to -10 ^{o}C increases the stereoselectivity of the reaction to 83% *ee*, but slows down the reaction significantly (entry 4). Surface modified TiO_2 **2** allows the reaction to run with green light (530 nm, entries 5 and 6) yielding 65% product in 81% *ee* at -10 ^{o}C. $PbBiO_2Br$ (**3**) absorbs in the visible range and catalyzes the reaction with blue light (entries 7 and 8). However, its surface area is with only 0.17 m^2/g small compared to TiO_2 (50 m^2/g). This explains the still rather long reaction time. Nanocrystalline $PbBiO_2Br$ (**4**) has a larger surface area of 10.8 m^2/g and at room temperature and 440 nm irradiation the product can be isolated with a yield of 84% and 72% *ee* after 20 h (entry 9). Again, the stereoselectivity increases to 83% *ee* at -10 ^{o}C, but with lower conversion (entry 10). The microreactor reduces reaction times to 3 or 10 h, resp. with yields of 69% and *ee´*s of 80% (entries 11 and 12). The reuse of **4** is possible, but black organic surface deposits lead to significantly slower conversions.

The mechanism of the alkylation reaction presumably follows the proposed pathway for photoredox catalysis (see SI for scheme): Electron transfer from the conduction band of the semiconductor to the halogenated carbonyl compound generates *via* the loss of a bromide anion the α-carbonyl radical, which adds to the enamine obtained by condensation of the chiral catalyst with octanal. The

α-amino radical is then oxidized by a hole of the valence band yielding the iminium ion that releases catalyst and product.

In an attempt to create a completely heterogeneous catalyst system we prepared the chiral amine phosphonate ester **11** (see Supporting Information for the synthesis) and immobilized it on TiO_2. However, the catalyst system is inactive and no product formation could be observed under identical conditions as used before. The close proximity of the secondary amine organocatalyst to the semiconductor surface may lead to its rapid oxidative photodecomposition. The non-immobilized catalyst, mostly present in solution as enamine, will only very rarely encounter the surface as the free amine and is thereby protected from oxidative decomposition.

Table 1. Enantioselective alkylations using MacMillan´s chiral secondary amine and inorganic semiconductors as photocatalysts.

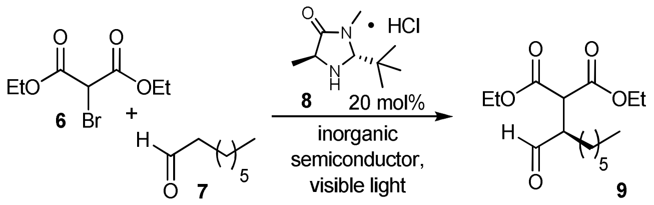

Entry	Photo-catalyst[a]	Wave-length[b] [nm]	Reaction time [h]	Reaction temp. [°C]	Yield **9** [%][c]	*ee* [%][d]
1	**1**	440	20	20	55	71
2	**1**[e]	440	20	20	60	72
3	**1**[f]	440	3	20	76	74
4	**1**	440	20	-10	40	83
5	**2**	530	20	20	55	72
6	**2**	530	20	-10	65	81
7	**3**	440	20	20	69	71
8	**3**	440	20	-10	40	84
9	**4**	440	20	20	84	72
10	**4**	440	20	-10	49	83
11	**4**[f]	455	3	20	41	71
12	**4**[f]	455	10	-10	69	80

[a] 64 mg photocatalyst/1 mmol of **6** in 2.5 mL of degassed CH_3CN. [b] high power LED (440, 455 or 530 nm ± 10 nm, 3 W, LUXEON as indicated). [c] isolated yield. [d] determined by chiral HPLC or by NMR using a chiral diol.[27] [e] photocatalyst reused. [f] irradiation in microreactor in 1.5 mL of CH_3CN.

Our attempts to use CdS (**5**) for this transformation were not successful. A comparison of the relevant potentials of the widely employed photocatalyst $Ru(bpy)_3Cl_2$ and the investigated semiconductors explains the observation. $Ru(bpy)_3^+$ is proposed as the electron donor with a potential of -1.33 V (SCE). The conduction band potential of TiO_2 at -2.0 V (SCE) in acetonitrile is sufficient for this step, while the respective reported potential for CdS in acetonitrile of -1.05 V may be too low (Figure 2).[28,29] On the other hand, the reductive quenching step potential of excited $Ru(bpy)_3^{2+*}$ leading to the oxidation of the α-aminoradical intermediate is estimated to be +0.84 V (SCE), which is matched by the hole potentials (all *vs.* SCE in acetonitrile) of TiO_2 (+1.0 V)[29, 30] and CdS (+1.6 V).

The combination of heterogeneous inorganic and homogeneous organic catalysts is applicable to other substrates, such as bromoacetophenone (**12a**). For the conversion of the more difficult to reduce dinitro benzylbromide (**12b**) iridium complexes are required in the case of homogeneous photocatalysis.[9c] However, the estimated conduction band potentials of TiO_2 and $PbBiO_2Br$ in acetonitrile (Figure 2) should be still sufficient and we indeed could observe the clean conversion to the expected products in good yield and high stereoselectivity (Scheme 2).

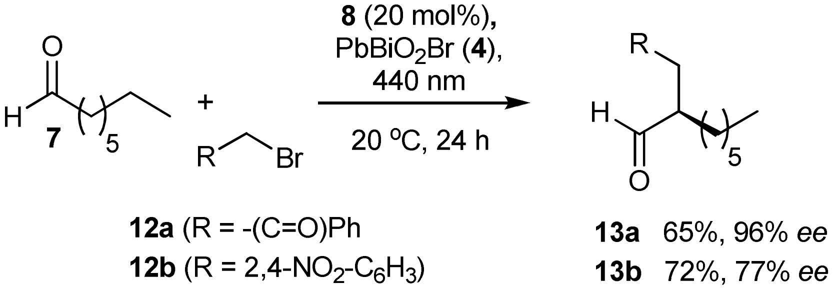

Scheme 2. Alkylations using bromoacetophenone (**12a**) in CH_3CN or 2,4-dinitrobenzylbromide (**12b**) in DMSO, chiral amine **7**, $PbBiO_2Br$ (**4**) and blue light.

Recently, several cross-dehydrogenative couplings[31] on tetrahydroisoquinolines by homogeneous photocatalysis using Ir- or Ru-based transition metal complexes[5b,5c,7d,8b,8d,15,32] or organic dyes,[33] such as Eosin Y[8a] have been reported. Here the photocatalytic key step is the reductive quenching of the excited chromophore leading to an amine radical cation, which subsequently can transform to an electrophilic iminium species. Considering the use of inorganic semiconductors for this reaction, the potential of the photogenerated holes in the valence band is now of importance. Based on the band gap and its redox potential (see Figure 2) CdS should be a suitable heterogeneous visible light photocatalysts for oxidations to generate the desired amine radical cation. The combination of proline as organocatalysts with CdS, as inorganic photocatalyst, indeed allows for a clean conversion of *N*-aryltetrahydroisoquinolines **14** in a photooxidative Mannich type reaction[32b,33a] with ketones **15** upon irradiation with blue light of 460 nm. The products **16a-d** arising from the reaction with acyclic or cyclic ketones can be obtained in good yields of 76-89% (Table 2).[34] While the reaction can also successfully be performed in CH_3CN with a significantly reduced amount of ketone (see Table 2, entry

1a-c), the reaction is most conveniently run in neat ketone if inexpensive (liquid) ketones are employed.

Table 2. Photocatalytic Mannich reaction of *N*-aryltetrahydroisoquinolines **14** with ketones **15** and L-proline on CdS (**5**)[a]

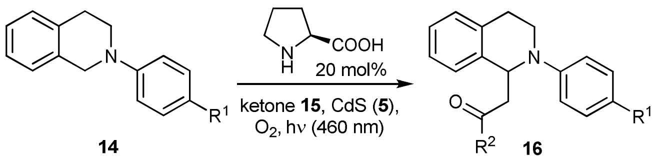

entry	R^1	ketone	product	reaction time [h]	yield [%][b]
1a	H	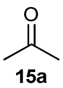 **15a**	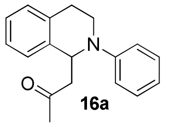 **16a**	24	86[c]
1b				24	90[d]
1c				24	100[e]
1d				24	87
2	OMe	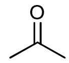 **15a**	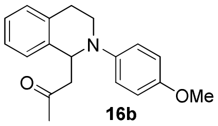 **16b**	18	89
3	H	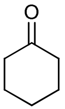 **15b**	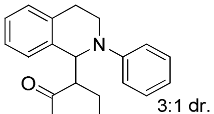 **16c** 3:1 dr.	24	79
4	H	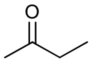 **15c**	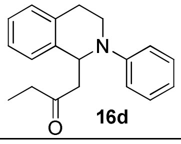 **16d**	15	76

[a] Unless otherwise noted all experiments were performed with amine (1 eq) and L-proline (0.2 eq) in a 5 mg/ml mixture of CdS in neat ketone (c_{amine}=0.25 mol/l). Reactions were run in schlenk tubes with an attached oxygen balloon and irradiated with high power LEDs (460 nm) for the time indicated. [b] Given yields correspond to isolated product. [c] Reaction performed in CH_3CN with 2 equiv. of acetone; the conversion was determined by GC analysis. [d] Reaction performed in CH_3CN with 5 equiv. of acetone; the conversion was determined by GC anaylsis. [e] Reaction performed in CH_3CN with 10 equiv. of acetone; the conversion was determined by GC analysis.

The flat band potentials of some common inorganic (and organic) semiconductors are summarized in Figure 2.[35] Importantly, with changing pH or upon exposure to different organic solvents these values shift significantly and the currently available data for organic solvents are limited. However, comparing the semiconductor flat band potentials with the potentials required for catalytic key steps from known photoredox catalysts (e. g. Ru-, Ir-complexes, xanthene dyes etc.) allows the prediction of suitable combinations of (inorganic) semiconductors with organocatalysts.

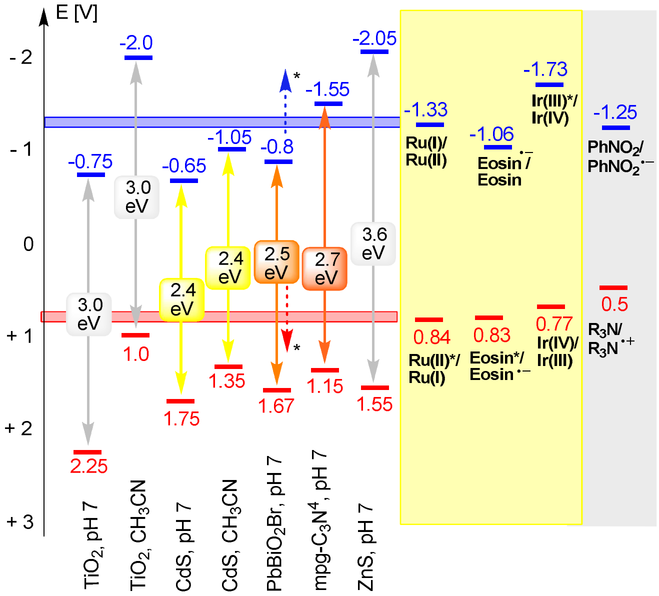

Figure 2. Band gaps (in eV) and redox potentials (in V *vs*. SCE) of common inorganic semiconductors in comparison with molecular photocatalysts and redox potentials of some photocatalytic key steps. *Estimated change of $PbBiO_2Br$ flat band potential in acetonitrile. Given values for Ru relate to $Ru(bpy)_3^{2+}$; values for Ir are related to *fac*-$Ir(ppy)_3$.

1.3.3 Conclusion

We have demonstrated that the well-directed combination of heterogeneous semiconductor photocatalysts with chiral organocatalysts allows for different types of stereoselective bond formation by visible light photocatalysis. Yields and stereoselectivity are comparable to previously reported homogeneous reactions using transition metal complexes or organic dyes. Electrons are exchanged in the course of the reaction between the chiral reaction intermediates in solution and the semiconductor surface, if the redox potentials of substrates and band gaps match. The covalent immobilization of the organocatalyst on the semiconductor surface leads to its oxidative decomposition and must be avoided.

The good availability of inorganic semiconductors with different band gaps and redox potentials, their simple removal and recycling make them the perfect partners for chiral organocatalysts in stereoselective photocatalysis.

1.3.4 Experimental Section

1.3.4.1 General Methods

For irradiation high power LEDs (440 nm, 455 nm or 530 nm±10 nm) with 3 W electrical power STAR LB BL ZXHL-LBBC LUXEON were used.

Commercial reagents and starting materials were purchased from Aldrich, Fluka, VWR or Acros and used without further purification. Solvents were used as p.a. grade or dried and distilled as described in common procedures.

For NMR-spectroscopy a Bruker Avance 300 (1H: 300 MHz, 13C: 75 MHz, T = 295 K), a Bruker Avance 400 (1H: 400 MHz, 13C: 100 MHz, T = 295 K) and Bruker Avance 600 (1H: 600MHz, 13C: 150 MHz, 31P: 243 MHz, T = 295 K) were used. The chemical shifts are reported in δ [ppm] relative to internal standards (solvent residual peak). The spectra were analyzed by first order, the coupling constants J are given in Hertz [Hz].

Absorption spectra were recorded on a Varian Cary BIO 50 UV/VIS/NIR spectrometer, 1 cm quartz cuvette (Hellma) was used.

Specific optical rotation was measured on Kruess (A. Kruess Optonics).

Preparative HPLC was performed on Agilent 1100 Series.

1.3.4.2 General procedures

General procedure 1 (aldehyde α-alkylation): Bromo-alkyl (1 equiv.), octanal (2.5 equiv.), (2*R*,5*S*)-2-*tert*-butyl-3,5-dimethylimidazolidin-4-one hydrochloride **8** (0.2 equiv.), 2,6-lutidine (2 equiv.) and the semiconductor (64mg/mol$_{\text{Br-alkyl}}$) in the indicated solvent were degassed by repeated freeze-pump-thaw cycles. The vial was irradiated with high power LEDs wavelength temperature and time as given in Table 1. For work up the reaction mixture was filtered with the aid of Acetonitrile (3×2ml) and EtOAc (2×2ml). The filtrates were washed with aqueous sat. solutions of $NaHCO_3$, NH_4Cl, NaCl. The aqueous layers were extracted with EtOAc (2×10 ml), the combined organic layers were evaporated to dryness, and the crude products were purified by column chromatography.

General procedure 2 (Aza-Henry reactions): 1,2,3,4-Tetrahydroisoquinoline derivative (1 equiv.), L-proline (0.2 equiv.) and ketone (c_{THIQ} = 0.25 mol/l) were mixed in a schlenk tube. CdS (5 mg/ml$_{\text{Ketone}}$) was added and an oxygen atmosphere was applied by balloon. The vial was irradiated with high power LEDs (460 nm) in a distance of approximately 5 cm for the indicated time. After full conversion of the Starting material (as judged by TLC) the crude mixture was purified by column chromatography (hexanes:ethyl acetate 9:1).

1.3.4.3 Proposed mechanism of the photocatalysis

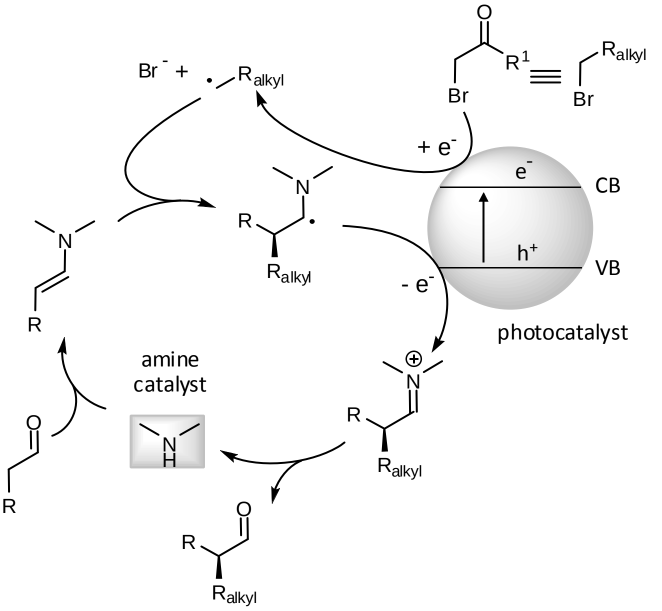

Scheme S-1. Proposed mechanism of the semiconductor photoredox catalysis of enamines and bromo malonate

1.3.4.4 Experimental data for Aldehyde α-alkylations

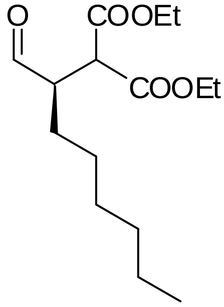

286,36 g/mol

(*R*)-Diethyl 2-(1-oxohexan-2-yl)propanedioate (9)

According to general procedure 1: Bromo-diethylmalonate 6 (133 µL, 0.78 mmol) catalyst 8 (33 mg, 156 µmol), octanal (305 µL, 195 µmol), 2,6-lutidine (182 µL, 156 µmol) and the semiconductor (50 mg, table 1) in acetonitrile (2.5 mL). Column chromatography (hexanes:diethylether, 6:1; $R_f = 0.3$) afforded 9 as a colorless oil. ^{1}H NMR (300 MHz, CD3CN): δ 9.67 (d, *J* = 1.1 Hz, 1H), 4.30 – 4.10 (m, 4H), 3.71 (dd, *J* = 8.6, 4.4 Hz, 1H), 3.04 – 2.96 (m, 1H), 1.71 – 1.51 (m, 2H), 1.28 – 1.16 (m, 14H), 0.87 (t, *J* = 6.7 Hz, 3H). For determination of the enantiomeric excess 20 mg of the product was dissolved in 5 ml of dichloromethane, 2S,4S-(+)-pentanediol (10 mg) and TsOH (3 mg) were added, the reaction mixture was stirred under nitrogen atmosphere for 5 h, the solvent was removed and the *ee* was determined by the integration of the NMR signals (400 MHz, CD_3CN) at 3.54 ppm (major) and 3.57 ppm (minor)[1]. Alternatively, the enantiomeric excess was determined by chiral HPLC using Phenomenex Lux Cellulose-1 column, 4.6×250 mm, 5 µm, *n*-heptane/*i*-propanol 1.0 ml/min.

(*R*)-2-(2-Oxo-2-phenylethyl)hexanal (13a)

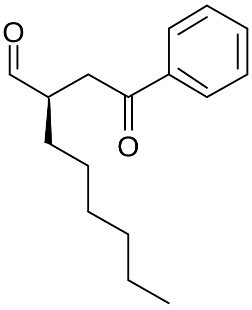

246,34 g/mol

According to general procedure 1: 2-Bromacetophenone 12a (100 mg, 0.5 mmol), catalyst 8 (21 mg, 0.1 mmol), octanal (195 µl, 1.25 mmol), 2,6-lutidine (116 µl, 1 mmol), PbBiO2Br *nano* (4, 32 mg) in acetonitrile (2 ml). Column chromatography (hexanes:diethylether; 10:1; *R*f = 0.3) afforded 13a (76.2 mg, 62 % yield, 96% ee) as a colorless oil. 1H NMR (300 MHz, CD3CN): δ 9.70 (d, *J* = 1.4 Hz, 1H), 8.01 – 7.94 (m, 2H), 7.65 – 7.59 (m, 1H), 7.53 – 7.48 (m, 2H), 3.44 (dd, *J* = 18.1, 8.4 Hz, 1H), 3.13 (dd, *J* = 18.1, 4.4 Hz, 1H), 2.99 – 2.89 (m, 1H), 1.79-1.70 (m, 1H), 1.55-1.46 (m, 1H), 1.41 – 1.24 (m, 8H), 0.88 (t, *J* = 6.8 Hz, 3H). The enantiomeric excess was determined by optical rotation $[\alpha]_D^{23}$ = +69.1 (c = 1.3, CHCl3, 96% ee)[36].

(*R*)-2-(2,4-Dinitrobenzyl)octanal (13b)

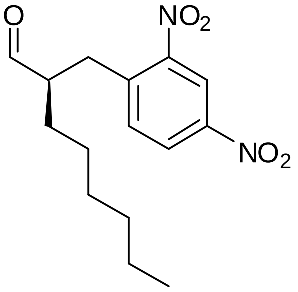

308,33 g/mol

According to general procedure 1: 2,4-dinitrobenzyl bromide 12b (100 mg, 0.38 mmol), catalyst 8 (16 mg, 0.076 mmol), octanal (149 µL, 0.95 mmol), 2,6-lutidine (89 µL, 0.76 mmol) and PbBiO$_2$Br *nano* (4, 25 mg) in DMSO (2 mL). Column chromatography (hexanes:diethyl ether; 7:1; R$_f$ = 0.23) afforded 13b (85.5 mg (72 % yield, 77 % ee) as a yellowish oil. ^{1}H NMR (300 MHz, CD$_3$CN): δ 9.58 (d, *J* = 2.0 Hz, 1H), 8.68 (d, *J* = 2.4 Hz, 1H), 8.37 (dd, *J* = 8.6, 2.4 Hz, 1H), 7.70 (d, *J* = 8.6 Hz, 1H), 3.34 (dd, *J* = 14.1, 8.5 Hz, 1H), 3.04 (dd, *J* = 14.1, 5.7 Hz, 1H), 2.82 – 2.70 (m, 1H), 1.79 – 1.65 (m, 1H), 1.60 – 1.47 (m, 1H), 1.37 – 1.22 (m, 8H), 0.88 (t, *J* = 6.8 Hz, 3H). For determination of the enantiomeric excess 20 mg of the product was dissolved in 5 ml of dichloromethane, 2S,4S-(+)-pentanediol (10 mg) and TsOH (3 mg) were added, the reaction mixture was stirred under dinitrogen atmosphere for 5 h, the solvent was removed and the *ee* was determined by the integration of the NMR resonance signals (400 MHz, CD$_3$CN) at 8.55 ppm (major) and 8.53 ppm (minor).

For microreactor reactions the reaction mixture was injected by syringe into a glass microreactor (1.5 mL acetonitrile) (LTF factory, 11 x 5.7 cm, 1.7 mL internal volume) previously flushed with nitrogen. For pictures see topic (9).

1.3.4.5 Synthesis and immobilization of compound 10

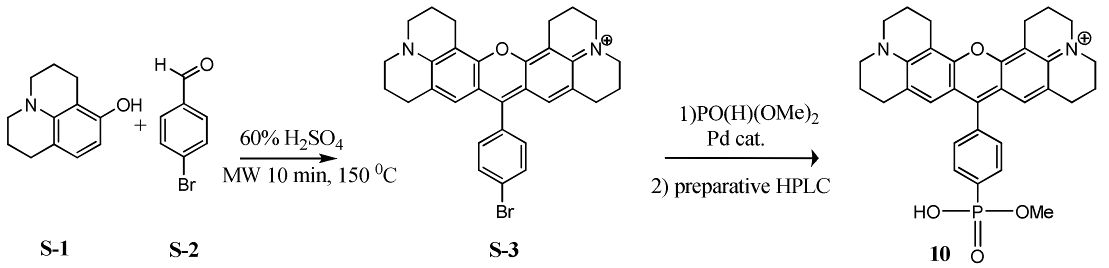

Scheme **S-2**. Synthesis of Phos-Texas Red (**10**) for surface modification of TiO_2.

Phos-TexasRed dye **10** was synthesized *via* Pd-catalyzed reaction of compound **S-3** with diethyl phosphate.[37] Compound **S-3** was obtained from the condensation of 8-hydroxyjuloidine (**S-1**) and 4-bromobenzaldehyde (**S-2**).[38] The synthetic procedure is simpler compared to the reported syntheses of other dyes of this type for surface immobilization[39] and the phosphonate group has excellent anchoring properties to the TiO_2 surface.[40] The absorption maximum of dye **10** in methanol solution is λ_{max} = 578 nm(c = 4.7×10^{-5} M) with an extinction coefficient of ε = 83000 $cm^{-1}M^{-1}$. TiO_2 was surface modified with Phos-Texas Red dye **10**. After immobilization the absorption maximum shifted slightly to 560 nm. The amount of immobilized dye was estimated from the UV-Vis spectra to be 9.3×10^{-3} mmol/50mg TiO_2. This corresponds to 1.2 mol% in respect to diethyl 2-bromomalonate used in the catalysis reaction.

Texas Red dye S-3.[41] *p*-Bromobenzaldehyde (90 mg, 0.5 mmol) and 8-hydroxyjulolidine (200 mg, 1.05 mmol) were dissolved in 10 ml of $CHCl_3$ and the solvent was removed *in vacuo* to give a homogenous mixture. The mixture was then suspended in 10 ml of 60% H_2SO_4, heated in the microwave reactor for 10 min to 150 ^{0}C with vigorous stirring. Chloranil (185 mg, 0.75 mmol) was added and the mixture was allowed to cool to room temperature. The reaction mixture was adjusted with 10 M NaOH to neutral pH and filtered. The filtered mixture was then extracted with dichloromethane (3×200 ml) and the combined organic layers were washed with brine and water, dried over $MgSO_4$ and the solvent was removed under reduced pressure. The residue was further purified by chromatography on silicagel (EtOAc/MeOH 4/1) to give the compound **S-3** as violet solid. ^{1}H NMR (300 MHz, MeOD) δ 7.76 (d, *J* = 8.4 Hz, 2H), 7.28 (d, *J* = 8.4 Hz, 2H), 6.79 (s, 2H), 3.56 (t, *J*=5.5 Hz, 4H), 3.53 (t, *J*=5.5 Hz, 4H), 3.02 (t, *J* = 6.4 Hz, 3H), 2.68 (t, *J* = 6.4 Hz, 3H), 2.10 – 2.00 (m, 4H), 1.98 – 1.86 (m, 4H). MS (ESI) m/z 526/528 (M^+).

Phos-Texas Red dye 10. Texas Red dye (**S-3**, 50 mg, 0.11 mmol), $Pd_2(dba)_3CHCl_3$ (11.4 mg, 0.011 mmol) and xantphos (12.7 mg, 0.022 mmol) were dissolved in 30 ml of dry dichloromethane under exclusion of air. The reaction mixture was refluxed in nitrogen atmosphere and diisopropylethyl amine (20 µl, 0.11 mmol) and dimethylphosphite (10.1 µl, 0.11 mmol) were added at once. The reaction mixture was allowed to reflux for 10 h, it was filtered and the solvent was removed under reduced pressure. The residue was further purified on Al_2O_3 (EtOAc/MeOH 4/1) and by preparative HPLC (Phenomenex Luna 250×21.2 mm, MeCN/H_2O) to give compound **10** as dark violet solid (20 mg, 33% yield). The compound dissolves in water, methanol, DMSO and is partially soluble in EtOAc. ^{1}H NMR (600 MHz, MeOD): δ 8.00 (dd, *J* = 12.2, 7.9 Hz, 2H), 7.45 (dd, *J* = 7.8, 2.7 Hz, 2H), 6.82 (s, 2H), 3.65 (s, 3H), 3.55 (m, 4H), 3.51 (m, 4H), 3.07 (t, *J* = 6.3 Hz, 4H), 2.70 (t, *J*=6.3 Hz, 4H), 2.12 – 2.07 (m, 4H), 1.98 – 1.92 (m, 4H), 1.40 (t, *J* = 7.15, 7,15 Hz, 6H). ^{13}C NMR (150 MHz, MeOD): δ 19.46, 19.56, 20.38, 21.60, 27.11, 50.04, 50.50, 51.06, 106.35, 112.33, 126.15, 129.00, 131.33. ^{31}P NMR (243 MHz, MeOD) δ 14.43. HRMS (ESI) m/z 541/543 (M^+).

Immobilization of dye 10 on TiO_2. TiO_2 particles (400 mg) were added to a solution of the Phos-Texas Red dye **10** (18.1 mg, 33.8 µmol) in 15 ml of methanol. The mixture was stirred for 2 days in nitrogen atmosphere. Then solvent was removed *in vacuo* and the solid particles were washed several times with methanol and dried in high vacuum.

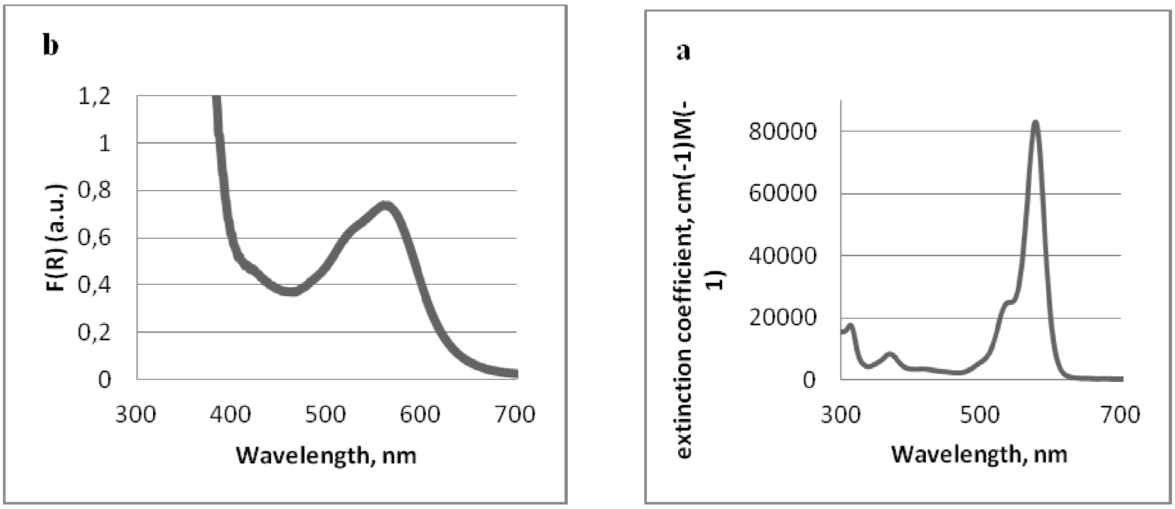

Figure **S-1**. UV/Vis absorption spectra of **10** in methanol solution (a, left). Diffuse UV/Vis reflectance spectra of Phos-Texas Red surface modified TiO_2 (**2)** plotted as the Kubelka-Munk function on the reflectance (R) (b, right).

1.3.4.6 Synthesis of compound 11

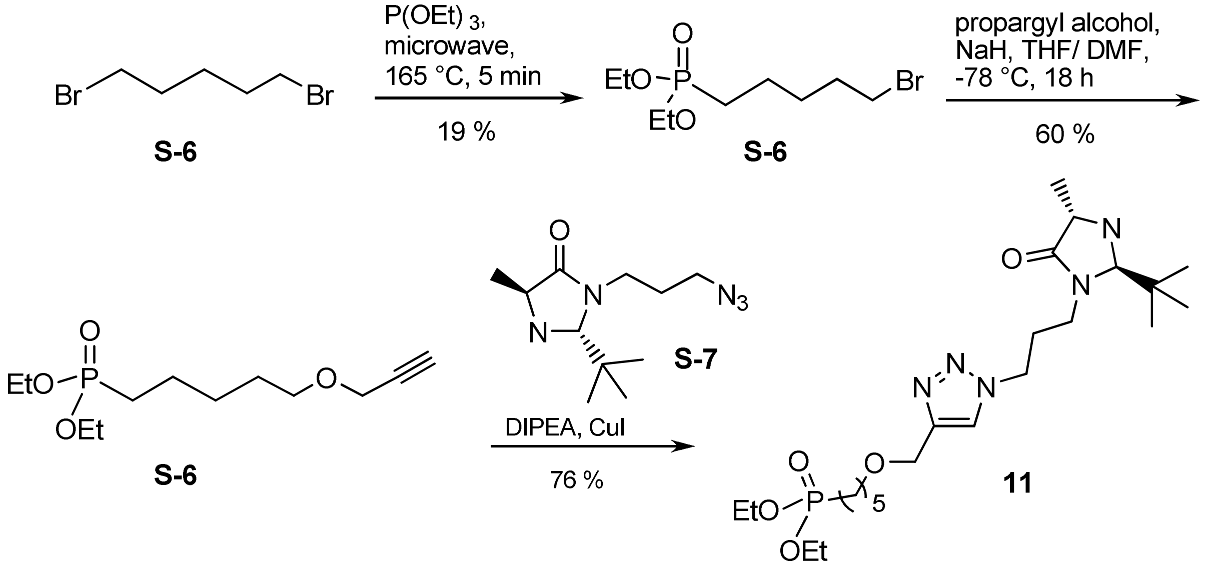
Br
Br
S-6
P(OEt) 3,
microwave,
165 °C, 5 min
19 %
O
EtO
P
EtO
Br
S-6
propargyl alcohol,
NaH, THF/ DMF,
-78 °C, 18 h
60 %
O
EtO
P
OEt
O
S-6
O
N
N
N3
S-7
DIPEA, CuI
76 %
O
N
O
N
N
N
N
O
O
EtO
P
5
OEt
11

Scheme **S-3**. Synthesis of diethyl 5-((1-(3-((2*R*,4*S*)-2-*tert*-butyl-4-methyl-5-oxoimidazolidin-1-yl) propyl)-1*H*-1,2,3-triazol-4-yl)methoxy)pentylphosphonate (**11**) for surface modification

Diethyl 5-bromopentylphosphonate (S-5)[42]

Distilled 1,5-dibromopentane (S-4, 5.45 mL, 40 mmol) and triethylphosphite (1.72 mL, 10 mmol) were placed in a quartz tube. Before the reaction vessel was closed it was saturated with argon. The solution was irradiated in the microwave (max. power: 150 Watt, temperature: 165 °C, pressure: 1 bar, time: 5 min). The excess dibromopentane was removed at 2 mbar and 130 °C. The crude product was purified by flash chromatography (silica gel, dichloromethane/ MeOH 30:1; R_f = 0.46, dichloromethane/ MeOH 20:1) to give 545 mg (yield: 19 %, literature:[6] 94 %) of the pure product as a colorless liquid and 1.18 g of a mixed fraction.

^{1}H NMR (300 MHz, $CDCl_3$, 22 °C, TMS): δ = 1.31 (t, J = 7.1 Hz, 6 H, 1/1'-H), 1.46-1.78 (m, 6 H, 3/4/5-H), 1.86 (tt, J = 7.2 Hz, 6.8 Hz, 2 H, 6-H), 3.39 (t, J = 6.8 Hz, 2 H, 7-H), 3.99-4.16 (m, 4 H, 2/2'-H).

^{31}P NMR (121 MHz, $CDCl_3$): δ = 32.52.

^{13}C NMR (75 MHz, $CDCl_3$): δ = 16.6 (d, J = 6.0 Hz, C-1/1'), 21.9 (d, J = 5.1 Hz, C-5), 25.7 (d, J = 141.1 Hz, C-3), 29.2 (d, J = 16.9 Hz, C-4), 32.3 (d, J = 1.1 Hz, C-6), 33.5 (C-7), 61.6 (d, J = 6.6 Hz, C-2/2').

Diethyl 5-(prop-2-ynyloxy)pentylphosphonate (S-6)[43]

In a 100 mL-Schlenk-flask sodium hydride (752 mg, 18.81 mmol, 60 wt% in oil) was washed with dry Et_2O (5 x 5 mL). The sodium hydride was dried under vacuum and freshly distilled THF (11 mL) was added. The suspension was cooled to -78 °C. A solution of propargyl alcohol (732 µL, 12.54 mmol) in THF (2.7 mL) was added drop wise. The mixture was stirred for 30 min at -78 °C. A solution of diethyl 5-bromopentylphosphonate S-5 (1.8 g, 6.27 mmol) in abs. DMF (11 mL) was added drop wise by syringe injection over a period of 25 min. The mixture was allowed to warm up to room temperature over night. The solution was evaporated to dryness *in vacuo*. Saturated NH_4Cl solution (20 mL) was added and the solution was extracted with dichloromethane (4 x 30 mL). The organic layer was dried over $MgSO_4$, filtered and concentrated. The crude product was purified by kugelrohr distillation (174 °C/ 0.017 mbar) to give 988 mg (yield: 60 %, literature:[7] 79 %) of a colorless liquid.

R_f = 0.32 (DCM/ MeOH 30:1).

^{1}H NMR (300 MHz, $CDCl_3$, 22 °C, TMS): δ = 1.31 (t, *J* = 7.1 Hz, 6 H, 1/1'-H), 1.42-1.78 (m, 8 H, 3/4/5/6-H), 2.41 (t, *J* = 2.4 Hz, 1 H, 10-H), 3.50 (t, *J* = 6.4 Hz, 2 H, 7-H), 4.01-4.14 (m, 6 H, 2/2'/8-H).

^{31}P NMR (121 MHz, $CDCl_3$): δ = 32.91.

^{13}C NMR (75 MHz, $CDCl_3$): δ = 16.6 (d, *J* = 6.0 Hz, C-1/1'), 22.4 (d, *J* = 5.1 Hz, C-5), 25.8 (d, *J* = 140.6 Hz, C-3), 27.3 (d, *J* = 17.4 Hz, C-4), 29.2 (d, *J* = 1.1 Hz, C-6), 58.2 (C-8), 61.5 (d, *J* = 6.4 Hz, C-2/2'), 69.9 (C-7), 74.3 (C-10), 80.0 (C-9).

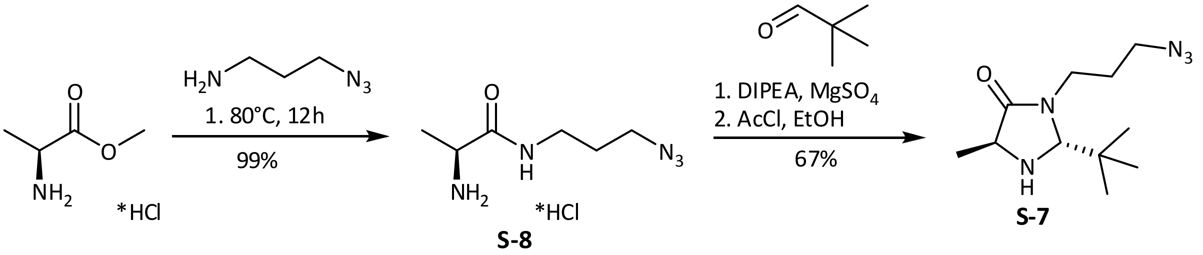

Scheme **S-4**. Synthesis of azido-modified MacMillan Imidazolidinone catalyst (**S-7**).

(*S*)-2-Amino-N-(3-azidopropyl)propanamide hydrochloride (S-8)

L-Alanine methyl ester hydrochloride (1 equiv.) and 3-aminopropane-1-azide[44] (1.2 equiv.) were dissolved in methanol (c_{Ala}= 7.5 mol/l) in a sealed tube. The mixture was heated to 80°C for 12h. After full conversion (as judged by IR spectra 1738 cm^{-1} (ester); 1655 cm^{-1} (amide)) the solvent and excess azide were removed in vacuum yielding quantitatively the pure product as a brown oil.

^{1}H NMR (300 MHz, $CDCl_3$) δ: 3.70 (q, *J* = 6.9 Hz, 1H), 3.47 (t, *J* = 6.4 Hz, 2H), 3.39 – 3.20 (m, 4H), 3.02 (t, *J* = 7.3 Hz, 2H), 2.07 – 1.88 (m, 2H), 1.85 – 1.66 (m, 2H), 1.37 (d, *J* = 7.0 Hz, 3H).

(2*R*,5*S*)-3-(3-Azidopropyl)-2-tert-butyl-5-methylimidazolidin-4-one (S-7)

(*S*)-2-Amino-N-(3-azidopropyl)propanamide hydrochloride (S-8, 1 equiv.), magnesium sulfate (2 equiv.), DIPEA (1 equiv.) and pivalaldehyde (70% in propanol, 2 equiv.) were mixed in dichloromethane $c_{S\text{-}8}$ = 0.5 mol/l. The flask was argon flushed and closed by an argon filled balloon, stirred at room temperature for 18h, as the reaction was completed (monitored by TLC) the magnesium sulfate was filtered off and the solution was concentrated in vacuum. The residue was redissolved in dry ethanol (c = 0.8 mol/l) and cooled to -10°C. Acetylchlorid (1.5 equiv.) was added drop wise via syringe over a period of 1.5h, the cooling bath was allowed to melt and stirring was continued for additional 12h. The reaction mixture was diluted with dichloromethane, neutralized by saturated $NaHCO_3$ solution; organic phase was separated, dried over magnesium sulfate and concentrated in vacuum. The crude product was purified by column chromatography (SiO_2, hexanes/ethyl acetate 1:1) yielding S-7 as yellow brown oil in 67% yield and 96 %de.

^{1}H NMR (400 MHz, $CDCl_3$) δ 4.14 (brs, 1H), 3.85 – 3.74 (m, 1H), 3.56 (q, *J* = 6.8 Hz, 1H), 3.38 – 3.25 (m, 2H), 3.19 (m, 1H), 2.04 – 1.91 (m, 1H), 1.89 – 1.69 (m, 2H), 1.26 (d, *J* = 6.8 Hz, 3H), 0.94 (s, 9H). ^{13}C NMR (75 MHz, $CDCl_3$) δ 177.2, 80.6, 54.3, 49.2, 41.0, 38.4, 26.4, 25.9, 25.6, 18.8.

Diethyl 5-((1-(3-((2*R*,4*S*)-2-*tert*-butyl-4-methyl-5-oxoimidazolidin-1-yl)propyl)-1*H*-1,2,3-triazol-4-yl)methoxy)pentylphosphonate (11)

In a 25 mL-round-bottom-flask (2*R*,5*S*)-3-(3-azidopropyl)-2-*tert*-butyl-5-methylimidazolidin-4-one (S-7, 130 mg, 0.54 mmol), diethyl 5-(prop-2-ynyloxy)pentylphosphonate S-6 (130 mg, 0.49 mmol) and copper(I) iodide (9.40 mg, 0.05 mmol) were dissolved in dichloromethane (5 mL) to give a colorless suspension. DIPEA (172 µL, 0.99 mmol) was added and the cooled mixture was degassed by argon purge for 5 min. The solution was stirred for 18 h under an argon atmosphere. The solution was diluted with dichloromethane (20 mL) and washed with saturated NH_4Cl solution (3 x 15 mL). The aqueous layer was extracted with dichloromethane (2 x 20 mL), the combined organic layers were washed with brine (1 x 30 mL), dried over $MgSO_4$ and evaporated to dryness. The crude product was purified by flash chromatography (silicagel, dichloromethane/ MeOH 15:1; R_f = 0.29) to give 188 mg (76 %, 10:1 dr (82 % *de*)) of a pale yellow oil. The diastereomeric excess was determined from integration of ^{1}H-NMR signals ($CDCl_3$) at 0.92 ppm (major) and 0.96 ppm (minor).

^{1}H NMR (300 MHz, CDCl$_3$, 22 °C, TMS): δ = 0.92 (s, 9 H, 20/20'/20''-H), 1.27 (d, *J* = 6.8 Hz, 3 H, 16-H), 1.31 (t, *J* = 7.1 Hz, 6 H, 1/1'-H), 1.38-1.76 (m, 8 H, 3/4/5-H), 2.09-2.42 (m, 3 H, 12/17-H), 3.17 (dt, *J* = 14.3, 6.9 Hz, 1 H, 13-H), 3.50 (t, *J* = 6.4 Hz, 2 H, 7-H), 3.58 (q, *J* = 6.8 Hz, 1 H, 15-H), 3.77 (dt, *J* = 14.3, 6.9 Hz, 1 H, 13-H), 4.00-4.13 (m, 4 H, 2/2'-H), 4.15 (d, *J* = 1.3 Hz, 1 H, 18-H), 4.25-4.43 (m, 2 H, 11-H), 4.59 (s, 2 H, 8-H), 7.65 (s, 1 H, 10-H). ^{31}P NMR (121 MHz, CDCl$_3$): δ = 32.95. ^{13}C NMR (75 MHz, CDCl$_3$): δ = 16.6 (d, *J* = 6.0 Hz, C-1/1'), 18.8 (C-16), 22.4 (d, *J* = 5.2 Hz, C-5), 25.7 (d, *J* = 140.7 Hz, C-3), 26.0 (C-20/20'/20''), 27.3 (d, *J* = 17.3 Hz, C-4), 27.9 (C-12), 29.3 (C-6), 38.5 (C-19), 40.8 (C-13), 47.9 (C-11), 54.5 (C-15), 61.6 (C-2/2'), 64.4 (C-8), 70.6 (C-7), 80.7 (C-18), 122.9 (C-9), 145.6 (C-10), 177.6 (C-14). UV-VIS (MeCN): λ_{max} (nm)/ ε(L·M^{-1}·cm^{-1}) = 217/ 4475.

IR: $\tilde{\nu}$ [cm^{-1}] = 3451, 2980, 2944, 2914, 2869, 1682, 1222, 1097, 1024, 960.

ESI-MS: m/z = 502.3 (MH$^+$).

Immobilization of diethyl 5-((1-(3-((2*R*,4*S*)-2-*tert*-butyl-4-methyl-5-oxoimidazolidin-1-yl) propyl)-1*H*-1,2,3-triazol-4-yl)methoxy) pentyl phosphonate (11) on TiO$_2$

TiO$_2$ (485 mg, 6.07 mmol), compound 11 (20.5 mg, 41 µmol) and MeCN (3 mL) were placed in a 5 mL snap cap vial equipped with a magnetic stirring bar. The vial was closed with a septum and the suspension was stirred at 40 °C. After 24 h the solvent was removed and the TiO$_2$ was dried for 1.5 h at 65 °C. The TiO$_2$ was suspended in MeCN (2 mL), centrifuged and the solvent was removed. The procedure was repeated three times, the modified TiO$_2$ was dried at 65 °C and under high vacuum over night. 79 % of the initial amount of compound 11 was immobilized as determined by UV spectroscopy.

1.3.4.7 Experimental Data for Aza-Henry reactions [45]

Screening of different ketone equivalents for Aza-Henry reactions:

2-Phenyl-1,2,3,4-tetrahydroisoquinoline **14a** (1 equiv., 52 mg; 0.25 mmol), L-proline (0.2 equiv., 6 mg; 0.05 mmol) and 2, 5 or 10 equiv. of ketone were mixed in a schlenk tube together with CH$_3$CN as solvent (total volume: 1 ml; c_{THIQ} = 0.25 mol/l)). CdS (5 mg/ml$_{solvent}$) was added and an oxygen atmosphere was applied by balloon. The vial was irradiated with high power LEDs (460 nm) in a distance of approximately 5 cm for 24h. Analysis by TLC and determination of conversion by gas chromatography.

Overview:
2 equiv. of ketone using 37 µl of acetone in 960 µl of CH_3CN
5 equiv. of ketone using 91 µl of acetone in 910 µl of CH_3CN
10 equiv. of ketone using 182 µl of acetone in 820 µl of CH_3CN

1-(2-phenyl-1,2,3,4-tetrahydroisoquinolin-1-yl)propan-2-one (16a)

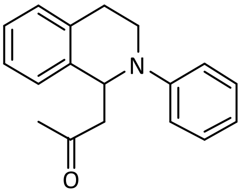

265,35 g/mol

According to general procedure 2: 2-phenyl-1,2,3,4-tetrahydroisoquinoline 14a (97 mg, 463 µmol), L-proline (10.5 mg, 91 µmol) and CdS (10mg, 69 µmol) in acetone 15a (1.8 ml) afforded 107 mg (87 %) of 16a after 24 h irradiation as a colorless solid. R_f (hexanes:ethyl acetate 3:1) = 0.51. ^{1}H NMR (300 MHz, $CDCl_3$) δ 7.31 – 7.21 (m, 2H), 7.17 (t, *J* = 2.9 Hz, 4H), 6.95 (d, *J* = 8.0 Hz, 2H), 6.79 (t, *J* = 7.3 Hz, 1H), 5.41 (t, *J* = 6.3 Hz, 1H), 3.72 – 3.60 (m, 1H), 3.60 – 3.46 (m, 1H), 3.14 – 2.97 (m, 2H), 2.90 – 2.75 (m, 2H), 2.08 (s, 3H). ^{13}C NMR (75 MHz, $CDCl_3$) δ 207.3, 148.9, 138.3, 134.5, 129.4, 128.7, 126.9, 126.8, 126.3, 118.3, 114.8, 54.8, 50.2, 42.1, 31.1, 27.2.

1-(2-(4-methoxyphenyl)-1,2,3,4-tetrahydroisoquinolin-1-yl)propan-2-one (16b)

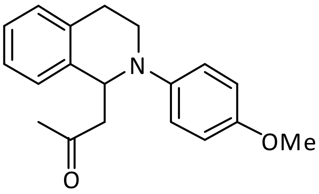

295,38 g/mol

According to general procedure 2: 2-(4-methoxyphenyl)-1,2,3,4-tetrahydroisoquinoline 14b (42 mg, 176 µmol), L-proline (4 mg, 35 µmol), and CdS (3.5 mg, 24 µmol) in acetone 15a (0.7 ml) afforded 46 mg (89 %) of 16b after 18 h irradiation as a colorless solid. R_f (hexanes:ethyl acetate 3:1) = 0.53. ^{1}H NMR (300 MHz, $CDCl_3$) δ 7.20 – 7.05 (m, 4H), 6.95 – 6.87 (m, 2H), 6.86 – 6.76 (m, 2H), 5.24 (t, *J* = 6.4 Hz, 1H), 3.75 (s, 3H), 3.61 – 3.38 (m, 2H), 3.08 – 2.92 (m, 2H), 2.82 – 2.67 (m, 2H), 2.06 (s, 3H). ^{13}C NMR (75 MHz, $CDCl_3$) δ 207.4, 153.3, 143.7, 138.3, 134.3, 129.0, 126.8, 126.7, 126.2, 118.4, 114.6, 56.0, 55.6, 50.0, 42.9, 30.9, 26.7.

2-(2-phenyl-1,2,3,4-tetrahydroisoquinolin-1-yl)cyclohexanone (16c)

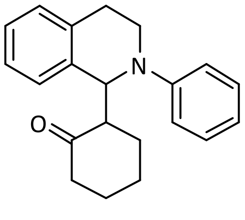
305,41 g/mol

According to general procedure 2: 2-phenyl-1,2,3,4-tetrahydroisoquinoline 14a (94 mg, 449 µmol), L-proline (10.3mg, 90 µmol) and CdS (10mg, 69 µmol) in cyclohexanone 15b (1.8 ml) afforded 108mg (79 %) 16c after 24 h irradiation as colorless oil after 24 h irradiation. R_f (hexanes:ethyl acetate 3:1) = 0.55. ^{1}H NMR (400 MHz, $CDCl_3$, *major diastereomer) δ 7.27 – 7.18 (m, 3H), 7.18 – 7.09 (m, 3H), 6.92*, 6.82 (d, 8.1 Hz, 2H), 6.76*, 6.68 (t, 7.2 Hz, 1H), 5.67, 5.63* (d, 6.6 Hz, 1H), 3.77 – 3.48 (m, 2H), 3.09 – 2.67 (m, 3H), 2.53 – 2.43 (m, 1H), 2.37 – 2.32 (m, 2H), 1.96 – 1.79 (m, 3H), 1.78 – 1.54 (m, 2H). ^{13}C NMR (101 MHz, $CDCl_3$) δ 211.9, 149.3, 136.0, 135.1, 129.4, 128.7, 128.0, 126.7, 125.8, 118.1, 114.9, 112.3, 56.5, 55.0, 42.6, 42.0, 41.4, 30.2, 27.3, 25.03, 23.8.

1-(2-phenyl-1,2,3,4-tetrahydroisoquinolin-1-yl)butan-2-one (16d)

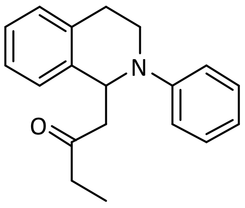
279,38 g/mol

According to general procedure 2: 2-phenyl-1,2,3,4-tetrahydroisoquinoline 14a (108 mg, 516 µmol), L-proline (11.9mg, 103 µmol) and CdS (10mg, 69 µmol) in 2-butanone 15c (1.8 ml) afforded 109mg (76 %) 16d after 15 h irradiation as brownish solid. R_f (hexanes:ethyl acetate 3:1) = 0.55. ^{1}H NMR (400 MHz, $CDCl_3$) δ 7.30 (m, 2H), 7.19 (m, 4H), 7.00 (d, *J* = 8.0 Hz, 2H), 6.82 (t, *J* = 7.3 Hz, 1H), 5.48 (t, *J* = 6.4 Hz, 1H), 3.73 – 3.63 (m, 1H), 3.62 – 3.52 (m, 1H), 3.10 (m, 2H), 2.92 – 2.78 (m, 2H), 2.34 (m, 2H), 1.03 (t, *J* = 7.3 Hz, 3H). ^{13}C NMR (101 MHz, $CDCl_3$) δ 210.0, 148.9, 138.5, 134.5, 129.4, 128.7, 126.9, 126.9, 126.3, 118.2, 114.7, 55.2, 49.0, 42.0, 37.3, 27.4, 7.6.

1.3.4.8 Synthesis and characterization of $PbBiO_2Br$ semiconductors

The **$PbBiO_2Br$ bulk semiconductor** was synthesized according to a literature procedure.[46]

$PbBiO_2Br$ *nano* semiconductor. For the synthesis of $PbBiO_2Br$ *nano* all chemicals were of analytical grade and were used as received.

$Bi_5O(OH)_9(NO_3)_4$ (2 mmol) were mixed with $Pb(CH_3COO)_2 \times 3H_2O$ (10 mmol) and NaBr (10 mmol). Subsequently, 200 ml of H_2O were added. The mixture was stirred for 24 h yielding a white suspension. About 100 ml of the suspension were heated under stirring for 72 h at 80°C in a round bottom flask with stopper. The suspension turned yellow. Then it was centrifuged at 6000 rpm for 30 min, the solid precipitate was dispersed in deionized water and centrifuged again. The procedure was repeated once and the yellow product was washed once with ethanol (99%) and again centrifuged at 6000rpm for 30 min. Ethanol was removed and the solid was dried at 50 °C for 3 days.

Characterization

X-ray powder diffraction (XRD) patterns of the products were measured by using a STOE STADI P (STOE & Cie GmbH, Darmstadt, Germany) at 40 kV and 40 mA(Cu Kα_1 radiation, Ge monochromator) equipped with a PSD unit. The diffractograms were measured at room temperature from $8° \leq 2\theta \leq 90°$ with a step size of $\Delta\theta = 0.02°$. Diffuse UV/Vis reflectance spectra were recorded by using a Bruins Instruments Omega 20 spectrometer. Data were transferred to absorption spectra by the Kubelka-Munk method.[47]

1.3.4.9 Glass microreactor and irradiation set up used for photocatalysis

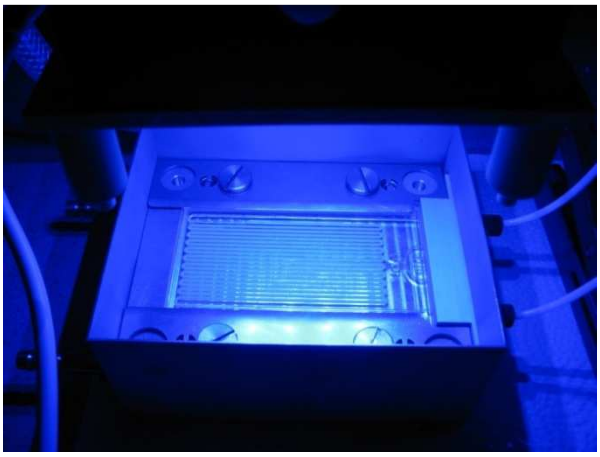

Figure **S-2**. Glass microreactor with suspension of reaction mixture and heterogeneous semiconductor catalyst (no-flow mode)

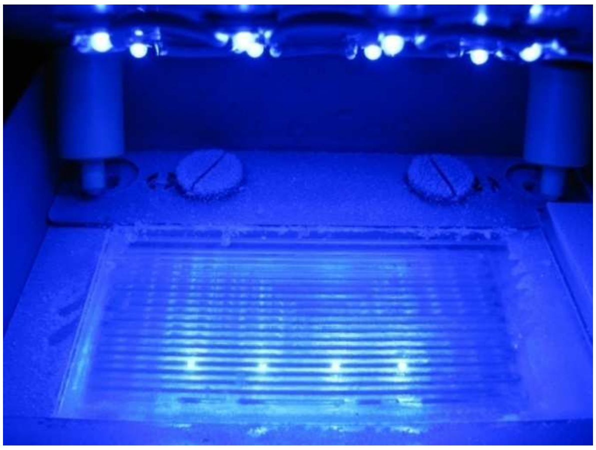

Figure**. S-3.** Irradiation set-up for the reaction in the microreactor.

1.3.4.10 Spectra of compounds 10, 11 and 13

Phos-TexasRed dye (10).

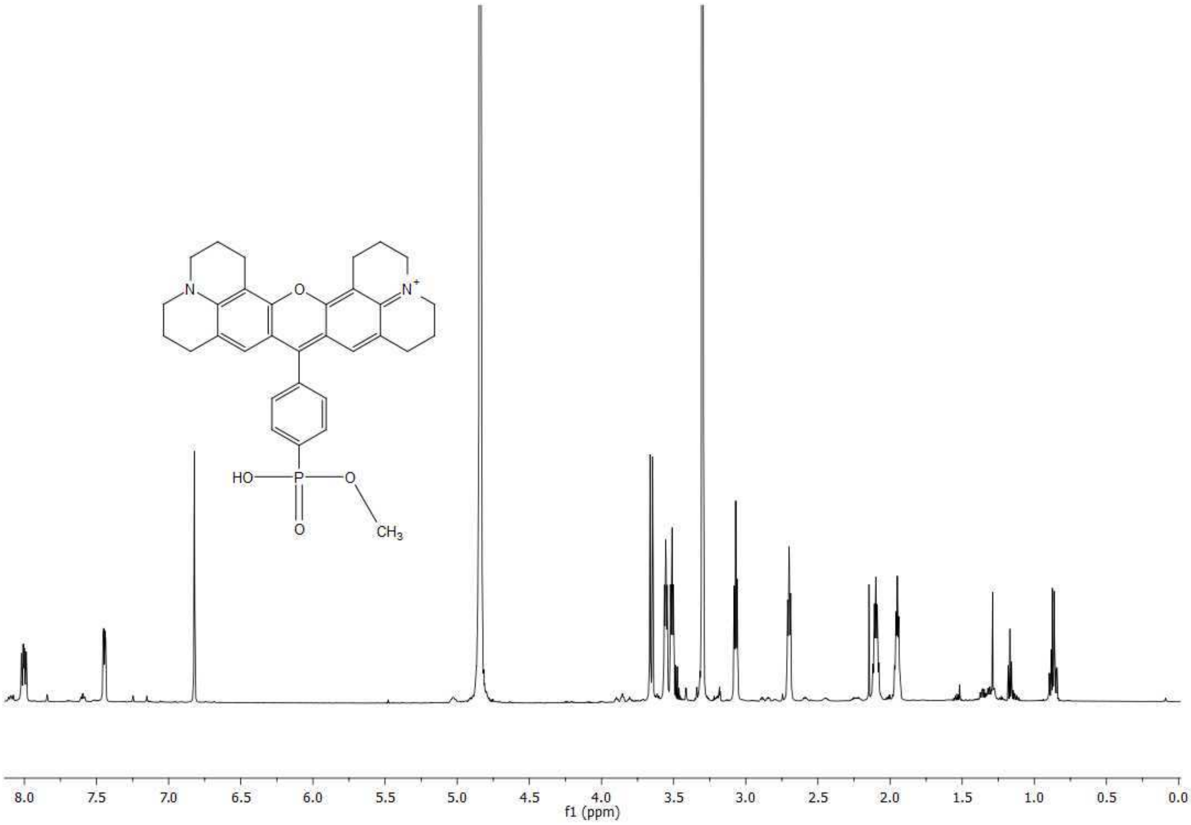

Figure **S-4.** ^{1}H NMR (600 MHz, MeOD): Phos-TexasRed dye (**10**).

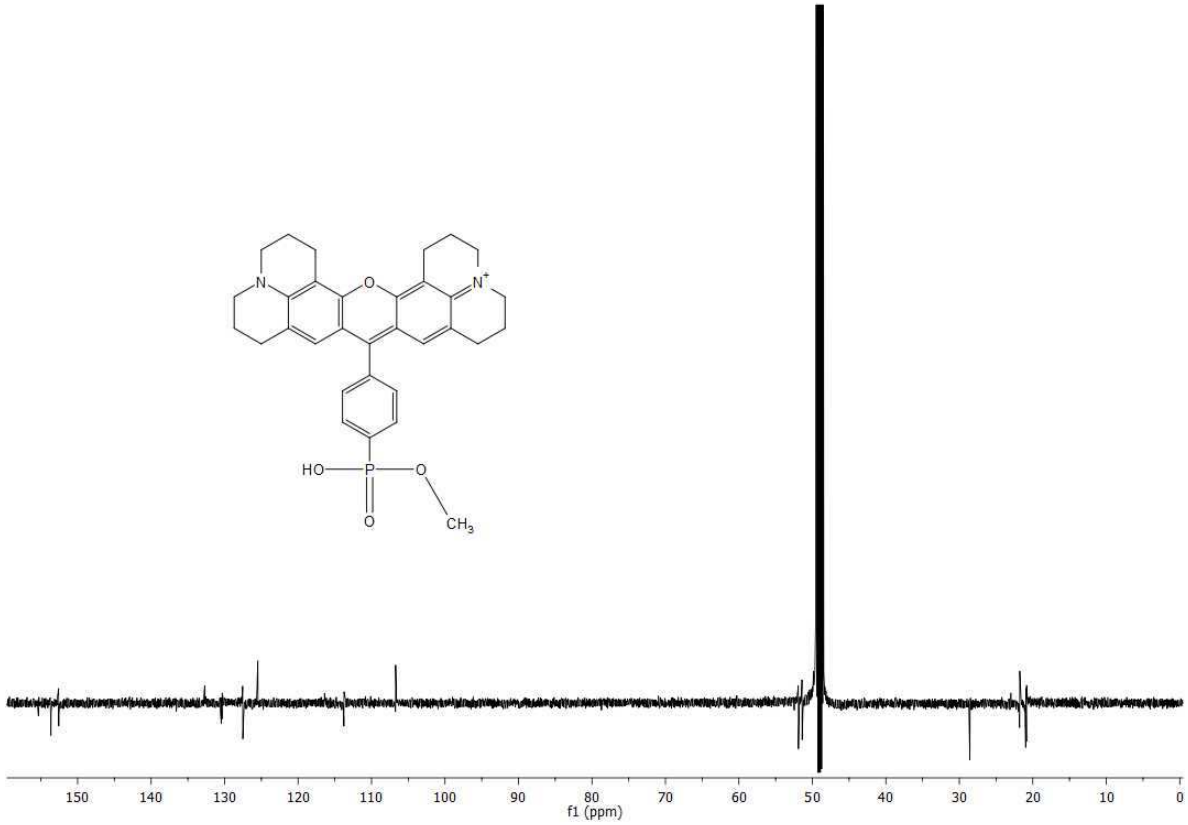

Figure **S-5.** ^{13}C NMR (150 MHz, MeOD): Phos-TexasRed dye (**10**).

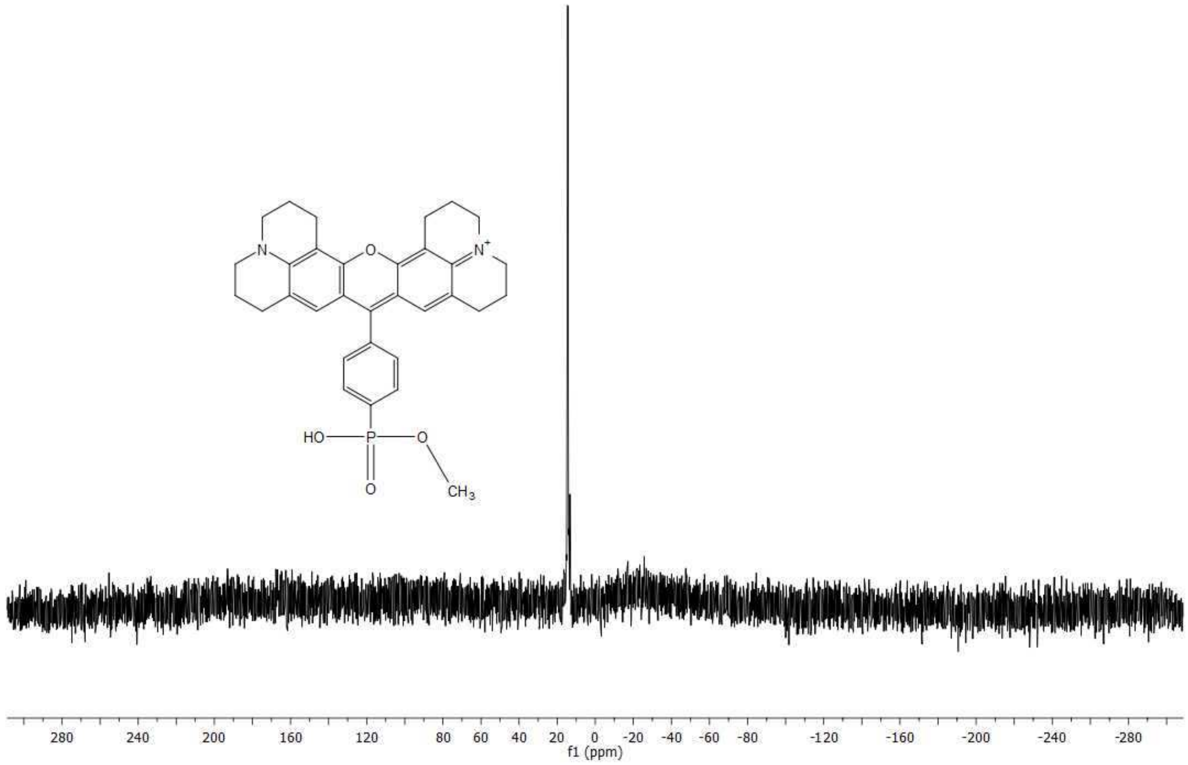

Figure **S-6.** ^{31}P NMR (243 MHz, MeOD): Phos-TexasRed dye (**10**).

Diethyl 5-((1-(3-((2*R*,4*S*)-2-*tert*-butyl-4-methyl-5-oxoimidazolidin-1-yl)propyl) -1*H*-1,2,3-triazol-4-yl)methoxy)pentylphosphonate (**11**)

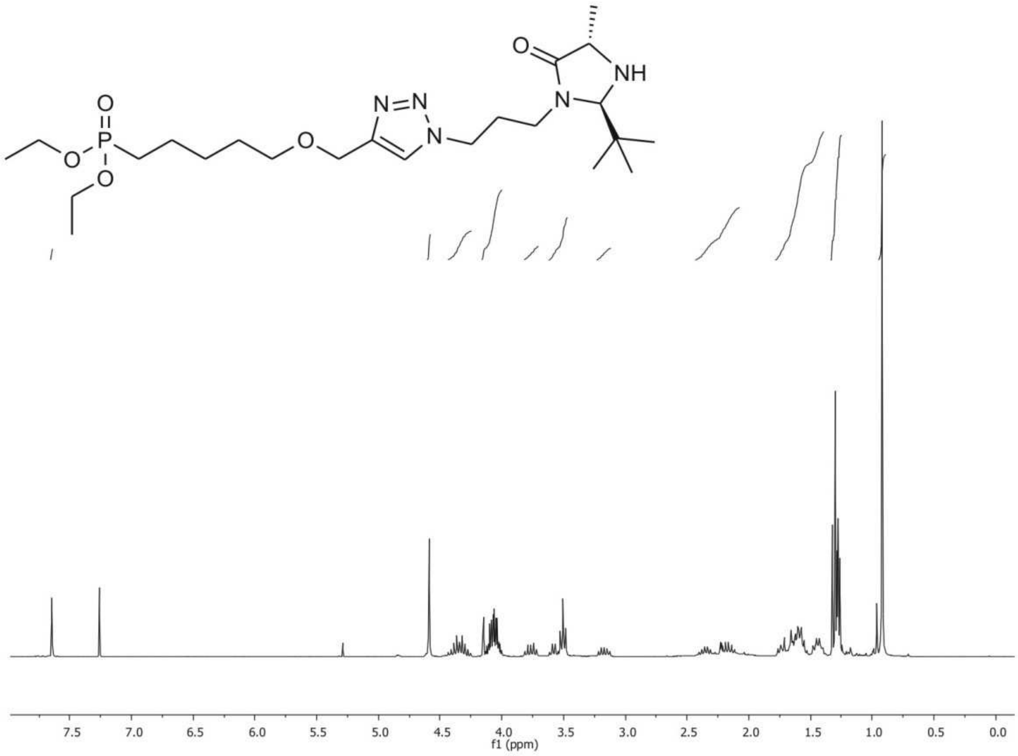

Figure **S-7**. ^{1}H NMR (300 MHz, CDCl$_3$): Diethyl 5-((1-(3-((2*R*,4*S*)-2-*tert*-butyl-4-methyl-5-oxoimidazolidin-1-yl) propyl)-1*H*-1,2,3-triazol-4-yl)methoxy)pentylphosphonate **(11).**

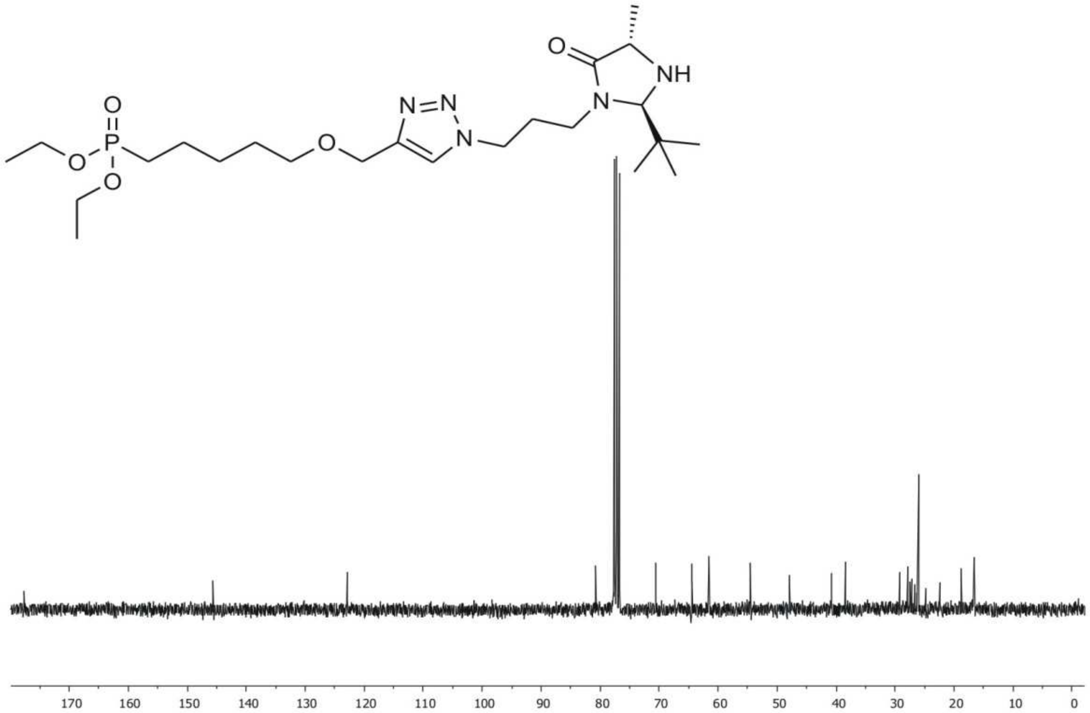

Figure **S-8:** ^{13}C NMR (75 MHz, CDCl$_3$): Diethyl 5-((1-(3-((2*R*,4*S*)-2-*tert*-butyl-4-methyl-5-oxoimidazolidin-1-yl) propyl)-1*H*-1,2,3-triazol-4-yl)methoxy)pentylphosphonate **11**.

1.3.5 References

[1] a) A. J. Bard, *Science* **1980**, *207*, 139–144. b) F. Teply, *Coll. Czech. Chem. Commun.* **2011**, *76*, 859–917. c) G. Pandey, M. K. Ghorai, S. Hazra, *Pure Appl. Chem.* **1996**, *68*, 653.

[2] For recent reviews, see: a) J. M. R. Narayanam, C. R. J. Stephenson. *Chem. Soc. Rev.* **2011**, *40*, 102–113. b) ref. 1b. c) T. P. Yoon; M. .A. Ischay; J. Du, *Nature Chem.* **2010**, *2*, 527–532. d) K. Zeitler, *Angew. Chem. Int. Ed.* **2009**, *48*, 9785–9789.

[3] C. Dai, J. M. R. Narayanam, C. R. J. Stephenson, *Nat. Chem*. **2011**, *3*, 140-145.

[4] a) M. A. Ischay, M. E. Anzovino, J. Du, T. P. Yoon, *J. Am. Chem. Soc*. **2008**, *130*, 12886–12887. b) J. Du, T. P. Yoon, *J. Am. Chem. Soc*. **2009**, *131*, 14604-14605. c) M. A. Ischay, Z. Lu, T. P. Yoon, *J. Am. Chem. Soc*. **2010**, *132*, 8572–8574. d) J. Du, L. Ruiz. Espelt, I. A. Guzei, T. P. Yoon, *Chem. Sci.* **2011**, *2*, 2115-2119.

[5] a) Z. Lu, M. Shen, T. P. Yoon, *J. Am. Chem. Soc*. **2011**, *133*, 1162–1164. b) Y.-Q. Zou, L.-Q. Lu, L. Fu, N.-J. Chang, J. Rong, J.-R. Chen, W.-J. Xiao, *Angew. Chem. Int. Ed.* **2011**, *50*, 7171–7175. c) M. Rueping, D. Leonori, T. Poisson, *Chem. Commun*. **2011**, *47*, 9615–9617. d) S. Maity, M. Zhu, R. S. Shinabery, N. Zheng, *Angew. Chem. Int. Ed.* **2012**, DOI: 10.1002/anie.201106162.

[6] a) A. E. Hurtley, M. A. Cismesia, Mi. A. Ischay, T. P. Yoon, *Tetrahedron* **2011**, *67*, 4442–4448. b) S. Lin, M. A. Ischay, C. G. Fry, T. P. Yoon, *J. Am. Chem. Soc*. 2**011**, *133*, 19350–19353.

[7] For selected recent examples: a) L. Furst, B. S. Matsuura, J. M. R. Narayanam, J. W. Tucker, C. R. J. Stephenson, *Org. Lett*. **2010**, *12*, 3104–3107. b) P. V. Pham, D. A. Nagib, D. W. C. MacMillan, *Angew. Chem. Int. Ed.* **2011**, *50*, 6119–6122. c) J. D. Nguyen, J. W. Tucker, M. D. Konieczynska, C. R. J. Stephenson, *J. Am. Chem. Soc.* **2011**, *133*, 4160-4163. d) M. Rueping, S. Zhu, R. M. Koenigs, *Chem. Commun*. **2011**, *47*, 12709–12711. e) A. McNally, C. K. Prier, D. W. C. MacMillan, *Science*, **2011**, *334*, 114–117. f) D. Kalyani, K. B. McMurtrey, S. R. Neufeldt, M. S. Sanford, *J. Am. Chem. Soc.* **2011**, *133*, 18566. g) D. A. Nagib, D. W. C. MacMillan, *Nature* **2011**, *480*, 224–228.

[8] For the formation of C-P bonds, see: a) D. P. Hari, B. König, *Org. Lett.* **2011**, *13*, 3852–3855. b) M. Rueping, S. Zhu, R. M. Koenigs, *Chem. Commun.* **2011**, *47*, 8679 - 8681. For the formation of C-S bonds, see: Y. Cheng, J. Yang, Y. Qu, P. Li, *Org. Lett.* **2011**, DOI: 10.1021/ol2028866. For the formation of C-N bonds, see: J. Xuan, Y. Cheng, J. An, L.-Q. Lu, X.-X. Zhang, W.-J. Xiao, *Chem. Commun.* **2011**, *47*, 8337–8339.

[9] a) D. A. Nicewicz, D. W. C. MacMillan, *Science* **2008**, *322*, 77–80. b) D. A. Nagib, M. E. Scott, D. W. C. MacMillan, *J. Am. Chem. Soc*. **2009**, *131*, 10875-10877. c) H.-W. Shih, M. N. Vander Wal, R. L. Grange, D. W. C. MacMillan, *J. Am. Chem. Soc*. **2010**, *132*, 13600–13603. d) M. Neumann, S. Füldner, B. König, K. Zeitler, *Angew. Chem. Int. Ed.* **2011**, *50,* 951-954.

[10] For seminal and recent examples of UV light promoted enantioselective photocatalytic reaction, see: a) A. Bauer, F. Westkämper, S. Grimme, T. Bach, *Nature* **2005**, *436*, 1139– 1140. b) Ch. Müller, A. Bauer, M. M. Maturi, M. C. Cuquerella, M. A. Miranda, T. Bach, *J. Am. Chem. Soc.* **2011**, *133*, 16689–16697. For a review on enantioselective photocatalysis using hydrogen-bonding templates, see: c) C. Müller, T. Bach, *Aust. J. Chem.* **2008**, *61*, 557-564.

[11] a) A. Atyaoui, L. Bousselmi, H. Cachet, Peng Pu, E. M. M. Sutter, *J. Photochem. Photobiol. A* **2011**, *224*, 71–79; b) F. Spadavecchia G. Cappelletti, S. Ardizzone, C. L. Bianchi, S. Cappelli, C. Oliva, P. Scardi, M. Leoni, P. Fermo, *Appl. Cat. B* **2010**, *96*, 314–322; c) M. K. Seery, R. George, P. Floris, S. C. Pillai, *J. Photochem. Photobiol. A* **2007**, *189*, 258–263; d) J. Tang, J. Ye, *Angew. Chem. Int. Ed.* **2004**, *43*, 4463–4466.

[12] An active area of current research is the use of inorganic semiconductors as photocatalysts for water splitting and hydrogen generation. For a recent review, see: a) X. Chen, S. S. Mao, *Chem. Rev*. **2007**, *107*, 2891–2959; b) R. M. Navarro, M. C. Álvarez-Galván, F. del Valle, J. A. Villoria de la Mano, J. L. G. Fierro, *ChemSusChem* **2009**, *2*, 471–485; c) H. Xu, R. Q. Zhang, A. N. C. Ng, A. B. Djurišić, H. T. Chan, W. K. Chan, S. Y. Tong, *J. Phys. Chem. C* **2011**, *115*, 19710-19715**;** d) M.

Antoniadou, P. Lianos, *Appl. Cat. B* **2011**, *107*, 188–196; e) M. Antoniadou, V. M. Daskalaki, N. Balis, D. I. Kondarides, C. Kordulis, P. Lianos. *Appl. Cat. B* **2011**, *107*, 188–196.

[13] a) H. Kisch, W. Schindler, *J. Photochem. Photobiol. A* **1993**, *103,* 257–264; b) H. Kisch, W. Linder, *Chem. Unserer Zeit* **2001**, *35*, 250–257; c) M. Gartner, H. Kisch, *Photochem. Photobiol Sci.* **2007**, *6*, 159–164; d) N. Zeug, J. Bücheler, H. Kisch, *J. Am. Chem Soc.* **1985**, *107*, 1459–1465; e) W. Hetterich, H. Kisch, *Chem. Ber.*1987, **121**, 15-20.

[14] L. Cermenati, C. Richter, A. Albini, *Chem. Commun*, **1998**, *7*, 805–806.

[15] For selective examples using metal-organic frameworks and polymers, see: a) Z. Xie, C. Wang, K. E. deKrafft, W. Lin, *J. Am. Chem. Soc.* **2011**, *133*, 2056–2059. b) C. Wang, Z. Xie, K. E. deKrafft, W. Lin, *J. Am. Chem. Soc.* **2011**, *133*, 13445–13454.

[16] For selective examples using organic semiconducting material, see: a) F: Su, S: C. M:, L: Möhlmann, M. Antonietti, X. Wang, S. Blechert, *Angew. Chem. Int. Ed.* **2010**, *49,* 657–660. b) F. Su, S. C. Mathew, G. Lipner, X. Fu, M. Antonietti, S. Blechert, X. Wang, *J. Am. Chem. Soc.* **2010**, *132*, 16299–16301.

[17] For selected recent reviews on organocatalysis, see: a) S. Bertelsen, K. A. Jørgensen, K. A. *Chem. Soc. Rev*. **2009**, *38*, 2178–2189. b) B. List, (Ed.) *Top. Curr. Chem*. **2010**, *291*, 1–456 (Asymmetric Organocatalysis). c) *Chem. Rev.* **2007**, *107* (12), 5413–5883 (special issue on organocatalysis).

[18] For a recent example combining organocatalysis and UV light TiO_2 photocatalyis, see: X.-H. Ho, M.-J. Kang, S.-J. Kim, E. D. Park, H.-Y. Jang, *Catal. Sci. Technol*. **2011**, ***1***, 923–926.

[19] P25 Degussa with an anatase: rutile ratio of 80:20 was used.

[20] a) P. Roy, S. Berger, P. Schmuki, *Angew. Chem. Int. Ed*. **2011**, *50*, 2904–2939; b) S. Higashimoto, N. Kitao, N. Yoshida, T. Sakura, M. Azuma, H. Ohue, Y. Sakata, *J. Catal.* **2009**, *266*, 279–285. c) The visible light absorption was attributed to surface deposits of organic material on TiO_2.

[21] a) S. U. M. Khan, M. Al-Shahry, W. B. Ingler Jr., *Science* **2002**, *297*, 2243-2245; b) X. Chen, L. Liu, P. Y. Yu, S. S. Maol, *Science* **2011**, *331*, 746–750.

[22] S. Füldner, R. Mild, H. I. Siegmund, J. A. Schroeder, M. Gruber, B. König, *Green Chem.* **2010**, *12*, 400–406.

[23] L. Xiong, F. Yang, L. Yan, N. Yan, X. Yang, M. Qiu, Y. Yu, *J. Phys. Chem. Solids* **2011** *72* , 1104–1109.

[24] D. Chatterjee, V. R. Patnama, A. Sikdar, P. Joshi, R. Misra, N. N. Rao. *J. Hazard. Mat*. **2008**, *156*, 435–441.

[25] A. Pfitzner, P. Pohla, *Z. Anorg. Allg. Chem.* **2009**, *635*, 1157–1159.

[26] M. Hopfner, H. Weiss, D. Meissner, F. W. Heinemann, H. Kisch, *Photochem. Photobiol. Sci.*, **2002**, *1*, 696–703.

[27] Procedure according to ref. 9a; for details please see the supporting information of this article.

[28] H. Kisch, *Adv. Photochem*. **2001**, *26*, 93–143.

[29] The flat band potential of $PbBiO_2Br$ in acetonitrile has not been determined. The expected shift of the potential is + 0.5 to + 1.0 V in acetonitrile compared to water, pH 7. This would be sufficient for the observed transformations. The potentials of $PbBiO_2Br$ in water were determined to 1.67 V for the valence band and -0.80 V for the conduction band.

[30] For the redox potential of Texas-Red, see: M. Torimura, S. Kurata, K. Yamada, T. Yokumaku, Y. Kamagata, T. Kanagawa, R. Kurane, *Analyt. Sci*. **2001**, *17*, 155–160.

[31] For recent reviews on dehydrogenative coupling using oxidation reagents: a) C.-J. Li, *Acc. Chem. Res.* **2009**, *42*, 335–344; b) C. J. Scheuermann , *Chem. Asian J***.** **2010**, *5*, 436 – 451; c) C. S. Yeung, V. M. Dong, *Chem. Rev*. 2011, **111**, 1215–1292.

[32] a) A. G. Condie, J.-C. González-Gómez C. R. J. Stephenson, J. Am. Chem. Soc. **2010**, 132, 1464. b) M. Rueping, C. Vila, R. M. Koenigs, K. Poscharny, D. C. Fabry, *Chem. Commun.* **2011**, *47*, 2360–2362.

[33] a) Y. Pan, C. W. Kee, L. Chen, C.-H. Tan, *Green Chem.*, **2011**, *13*, 2682-2685. b) Y. Pan, S. Wang, C. W. Kee, E. Dubuisson, Y. Yang, K. P. Loh, C.-H, Tan, *Green Chem***.**, **2011**, *13*, 3341–3344.

---

[34] Klussmann et al. reported slow racemization of the products under their oxidative reaction conditions: A. Sud, D. Sureshkumarz, M. Klussmann *Chem. Commun.*, **2009**, 3169–3171. Our stereochemical analysis also reveals only low *ee* values as similarly noted in previous reports by Rueping (see ref. 32b) and Tan (see ref. 33a).

[35] For a recent paper on the calculation of flat band potentials of semiconductor oxides, see: M. C. Toroker, D. K. Kanan, N. Alidoust, L. Y. Isseroff, P. Liaob, E. A. Carter, *Phys. Chem. Chem. Phys.*, **2011**, *13*, 16644–16654.

[36] D. A. Nicewicz, D. W. C. MacMillan, *Science* **2008**, *322*, 77-80.

[37] G. Laven, M. Kalek, M. Jezowska, J. Stawinski, *New J. Chem.*, **2010**, *34*, 967–975.

[38] G.-S. Jiao, J. C. Castro, L. H. Thoresen, K. Burgess.*Org. Lett.* **2003**, *5*, 3675-3677.

[39] Y. Yang, J. O. Escobedo, A. Wong, C. M. Schowalter, M. C. Touchy, L. Jiao, W. E. Crowe, F. R. Fronczek, R. M. Strongin, *J. Org. Chem*. **2005**, *70*, 6907-6912.

[40] P. Hubert Mutin, Gilles Guerrero and Andre´ Vioux, J. Mater. Chem., **2005**, *15*, 3761-3768.

[41] G. Jiao, J. C. Castro, L. H. Thoresen, K. Burgess, *Org. Lett.* **2003**, *5*, 3675-3677.

[42] D. Villemina, F. Simeona, H. Decreusa, P.-A. Jaffres, *Phosphorus, Sulfur and Silicon* **1998**, *133*, 209-213.

[43] L. Delain-Bioton, D. Villemin, P.-A. Jaffrès*, Eur. J. Org. Chem.* **2007**, 1274-1286.

[44] J. Hannant, J. H. Hedley, J. Pate, A Walli, Said A. Farha Al-Said, M. A. Galindo, B. A. Connolly, B. R. Horrocks, A. Houlton and A. R. Pike, ***Chem. Commun.***, **2010**, **46**, 5870.

[45] a) M. Rueping, C. Vila, R. M. Koenigs, K. Poscharny, D. Fabry, *Chem. Commun.* **2011**, *47*, 2360 - 2362. b) A. Sud, D. Sureshkumar, M. Klussmann, *Chem. Commun.* **2009**, 3169–3171

[46] A. Pfitzner, P. Pohla. *Z. Anorg. Allg. Chem*., **2009**, *635*, 1157-1159.

[47] P. Kubelka, F. Munk, *Z. Tech. Phys.* **1931**, *12*, 593–601.

1.4 Application of Microflow Conditions to Visible Light Photoredox Catalysis[i]

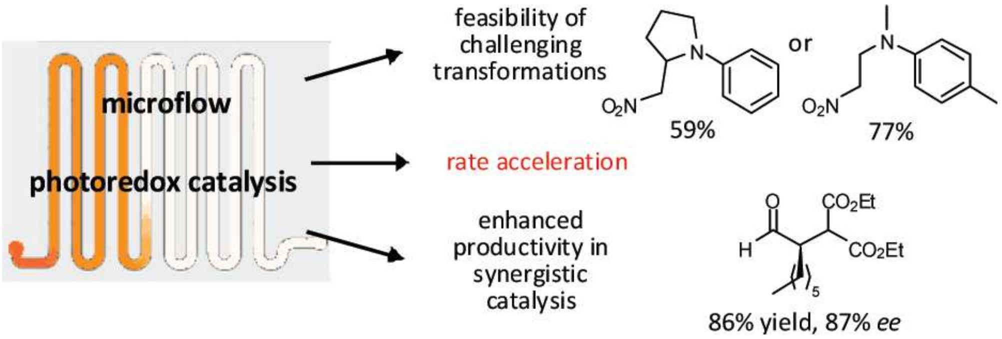
microflow
photoredox catalysis
feasibility of challenging transformations
59%
or
77%
rate acceleration
enhanced productivity in synergistic catalysis
86% yield, 87% ee

Applications of microflow conditions for visible light photoredox catalysis have successfully been developed. Operationally simple microreactor and FEP (fluorinated ethylene propylene copolymer) tube reactor systems enable significant improvement of several photoredox reactions using different photocatalysts such as $[Ru(bpy)_3]^{2+}$ and Eosin Y. Apart from rate acceleration, this approach facilitates previously challenging transformations of nonstabilized intermediates. Additionally, the productivity of the synergistic, catalytic enantioselective photoredox α-alkylation of aldehydes was demonstrated to be increased by 2 orders of magnitude.[ii]

---

[i] Reproduced with permission from: M.Neumann, K. Zeitler, *Org. Lett.,* **2012**, 14, 2658. Copyright 2012 American Chemical Society

[ii] All experiments were carried out by M.Neumann

1.4.1 Introduction

Visible light promoted photochemistry has already been recognized as a highly valuable tool for synthesis a century ago.[1] Only recently, photocatalytic (redox) transformations[2] have again been gaining increasing attention not only as interesting synthetic methodology in the context of green chemistry, but also due to their potential for developing new chemical reactions. While efficiency is typically not an issue for the classic laboratory scale, larger practical synthetic applications of photoredox catalysis and photosensitization are scarce as they often require specialized equipment. is required. Furthermore, the productivity in batch reactors is impeded by the limited light penetration through the reaction media as rationalized by Lambert-Beer´s law. In this context, continuous microflow methods present a valuable alternative approach to circumvent known drawbacks. Their high surface-to-volume ratio (small channel depth) not only ensures improved sample irradiation,[3] but also contributes to spatial homogeneity, resulting in greatly enhanced heat and mass transfer as compared to common batch systems.[4] Shortened reaction times and hence prevention of undesired side reactions may contribute to higher selectivity and product purity.[5] Although well established for UV photochemistry,[6] microreactors have until now only found limited applications for visible-light photocatalytic transformations.[7], [8] Likewise, there are only few reports on (homogenous) enantioselective catalysis in microflow systems;[9, 10] especially examples dealing with synergistic catalysis[11] have not yet been described. For instance, the merging of photoredox catalysis with organocatalysis as pioneered by MacMillan and co-workers[12, 13] provides access to important chiral α-alkylated aldehyde building blocks. Proceeding under the *simultanous* activation of both the nucleophile and the electrophile (within two distinct intersecting catalytic cycles) this powerful concept poses an additional challenge for the transfer to flow systems due to the inherent low concentration of the key intermediates.[11a]

1.4.2 Results and discussion

The obvious benefits of microstructured reactors known from classical photochemistry prompted us to investigate the influence of microreactors on visible-light photoredox catalysis. Herein, we disclose the successful development of flow conditions to both enhance productivity of (enantioselective) photocatalytic reactions and facilitate challenging transformations involving instable intermediates. We recently reported[14] that the photoredox dehalogenation[15] of activated halogenides upon irradiation with visible light can also be effected by simple organic dyes[16] and chose this

Eosin Y-mediated transformation as a first benchmark reaction for the evaluation of flow conditions using a commercially available microreactor setup.[17] In fact, within the flow regime, by employing similar conditions as described previously,[14] we noticed a tremendous acceleration for the dehalogenation of α-bromoacetophenone **1a** (Table 1, entry 1). Full defunctionalization yielding product **2a** could be reached in less than one minute. Similiarly, the conversion of the less activated α-carbonyl chloride **1b** (entry 2) was significantly increased without loss of selectivity as the aromatic bromide remained untouched.

Table 1. Acceleration of the Photocatalytic Reductive Dehalogenation within a Microreactor.[a]

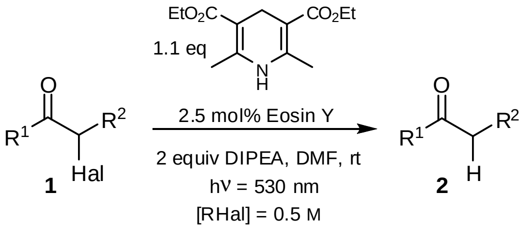

entry	R-Hal	product	$t_{reaction}$ batch	$t_{residence}$ microreactor (yield [%])
1	**1a** R^1 = Ph R^2 = H Hal = Br	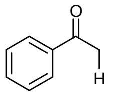 **2a**	12 h	40 s (97[b])
2	**1b** R^1 = (*p*-Br)BnO R^2 = Ph Hal = Cl	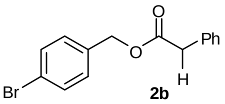 **2b**	18 h	20 min (89[b])

[a] Reaction conditions according to ref 14, c_{RHal} = 0.5 M. [b] Isolated yield.

We assume that in the presence of sacrificial electron donors (such as di*iso*propylethylamine (DIPEA) and/or Hantzsch ester) the strongly improved light penetration results in the efficient formation of the excited $^1EY^*$ and subsequent intersystem crossing to the corresponding triplet state $^3EY^*$ and hence in a higher concentration of the strong reductant Eosin Y radical anion $EY^{\bullet-}$ being capable to reduce the α-halogen carbonyl compounds. The observed temporary decolorization of the usually orange reaction mixture during irradiation might also indicate the accumulation of this active catalyst species.[18]

Encouraged by these initial results we turned our attention to Aza-Henry reactions, representing an example for oxidative α-amino C–H functionalizations *via* visible-light photoredox catalysis.[19] Quite a number of related transformations employing different nucleophiles[20] and also "follow-up" reactions[21] with the help of various photoredox catalysts[22] have been published recently. Upon irradiation, initial formation of an α-amino radical cation by reductive quenching of the photoexcited catalyst is commonly proposed to be the starting point for a subsequent generation of a electrophilic iminium intermediate **5**.[23] This can then be trapped by different nucleophiles[20] such as nitromethane in the case of aza-Henry reactions. Despite of known side reactions such as the undesired amide formation in non-degassed reaction mixtures these transformations only work well if stabilized iminium ions (e. g. stemming from benzylic amines such as *N*-aryl tetrahydro isoquinolines (THIQs)) are involved;[24] other tertiary amines, such as *N*-phenyl pyrrolidine **4b** or dimethylaniline **4c** are known to be difficult substrates that require long reaction times (Table 2, entries 3 and 4) and often fail to reach full conversion.[25] We envisioned our microflow conditions to be beneficial for these critical transformations as the improved mass transfer could ensure a fast reaction of the instable iminium intermediates with their corresponding reaction partner.[26]

To test our hypothesis, we launched aza-Henry reactions of different substrates under microflow conditions with conditions reported by Stephenson[19] using both $[Ru(bpy)_3]Cl_2$ **6** and $[Ir(ppy)_2(dtbbpy)]PF_6$ **7** as catalysts.

Having established an amine concentration of c = 0.25 mol/L as optimal, we started to compare our results regarding conversion, time and yield with the literature data of the optimized batch conditions.[19] With THIQ **4a** as "iminium precursor" we could solely identifiy the generation of the corresponding aza-Henry product with an approximate 20-30-fold acceleration without formation of any side products. Unlike to the batch conditions[19] the choice of Ru or Ir catalyst indeed slightly altered the reaction time, but did not influence the isolated yield of the product (see Table 2, entries 1 and 2). Remarkably, using 2 mol% of the Ir catalyst **7** the more challenging substrate *N*-phenyl pyrrolidine **4b** could smoothly be converted to the desired nitromethane addition product (entry 3). This clearly demonstrates the superiority of the flow conditions for aza-Henry reaction as compared to batch transformations. Likewise, we also noticed a considerable enhancement in reaction rate. Even substrates requiring the intermediate formation of a non-stabilized iminium ion containing a primary carbon atom such as aniline **3c** (which completely failed to react under batch conditions)[19] could be successfully converted to the correponding product **4c** (entry 4) in good yield within in the microreactor. However, we still could not achieve full conversion as further prolonged reaction times led to degradation of the Ir photocatalyst.

Table 2. Comparison of Visible Light Photoredox Aza-Henry Reactions conducted in Batch and Flow Reactor.[a]

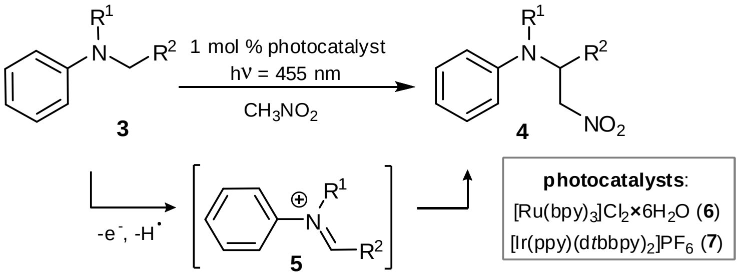

entry	product	rxn time[b] batch	Yield[b] (conversion)[b] [%]	residence time microreactor	Yield[c] (conversion)[d] [%]
1	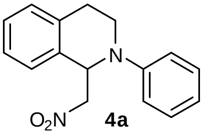 **4a**	10 h	92 (100)	30 min	93 (100)
2		20 h[e]	81 (100)	40 min	93 (100)
3	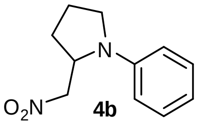 **4b**	72 h	27 (40)	60 min	59[f] (100)
4	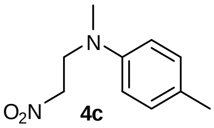 **4c**	72 h	0 (0)	130 min	77 (85[h])

[a] Conditions: 1 mol % Ir catalyst **7**, nitromethane, c_{amine} = 0.25 M. [b] According to ref 19. [c] Yield of isolated product. [d] Determined by GC analysis using an internal standard. [e] Conducted using 1 mol % of Ru catalyst **6**. [f] Volatile compound. [g] Longer residence times could not improve conversion due to photocatalyst bleaching.

We then sought to further investigate the full potential of the microflow approach. While in the previous examples the photocatalytically generated electrophiles were reacted with an excess of (pro)nucleophile, we wondered whether an extension to a more challenging enantioselective, cooperative catalytic system, such as the aminocatalyzed α-alkylation of aldehydes[12a, 14] would be possible. Here, it is critical to match the photoredox catalytic generation of the electron-deficient stabilized α-carbonyl alkyl radicals from the corresponding halides with the aminocatalyzed formation of the nucleophilic enamine intermediate; too low enamine concentrations would promote dehalogenation as side reaction. Additionally, one must ensure the sufficiently fast oxidation of the intermediary aminoradical to both allow for regeneration of the imidazolidinone catalyst **10** and ensure the availability of the reductive species of the photocatalyst. We were pleased to find that the cooperative catalysis using previously established Eosin Y-catalyzed conditions[14] indeed performed extremely well within the microreactor flow regime (Table 3). While no erosion of yield or enantiomeric excess was noticed, we could significantly shorten the reaction time. In an effort to lower the amount of organocatalyst we investigated the influence of the microflow conditions on the enamine formation by a stepwise reduction of the loading of catalyst **10** monitoring both yield and enantiomeric excess as a function of the reaction temperature. Residence times (Table 3) were each adjusted to reach full conversion. At 20 °C reduced amounts of amino catalyst (down to 10 mol%) still allowed for full conversion and good isolated yields, albeit requiring longer reaction times (entries 1, 4 and 7). Lowering the reaction temperature to -5 °C could considerably improve the enantioselectivity (as also previously observed for our batch conditions[14]) at a catalyst loading of 20 mol% (entries 2, 3). However, this turned out to be difficult for lower catalyst amounts, as we could not detect a comparable improvement and noticed even further prolonged reaction times (entries 5 and 8). Using 15 mol% of catalyst **10** at -5 °C, full conversion was not reached even after 2 hours (entry 6), indicating the limitations of the reducing the applied catalyst amounts.

Table 3. Comparison of Batch and Microflow for Cooperative Organocatalytic Photoredox α–Alkylation and Survey of Microflow Experiments with Catalyst **10** and Eosin Y.[a]

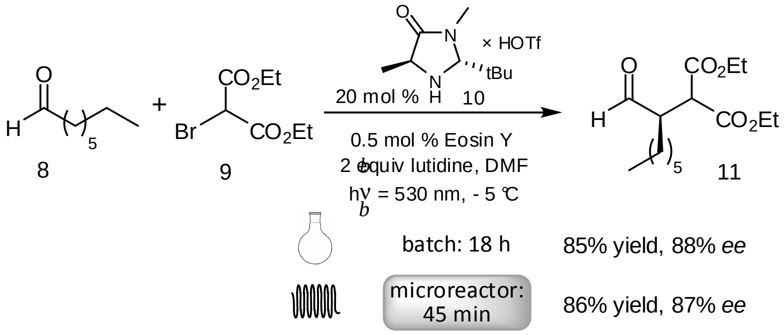

entry	mol% of catalyst **10**	T [°C]	residence time [min]	yield[c] [%]	*ee* [%]
1	20	20	45	87	76
2	20	0	45	88	81
3	20	-5	45	86	87
4	15	20	60	86	75
5	15	0	90	85	72
6	15	-5	120	82	n. d.
7	10	20	90	81	75
8	10	0	120	84	73
9	5	20	120	15[d]	n.d.

[a] Reactions conducted at $c_{\text{bromoalkyl}}$ = 0.5 M; yields refer to isolated product. [b] Determined *via* NMR after acetalization with (2*S*,4*S*)-2,4-pentanediol.[12a] [c] Isolated yields. [d] Determined by GC analysis.

We finally investigated the scalability of this approach. As microstructured flow reactors with their low flow rates and small internal volumes (ca. 100 µl) are ideally suited for reaction optimization, greater amounts of product are only available on "numbering up". In order to increase the material throughput we decided to construct a modified Booker-Milburn system[27] as micro photoreactor. Using the highly transparent, solvent-resistant and flexible FEP polymer (ID 0.8 mm) we coiled the tubing around a glass beaker which was equipped with an internal household fluorescent bulb (23 W);[17] the whole system was then placed in a cooling bath for temperature regulation. Our initial approach to directly transfer the optimized microreactor conditions to this 1st generation reactor (tubing length 8.5 m, V_{int}≈4.3 mL) failed due to clogging by 2,6-lutidine hydrobromide which precipitates from the reaction mixture. Higher flow rates in combination with ultrasonic treatment[28] and a slightly higher dilution (c=0.4 mmol/mL) prevented precipitation, but full conversion could not be attained.

Table 4. Comparison of the Performance of Different Reactors.[a]

entry	reactor type	yield[b] [%]	ee [%]	productivity [mmol/h]]	relative factor
1	batch	85	88	0.018	1
2	micro reactor	86	87	0.037	2
3	tube reactor	92	82	1.92	107

[a] Conditions as described in Table 3, but performed with $c_{bromoalkyl}$ = 0.4 M. [b] Isolated yield.

The 2nd generation set-up with an enlarged irradiation zone by coiling the tubing around the beaker in two layers (length 21 m, V_{int}≈10.5 mL) allows for full conversion at high flow rates and low temperature (maintaining the previously optimized residence time). Comparing the performance of the three examined reactor types (Table 4) clearly demonstrates the advantage of the tube flow system with respect to productivity.

In conclusion, we have developed microflow conditions for visible light photoredox processes, which can be significantly accelerated. Especially transformations involving the conversion of instable intermediates can be improved. Applying our simple, inexpensive tube reactor enantioselective, cooperative photocatalytic reactions can be easily scaled up, thereby generating useful amounts of enantiopure products. We expect the merging of flow chemistry and photoredox catalysis to be of broad utility for future applications.

1.4.3 Experimental section

1.4.3.1 General Methods

Unless noted otherwise, all commercially available compounds were used as provided without further purification

NMR spectra were recorded on a Bruker Avance 300 (300.13 MHz) and Bruker Ultrashield Plus 400 MHz (400.13 MHz) using the solvent peak as internal reference ($CDCl_3$: δ H 7.26; δ C 77.0). Multiplicities are indicated, s (singlet), d (doublet), t (triplet), q (quartet), quint (quintet), sept (septet), m (multiplet)); coupling constants (*J*) are in Hertz (Hz). All reactions were monitored by thin-layer chromatography using Merck silica gel plates 60 F_{254}; visualization was accomplished with UV light and/or staining with appropriate stains (anisaldehyde, phosphomolybdic acid). Standard chromatography procedures were followed (particle size 63-200 µm). Gas chromatographic analysis was performed on a Fisons Instrument GC 8130, (capillary column J&W Scientific DB-1 / 30 m x 0.25 mm / 0.25 µm film). The microflow reactors (M-111 effective volume 100 µL, channel width 0.6 mm channel depth 0.5 mm, borosilicate glass) were manufactured by Micronit Microfluidics and operated in a FutureChemistry Holding BV *Flow*Start B-200 setup. For temperature control below 0° C the reactor holder was mounted on an aluminium cooling device which was connected to a Huber Minichiller. Irradiation was performed with a modified FutureChemistry Holding BV photochemistry module equipped with two CREE XP-E Q4 green (530 nm) or royal blue (455 nm) LEDs operated at 700 mA (approx. 145 lm per LED). Irradiation within the tube reactor was accomplished using a household fluorescent bulb (23 W, OSRAM®, 6500 K, 1470 lm).

1.4.3.2 General procedures

General Procedure 1 (Reductive Dehalogenation):

The microreactor inlet tubing was connected to a gastight luerlock syringe while the outlet tubing was connected to a schlenk tube through septum. The whole system was deoxygenated by several cycles of evacuation and subsequent nitrogen backfill. The inlet tubing and syringe were removed while a nitrogen counterflow was maintained through the reactor.

In a 10 mL schlenk tube α-bromo-carbonyl compound (1 equiv.), Eosin Y (0.025 equiv.), diethyl 2,6-dimethyl-1,4-dihydropyridine-3,5-dicarboxylate and DIPEA (2 equiv.) were dissolved in DMF ($c_{haloalykl}$ = 0.5 mol/L). The mixture was degassed *via* freeze-pump-thaw approach (3 cycles) and transferred to the inlet syringe. The inlet syringe was reconnected to the reactor maintianing a nitrogen counterflow. The vacuum/nitrogen line at the schlenk tube was replaced by a nitrogen filled balloon.

Irradiation was started as the reaction mixture was pumped through the reactor with the indicated flow. The collected outlet mixture was analysed by GC and/or TLC prior to workup.

General Procedure 2 (Aza-Henry-Reaction):

Tertiary amine (1 equiv.) and photocatalyst as indicated were dissolved in nitromethane (c_{amine} = 0.25 mol/L). The mixture was transferred to a syringe and pumped through the irradiated reactor with the indicated flow. The collected outlet mixture was analysed by GC and/or TLC prior to workup. Purification of products was accomplished by column chromatography using the indicated eluents.

General Procedure 3 (α-Alkylation of Aldehydes):

The microreactor inlet tubing was connected to a gastight luerlock syringe while the outlet tubing was connected to a schlenk tube through septum. The whole system was deoxygenated by several cycles of evacuation and subsequent nitrogen backfill. The inlet tubing and syringe were removed while a nitrogen counterflow was maintained through the reactor.

In a 10 mL schlenk tube octanal (2 equiv), (2*R*, 5*S*)-2-*tert*-butyl-3,5-dimethylimidazolidin-4-one ×TfOH (0.2 equiv), Eosin Y (0.005 equiv), 2,6-lutidine (2 equiv) and diethylbromomalonate (1 equiv.) were dissolved in DMF (0.5 M). The mixture was degassed *via* freeze-pump-thaw and transferred to the inlet syringe. The inlet syringe was reconnected to the reactor maintaining a nitrogen counterflow. The vacuum/nitrogen line was replaced by a nitrogen filled balloon.

Irradiation was started and the reaction mixture was pumped through the reactor with the indicated flow using a syringe pump. The collected outlet mixture was analysed by GC and/or TLC prior to workup.

1.4.3.3 Experimental data for the products

Acetophenone (2a)

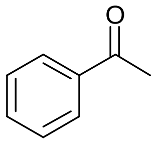

C_8H_8O
120.15 g/mol

according to the **general procedure 1**: flow 150 µL/min. GC analysis with internal standard (trichloroethylene) showed full conversion and yield >99%. GC (40° C, 1 min, 15.0° C/min, 250° C) t_R : = 2.7 min (trichloroethylene), 4.2 min (DIPEA), 6.9 min (acetophenone), 10.5 min (bromoacetophenone), 13.7 min (diethyl 2,6-dimethylpyridine-3,5-dicarboxylate).

4-Bromobenzyl 2-phenylacetate (2b)[i]

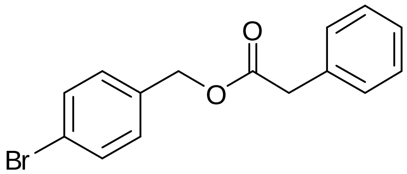

$C_{15}H_{13}BrO_2$
305.17 g/mol

according to the **general procedure 1**: flow 300 µL/h. 4-bromobenzyl 2-chloro-2-phenylacetate (1b) (125 mg, 368 µmol), 2,6-dimethyl-1,4-di-hydropyridine-3,5-dicarboxylate (103 mg, 405 µmol), Eosin Y (6.4 mg, 9.2 µmol), DIPEA (160 µl, 920 µmol) in 1.4 mL DMF 1.2 mL of the collected outlet was purified by SiO_2 column chromatography yielding 51 mg (76 %, i. e. 89% as only 85% of the reaction mixture were worked up)of 2b. R_f (hexanes/EtOAc 9/1) = 0.38. ^1H NMR (300 MHz, $CDCl_3$): δ 7.49 - 7.11 (m, 9H, ArH), 5.08 (s, 2H, Ar-CH_2-O), 3.67 (s, 2H, C(O)-CH_2-Ph). ^{13}C NMR (75.5 MHz, CDCl3) δ 171.3, 135.5, 134.8, 131.8, 129.8, 129.3, 128.7, 128.0, 127.3, 122.3, 65.8, 41.3. GC (40° C, 1 min, 15.0° C/min, 300° C): t_R(product) = 16.0 min, t_R(starting material) = 17.1 min.

1-(Nitromethyl)-2-phenyl-1,2,3,4-tetrahydroisoquinoline (4a)[ii]

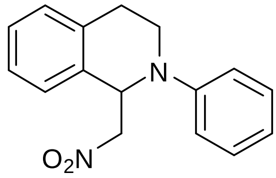

$C_{16}H_{16}N_2O_2$
268.31 g/mol

according to the **general procedure 2**: a) $[Ru(bpy)_3]Cl_2 \times 6H_2O$ flow 150 µL/h, GC analysis revealed yield >99%. b) $[Ir(dtbbpy)(ppy)_2]PF_6$ pump speed 200 µL/h, GC analysis revealed yield >99%. 2-phenyl-1,2,3,4-tetrahydroisoquinoline (205 mg, 980 µmol), $[Ir(dtbbpy)(ppy)_2]PF_6$ (10.5 mg, 9.8 µmol), nitromethane 3.9 mL. 3 mL of the collected outlet was filtered through a pad of SiO_2 with the aid of diethylether affording 183 mg (93 %) 4a as yellowish solid. GC (150° C, 1 min, 10° C/min, 300° C): t_R(starting material) = 9.6 min; t_R(product)

---

[i] Narayanam, J. M. R.; Tucker, J. W.; Stephenson, C. J. R. *J. Am. Chem. Soc.* **2009**, *131*, 8756.
[ii] Li, Z.; Li, C.-J. *J. Am. Chem. Soc.* **2005**, *127*, 3672.

= 13.0 min, ^{1}H NMR (300 MHz, $CDCl_3$) δ 7.35 - 7.10 (m, 6H), 7.04 - 6.94 (m, 2H), 6.91 - 6.81 (m, 1H), 5.56 (t, *J* = 7.2 Hz, 1H), 4.88 (dd, *J* = 11.8, 7.8 Hz, 1H), 4.57 (dd, *J* = 11.8, 6.6 Hz, 1H), 3.77 - 3.57 (m, 2H), 3.19 - 3.02 (m, 1H), 2.80 (dt, *J* = 16.4, 5.0 Hz, 1H). ^{13}C NMR (75.5 MHz, $CDCl_3$) δ 148.5, 135.3, 132.9, 129.5, 129.2, 128.2, 127.0, 126.7, 119.5, 115.1, 78.8, 58.2, 42.1, 26.5.

2-(Nitromethyl)-1-phenylpyrrolidine (4b)[ii]

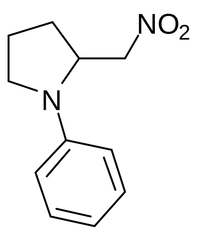

$C_{11}H_{14}N_2O_2$
206.24 g/mol

according to the **general procedure 2**: flow 100 µL/h; 1-phenylpyrrolidine (89 mg, 592 µmol), $[Ir(dtbbpy)(ppy)_2]PF_6$ (11 mg, 12 µmol); GC analysis revealed yield >99%. Dry loaded silica column (hexanes/ethyl acetate, 60/1) yielded 48mg of 4b as a yellow volatile oil. GC 150 °C 1min, 10° C/min, 300° C): t_R(starting material) = 10.6 min; t_R(product) = 13.9 min. ^{1}H NMR (300 MHz, $CDCl_3$) δ 7.36 - 7.26 (m, 2H), 6.80 (m, 1H), 6.75 - 6.65 (m, 2H), 4.64 (dd, *J* = 11.3, 3.0 Hz, 1H), 4.49 - 4.35 (m, 1H), 4.20 (dd, *J* = 11.3, 9.8 Hz, 1H), 3.51 (m, 1H), 3.23 (m, 1H), 2.21 - 2.01 (m, 4H). ^{13}C NMR (75.5 MHz, $CDCl_3$) δ 145.8, 129.7, 117.3, 112.0, 75.8, 57.5, 48.1, 29.3, 22.8.

N,4-Dimethyl-*N*-(2-nitroethyl)aniline (4c)[ii]

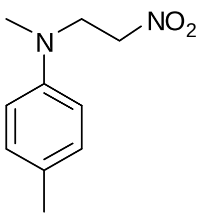

$C_{10}H_{14}N_2O_2$
194.23 g/mol

according to the **general procedure 2**: flow 45 µL/h; *N,N*,4-trimethylaniline (50 µL, 339 µmol), $[Ir(dtbbpy)(ppy)_2]PF_6$ (7.8 mg, 8.5 µmol), GC analysis revealed yield 85 %. Dry loaded silica column (hexanes/ethyl acetate, 19/1) yielded 51 mg of 4c as a yellow oil. GC 150 °C 1min, 10° C/min, 300°C): t_R(product) = 4.3 min, t_R(starting material) = 8.3 min. ^{1}H NMR (400 MHz, $CDCl_3$) δ 7.08 (d, *J* = 8.3 Hz, 2H), 6.67 (d, *J* = 8.7 Hz, 2H), 4.56 (t, *J* = 6.4 Hz, 2H), 3.97 (t, *J* = 6.4 Hz, 2H), 2.95 (s, 3H), 2.26 (d, *J* = 8.2 Hz, 3H). ^{13}C NMR (101 MHz, $CDCl_3$) δ 145.9, 130.0, 127.5, 113.2, 72.6, 51.0, 39.0, 20.3.

(*R*)-Diethyl 2-(1-oxooctan-2-yl)malonate (11)[iii]

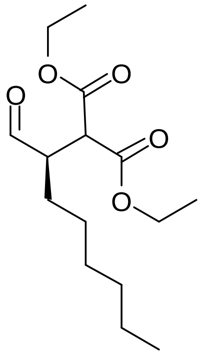

$C_{15}H_{26}O_5$
286.36 g/mol

according to the **general procedure 3**: composition and yields as indicacted in Table 4. Column chromatography (hexanes/diethylether 6/1) yielded 11 as colorless oil. ^{1}H NMR (300 MHz, $CDCl_3$): δ 9.74 (d, *J* = 1.2 Hz, 1H), 4.25 - 4.17 (m, 4H), 3.71 (d, *J* = 8.8 Hz, 1H), 3.12-3.05 (m, 1H), 1.75-1.45 (m, 2H,), 1.44-1.22 (m, 14H), 0.87 (m, 3H, CH2(CH2)4CH3); ^{13}C NMR (75.5 MHz, CDCl3) δ 201.6, 168.1, 168.0, 61.9, 61.8, 51.7, 50.2, 31.4, 29.3, 27.0, 26.4, 22.5, 14.1, 14.0, 14.0; GC (40° C, 1 min, 15.0° C/min): t_R (starting material) = 9.0 min; t_R (product) = 13.8 min, Enantiomeric excess was determined after acetalization of the aldehyde with (2*S*, 4*S*)-(+)-2,4-pentanediol *via* integration of ^{1}H NMR signals of the diastereomeric acetals ($CDCl_3$, both doublets) at 3.63 ppm (minor) and 3.59 ppm (major).

1.4.3.4 Overview on Cooperative Catalysis in Different Reactor Types and Calculation of Productivity

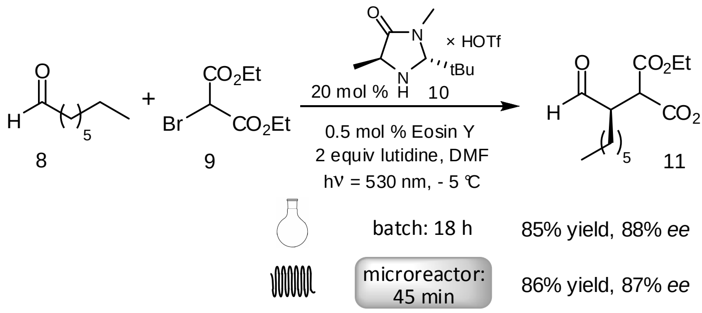

$$\boxed{productivity = \frac{yield[mmol]}{time[h]}}$$

Table 4. Comparison of the Performance of Different Reactors.[a]

entry	reactor type	yield[b] [%]	ee [%]	flow rate [ml/h]]	rxn size	productivity [mmol/h]]	relative factor
1	batch	85	88	0	0.4 mmol	0.018	1
2	micro reactor	86	87	0.134	0.4 mmo	0.037	2
3	FEP tube reactor	92	82	6.0	5.57 mmol	1.92	106

[a] Conditions as described in Table 3, but performed with $c_{bromoalkyl}$ = 0.4 M. [b]Isolated yield.

[iii] Nicewicz, D. A.; MacMillan, D. W. C. *Science* **2008**, *322*, 77.

Productivity:
According to the equation above the productivity balances the gained yield against the time needed. For the continous flow systems this calculates from the actual concentration of the material in the reaction mixture (which might differ from the indicated concentration (e. g. of bromomalonate in DMF $c_{bromoalkyl}$ = 0.5 resp. 0.4 mmol/L) according to a reagent if liquid reaction partners are involved.).

Batch:
reaction in classic reaction flask resp. reaction vial. The scale of the typical batch test reaction was 0.40 mmol according to our earlier descibed conditions.[iv]
Productivity: (0.85 • 0.40 mmol)/18 h = 0.018 mmol/h

Microreactor:
Flow rate: 100 µL /45 min = 0.134 mL/h; yield: 86%;[v] actual concentration: 0.39 mmol/1.2 mL = 0.325 mmol/L.
Productivity: 0.86 • (0.325 mmol/mL • 0.134 mL/h) = 0.037 mmol/h

FEP tube microcapillary reactor:
Flow rate: 6.0 mL/h; yield: 92%;[v] actual concentration: 5.57 mmol/16 mL = 0.348 mmol/L.
Productivity: 0.86 • (0.348 mmol/mL • 6.0 mL/h) = 1.92 mmol/h

1.4.3.5 Setup for Microreactor Experiments

Characteristic Data for the used Basic Microreactor M-111

Specifications
Outer dimensions 45.3 x 15.3 x 2.2 mm

Material: Borosilicate glass

Channel width (maximum): 600 µm

Channel depth: 500 µm

Effective reaction volume: 100 µL

[iv] Neumann, M.; Füldner, S.; König, B.; Zeitler, K. *Angew. Chem. Int. Ed.* **2011**, *50*, 951.
[v] Yield of isolated product determined from a defined certain aliquot of the reacted solution.

Schematic View on microreactor:

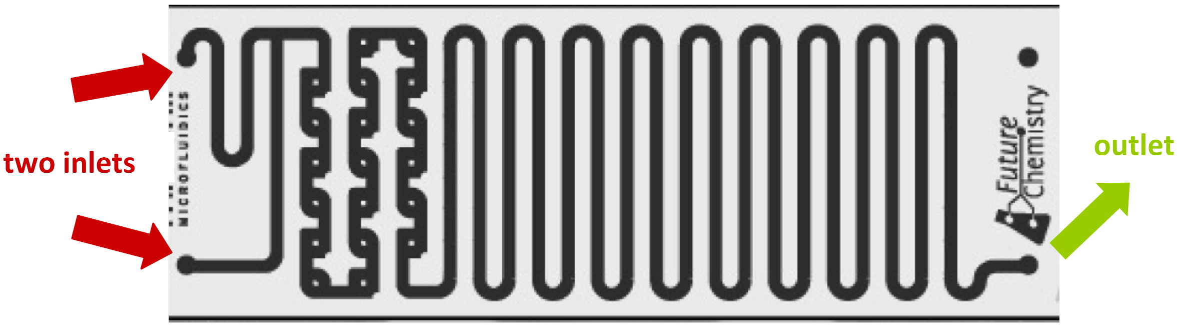
two inlets
MICROFLUIDICS
Future Chemistry
outlet

Continous flow is maintained with a standard syringe pump which (in our application) is used to slowly dispense the pre-mixed reaction mixture through the reactor at a defined flow rate.

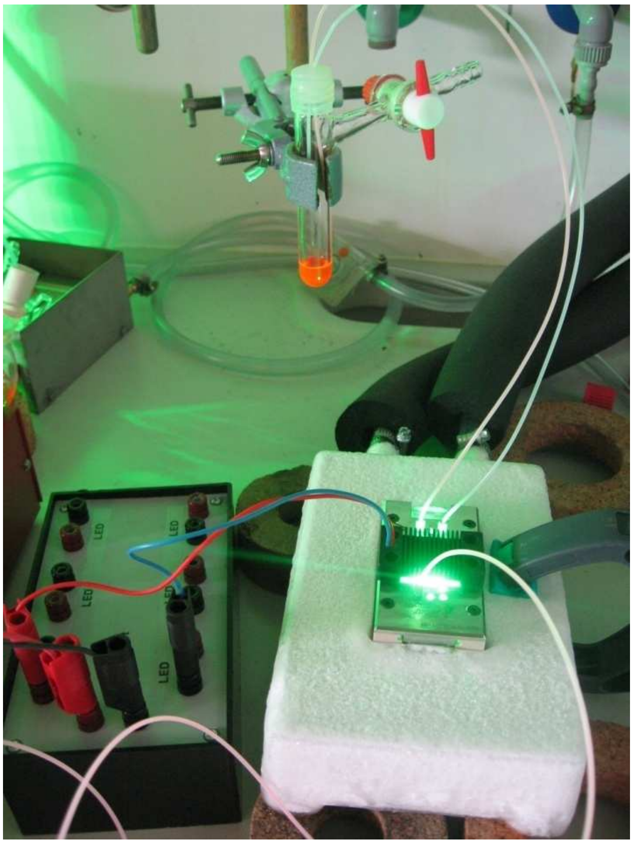
LED
LED
LED
LED
LED

Photomodule

2 LEDs[vi] were mounted on a cooling finned aluminium frame (black colored in the photo, *vide supra*), which also minimizes outgoing light from the irradiation system.

[vi] For detailed specification, please see "General Methods".

1.4.3.6 Setup for Upscale Experiments

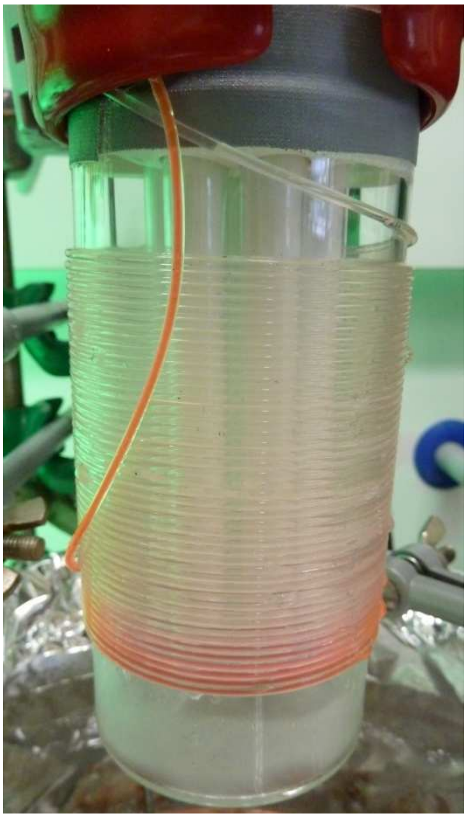

Figure 1: Reactor setup in operation; reaction mixture is reversibly discoloured over the course of reaction.

According to the setup described by Booker-Milburn[vii] a FEP tubing (fluorinated ethylene propylene) with 1.58 mm O.D. and 0.8 mm I.D. was coiled round a 60 mm Ø glass beaker with 53 windings per layer in two layers. An Osram® Dulux Superstar 23 W household fluorescent bulb[vi] was placed inside the beaker and fixed with duct tape. The whole setup was immersed in a cooling bath and operated according to general procedure 3.

First generation reactor used FEP tubing of a length of 8.5 m (corresponding to an internal volume $\underline{V_{int} = 4.3\ \mathrm{mL}}$).

Second generation tube reactor had a length of 21 m (corresponding to an internal volume $\underline{V_{int} = 10.5\ \mathrm{mL}}$) coiled around the lamp-containg beaker in two layers.

[vii] Hook, B. D. A.; Dohle, W.; Hirst, P. R.; Pickworth, M.; Berry, M. B.; Booker-Milburn, K. I. *J. Org. Chem.* **2005**, *70*, 7558.

References

---

[1] (a) Ciamician, G. *Science* **1912**, *36*, 385. Reviews on synthetic photochemistry: (b) Hoffmann, N. *Chem. Rev*. **2008**, *108*, 1052. (c) Hehn, J. P.; Bach. T. *Angew. Chem. Int. Ed.* **2011**, *50*, 1000.

[2] (a) Tucker, J. W.; Stephenson, C. R. J. *J. Org. Chem.* **2012**, 77, 1617. (b) Teplý, F. *Collect. Czech. Chem. Commun*. **2011**, *76*, 859. (c) Yoon, T. P.; Ischay, M. A.; Du, J. *Nat. Chem.* **2010**, *2*, 527. (d) Zeitler, K. *Angew. Chem. Int. Ed.* **2009**, *48*, 9785. (e) Narayanam, J. M. R.; Stephenson, C. R. J. *Chem. Soc. Rev.* **2011**, *40*, 102.

[3] For an example where stronger light emission proved unfavorable: Rueping, M.; Vila, C.; Koenigs, R. M.; Poscharny, K.; Fabry, D. C. *Chem. Commun.* **2011**, *47*, 2360.

[4] Recent reviews on microreactors: (a) Yoshida, J.; Kim. H.; Nagaki, A. *ChemSusChem* **2011**, *4*, 331. (b) Wiles, C.; Watts, P. *Chem. Commun.* **2011**, *47*, 6512. (c) Wegner, J, Ceylan, S.; Kirschning, A. *Chem. Commun*. **2011**, *47*, 4583. (d) *Microreactors in Organic Synthesis and Catalysis*; Wirth, T., Ed.; Wiley- VCH, Weinheim, 2008.

[5] Flow conditions lower products´ exposure to light and hence limit degradation. Additional advantages include both the possibility of rapid analysis and fast reaction screening as well as of parallelization to allow for simple scaling up, see ref. 4.

[6] (a) Oelgemöller, M.; Shvydkiv, O. *Molecules* **2011**, *16*, 7522. (b) Coyle, E: E:; Oelgemöller, M. *Photochem. Photobiol. Sci.* **2008**, *7*, 1313. (c) Wiles, C.; Watts, P. *Microreaction Technology in Organic Synthesis*; Taylor and Francis Group, Boca Raton, 2011, Ch. 5. (d) Fukuyama, T.; Rahman, T.; Sato, M.; Ryu, I. *Synlett* **2008**, 151.

[7] For recent examples on photocatalytic triplet sensitization, see: (a) Lévesque, F.; Seeberger, P. H. *Org. Lett.* **2011**, *13*, 5008. (b) Lévesque, F.; Seeberger, P. H. *Angew. Chem. Int. Ed.* **2012**, *51*, 1706.

[8] For a recent report on accelerating [Ru(bpy)$_3$]$^{2+}$-catalyzed reactions, see: (a) Bou-Hamdan, F. R.; Seeberger, P. H. *Chem. Sci.* **2012**, *3*, 1612. Two further applications of photoredox catalysis in flow systems have been reported while this manuscript was under review: (b) Tucker, J. W.; Zhang, Y.; Jamison, T. F.; Stephenson, C. R. J. *Angew. Chem. Int. Ed.* **2012**, DOI: 10.1002/anie.201200961. (c) Andrews, R. S.; Becker, J. J.; Gagné, M. R. *Angew. Chem. Int. Ed.* **2012**, 10.1002/anie.201200593.

[9] (a) Rasheed, M; Elmore, S. C.; Wirth, T. in *Catalytic Methods in Asymmetric Synthesis: Advanced Materials, Techniques and Applications*; Gruttadauria, M.; Giacalone, F*.*, Eds.; Wiley: Hoboken, 2011; 345. (b) Mak, X. Y.; Laurino, P.; Seeberger, P. H. *Beilstein J. Org. Chem.* **2009**, *5*, doi:10.3762/bjoc.5.19. Selected recent examples of enantioselective flow chemistry: (c) Odedra, A.; Seeberger, P. H. *Angew. Chem. Int. Ed.* **2009**, *48*, 2699. (d) Fritzsche, S.; Ohla, S.; Glaser, P.; Giera, D. S.; Sickert, M.; Schneider, C.; Belder, D. *Angew. Chem. Int. Ed.* **2011**, *50*, 9467.

[10] For a seminal example of enantioselective photochemistry in a micoreactor (≈ 2% *ee*), see: Maeda, H.; Mukae, H.; Mizuno, K. *Chem. Lett.* **2005**, *34*, 36.

[11] For a recent review, see: Allen, A. E.; MacMillan, D. W. C.; *Chem. Sci.* **2012**, *3*, 633.

[12] (a) Nicewicz, D. A.; MacMillan, D. W. C. *Science* **2008**, *322*, 77. (b) Nagib, D. A.; Scott, M. E.; MacMillan, D. W. C. *J. Am. Chem. Soc.* **2009**, *131*, 10875. (c) Shih, H.-W.; Vander Wal, M. N.; Grange, R. L.; MacMillan, D. W. C. *J. Am. Chem. Soc.* **2010**, *132*, 13600.

[13] For another example of cooperative photoredox organocatalysis (albeit with only poor enantioselectivity), see ref. 3.

[14] Neumann, M.; Füldner, S.; König, B.; Zeitler, K. *Angew. Chem. Int. Ed.* **2011**, *50*, 951.

[15] Narayanam, J. M. R.; Tucker, J. W.; Stephenson, C. J. R. *J. Am. Chem. Soc.* **2009**, *131*, 8756.

[16] For selected recent applications using organic photoredox catalysts, see: (a) Pan, Y.; Kee, C. W.; Chen, L.; Tan, C.-H. *Green Chem.* **2011**, *13*, 2682; (b) Pan, Y.; Wang, S.; Kee, C. W.; Dubuisson, E.; Yang, Y.; Loh, K. P.; Tan, C.-H. *Green Chem.* **2011**, *13*, 3341. (c) Hari, D. P.;

Schroll, P.; König; B. *J. Am. Chem. Soc.* **2012**, *134*, 2958. (d) Hari, D. P. ; B. König, B. *Org.Lett.* **2011**, *13*, 3852. (e) Zou, Y.-Q.; Chen, J.-R.; Liu, X.-P.; Lu, L.-Q.; Davis, R. L.; Jørgensen, K. A.; Xiao, W.-J. *Angew. Chem. Int. Ed.* **2012**, *51*, 784. For a review see: (f) Ravelli, D. Fagnoni, M. *ChemCatChem* **2012**, *4*, 169. (g) Pandey, G.; Ghorai, M. K.; Hajra, S. *Pure Appl. Chem.* **1996**, *68*, 653.

[17] For details see supporting information.

[18] (a) Neckers, D. C.; Valdes-Aguilera, O.M. *Adv. Photochem* **1993**, *18*, 315. For recent spectroelectrochemical studies on redox reactions of Eosin Y, see: (b) Zhang, J.; Sun, L.; Yoshida, T. *J. Electroanal. Chem.* **2011**, *662*, 384.

[19] Condie, A. G.; González-Gómez, J.-C.; Stephenson, C. R. J. *J. Am. Chem. Soc.* **2010**, *132*, 1464.

[20] For selected examples using Ir or Ru-based catalysts: (a) Freeman, D. B.; Furst, L.; Condie, A. G.; Stephenson, C. R. J. *Org. Lett.* **2012**, *14*, 94. (b) Rueping, M.; Zhu, S.; Koenigs, R. M. *Chem. Commun.* **2011**, *47*, 12709. (c) Xuan, J.; Cheng, Y.; An, J.; Lu, L.-Q.; Zhang, X.-X.; Xiao, W.-J. *Chem. Commun.* **2011**, *47*, 8337. See also ref. 3.

[21] (a) Rueping, M.; Leonori, D.; Poisson, T. *Chem. Commun.* **2011**, *47*, 9615. (b) Zou, Y.-Q.; Lu, L.-Q.; Fu, L.; Chang, N.-J.; Rong, J.; Chen, J.-R.; Xiao, W.-J. *Angew. Chem. Int. Ed.* **2011**, *50*, 7171.

[22] Examples with organic photocatalysts, see refs. 16a,b,d and 23a. For solid inorganic cats, see: (a) Rueping, M.; Zoller, J.; Fabry, D. C.; Poscharny, K.; Koenigs, R. M.; Weirich, T. E.; Mayer, J. *Chem. Eur. J.* **2012**, *18*, 3478. (b) Cherevatskaya, M.; Neumann, M.; Füldner, S.; Harlander, C. ; Kümmel, S.; Dankesreiter, S.; Pfitzner, A.; Zeitler, K.; König, B. *Angew. Chem. Int. Ed.* **2012**, DOI: 10.1002/anie.201108721. (c) Xie, Z.; Wang, C.; deKrafft, K. E.;. Lin, *W. J. Am. Chem. Soc.* **2011***, 133*, 2056.

[23] For selected recent mechanistic studies, see: (a) Liu, Q.; Li, Y.-N.; Zhang, H.-H.; Chen, B.; Tung, C.-H.; Wu, L.-Z. *Chem. Eur. J.* **2012**, *18*, 620. (b) see ref. 20a.

[24] Successful photoredox reactions of non-benzylic amines often follow a different α-amino radical mechanism: (a) McNally, A.; Prier, C. K.; MacMillan, D. W. C. *Science* **2011**, *334*, 1114. (b) Kohls, P.; Jadhav, D.; Pandey, G.;Reiser, O. *Org. Lett.* **2012**, *14*, 672. (c) Miyake, Y.; Nakajima, K.; Nishibayashi, Y. *J. Am. Chem. Soc.* **2012***, 134*, 3338.

[25] For other documented examples (rxn time up to 96 h) please refer to refs. 16a and d.

[26] The transformation of instable intermediates under flow conditions is known: Yoshida, J. *Flash chemistry: fast organic synthesis in microsystems*, Wiley, Hoboken, 2008. For the recent transformation of instable silyl enolethers, see: Kurahashi, K.; Takemoto, Y.; Takasu, K. *ChemSusChem* **2012**, *5*, 270.

[27] Hook, B. D. A.; Dohle, W.; Hirst, P. R.; Pickworth, M.; Berry, M. B.; Booker-Milburn, K. I. *J. Org. Chem***.** **2005**, *70*, 7558.

[28] Representative examples for application of ultrasound in continuous flow reactions, see: (a) Shu, W.; Pellegatti, L.; Oberli, M. A.; Buchwald, S. L. *Angew. Chem. Int. Ed.* **2011**, *50*, 10665. (b) Hartman, R. L.; Naber, J. R.; Zaborenko, N. Buchwald, S. L.; Jensen; K. F. *Org. Proc. Res. Dev.* **2010**, *14*, 347. (c) Horie, T.; Sumino, M.; Tanaka, T.; Matsushita, Y.; Ichimura, T.; Yoshida, J.-i. *Org. Proc. Res. Dev.* **2010**, *14*, 405.

1.5 A Cooperative Hydrogen Bond Promoted Organophotoredox Catalysis Strategy for Highly Diastereoselective, Reductive Enone Cyclizations

1.5.1 Introduction

Mild and efficient methods for catalytic C-C bond formations are of central importance to both academic and industrial research; here, lately green and sustainability aspects pose an additional major challenge for synthetic organic chemists. Over the last decade organocatalysis has successfully started to seize the mantle and especially multicatalysis concepts, combining robust, metal-free catalysts, allow access to complex (asymmetric) structures and many formerly elusive transformations.[1] Only recently has the combination of organocatalytic activation modes[2] with other sustainable methods begun to evolve. In this context in particular the merger with visible light photoredox chemistry[3] has emerged as a powerful approach as evidenced by pioneering examples by MacMillan[4], Rueping[5] and Rovis[6]. Secondary amine and NHC catalysis were successfully combined in synergistic processes with $[Ru(bpy)_3]^{2+}$–mediated photoredox catalysis. While metal-complex promoted photocatalysis – often based on expensive Ru and Ir of limited availability[7] – is still mandatory for some applications, we have recently developed a photoredox protocol demonstrating the applicability of Eosin Y as a potent metal-free surrogate for $[Ru(bpy)_3]^{2+}$.[8]

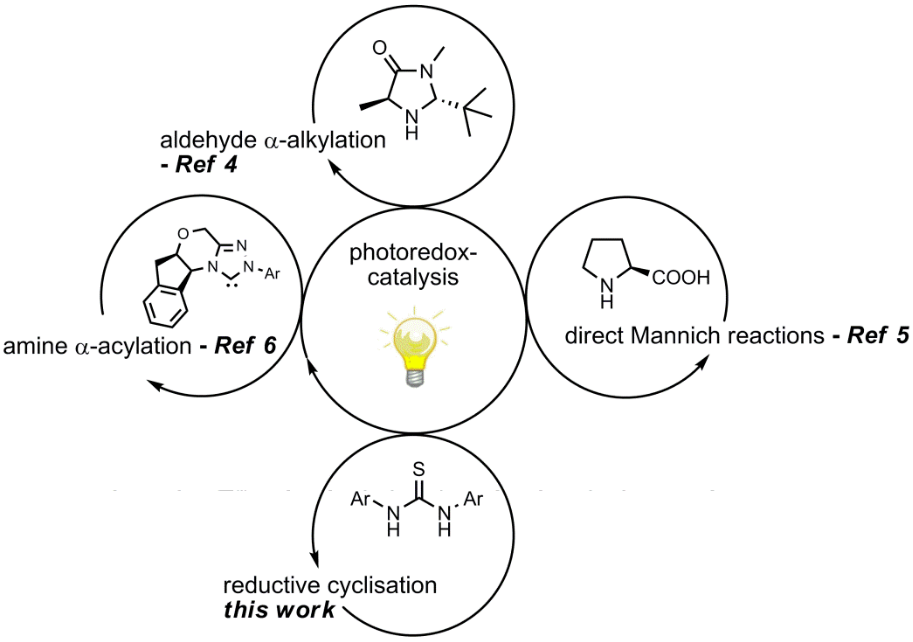

Scheme 1. Multicatalytic photoredox approaches.

In this context we could also show that simple *organic* photoredox catalysts can participate in highly enantioselective synergistic transformations having two catalytic cycles working perfectly in concert.[8a] Continuing this theme, we questioned whether the photoredox multicatalysis strategy could be extended to other organocatalytic activation modes. Apart from the above mentioned successful examples to combine photoredox catalysis with amine resp. NHC catalysis, a merger with metal-free carbonyl activation has not yet been described. As hydrogen-bonding catalysis,[9] mimicking enzymatic general acid catalysis, is well-known for being a powerful tool for mild LUMO-lowering carbonyl activation, we sought to transfer this attractive alternative to Lewis acids to *cooperative photoredox catalysis* for activating carbonyl groups towards electron acceptance. We anticipated that this non-covalent, weak interaction would be favorable in terms of catalyst loading to avoid the need of (super)stoichiometric amounts of Lewis acid activators.

Herein, we describe a highly diastereoselective H-bond promoted reductive cyclization of bisenones *via* cooperative organic photoredox catalysis. These reactions proceed efficiently and fast at room temperature using simple commercially available, inexpensive material as catalysts.

1.5.2 Results and Discussion

As outlined in scheme 2, we considered the versatile class of SET (*single electron transfer*)-promoted cyclization reactions of bisenones as a suitable model system to prove our concept. These cyclizations are not only interesting due to the formal umpolung[10] triggered by electron donation and hence the possible access to 1,4-difunctionalized products, but also have already been studied extensively for a number of catalyst systems and initiators. Early examples use stannyl radical chain reactions,[11] alternative methods range from metal catalysis,[12] arene radical anions[13] and electrochemical activation[12b, 14] to photocatalysis.[15] Besides the common need of high loadings of additives and/or catalysts product- and diastereoselectivity present possible issues.

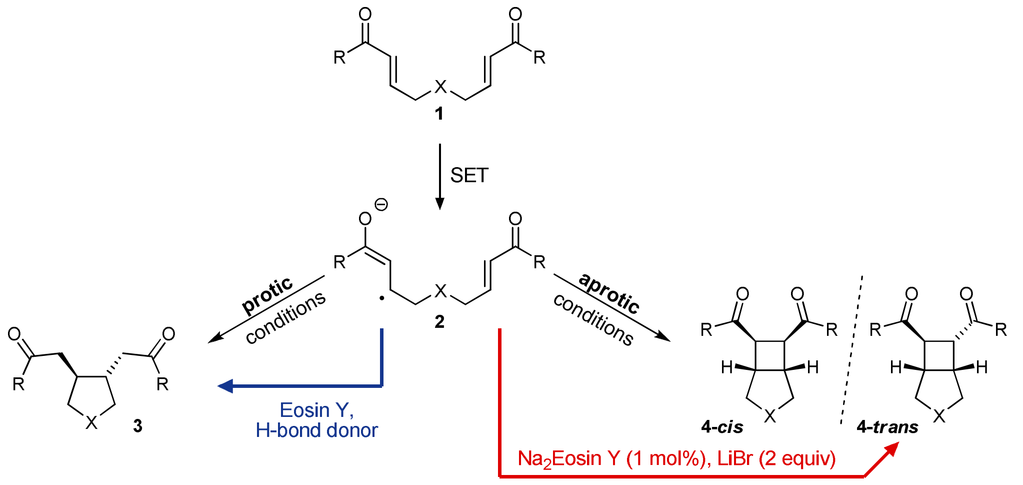

Pandey 1994: DMF/^{i}PrOH/H$_2$O, $\lambda = 405$ nm, DCA (40 mol%), PPh$_3$ (60 mol%)
Bauld/Krische 2004: electrochemical in 1.6 M AcOH
Yoon 2011: CH_3CN/HCOOH (5 equiv)/DIPEA (10 equiv) fluorescent bulb, $[Ru(bpy)_3]^{2+}$ (2.5 mol%)

Krische 2001: DCE, Co(dpm)2, $PhMeSiH_2$ (4 equiv)
Krische 2004: THF, chrysene radical anion sodium salt
Yoon 2008: CH_3CN/ DIPEA (2 equiv)/ $LiBF_4$ (2 equiv) 275 W GE sunlamp, $[Ru(bpy)_3]^{2+}$ (5 mol%) *cis*-selective

Scheme 2. Single electron transfer triggered electrocyclization of bisenones. [14b, 16]

The fate of the initially formed distonic radical is known to be strongly dependent on the reaction conditions. While the presence of protic solvents or acids as activators causes protonation resp. H-transfer of the primarily cyclized product generating the monocyclic products **3** in a reductive cyclization, non-protic conditions favor the formation of the bicyclic, formal [2+2]-cycloaddition products **4** in a *netto* redox neutral reaction.[14b, 15c] Using *iso*-propanol solvent mixtures with DCA (dicyanoanthracene) as photoredox catalyst Pandey describes the formation of **3** under irradiation ($\lambda = 405$ nm).[15a-c] In the presence of $[Ru(bpy)_3]^{2+}$ as photocatalyst Yoon and co-workers[17] could either access bicyclic products **4-*cis*** using an excess of $LiBF_4$ as Lewis acid activator or reductively cyclize the tethered bisenones to yield *trans*-configurated products **3** if superstoichiometric amounts of HCOOH were applied.

Our investigation began with an examination of the general feasibility to substitute $[Ru(bpy)_3]^{2+}$ with Eosin in the presence of Lewis acids. Both the intramolecular as well as the crossed intermolecular formal [2+2]-cycloaddition of acyclic enones could be realized using the organophotoredox catalyst with excellent yields and diastereoselectivity. Albeit, unlike to former results we could only detect the (thermodynamically more stable)[13] *trans*-products **6** and **9.**[i]

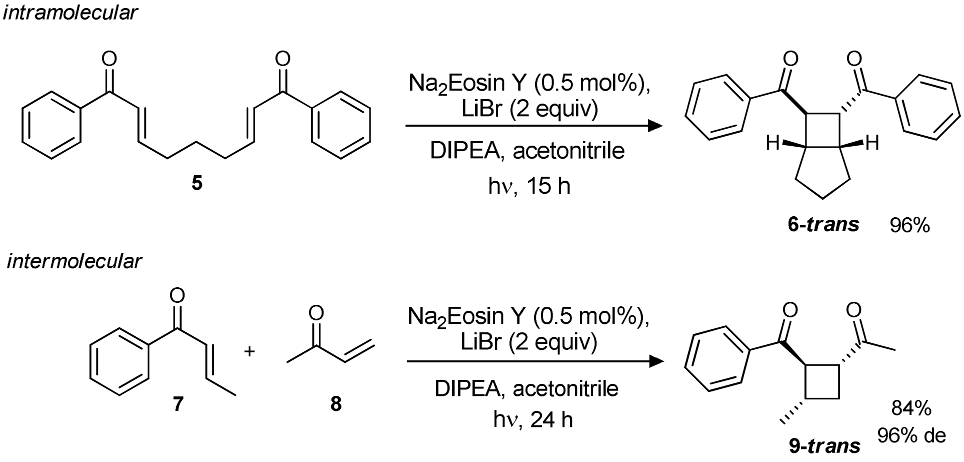

Scheme 3: Intra- and intermolecular formal [2+2] cycloadditions of enones with Eosin Y as photoredox catalyst.

Having demonstrated that Eosin could serve as a powerful organic photoredox catalyst to access ketyl radical anions we next turned our attention to combining Eosin in a cooperative manner with hydrogen-bond donor catalysts for carbonyl activation. We speculated that this catalytic combination with its additional suitability to mediate proton transfers would allow for selective reductive bisenone cyclizations. As common and easily accessible hydrogen-bonding organocatalysts performing as Lewis-acid type surrogates for carbonyl activation we chose TADDOL **11**[9e, 18] and thiourea **12** ("Schreiner´s catalyst").[19] As revealed in table 1 our design rendered successful with both catalysts providing the expected, more stable *trans*-configurated racemic cyclopentanes **10** with excellent diastereoselectivity, but in initially poor to moderate yield requiring long reaction times of up to 48 h for full conversion. Control experiments without irradiation left the substrate unchanged; neither could we observe reductive cyclization if organocatalyst or Eosin Y were missing (entries 9 and 10) verifying the need of all employed reaction components. Due to solubility problems with the acidic TADDOL **11** in the presence of DIPEA good yields only were obtained when DIPEA hydrochloride was used as reductive quencher instead. Nevertheless thiourea **12** proved to be superior regarding solubility and activity.

Quenching of the α-carbonyl radical resulting from the reductive cyclization *via* oxidation and hydride transfer or direct transfer of a hydrogen radical each by the radical cation of DIPEA stemming from reductive quenching of the photocatalyst might be critical for the successful catalysis.[20] As DIPEA is a rather poor hydride donor we rationalized that exchanging DIPEA a more powerful donor such as the commonly used Hantzsch ester, which also can be used as reductive quencher[21], could be beneficial; indeed we found the reaction to be significantly accelerated acceleration. After a survey to optimize the solvent the reaction time could be reduced to 3.5 h and in the presence of 1 equivalent DIPEA as additive even to 2h, respectively. For irradiation we used an array of two green 1 W LEDs[22] (emission maximum: λ=530 nm) that ideally matches the absorption maximum of Eosin Y. Chancing the light source to a more energy consuming 23 W household fluorescent bulb resulted in elongated reaction time, but afforded comparable yield.

---

[i] As our conditions if compared to Yoon´s experiments (23 W fluorescent bulb resp. green LEDs instead of a 275 W sunlight lamp with a considerable percentage of UV irradiation) resulted in longer reaction times (14 h *vs.* 1 h), we assume this to be responsible for obtaining the alternate relative stereochemistry. For the spectral distribution of a 275 W sunlight lamp (GE), see: T. P. Dryja, G. P. Kimball, D. M. Albert, . *Invest. Ophthalmol. Vis. Sci.* **1980**, *19*, **559.**

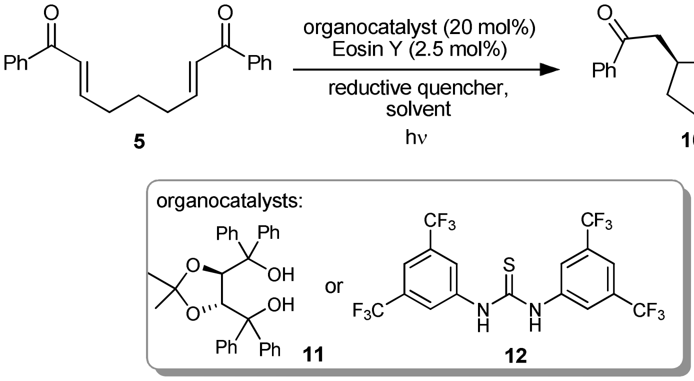

entry	organocatalyst	reductive quencher	solvent	time [h]	yield of **10** [%][a, b]
1	**1**	DIPEA (2 equiv)	MeCN	48	traces
2	**1**	DIPEA (2 equiv)	THF	48	8
3	**1**	DIPEA x HCl (2 equiv)	THF	48	62
4	**2**	DIPEA (2 equiv)	MeCN	48	78
5	**2**	HE (1.1 equiv)	MeCN	12	84
6	**2**	HE (1.1 equiv)	DCM	3.5	93
7	**2**	HE (1 equiv) + DIPEA (1 equiv)	DCM	2	92
8	**2**	HE (1 equiv) + DIPEA (1 equiv)	DCM	5.5	89[c]
9	**-**	HE (1 equiv) + DIPEA (1 equiv)	DCM	48	0
10[d]	**2**	HE (1 equiv) + DIPEA (1 equiv)	DCM	48	0

Table 1. Optimization of reaction conditions. [a]Typical procedure: all components were dissolved in a schlenk tube and degassed by freeze pump thaw cycles and irradiated for the indicated time by two green LEDs (530 nm, 1 W each). [b]isolated yield. [c] A 23 W fluorescent bulb was used instead of LEDs. [d]without Eosin Y.

With these best conditions in hand we investigated the scope of this reaction in electrocyclization of symmetrical bisenones. All tested aryl bisenones with both electron withdrawing and donating substitution pattern proved to be very good substrates yielding *trans*-selective the desired cyclopentanes in very good yields and short reaction time (entries 1-3). In the case of aliphatic enones (entries 4 and 5) the active photocatalyst species Eosin Y radical anion turned out to have a insufficient reduction potential (-1.06 V *vs.* SCE) as only trace amounts of product could be observed after 24 h reaction time. Usage of the more potent [Ir(d*t*bbpy)(ppy)$_2$]PF$_6$[23] (Ir (III)/Ir(II) -1.51 V *vs.* SCE) instead gave the product in excellent yield and short reaction times. Also heterocycles (entry 6) and cyclohexanes (entry 7) were obtained analogously whereas cycloheptanes were not accessible (entry 8). A whole different reactivity was observed shortening the alkylchain to four carbons. Along with the Baldwin rules[24] the expected 4-*exo*-trig cyclization should result in the formation of a cyclobutane but we observed formation of rearranged cyclopentene in good yield (enty 9). As 5-*endo*-trig cyclizations are strongly disfavoured and the formation *via* Rauhut Currier pathway[25] can be ruled out[26] the product might result from a vinylogous deptoronation/enolate addition sequence promoted by a photogenerated strong base; a ring expansion-rearrangement- oxidation-deprotonation sequence cannot be ruled at that time.

entry	substrate	product	time [h]	yield [%]
	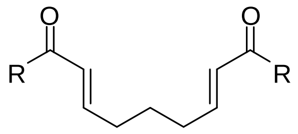	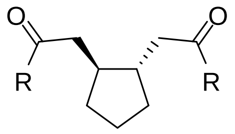		
1	R = Ph		2	92
2	R = PMP (*p*-methoxy phenyl)		1.5	95
3	R = *p*-Cl-C_6H_4		2.5	96
4[b]	R = CH_2CH_2Ph		2.5	91
5[b]	R = Me		0.5	93
	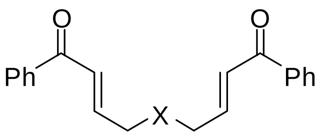	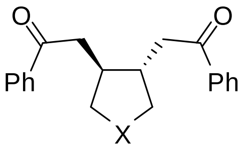		
6	X = O		8	95
7	X = CH_2CH_2		4.5	91
8	X = $CH_2CH_2CH_2$		24	0
9[c]	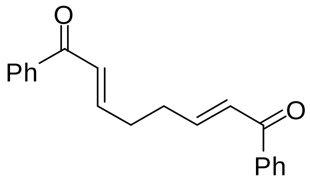	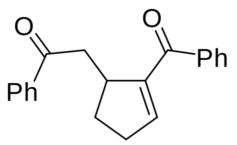	48	71

Table 2. Substrate scope of symmetrical enones. [a)]Thiourea **12** (20mol%), Eosin Y (2.5 mol%), Hantzsch ester (1 equiv), DIPEA (1 equiv), DCM (c_{enone} = 0.2 mol/l). [b)] Ir(d*t*bbpy)(ppy)$_2$PF$_6$ (1 mol%) was used instead of Eosin Y. [c)]no Hantzsch ester, DIPEA (2 equiv) instead.

In order to investigate the scope of this catalytic approach we proceeded screening a variety of unsymmetrical enones with respect to functional group tolerance. All substrates containing ester, ketone or nitrile Michael systems smoothly underwent reductive cyclization. Also thioester and electron deficient alkyne resulted in the desired products in good to excellent yields. Terminal alkenes (entries 9 and 10) did not react at all indicating the lacking stabilization of intermediary radical prior to final oxidation step.

entry	substrate	product	time [h]	yield [%]
	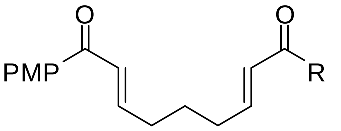	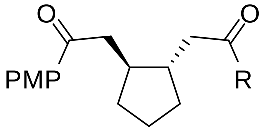		
1	R = OMe		6	85
2	R = SEt		5.5	86
3	R = Me		5	87
4	R = ^{t}Bu		4	95
5	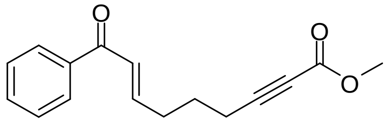	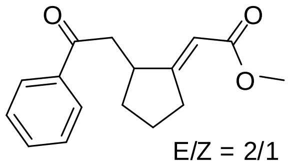 E/Z = 2/1	8	82
6	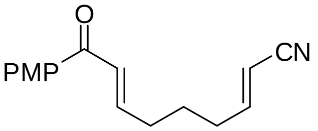	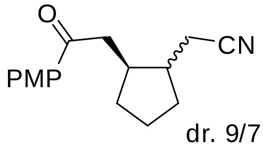 dr. 9/7	7.5	85
	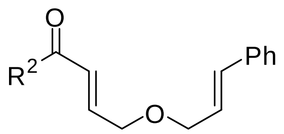	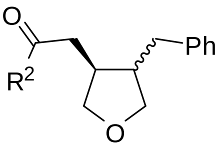		
7[b]	R^2 = Ph		12	0
8[b]	R^2 = CH$_2$CH$_2$Ph		2.5	72[c]
	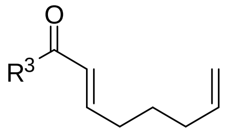	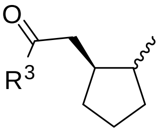		
9[b]	R^3 = Ph		12	0
10[b]	R^3 = CH$_2$CH$_2$Ph		12	0

Table 3. Substrate scope of unsymmetrical enones. [a)]Thiourea 12 (20mol%), Eosin Y (2.5 mol%), Hantzsch ester (1 equiv), DIPEA (1 equiv), DCM (c_{enone} = 0.2 mol/l). [b)] Ir(d*t*bbpy)(ppy)$_2$PF$_6$ (1 mol%) was used instead of Eosin Y. [c)]1:1 diastereomeric mixture

The propsed mechanistic picture as deduced from of the above observations starts with the reductive quenching of excited state Eosin Y by either DIPEA or Hantzsch ester generating the strong reductant Eosin Y radical anion which then can reduce hydrogen bond activated aryl ketones returning to its groundstate. The resulting 1,4-distonic radical anion undergoes 5-*exo*-trig cyclization to the corresponding Michael acceptor generating a stabilized α-carbony radical which is quenched either by oxidation through the radical cation of the reductive quencher and subsequent hydride transfer or *via* direct hydrogen radical transfer from the reductive quencher radical cation.

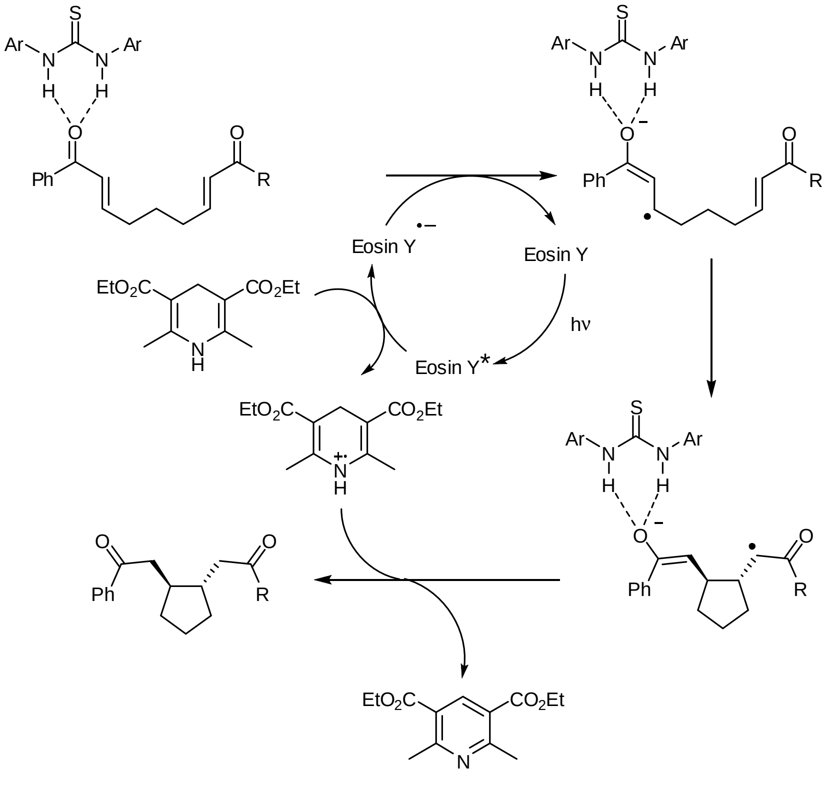

Scheme 4. Proposed mechanism of cooperative reductive cyclization.

To prove our mechanistic picture we used d$_2$-Hantzsch ester **13** as hydride source and were able to observe a 60% deuteration on the expected position. Moreover, the intermediary α-carbonyl radical could be trapped by allyltributyl stannane in analogy to a very recent publication of Reiser et al.[7] In order to prevent hydrogen transfer prior to nucleophilic attack of allylstannane we had to switch to a different photoredox catalyst that is able to perform reduction directly from its excited state without the need of additional reductive quencher. For this purpose we choose *fac*-Ir(ppy)$_3$[27] and were able to obtain the desired domino cyclization allylation product **15** in good yield and excellent diasteroselectivity.

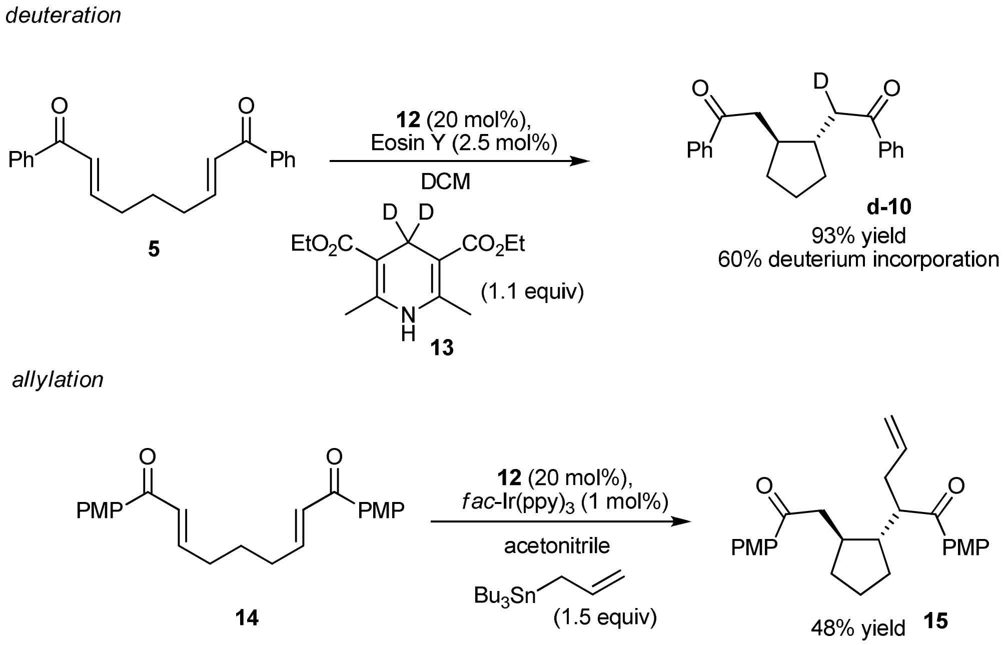
deuteration
5
12 (20 mol%),
Eosin Y (2.5 mol%)
DCM
13 (1.1 equiv)
d-10
93% yield
60% deuterium incorporation
allylation
14
12 (20 mol%),
fac-Ir(ppy)3 (1 mol%)
acetonitrile
Bu3Sn (1.5 equiv)
15
48% yield

Scheme 5. Mechanistic studies

1.5.3 Conclusion

In conclusion, we have demonstrated the applicability of Eosin Y as photocatalyst for the generation of ketyl radical anions and have developed a new efficient, cooperative organophoto-redox/organocatalysis protocol that allows the rapid and highly diastereoselective construction of various *trans*-1,2-substituted cycloalkanes and heterocycles. This operationally simple, room temperature, mild and metal-free method should also be a highly valuable, cost-effective alternative to metal-based photoredox approaches given the catalysts and catalyst loadings employed.

1.5.4 Experimental section

1.5.4.1 General Methods

Unless noted otherwise, all commercially available compounds were used as provided without further purification

NMR spectra were recorded on a Bruker Avance 300 (300.13 MHz) and Bruker Ultrashield Plus 400 MHz (400.13 MHz) using the solvent peak as internal reference ($CDCl_3$: δ H 7.26; δ C 77.0). Multiplicities are indicated, s (singlet), d (doublet), t (triplet), q (quartet), quint (quintet), sept (septet), m (multiplet)); coupling constants (*J*) are in Hertz (Hz).

Infrared Spectra were obtained using samples on a Biorad Excalibur FTS 3000 FT IR spectrometer equipped with a universal ATR sampling accessory (Specac Golden Gate Diamond Single Reflection ATR system); wave numbers $\tilde{\nu}$ are reported in cm^{-1}.

All reactions were monitored by thin-layer chromatography using Merck silica gel plates 60 F_{254}; visualization was accomplished with UV light and/or staining with appropriate stains (anisaldehyde, phosphomolybdic acid). Standard chromatography procedures were followed (particle size 63-200 µm). Gas chromatographic analysis was performed on a Fisons Instrument GC 8130, (capillary column J&W Scientific DB-1 / 30 m × 0.25 mm / 0.25 µm film). Irradiation was performed with CREE XP-E Q4 green (530 nm) or royal blue (455 nm) LEDs operated at 700 mA (approx. 145 lm per LED) or with household fluorescent bulb (23 W, OSRAM®, 6500 K, 1470 lm).

1.5.4.2 Lithium Mediated [2+2] Cyclizations

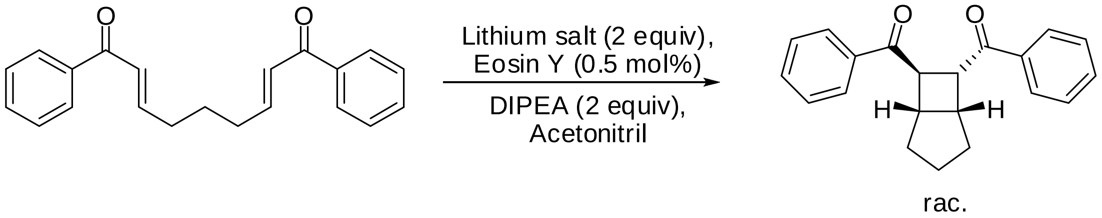

entry	lithium salt	photocatalyst	reaction time [h]	yield [%]
1	$LiBF_4$	Eosin Y	48	traces
2	$LiBF_4$	Na_2Eosin Y	48	60
3	LiCl	Na_2Eosin Y	48	traces
4	LiBr	Na_2Eosin Y	15	96

trans-Bicyclo[3.2.0]heptane-6,7-diylbis(phenylmethanone)[S1]

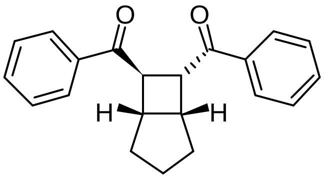

$C_{21}H_{20}O_2$
304.38 g/mol

LiBr (57 mg, 657 µmol) and Eosin Y disodium salt (1.2 mg, 1.7µmol) in 3.3 ml acetonitrile were treated with ultrasonic sound for 10 min. The mixture was filtered through a syringe filter cap into a 10 ml schlenk tube. (2*E*,7*E*)-1,9-diphenylnona-2,7-diene-1,9-dione (100 mg, 329 µmol), and DIPEA (114 µl, 657 µmol) were added followed by degassing *via* freeze-pump-thaw cycles. The solution was irradiated with a 26W fluorescent bulb until all starting material was consumed as judged by TLC (total 15h). Solvents were removed *in vacuo* and the residue was purified by silica column chromatography (hexanes/ethyl acetate, 19/1) yielding the pure product as colorless solid (96 mg, 315 µmol, 96%). ^{1}H NMR (300 MHz, $CDCl_3$) δ 8.02 (m, 2H), 7.94 (m, 2H), 7.55 (m, 2H), 7.45 (m, 4H), 4.57 (dd, *J* = 10.3, 7.9 Hz, 1H), 4.29 (m, 1H), 3.24 (m, 1H), 3.06 (q, *J* = 6.9 Hz, 1H), 1.84 (m, 3H), 1.53 (m, 1H), 1.42 (m, 2H). ^{13}C NMR (75 MHz, $CDCl_3$) δ 200.3, 198.1, 136.2, 135.7, 133.2, 133.1, 128.8, 128.6, 128.3, 128.1, 43.1, 43.0, 40.5, 40.4, 32.1, 28.5, 25.6.

trans-2-Benzoyl-3-methylcyclobutyl)ethanone[S2]

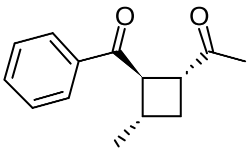

$C_{14}H_{16}O_2$
216.28 g/mol

LiBr (119 mg, 1370 µmol) and Eosin Y disodium salt (1.2 mg, 1.7µmol) in 3.4 ml acetonitrile were treated with ultrasonic sound for 10 min. The mixture was filtered through a syringe filter cap into a 10 ml schlenk tube. Methyl vinyl ketone (85 µl, 1026 µmol), (*E*)-1-phenylbuten-2-en-1-one (50 mg, 342 µmol) and DIPEA (119 µl, 684 µmol) were added followed by degassing *via* freeze-pump-thaw cycles. The solution was irradiated with a 26W fluorescent bulb until all starting material was consumed as judged by TLC (total 24h). Solvents were removed *in vacuo* and the residue was purified by PTLC using (hexanes/ethyl acetate, 3/1) yielding the pure product as yellowish oil (6 2mg, 287 µmol, 84%, 96% de). ^{1}H NMR (300 MHz, $CDCl_3$) δ 7.97 (m, 2H), 7.56 (m, 1H), 7.46 (m, 2H), 3.90 (t, *J* = 8.2 Hz, 1H), 3.61 (q, *J* = 9.3 Hz, 1H), 2.48 (m, 1H), 2.37 (m, 1H), 2.07 (s, 3H), 1.73 (m, 1H), 1.17 (d, *J* = 6.6 Hz, 3H). ^{13}C NMR (75 MHz, $CDCl_3$) δ 208.3, 199.4, 136.1, 133.3, 128.7, 49.7, 43.4, 31.0, 29.3, 27.7, 21.0.

1.5.4.3 Organophotoredox Cyclizations

Substrate Synthesis

(4-Methoxyphenyl)-7-oxohept-5-enal[S3]

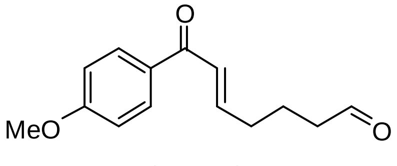

$C_{14}H_{16}O_3$
232.28 g/mol

Glutardialdeyhde (50% in water, 6.55 ml, 36mmol) was added to a stirred solution of 1-(4-methoxyphenyl)-2-(triphenylphosphoranylidene) (7.4 g, 13 mmol) in DCM (50 ml) and stirring was continued for 18 h. Volatiles were removed *in vacuo* and the crude product was purified by column chromatography on silica gel (hexanes/ethyl acetate, 3/1) yielding the product as colorless oil as a mixture of *E*/*Z* isomers (3.6 g, 15.5 mmol, 86% yield). ^{1}H NMR (300 MHz, $CDCl_3$) δ 9.79 (t, *J* = 1.3 Hz, 1H), 8.01 – 7.88 (m, 2H), 7.10 – 6.85 (m, 4H), 3.88 (s, 3H), 2.53 (m, 2H), 2.37 (m, 2H), 2.01 – 1.82 (m, 2H). ^{13}C NMR (75 MHz, $CDCl_3$) δ 201.4, 188.8, 147.0, 130.8, 126.3, 113.8, 55.5, 43.1, 42.8, 31.8, 20.6, 14.4.

(2*E*,7*E*)-Methyl 9-(4-methoxyphenyl)-9-oxonona-2,7-dienoate (table 3, entry 1)

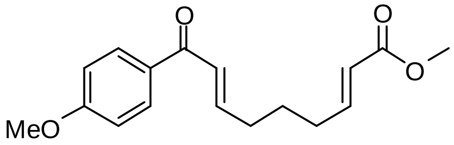

$C_{17}H_{20}O_4$
288.34 g/mol

To a solution of (4-Methoxyphenyl)-7-oxohept-5-enal (**S1**) (400 mg, 1.72 mmol) in DCM (10 ml) was added methyl 2-(triphenyl phosphoranylidene)acetate (1.15 g, 3.44 mmol) in small portions. The solution was stirred for 2 d before being concentrated *in vacuo* and purified by column chromatography on silica gel (hexanes/ethyl acetate, 3/1) yielding the product as colorless oil (427 mg, 1.48 mmol, 86% yield). IR (thin film): 2937, 1718, 1664, 1596, 1256, 1168. ^{1}H NMR (400 MHz, $CDCl_3$) δ 7.94 (d, *J* = 8.9 Hz, 2H), 7.05 – 6.87 (m, 5H), 5.85 (d, *J* = 15.7 Hz, 1H), 3.87 (s, 3H), 3.73 (s, 3H), 2.37 – 2.23 (m, 4H), 1.75 – 1.66 (m, 2H). ^{13}C NMR (101 MHz, $CDCl_3$) δ 188.8, 167.0, 163.4, 148.5, 147.4, 130.8, 130.7, 126.1, 121.6, 113.8, 55.5, 51.5, 32.0, 31.6, 26.6. HRMS (ESI$^+$) calculated for $[C_{17}H_{21}O_4]^+$ *m/z* 289.1434, found *m/z* 289.1432.

(2*E*,7*E*)-1-(4-Methoxyphenyl)deca-2,7-diene-1,9-dione (table 3, entry 3)

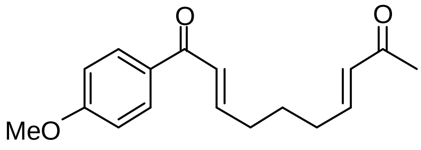

$C_{17}H_{20}O_3$
272.34 g/mol

To a solution of (4-Methoxyphenyl)-7-oxohept-5-enal **(S1)** (450 mg, 1.94 mmol) in DCM (10 ml) was added 1-(triphenylphosphoranylidene)-2-propanone (925 mg, 2.91 mmol) in small portions. The solution was stirred for 2 d before being concentrated *in vacuo* and purified by column chromatography on silica gel (hexanes/ethyl acetate, 3/1) yielding the product as colorless oil (493 mg, 1.81 mmol, 93% yield). IR (thin film): 2937, 1665, 1597, 1256, 1170. ^{1}H NMR (300 MHz, $CDCl_3$) δ 7.94 (d, *J* = 9.0 Hz, 2H), 7.10 – 6.87 (m, 4H), 6.78 (m, 1H), 6.15 – 6.03 (m, 1H), 3.87 (s, 3H), 2.42 – 2.20 (m, 7H), 1.80 – 1.65 (m, 2H). ^{13}C NMR (75 MHz, $CDCl_3$) δ 198.6, 188.8, 163.4, 147.3, 146.9, 131.8, 130.8, 126.1, 113.8, 55.5, 32.1, 31.8, 31.8, 27.0, 26.6. HRMS (ESI$^+$) calculated for $[C_{17}H_{21}O_3]^+$ *m/z* 273.1485, found *m/z* 273.1494.

(2*E*,7*E*)-9-(4-Methoxyphenyl)-9-oxonona-2,7-dienenitrile (table 3, entry 6)

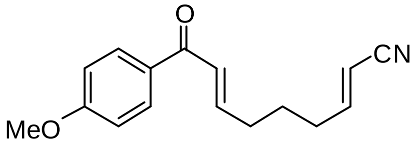

$C_{16}H_{17}NO_2$
255.31g/mol

To a solution of (4-Methoxyphenyl)-7-oxohept-5-enal **(S1)** (390 mg, 1.68 mmol) in DCM (10 ml) was added 2-(triphenylphosphoranylidene)acetonitrile (1.28 g, 3.36 mmol) in small portions. The solution was stirred for 2 d before being concentrated *in vacuo* and purified by column chromatography on silica gel (hexanes/ethyl acetate, 3/1) yielding the product as colorless oil (425 mg, 1.67 mmol, 99% yield). IR (thin film): 2935, 2221, 1596, 1257, 1170. ^{1}H NMR (400 MHz, $CDCl_3$) δ 7.94 (d, *J* = 8.9 Hz, 2H), 7.09 – 6.87 (m, 4H), 6.76 – 6.41 (m, 1H), 5.41 – 5.31 (m, 1H), 3.87 (s, 3H), 2.55 – 2.44 (m, 1H), 2.40 – 2.25 (m, 3H), 1.77 – 1.61 (m, 2H). ^{13}C NMR (101 MHz, $CDCl_3$) δ 188.6, 163.4, 155.0, 154.1, 146.7, 130.9, 130.6, 126.1, 113.8, 100.5, 55.5, 32.7, 31.4, 26.3. HRMS (ESI$^+$) calculated for $[C_{16}H_{18}NO_2]^+$ *m/z* 256.1332, found *m/z* 256.1337.

Experimental Data for the Products

General Procedure for Organophotoredox Cyclizations: In a 10 ml schlenk tube bisenone (1 equiv), Hantzsch ester (1 equiv), DIPEA (1 equiv), 1,3-bis(3,5-bis(trifluoromethyl)phenyl)thiourea[S4] + 2 (20 mol%) and photocatalyst (1 or 2.5 mol%) in DCM (c_{enone} = 0.2 mol/l) were degassed by freeze pump thaw cycles under nitrogen. The tube was then irradiated by two LEDs (530 nm in case of Eosin Y, 455nm in case of [Ir(dtbbpy)(ppy)2]PF6,) in a distance of 5 cm. After completion of the reaction (as judged by TLC) the products were isolated by column chromatography on silica gel.

(*trans*-Cyclopentane-1,2-diyl)bis(1-phenylethanone)[S5] (table 1)

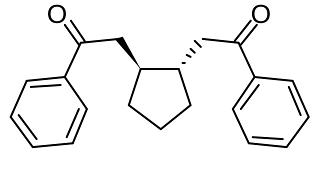

$C_{21}H_{22}O_2$
306.40 g/mol

Prepared according to general procedure: Using (2*E*,7*E*)-1,9-diphenylnona-2,7-diene-1,9-dione (103 mg, 338 µmol), 1,3-bis(3,5-bis(trifluoromethyl)phenyl)thiourea (34 mg, 68 µmol), Eosin Y (5.5 mg, 8.5 µmol), Hantzsch ester (86 mg, 338 µmol) and DIPEA (59 µl, 338 µmol) in DCM (1.7 ml). Irradiation for 2h. The product was isolated as a colorless oil (95 mg, 310 µmol, 92% yield). ^{1}H NMR (400 MHz, $CDCl_3$) δ 7.94 (m, 4H), 7.58 – 7.50 (m, 2H), 7.44 (t, *J* = 7.6 Hz, 4H), 3.20 (dd, *J* = 16.5, 4.5 Hz, 2H), 2.94 (dd, *J* = 16.5, 8.3 Hz, 2H), 2.26 – 2.11 (m, 2H), 1.98 (m, 2H), 1.69 – 1.56 (m, 2H), 1.27 (m, 2H). ^{13}C NMR (101 MHz, $CDCl_3$) δ 200.3, 137.2, 133.0, 128.6, 128.1, 44.0, 41.6, 32.6, 23.7.

(*trans*-Cyclopentane-1,2-diyl)bis(1-(4-methoxyphenyl)ethanone)[S5] (table 2, entry 2)

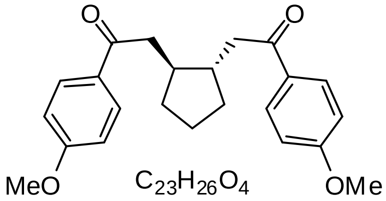

$C_{23}H_{26}O_4$
366.45 g/mol

Prepared according to general procedure: Using (2*E*,7*E*)-1,9-bis(4-methoxyphenyl)nona-2,7-diene-1,9-dione (120 mg, 329 µmol), 1,3-bis(3,5-bis(trifluoromethyl)phenyl)thiourea (33 mg, 66 µmol), Eosin Y (5.3 mg, 8.2 µmol), Hantzsch ester (83 mg, 329 µmol) and DIPEA (57 µl, 329 µmol) in DCM (1.7 ml). Irradiation for 1.5 h. The product was isolated as a colorless oil (99 mg, 313 µmol, 95% yield). ^{1}H NMR (400 MHz, $CDCl_3$) δ 7.92 (d, *J* = 8.9 Hz, 4H), 6.90 (d, *J* = 8.9 Hz, 4H), 3.84 (s, 6H), 3.12 (dd, *J* = 16.0, 4.4 Hz, 2H), 2.85 (dd, *J* = 16.0, 8.4 Hz, 2H), 2.14 (m, 2H), 1.95 (m, 2H), 1.59 (m, 2H), 1.25 (m 2H). ^{13}C NMR (101 MHz, $CDCl_3$) δ 198.9, 163.4, 130.4, 130.3, 113.7, 55.5, 43.6, 41.9, 32.5, 23.7.

(*trans*-Cyclopentane-1,2-diyl)bis(1-(4-chlorophenyl)ethanone)[S5] (table 2, entry 3)

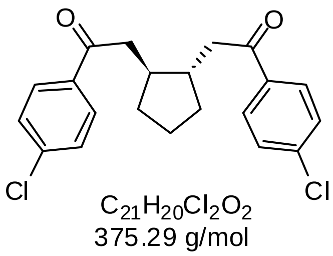

Prepared according to general procedure: Using (2*E*,7*E*)-1,9-bis(4-chlorophenyl)nona-2,7-diene-1,9-dione (135 mg, 362 µmol), 1,3-bis(3,5-bis(trifluoromethyl)phenyl)thiourea (36 mg, 72 µmol), Eosin Y (5.9 mg, 9 µmol), Hantzsch ester (92 mg, 362 µmol) and DIPEA (63 µl, 362 µmol) in DCM (1.8 ml). Irradiation for 2.5 h. The product was isolated as a colorless solid (130 mg, 346 µmol, 96% yield). ^{1}H NMR (300 MHz, $CDCl_3$) δ 7.87 (d, *J* = 8.7 Hz, 4H), 7.41 (d, *J* = 8.7 Hz, 4H), 3.16 (dd, *J* = 16.7, 4.9 Hz, 2H), 2.91 (dd, *J* = 16.7, 7.9 Hz, 2H), 2.16 (m, 2H), 1.97 (m, 2H), 1.63 (m, 2H), 1.27 (m, 2H). ^{13}C NMR (75 MHz, $CDCl_3$) δ 198.9, 139.4, 135.4, 129.5, 128.9, 44.0, 41.4, 32.6, 23.7.

1,1'-(*trans*-Cyclopentane-1,2-diyl)bis(4-phenylbutan-2-one)[S5] (table 2, entry 4)

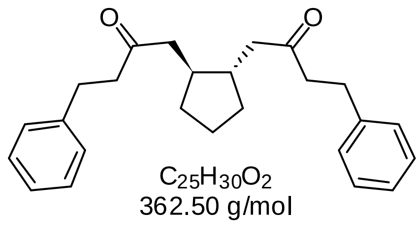

Prepared according to general procedure: Using (4*E*,9*E*)-1,13-diphenyltrideca-4,9-diene-3,11-dione (125 mg, 347 µmol), 1,3-bis(3,5-bis(trifluoromethyl)phenyl)thiourea (35 mg, 69 µmol), [Ir(d*t*bbpy)(ppy)$_2$]PF$_6$ (3.2 mg, 3.5 µmol), Hantzsch ester (88 mg, 347 µmol) and DIPEA (60 µl, 347 µmol) in DCM (1.7 ml). Irradiation for 1 h. The product was isolated as a colorless oil (116 mg, 320 µmol, 92% yield). ^{1}H NMR (400 MHz, $CDCl_3$) δ 7.27 (m, 4H), 7.18 (m, 6H), 2.87 (t, *J* = 7.6 Hz, 4H), 2.69 (m, 4H), 2.49 (dd, *J* = 16.6, 4.1 Hz, 2H), 2.29 (dd, *J* = 16.5, 7.4 Hz, 2H), 1.84 (m, 4H), 1.53 (m, 2H), 1.10 (m, 2H). ^{13}C NMR (75 MHz, $CDCl_3$) δ 210.7, 140.9, 128.5, 128.3, 126.2, 48.3, 44.6, 40.8, 32.3, 29.8, 23.5.

1,1'-(*trans*-Cyclopentane-1,2-diyl)dipropan-2-one[S6] (table 2, entry 5)

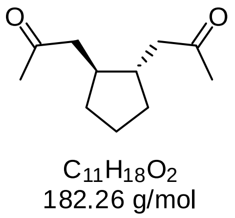

Prepared according to general procedure: Using (3*E*,8*E*)-undeca-3,8-diene-2,10-dione (110 mg, 610 µmol), 1,3-bis(3,5-bis(trifluoromethyl)phenyl)thiourea (61 mg, 69 µmol), [Ir(d*t*bbpy)(ppy)$_2$]PF$_6$ (5.6 mg, 6.1 µmol), Hantzsch ester (155 mg, 610 µmol) and DIPEA (106 µl, 610 µmol) in DCM (3 ml). Irradiation for 0.5 h. The product was isolated as a colorless oil (103 mg, 565 µmol, 93% yield). ^{1}H NMR (300 MHz, $CDCl_3$) δ 2.53 (dd, *J* = 16.7, 4.3 Hz, 2H), 2.29 (dd, *J* = 16.8, 7.5 Hz, 2H), 2.06 (s, 6H), 1.81 (m, 4H), 1.51 (m, 2H), 1.09 (m, 2H). ^{13}C NMR (75 MHz, $CDCl_3$) δ 208.9, 48.9, 40.8, 32.3, 30.3, 23.4.

1,1'-(*trans*-Tetrahydrofuran-3,4-diyl)bis(1-phenylethanone)[S5] (table 2, entry 6)

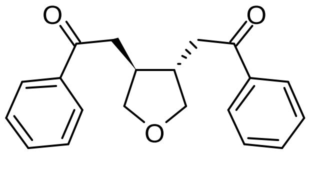
$C_{20}H_{20}O_3$
308.37 g/mol

Prepared according to general procedure: Using (2*E*,2'*E*)-4,4'-oxybis(1-phenylbut-2-en-1-one) (127 mg, 415 µmol), 1,3-bis(3,5-bis(trifluoromethyl)phenyl)thiourea (42 mg, 83 µmol), Eosin Y (6.7 mg, 10 µmol), Hantzsch ester (105 mg, 415 µmol) and DIPEA (72 µl, 415 µmol) in DCM (2 ml). Irradiation for 8 h. The product was isolated as a colorless oil (121 mg, 392 µmol, 95% yield). ^{1}H NMR (400 MHz, CDCl$_3$) δ 7.97 – 7.89 (m, 4H), 7.54 (d, *J* = 7.4 Hz, 2H), 7.44 (dd, *J* = 10.8, 4.4 Hz, 4H), 4.15 (dd, *J* = 8.9, 6.7 Hz, 2H), 3.48 (dd, *J* = 9.0, 5.9 Hz, 2H), 3.37 (dd, *J* = 17.7, 5.1 Hz, 2H), 3.09 (dd, *J* = 17.8, 8.2 Hz, 2H), 2.60 – 2.50 (m, 2H). ^{13}C NMR (101 MHz, CDCl$_3$) δ 199.1, 136.8, 133.3, 128.7, 128.0, 73.4, 42.6, 40.6.

(*trans*-Cyclohexane-1,2-diyl)bis(1-phenylethanone)[S7] (table 2, entry 7)

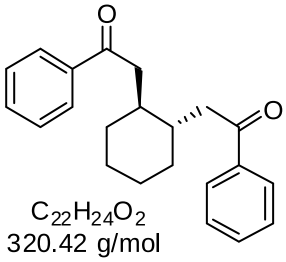
$C_{22}H_{24}O_2$
320.42 g/mol

Prepared according to general procedure: Using (2*E*,8*E*)-1,10-diphenyldeca-2,8-diene-1,10-dione (105 mg, 330 µmol), 1,3-bis(3,5-bis(trifluoromethyl)phenyl)thiourea (33 mg, 66 µmol), Eosin Y (5.3 mg, 8.2 µmol), Hantzsch ester (84 mg, 330 µmol) and DIPEA (57 µl, 330 µmol) in DCM (1.7 ml). Irradiation for 4.5 h. The product was isolated as a colorless oil (96 mg, 300 µmol, 91% yield). ^{1}H NMR (300 MHz, CDCl$_3$) δ 7.91 (m, 4H), 7.54 (m, 2H), 7.44 (m, 4H), 3.07 (dd, *J* = 16.4, 4.0 Hz, 2H), 2.84 (dd, *J* = 16.4, 7.7 Hz, 2H), 1.99 (m, 2H), 1.71 (m, 4H), 1.241 (m, 4H). ^{13}C NMR (75 MHz, CDCl$_3$) δ 200.5, 137.4, 133.0, 128.6, 128.1, 43.6, 38.8, 33.2, 26.0.

2-(2-Benzoylcyclopent-2-enyl)-1-phenylethanone[S8] (table 2, entry 9)

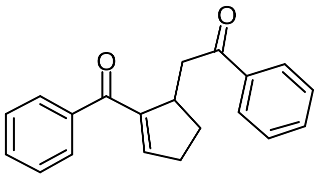
$C_{20}H_{18}O_2$
290.36 g/mol

Prepared according to general procedure: Using 1,8-diphenylocta-2,6-diene-1,8-dione (104 mg, 358 µmol), 1,3-bis(3,5-bis(trifluoromethyl)phenyl)thiourea (36 mg, 72 µmol), Eosin Y (5.8 mg, 8.9 µmol), and DIPEA (125 µl, 716 µmol) in DCM (1.8 ml). Irradiation for 48 h. The product was isolated as a colorless oil (74 mg, 255 µmol, 71% yield). ^{1}H NMR (300 MHz, CDCl$_3$) δ 8.04 (m, 2H), 7.75 (m, 2H), 7.49 (m, 6H), 6.59 (t, *J* = 2.6 Hz, 1H), 3.74 (m, 2H), 2.82 (m, 1H), 2.59 (m, 2H), 2.32 (m, 1H), 1.78 (m, 1H). ^{13}C NMR (75 MHz, CDCl$_3$) δ 199.8, 194.5 148.1, 146.2, 139.0, 136.9, 133.0, 132.0, 128.9, 128.6, 128.3, 42.4, 41.6, 32.7, 29.6, 21.5.

Methyl 2-(*trans*-2-(2-(4-methoxyphenyl)-2-oxoethyl)cyclopentyl)acetate (table 3, entry 1)

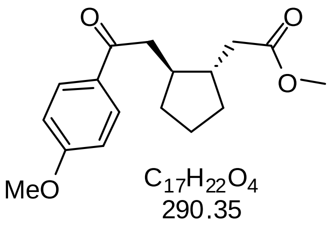

Prepared according to general procedure: Using (2*E*,7*E*)-methyl 9-(4-methoxyphenyl)-9-oxonona-2,7-dienoate (120 mg, 416 µmol), 1,3-bis(3,5-bis(trifluoromethyl)phenyl)thiourea (42 mg, 83 µmol), Eosin Y (6.7 mg, 10 µmol), Hantzsch ester (105 mg, 416 µmol) and DIPEA (72 µl, 416 µmol) in DCM (2 ml). Irradiation for 6 h. The product was isolated as a colorless oil (103 mg, 355 µmol, 85% yield). IR (thin film): 2950, 1732, 1673, 1599, 1256, 1170. ^{1}H NMR (300 MHz, CDCl$_3$) δ 7.92 (d, *J* = 9.0 Hz, 2H), 6.91 (d, *J* = 9.0 Hz, 2H), 3.85 (s, 3H), 3.63 (s, 3H), 3.08 (dd, *J* = 16.1, 4.6 Hz, 1H), 2.81 (dd, *J* = 16.1, 8.7 Hz, 1H), 2.52 (dd, *J* = 15.1, 4.9 Hz, 1H), 2.23 (dd, *J* = 15.1, 8.4 Hz, 1H), 2.05 (m, 1H), 1.95 (m, 2H), 1.59 (m, 2H), 1.24 (m, 2H). ^{13}C NMR (75 MHz, CDCl$_3$) δ 198.6, 173.8, 163.4, 130.4, 130.2, 113.7, 55.5, 51.5, 43.4, 42.3, 41.4, 39.2, 32.5, 32.2, 23.5. HRMS (ESI$^+$) calculated for $[C_{17}H_{23}O_4]^+$ *m/z* 291.1591, found *m/z* 291.1594.

S-Ethyl 2-(*trans*-2-(2-(4-methoxyphenyl)-2-oxoethyl)cyclopentyl)ethanethioate[S5] (table 3, entry 2)

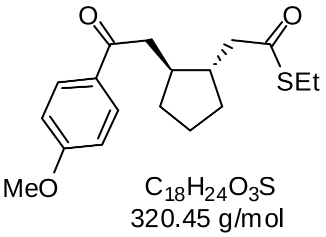

Prepared according to general procedure: Using (2*E*,7*E*)-*S*-ethyl 9-(4-methoxyphenyl)-9-oxonona-2,7-dienothioate (130 mg, 408 µmol), 1,3-bis(3,5-bis(trifluoromethyl)phenyl)thiourea (41 mg, 82 µmol), Eosin Y (6.7 mg, 10 µmol), Hantzsch ester (103 mg, 408 µmol) and DIPEA (71 µl, 408 µmol) in DCM (2 ml). Irradiation for 6 h. The product was isolated as a colorless oil (113 mg, 353 µmol, 86% yield). ^{1}H NMR (300 MHz, CDCl$_3$) δ 7.85 (d, *J* = 9.0 Hz, 2H), 6.86 (d, *J* = 8.9 Hz, 2H), 3.80 (s, 3H), 3.02 (dd, *J* = 16.0, 4.2 Hz, 1H), 2.88 – 2.70 (m, 3H), 2.66 (dd, *J* = 14.6, 4.9 Hz, 1H), 2.41 (dd, *J* = 14.6, 8.3 Hz, 1H), 1.97 (m, 2H), 1.88 (m, 2H), 1.52 (m, 2H), 1.20 (m, 5H). ^{13}C NMR (75 MHz, CDCl$_3$) δ 199.8, 199.2, 163.4, 132.2, 131.7, 113.8, 55.5, 49.0, 43.5, 42.8, 41.6, 32.3, 31.9, 23.4, 23.3, 14.7.

1-(*trans*-2-(2-(4-Methoxyphenyl)-2-oxoethyl)cyclopentyl)propan-2-one (table 3, entry 3)

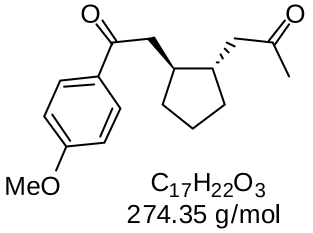

Prepared according to general procedure: Using (2E,7E)-1-(4-methoxyphenyl)deca-2,7-diene-1,9-dione (120 mg, 441 µmol), 1,3-bis(3,5-bis(trifluoromethyl)phenyl)thiourea (44 mg, 88 µmol), Eosin Y (7.1 mg, 11 µmol), Hantzsch ester (112 mg, 441 µmol) and DIPEA (77 µl, 441 µmol) in DCM (2.2 ml). Irradiation for 5 h. The product was isolated as a colorless oil (105 mg, 383 µmol, 87% yield). IR (thin film): 2944, 1710, 1672, 1597, 1254, 1169. 1H NMR (300

MHz, CDCl3) δ 7.93 (d, J = 9.0 Hz, 2H), 6.92 (d, J = 9.0 Hz, 2H), 3.86 (s, 3H), 3.06 (dd, J = 16.2, 4.7 Hz, 1H), 2.84 (dd, J = 16.2, 8.0 Hz, 1H), 2.65 (dd, J = 16.5, 4.2 Hz, 1H), 2.38 (dd, J = 16.4, 8.2 Hz, 1H), 2.12 (s, 3H), 1.97 (m 4H), 1.61 (m, 2H), 1.20 (m, 2H). ^{13}C NMR (75 MHz, $CDCl_3$) δ 209.1, 198.8, 163.4, 130.4, 130.3, 113.7, 55.5, 49.0, 43.5, 41.5, 41.2, 40.8, 32.5, 30.4, 23.6. HRMS (ESI$^+$) calculated for $[C_{17}H_{23}O_3]^+$ *m/z* 275.1642, found *m/z* 275.1646.

***trans*-2-(2-(4-Methoxyphenyl)-2-oxoethyl)cyclopentyl)-3,3-dimethylbutan-2-one**[S5] (table 3, entry 4)

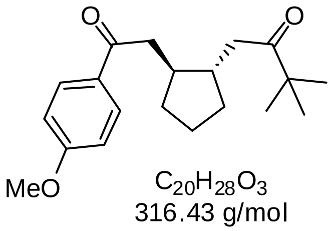

Prepared according to general procedure: Using (2*E*,7*E*)-1-(4-methoxyphenyl)-10,10-dimethylundeca-2,7-diene-1,9-dione (120 mg, 382 µmol), 1,3-bis(3,5-bis(trifluoromethyl)phenyl)thiourea (38 mg, 76 µmol), Eosin Y (6.2 mg, 11 µmol), Hantzsch ester (97 mg, 382 µmol) and DIPEA (66 µl, 382 µmol) in DCM (1.9 ml). Irradiation for 4 h. The product was isolated as a colorless oil (115 mg, 363 µmol, 95% yield). ^{1}H NMR (400 MHz, $CDCl_3$) δ 7.91 (d, *J* = 8.9 Hz, 2H), 6.90 (d, *J* = 8.9 Hz, 2H), 3.83 (s, 3H), 3.04 (dd, *J* = 16.1, 4.2 Hz, 1H), 2.86 – 2.78 (dd, *J* = 16.2, 8.7 Hz,, 1H), 2.60 (dd, *J* = 17.5, 4.6 Hz, 1H), 2.49 (dd, *J* = 17.5, 8.1 Hz, 1H), 2.02 (m, 2H), 1.96 – 1.84 (m, 2H), 1.61 – 1.50 (m, 2H), 1.27 – 1.16 (m, 1H), 1.13 – 1.04 (m, 1H), 1.09 (s, 9H). ^{13}C NMR (101 MHz, $CDCl_3$) δ 216.0, 199.0, 163.4, 130.4, 113.7, 55.4, 44.1, 43.6, 42.0, 41.6, 40.9, 32.6, 26.4, 23.7.

(*E*)-Methyl 2-(2-(2-oxo-2-phenylethyl)cyclopentylidene)acetate[S9] (table 3, entry 5)

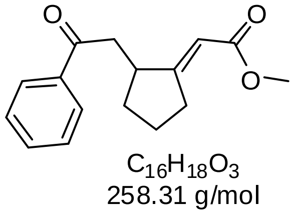

Prepared according to general procedure: Using (*E*)-methyl 9-oxo-9-phenylnon-7-en-2-ynoate (110 mg, 429 µmol), 1,3-bis(3,5-bis(trifluoromethyl)phenyl)thiourea (43 mg, 86 µmol), Eosin Y (6.9 mg, 11 µmol), Hantzsch ester (109 mg, 429 µmol) and DIPEA (75 µl, 429 µmol) in DCM (1.9 ml). Irradiation for 7 h. The product was isolated as a colorless oil (91 mg, 352 µmol, 82% yield). ^{1}H NMR (400 MHz, $CDCl_3$) δ 7.96 – 7.91 (m, 2H), 7.62 – 7.42 (m, 3H), 5.73 (q, *J* = 1.8 Hz, 1H), 3.68 (s, 3H), 3.00 (m, 5H), 2.05 (m, 1H), 1.87 (m, 1H), 1.64 (m, 1H), 1.31 (m, 1H). ^{13}C NMR (101 MHz, $CDCl_3$) δ 199.0, 171.5, 167.6, 136.8, 133.7, 128.8, 111.3, 51.0, 42.7 42.3, 33.0, 32.4, 24.2.

2-(*trans*-2-(2-(4-Methoxyphenyl)-2-oxoethyl)cyclopentyl)acetonitrile (table 3, entry 6)

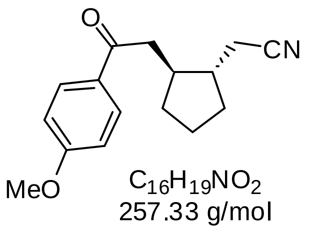

Prepared according to general procedure: Using (2*E*,7*E*)-9-(4-methoxyphenyl)-9-oxonona-2,7-diene nitrile (120 mg, 470 µmol), 1,3-bis(3,5-bis(trifluoromethyl)phenyl)thiourea (47 mg, 94 µmol), Eosin Y (7.6 mg, 12 µmol), Hantzsch ester (119 mg, 470 µmol) and DIPEA (82 µl, 470 µmol) in DCM (2,3 ml). Irradiation for 7.5 h. The product was isolated as a colorless oil (103 mg, 400 µmol, 85% yield). IR (thin film): 2954, 1672, 1599, 1258, 1171. ^{1}H NMR (300 MHz, $CDCl_3$) δ 7.92 (d, *J* = 8.8 Hz, 2H), 6.93 (m, 2H), 3.86 (s, 3H), 3.11 (m, 1H), 2.84 (m, 1H), 2.55 (m, 1H), 2.39 (m, 1H), 2.16 (m, 1H), 1.93 (m, 2H), 1.64 (m, 2H), 1.38 (m, 2H). ^{13}C NMR (75 MHz, $CDCl_3$) δ 198.9, 163.6, 130.4, 119.4, 113.8, 55.5, 43.4, 42.0, 41.9, 40.9, 32.9, 32.2, 23.7, 22.2. HRMS (ESI$^+$) calculated for $[C_{16}H_{20}NO_2]^+$ *m/z* 258.1489, found *m/z* 258,1495.

1.5.4.4 Mechanistic Studies

1-(4-Methoxyphenyl)-2-(*trans*-2-(2-(4-methoxyphenyl)-2-oxoethyl)cyclopentyl)pent-4-en-1-one

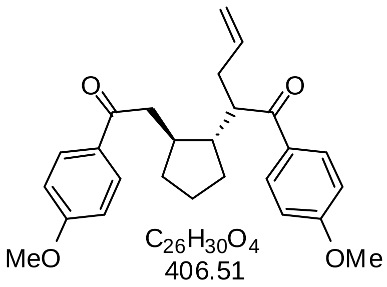

In a 10 ml Schlenk tube (2*E*,7*E*)-1,9-bis(4-methoxyphenyl)nona-2,7-diene-1,9-dione (100 mg, 274 µmol), 1,3-bis(3,5-bis(trifluoromethyl)phenyl)thiourea (28 mg, 55 µmol), allytributylstannane (132 µl, 412 µmol), and *fac*-Ir(ppy)$_3$ were dissolved in acetonitrile (1.4 ml). The mixture was degassed by freeze pump thaw cycles and then irradiated for 3 h. The product was isolated by column chromatography on silica gel (hexanes/ethyl acetate, 9/1) yielding a colorless oil (56 mg (purity 95%), 131 µmol, 48% yield). ^{1}H NMR (400 MHz, $CDCl_3$) δ 7.92 (d, *J* = 8.9 Hz, 2H), 7.79 (d, *J* = 8.9 Hz, 2H), 6.91 (m, 2H), 6.83 (d, *J* = 8.9 Hz, 2H), 5.66 (m 1H), 4.94 (m, 2H), 3.84 (s, 3H), 3.82 (s, 3H), 3.53 (m, 1H), 3.05 (m, 1H), 2.71 (dd, *J* = 15.5, 9.6 Hz, 1H), 2.57 (m, 1H), 2.29 (m, 1H), 2.17 (m, 1H), 2.3 (m, 1H), 1.78 (m, 2H), 1.45 (m, 4H). ^{13}C NMR (101 MHz, $CDCl_3$) δ 202.1, 198.9, 163.5, 163.4, 131.0, 130.7, 130.4, 116.4, 113.9, 113.8, 113.6, 55.5, 55.4, 49.5, 47.6, 44.7, 40.0, 34.2, 32.6, 29.8, 24.0. HRMS (ESI$^+$) calculated for $[C_{26}H_{31}O_4]^+$ *m/z* 406.2225, found *m/z* 407.2217.

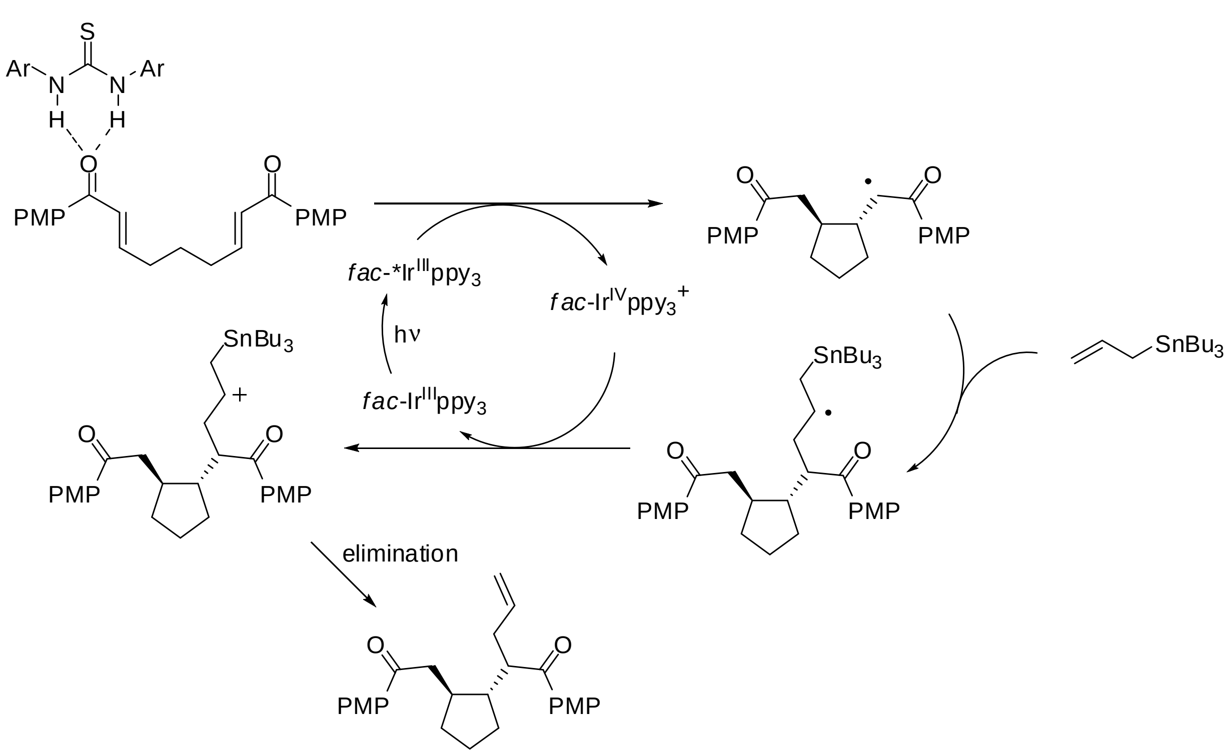
Ar
Ar
S
N
N
H
H
O
O
PMP
PMP
fac-*Ir^III^ppy3
hν
fac-Ir^III^ppy3
fac-Ir^IV^ppy3+
SnBu3
SnBu3
SnBu3
elimination

Scheme 6. Mechanistic proposal for domino cyclization allylation reaction.

Deuteration with d_2-Hantzsch Ester

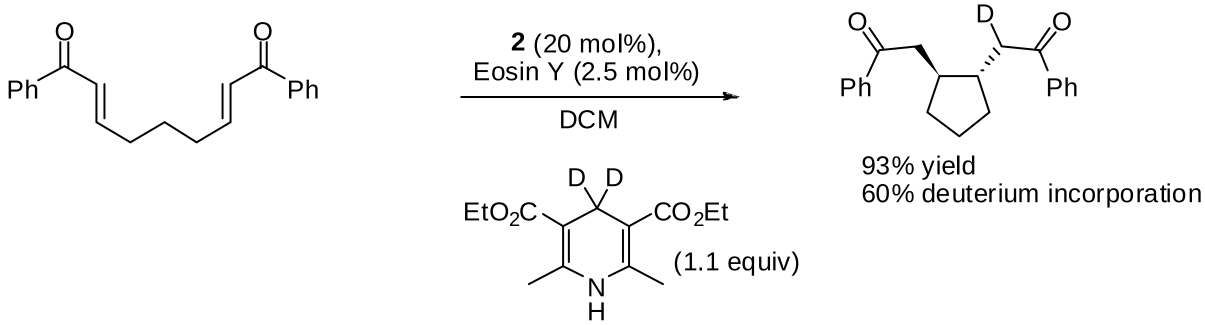
Ph
Ph
O
O
2 (20 mol%), Eosin Y (2.5 mol%)
DCM
D
D
D
EtO2C
CO2Et
N
H
(1.1 equiv)
93% yield
60% deuterium incorporation

Reaction was performed according to general procedure: Using (2*E*,7*E*)-1,9-diphenylnona-2,7-diene-1,9-dione (76 mg, 338 µmol), 1,3-bis(3,5-bis(trifluoromethyl)phenyl)thiourea **2** (25 mg, 50 µmol), Eosin Y (3.2 mg, 5 µmol) and d_2-Hantzsch ester (70 mg, 274 µmol) in DCM (1.7 ml). Irradiation for 4.5 h. The product was isolated as a colorless oil (71 mg, 231 µmol, 93% yield). Deuterium incorporation was determined by integration of the corresponding ^{1}H NMR signals 2.94 ppm (dd, 2H – one of the diastereotopic α-Hs; the integral of the second diastereotopic α-H signal used for comparison possess a 2H integral - also if compared to other signals within the molecule).

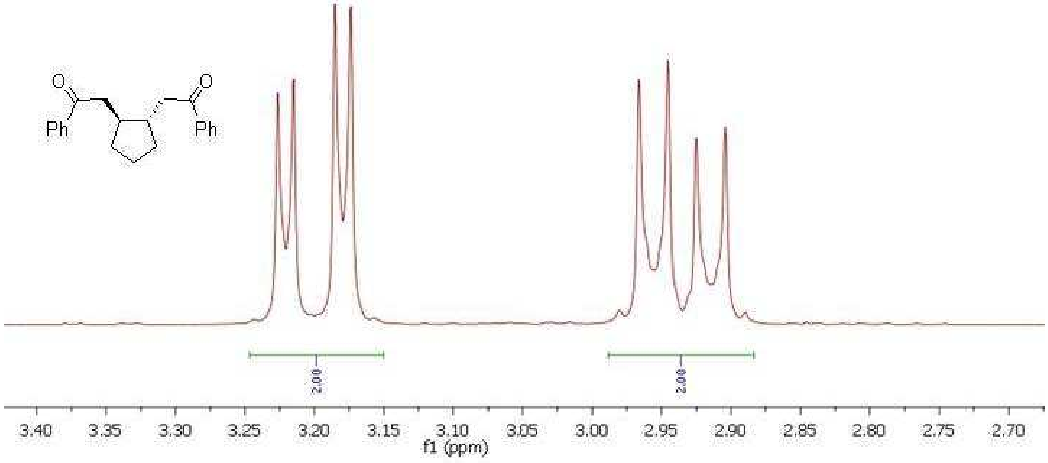

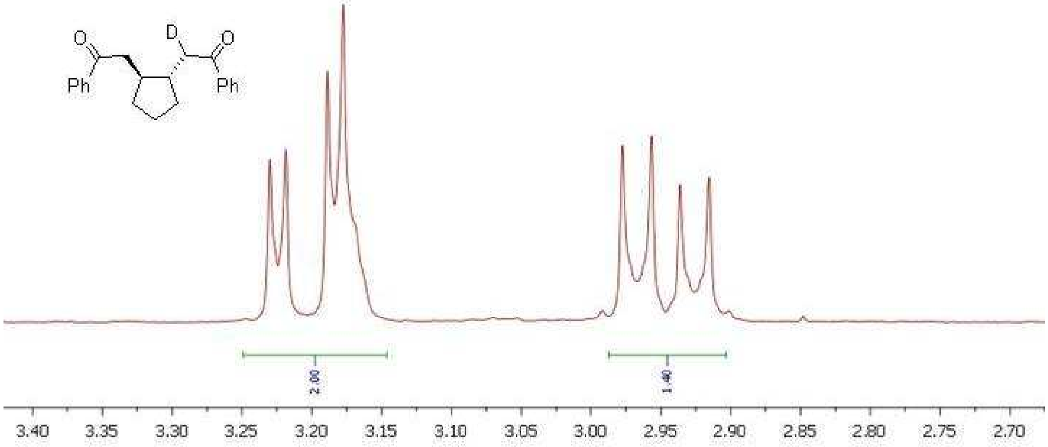

References:

[S1] G. A. N. Felton, N. L. Bauld, *Tetrahedron* **2004**, *60*, 10999.

[S2] J. Du, T. P. Yoon, *J. Am. Chem. Soc.* **2009**, *131*, 14604.

[S3] H.-Y. Jang, R. R. Huddleston, M. J. Krische, *J. Am. Chem. Soc.* **2002**, *124*, 15156.

[S4] M. Kotke, P. R. Schreiner, *Tetrahedron* **2006**, *62*, 434.

[S5] J. Du, L. R. Espelt, I. A. Guzei, T. P. Yoon, *Chem. Sci.* **2011**, *2*, 2115.

[S6] E. J. Enholm, K. S. Kinter, *J. Org. Chem* **1995**, *60*, 4850.

[S7] A. E. Hurtley, M. A. Cismesia, M. A. Ischay, T. P. Yoon, *Tetrahedron* **2011**, *67*, 4442.

[S8] L.-C. Wang, A. L. Luis, K. Agapiou, H.-Y. Jang, M. J. Krische, *J. Am. Chem. Soc.* **2002**, *124*, 2402.

[S9] H.-Y. Jang, F. W. Hughes, H. Gong, J. Zhang, J. S. Brodbelt, M. J. Krische, *J. Am. Chem. Soc.* **2005**, *127*, 6174.

1.5.4.5 ^{1}H, ^{13}C NMR and DEPT-135 Spectra for new compounds and products

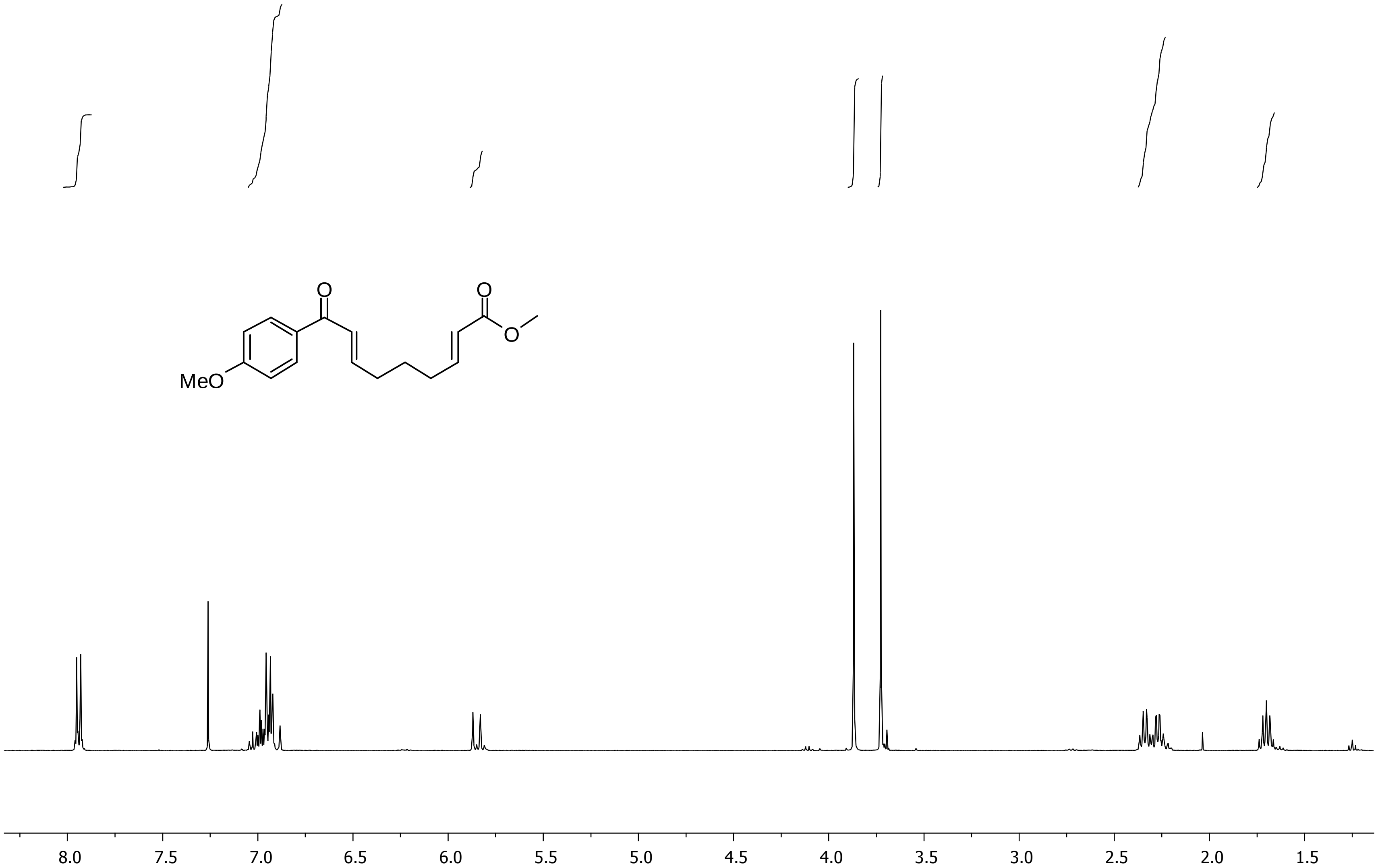

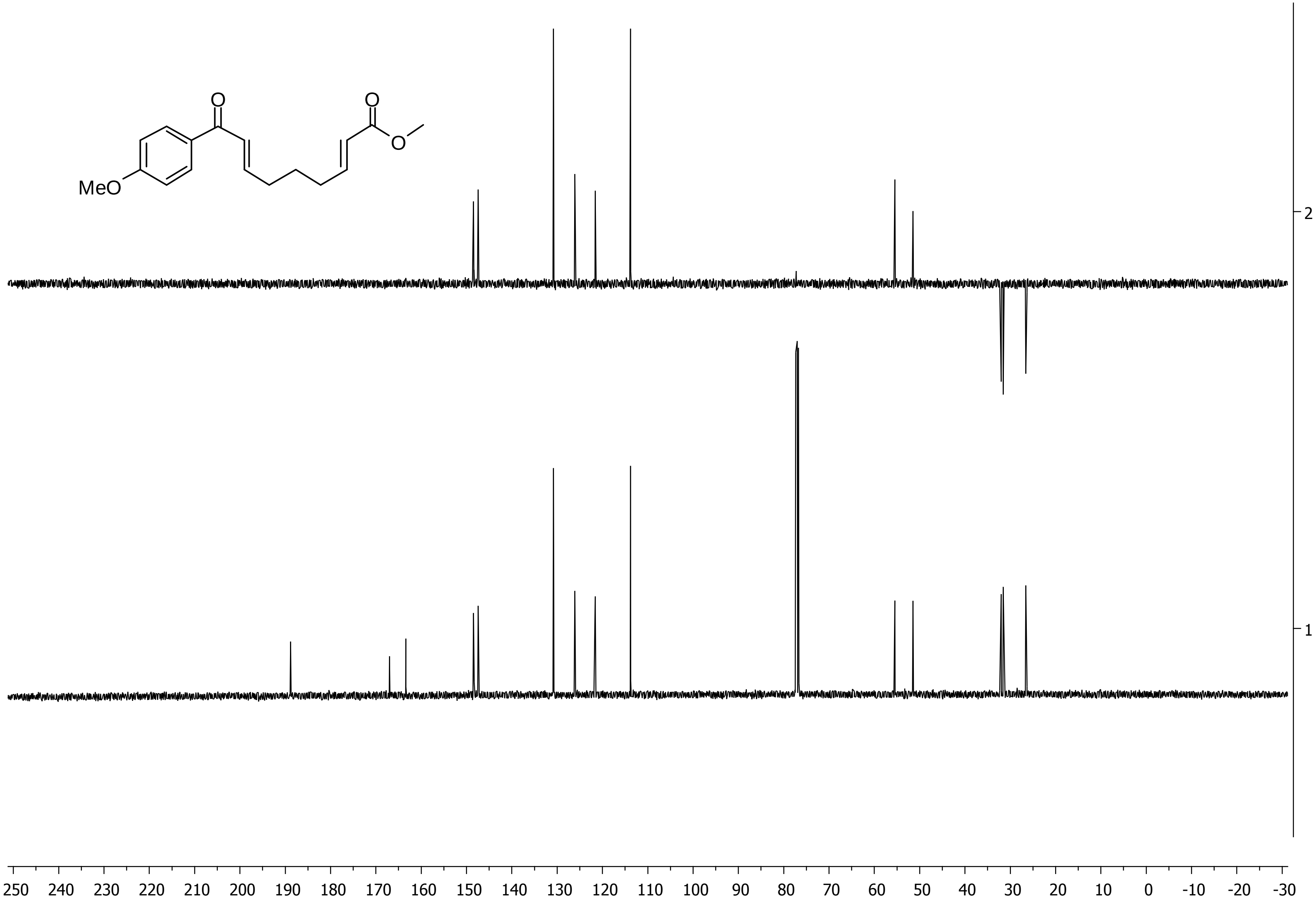
MeO
O
O
O
2
1
250
240
230
220
210
200
190
180
170
160
150
140
130
120
110
100
90
80
70
60
50
40
30
20
10
0
-10
-20
-30

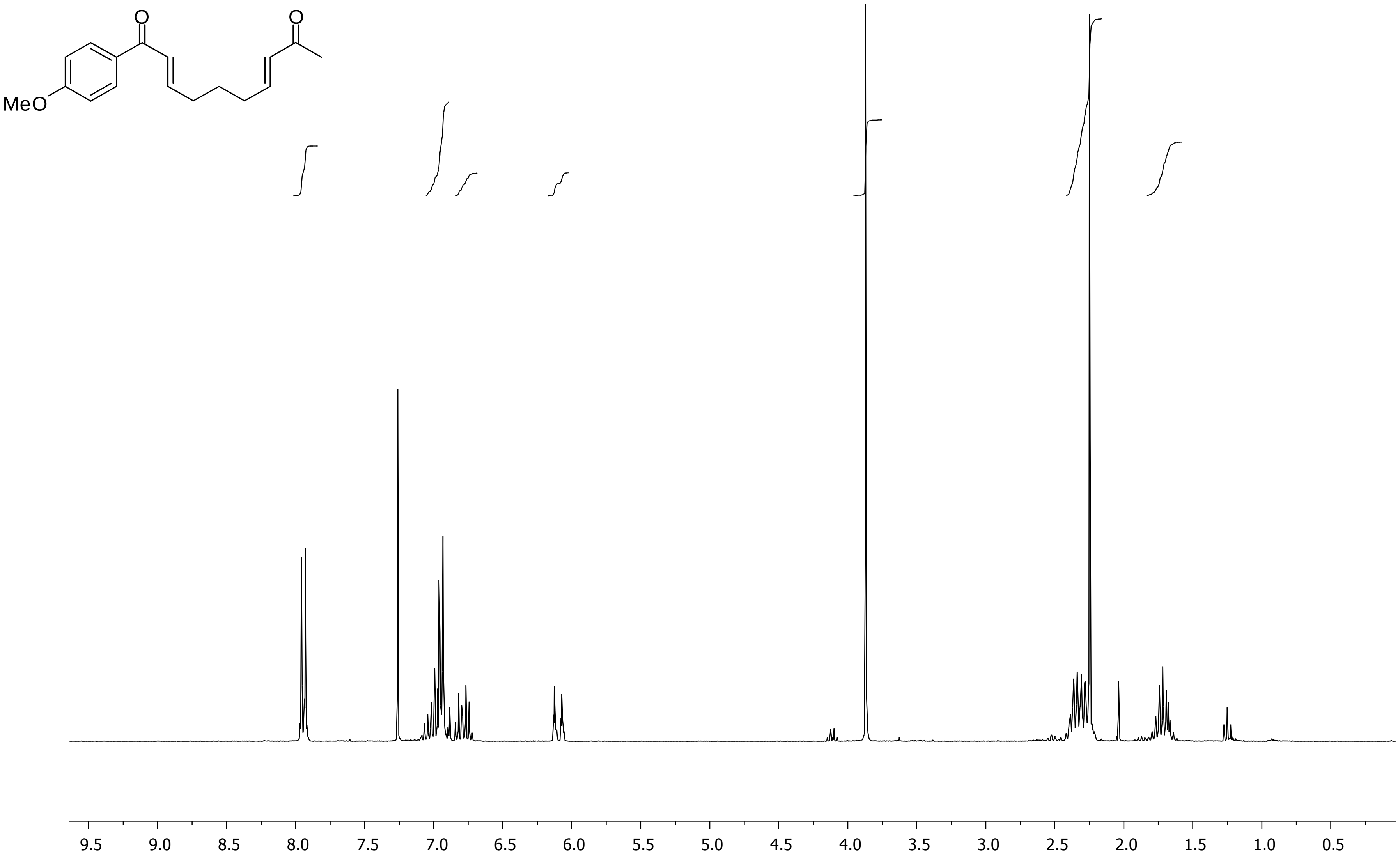
O
O
MeO
9.5
9.0
8.5
8.0
7.5
7.0
6.5
6.0
5.5
5.0
4.5
4.0
3.5
3.0
2.5
2.0
1.5
1.0
0.5

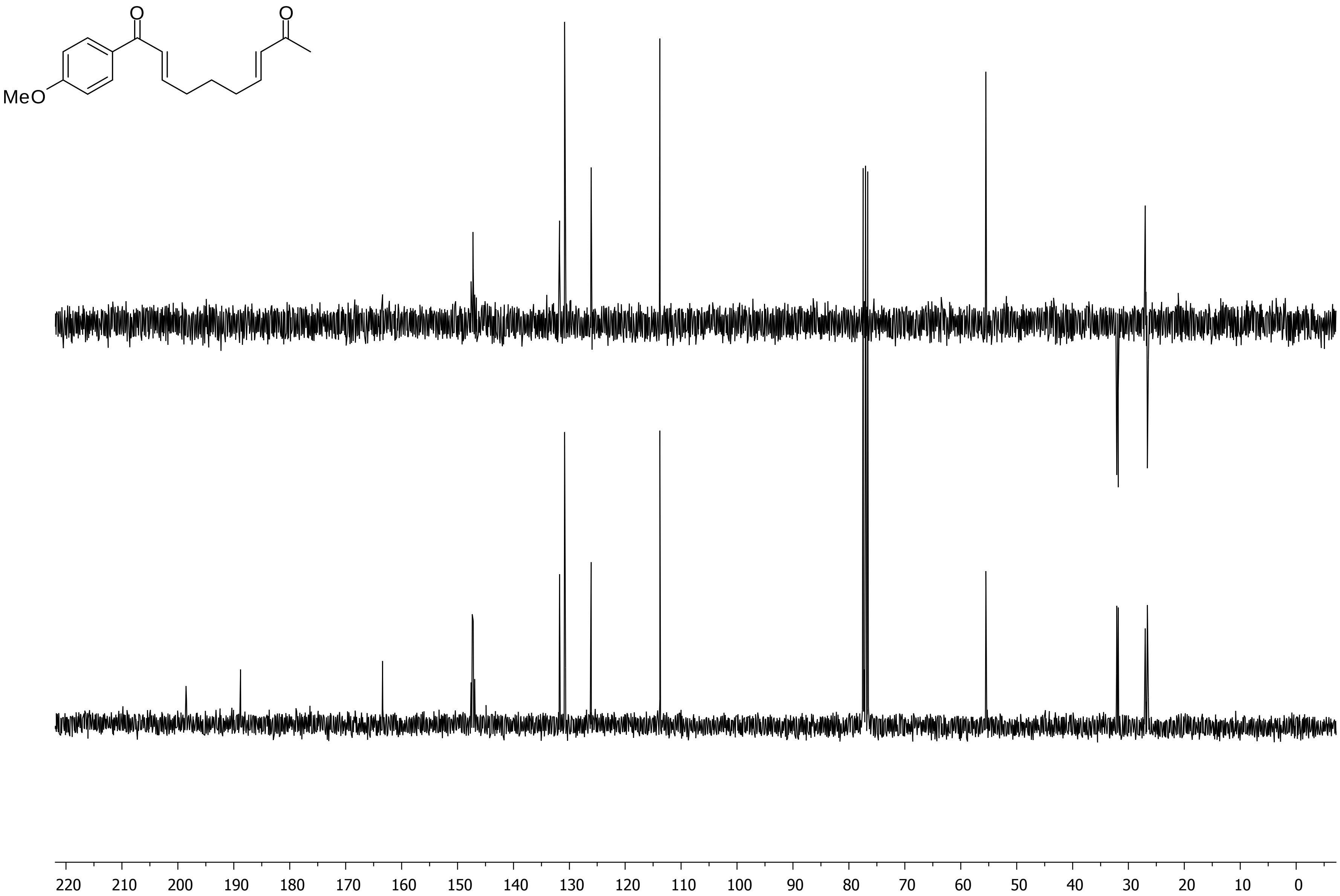
O
O
MeO
220
210
200
190
180
170
160
150
140
130
120
110
100
90
80
70
60
50
40
30
20
10
0

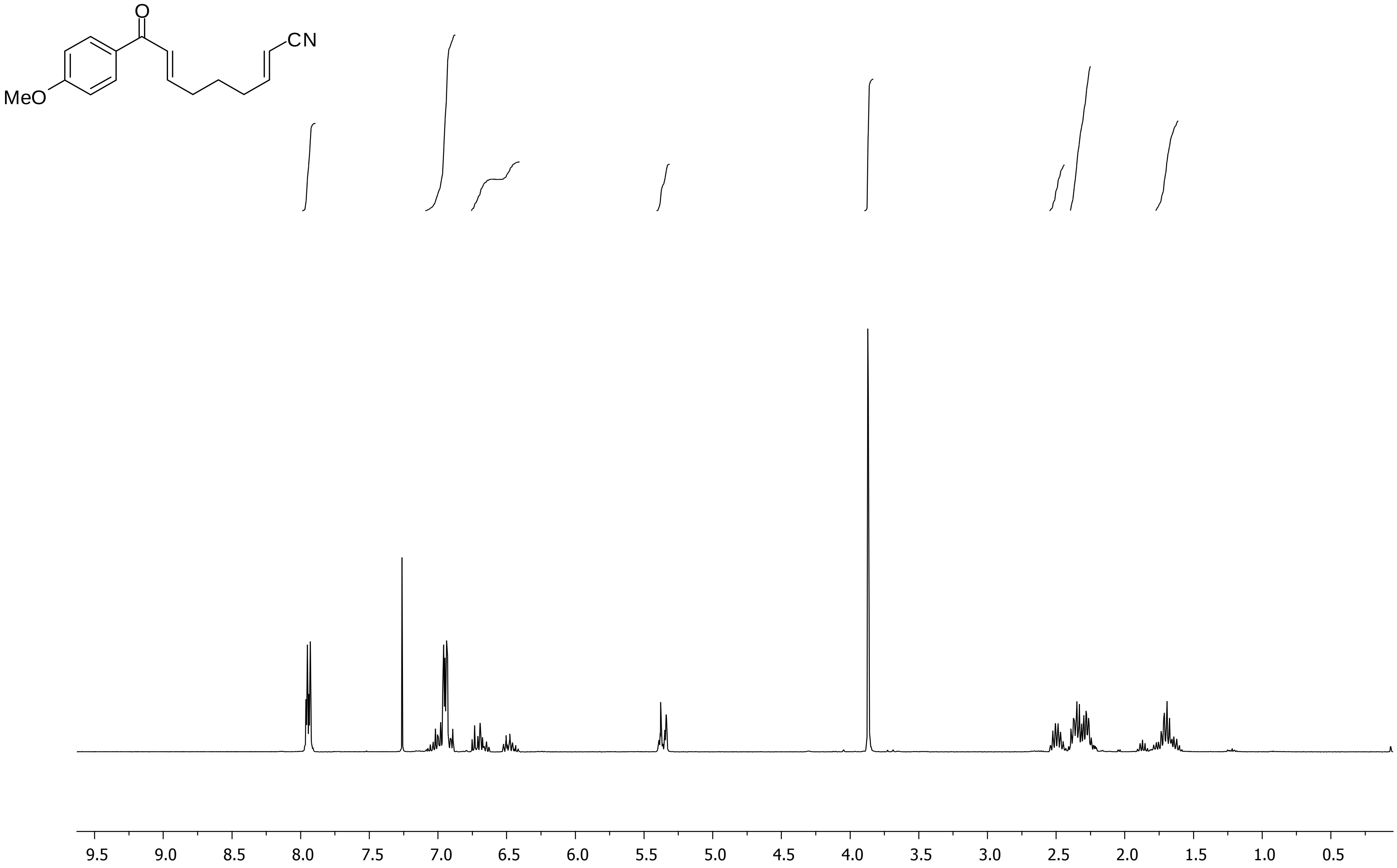
O
CN
MeO
9.5
9.0
8.5
8.0
7.5
7.0
6.5
6.0
5.5
5.0
4.5
4.0
3.5
3.0
2.5
2.0
1.5
1.0
0.5

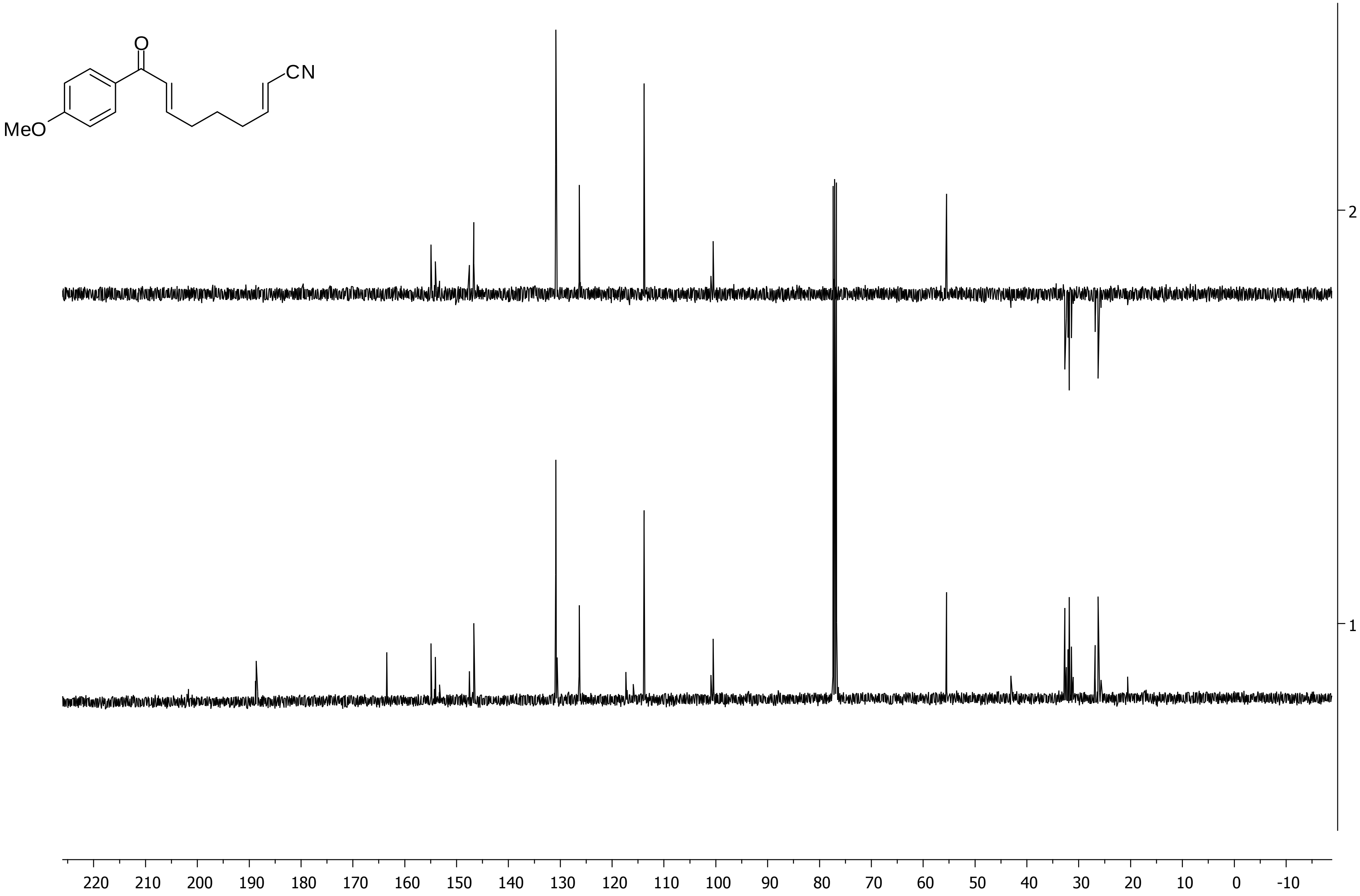
O
CN
MeO
2
1
220
210
200
190
180
170
160
150
140
130
120
110
100
90
80
70
60
50
40
30
20
10
0
-10

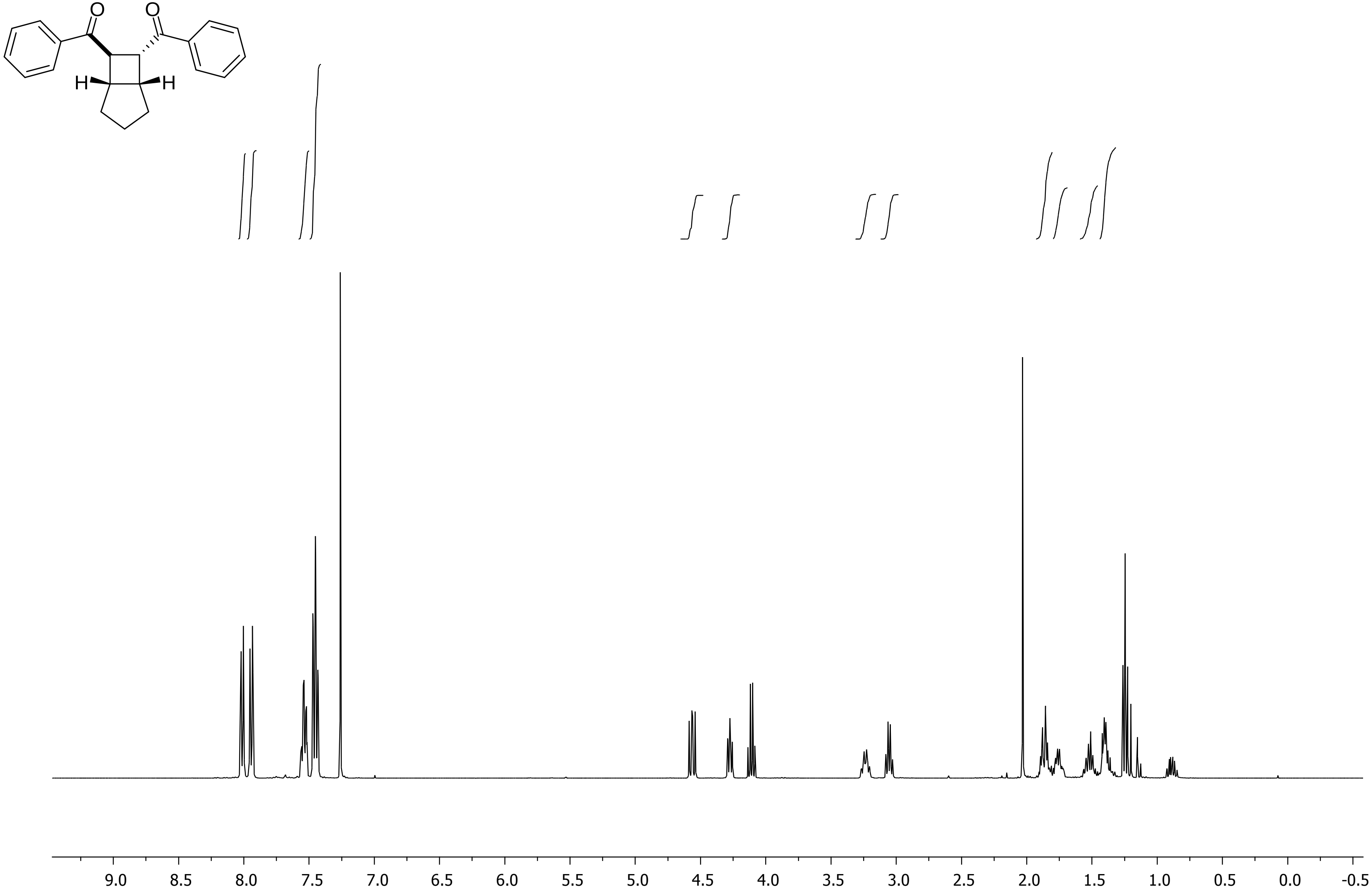
O
O
H
H
9.0
8.5
8.0
7.5
7.0
6.5
6.0
5.5
5.0
4.5
4.0
3.5
3.0
2.5
2.0
1.5
1.0
0.5
0.0
-0.5

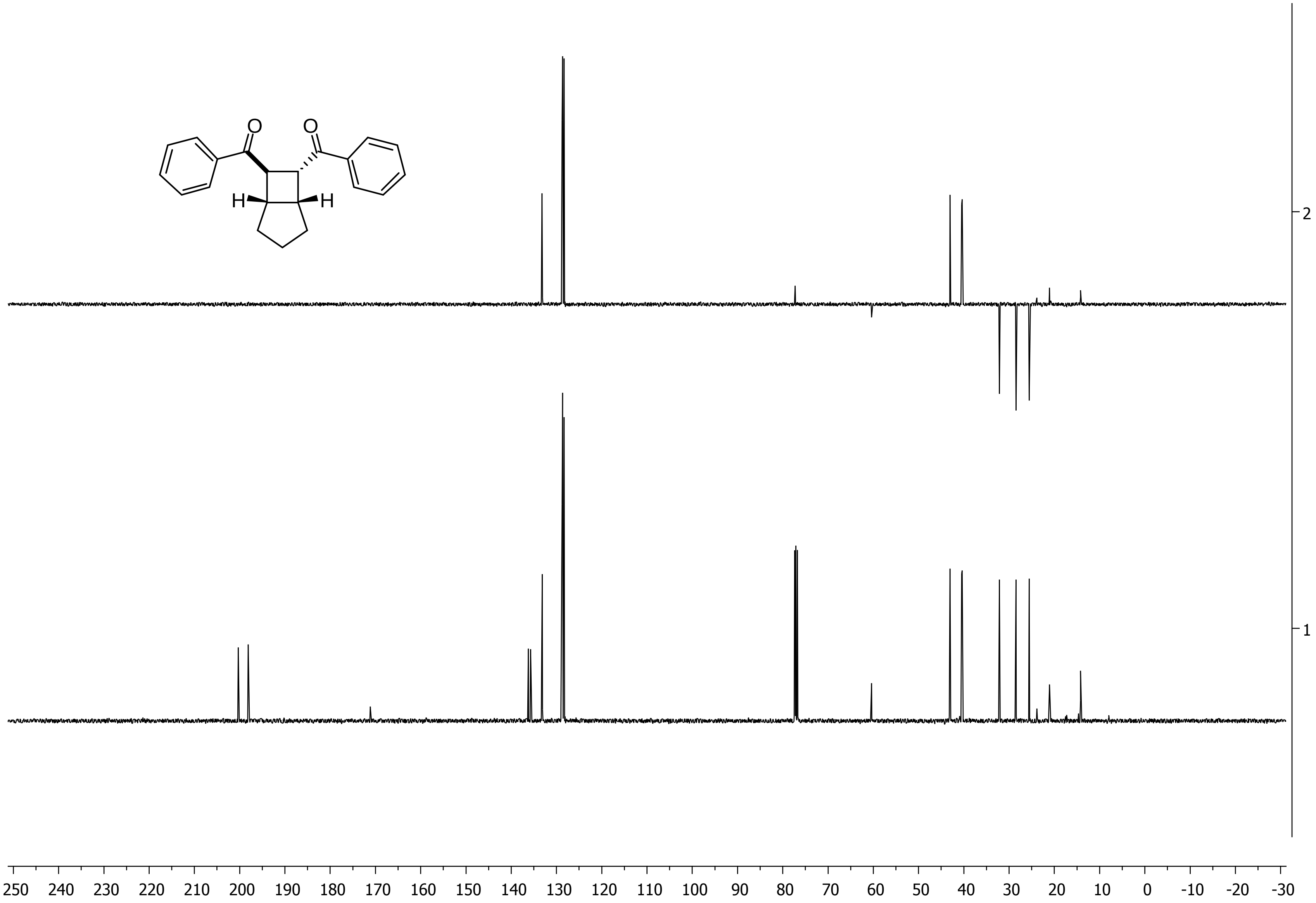
O
O
H
H
2
1
250
240
230
220
210
200
190
180
170
160
150
140
130
120
110
100
90
80
70
60
50
40
30
20
10
0
-10
-20
-30

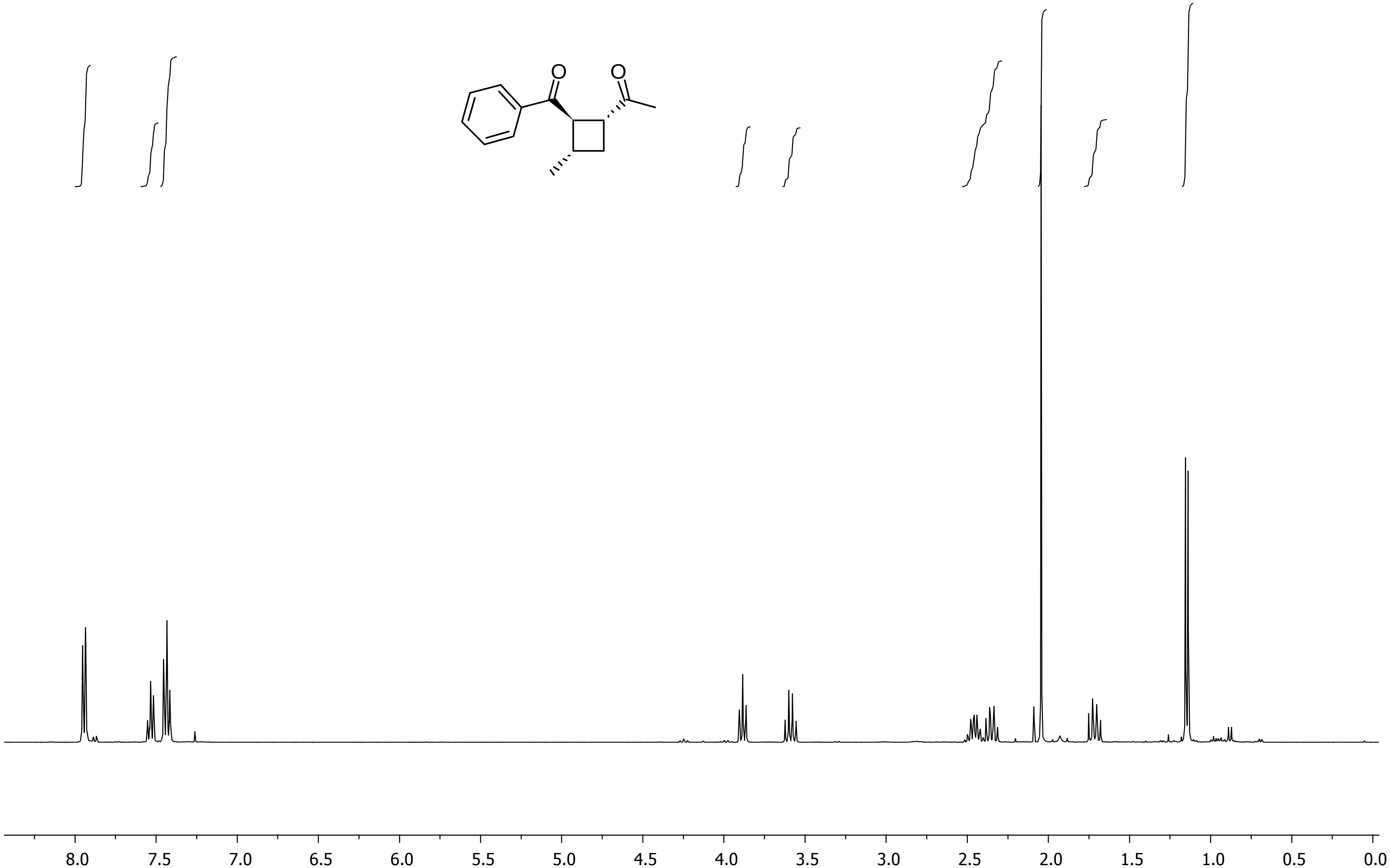
O
O
8.0
7.5
7.0
6.5
6.0
5.5
5.0
4.5
4.0
3.5
3.0
2.5
2.0
1.5
1.0
0.5
0.0

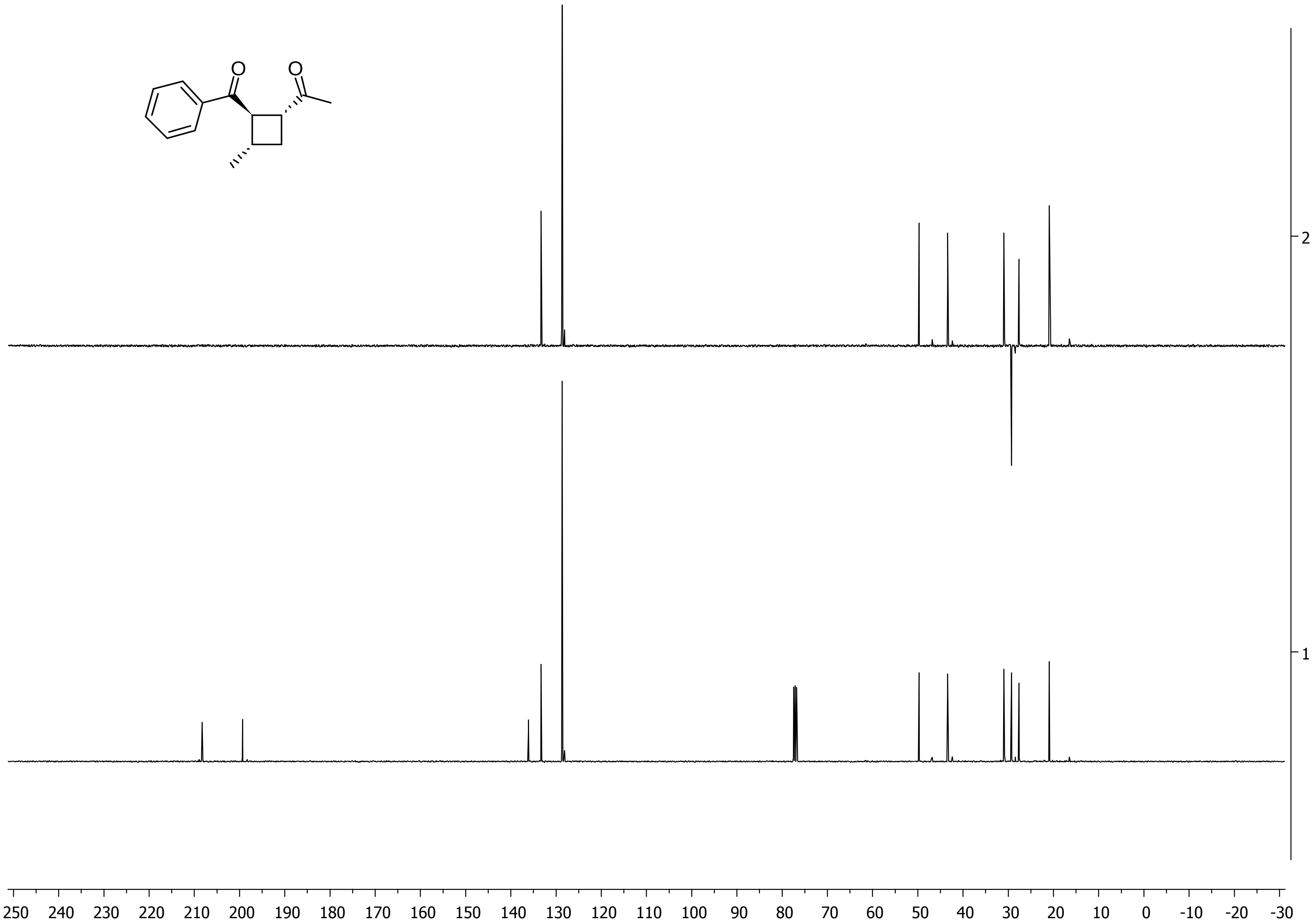
O
O
2
1
250
240
230
220
210
200
190
180
170
160
150
140
130
120
110
100
90
80
70
60
50
40
30
20
10
0
-10
-20
-30

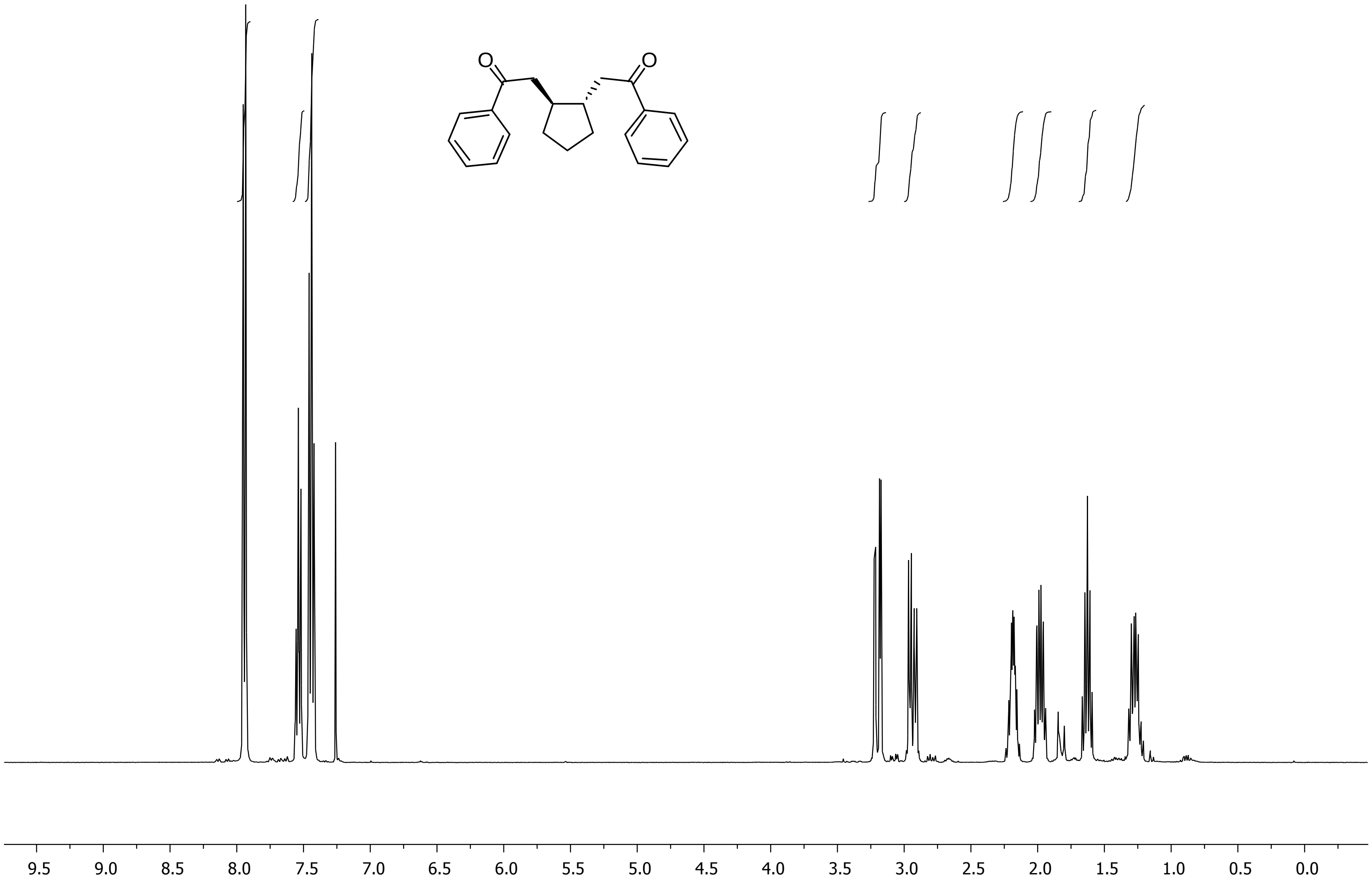
9.5
9.0
8.5
8.0
7.5
7.0
6.5
6.0
5.5
5.0
4.5
4.0
3.5
3.0
2.5
2.0
1.5
1.0
0.5
0.0
O
O

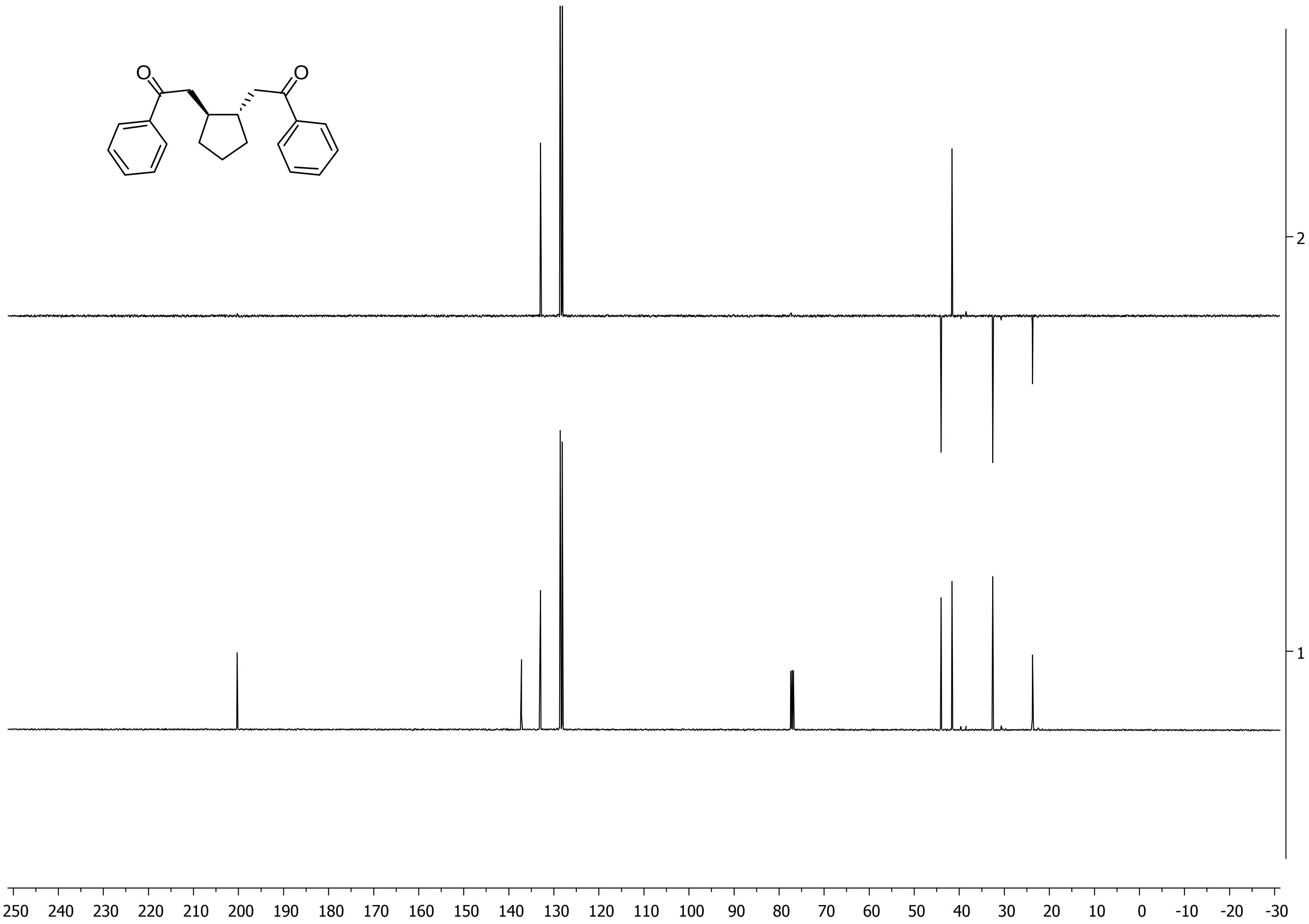
O
O
2
1
250 240 230 220 210 200 190 180 170 160 150 140 130 120 110 100 90 80 70 60 50 40 30 20 10 0 -10 -20 -30

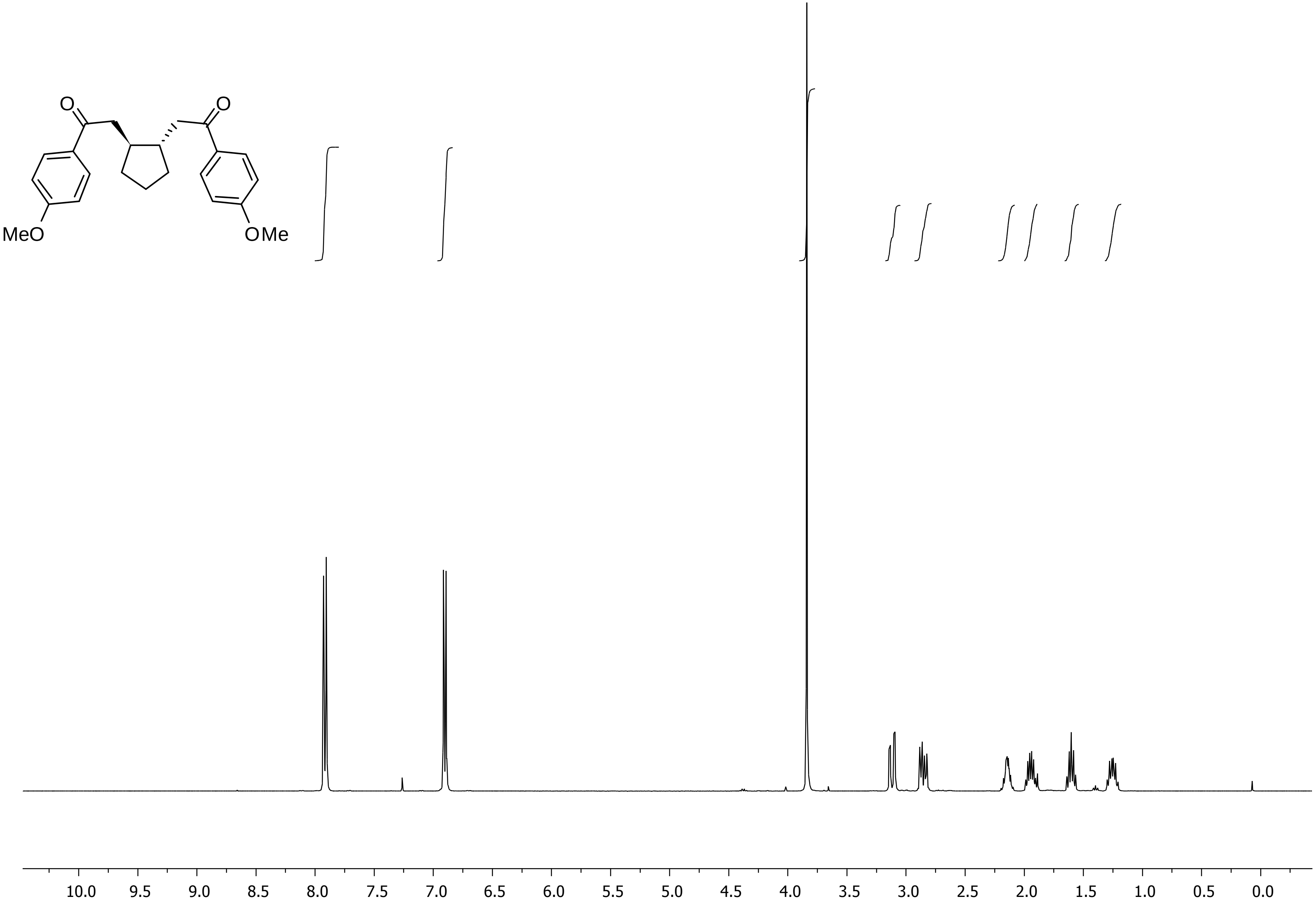
MeO
OMe
O
O
10.0
9.5
9.0
8.5
8.0
7.5
7.0
6.5
6.0
5.5
5.0
4.5
4.0
3.5
3.0
2.5
2.0
1.5
1.0
0.5
0.0

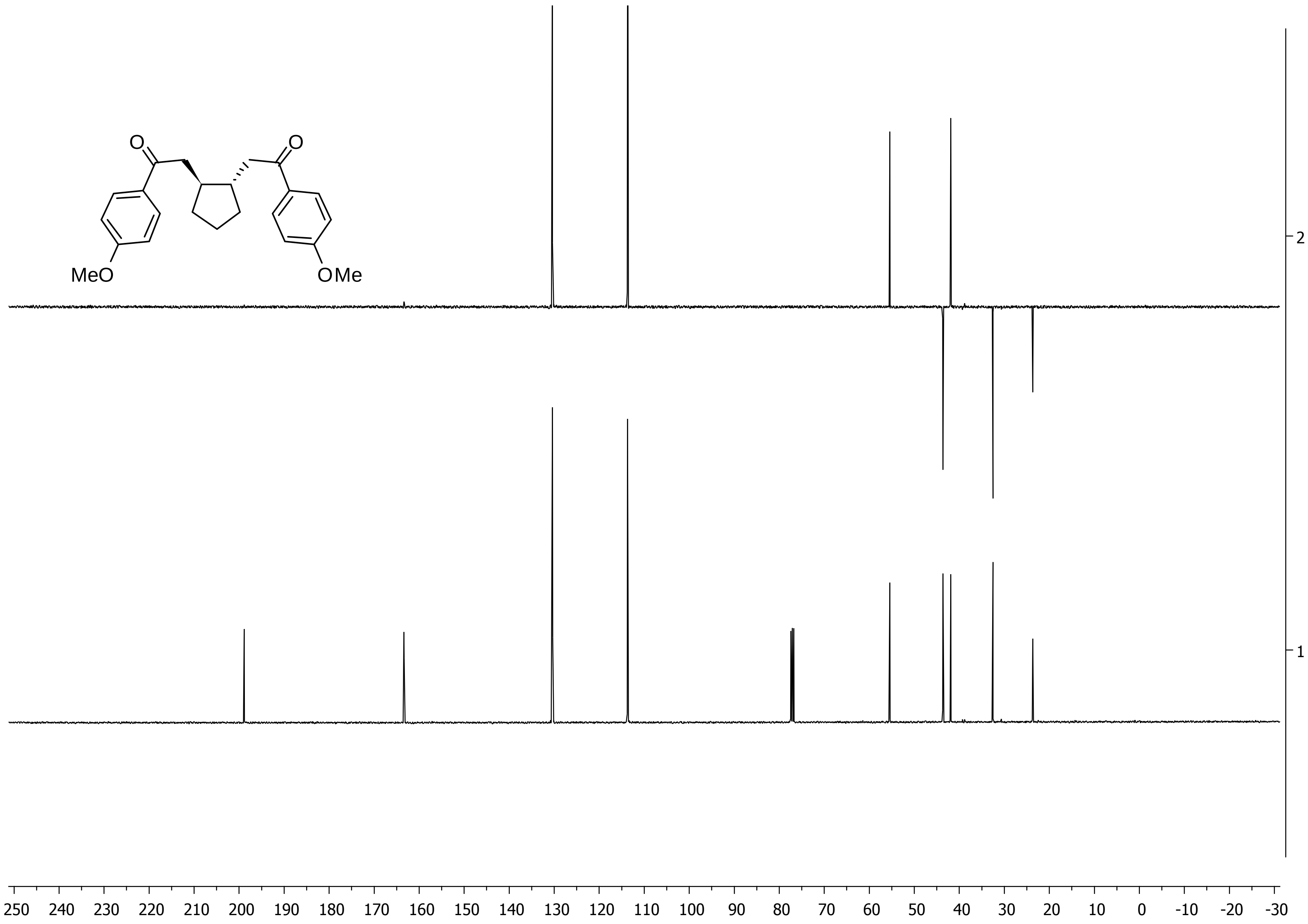
O
O
MeO
OMe
2
1
250
240
230
220
210
200
190
180
170
160
150
140
130
120
110
100
90
80
70
60
50
40
30
20
10
0
-10
-20
-30

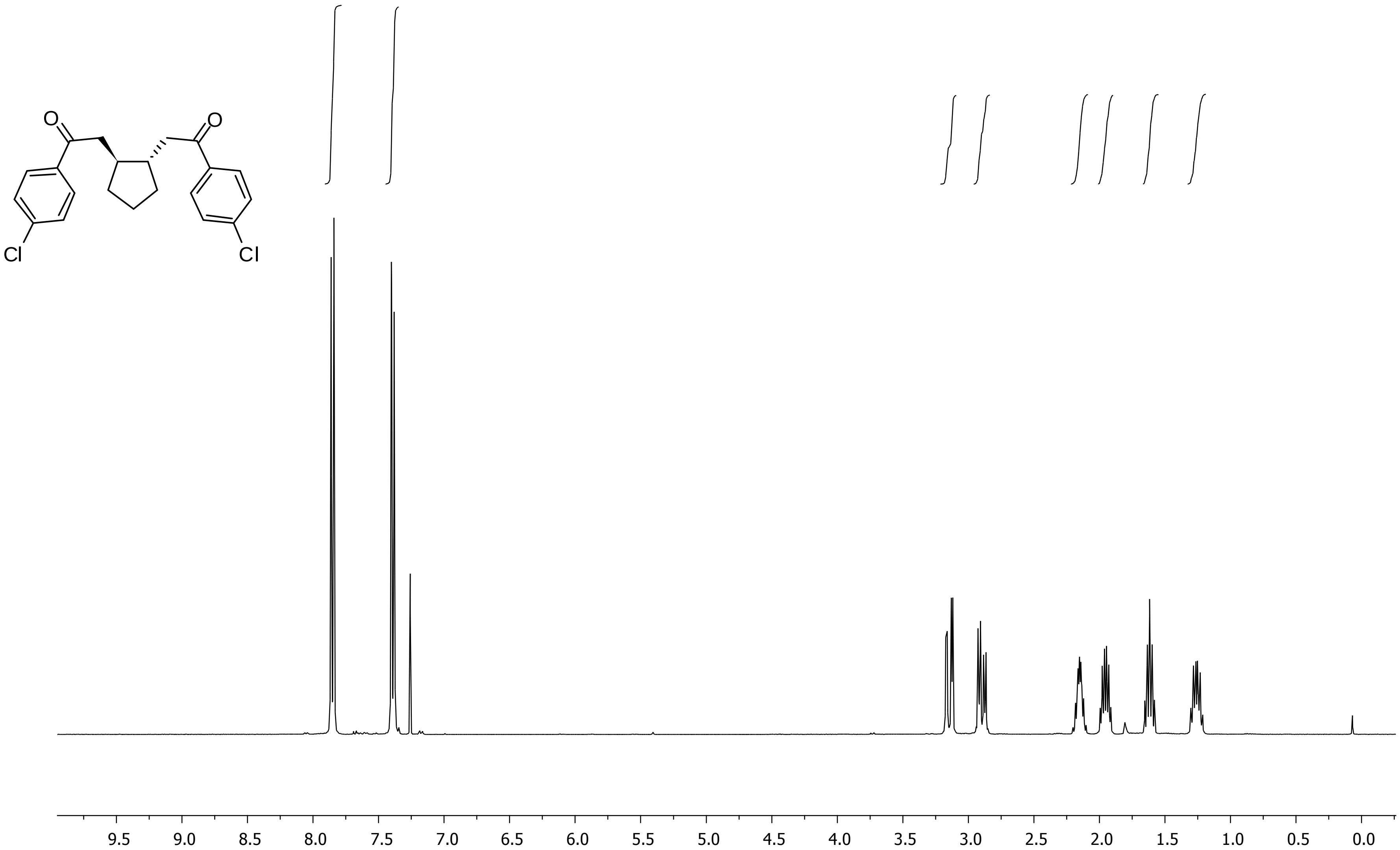
O
O
Cl
Cl
9.5
9.0
8.5
8.0
7.5
7.0
6.5
6.0
5.5
5.0
4.5
4.0
3.5
3.0
2.5
2.0
1.5
1.0
0.5
0.0

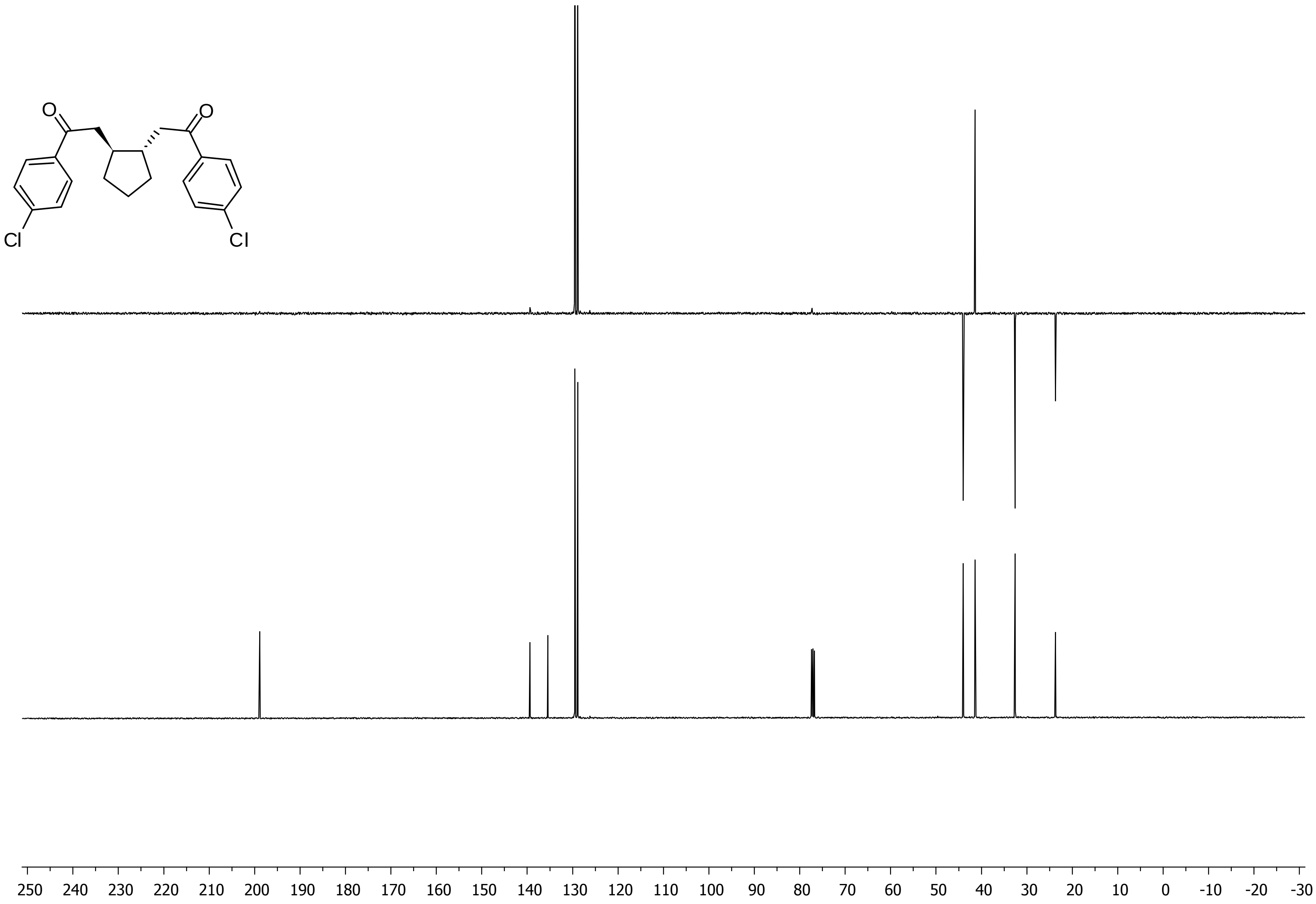
O
O
Cl
Cl
250 240 230 220 210 200 190 180 170 160 150 140 130 120 110 100 90 80 70 60 50 40 30 20 10 0 -10 -20 -30

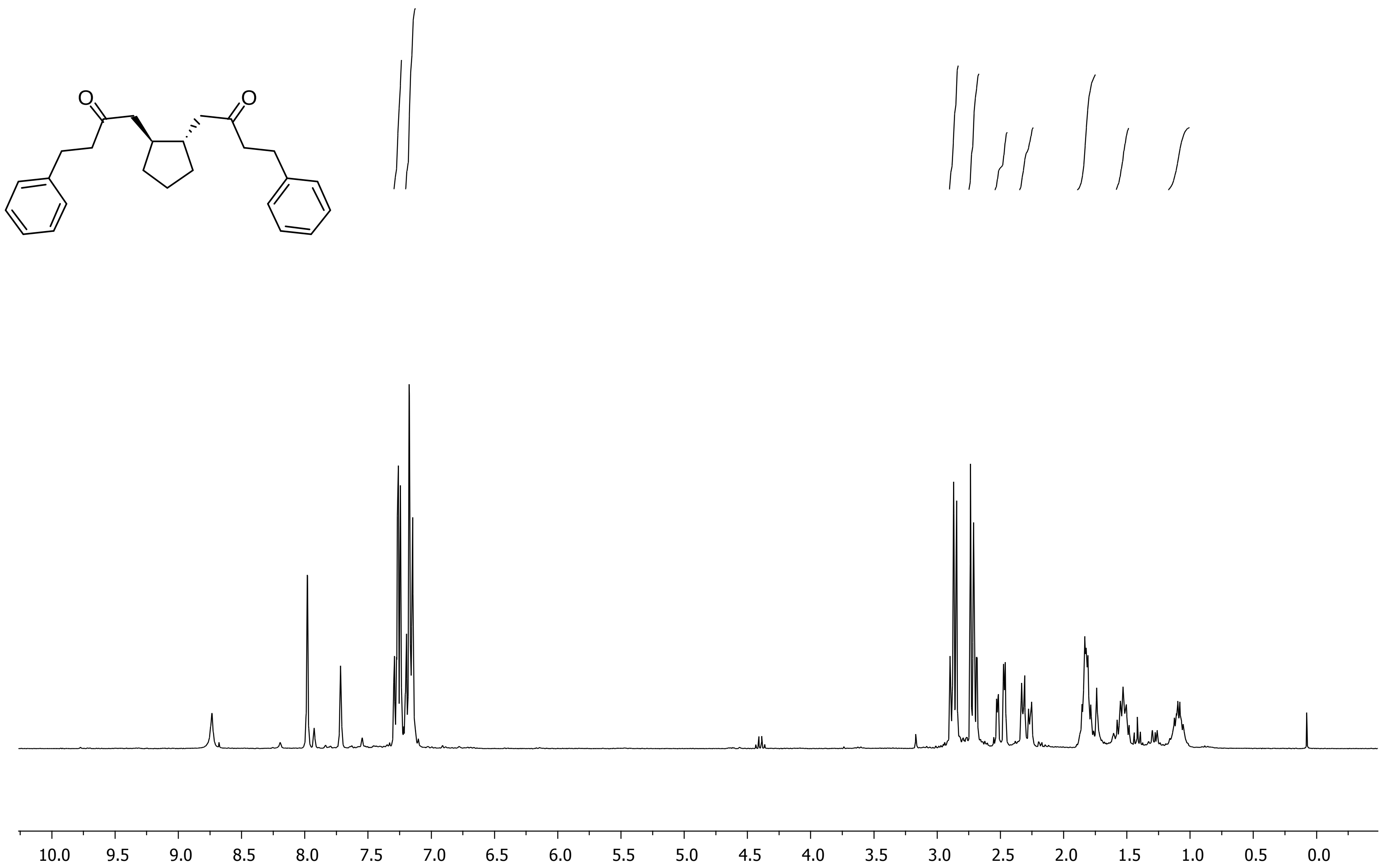
O
O
10.0
9.5
9.0
8.5
8.0
7.5
7.0
6.5
6.0
5.5
5.0
4.5
4.0
3.5
3.0
2.5
2.0
1.5
1.0
0.5
0.0

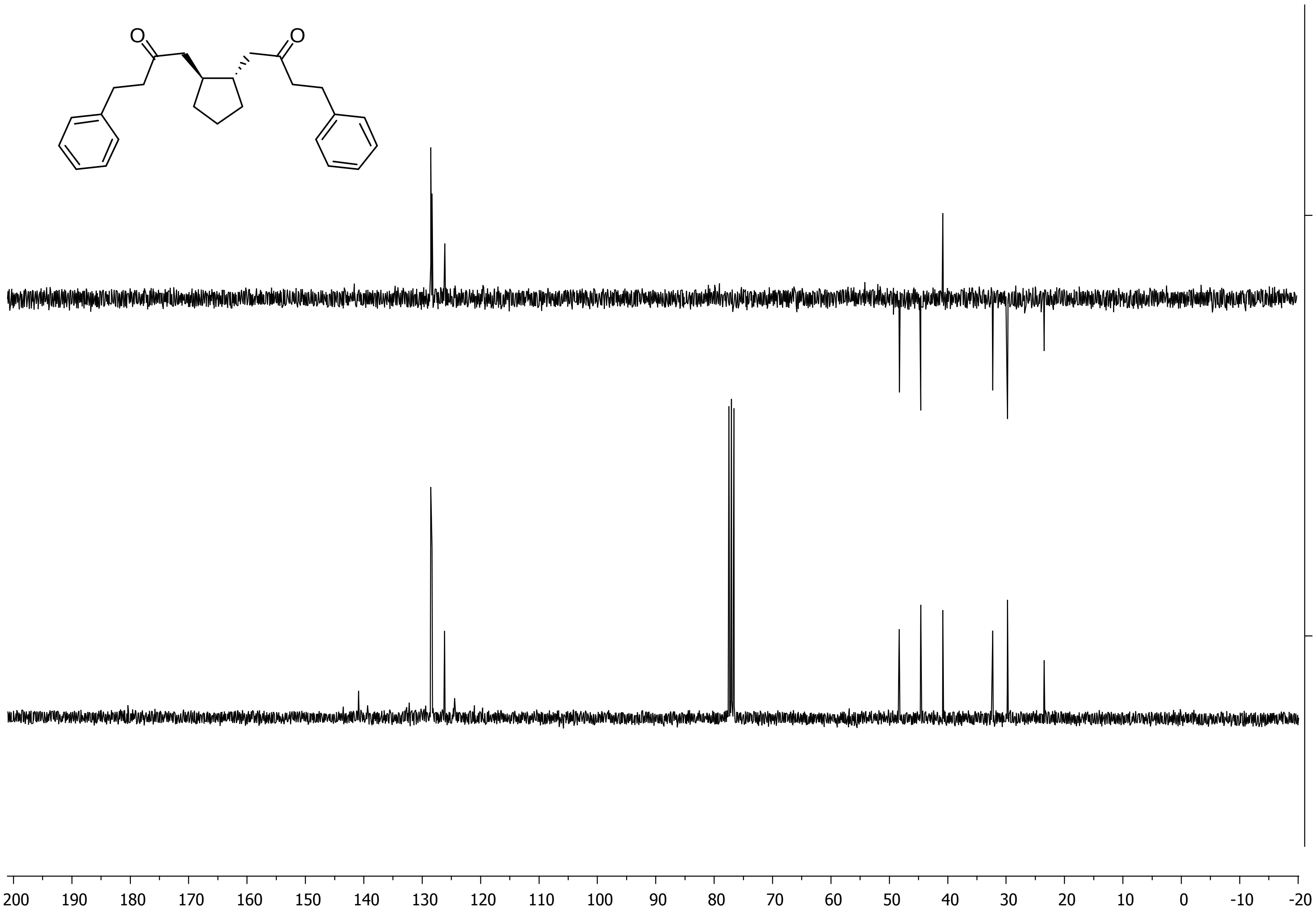
O
O
2
1
200
190
180
170
160
150
140
130
120
110
100
90
80
70
60
50
40
30
20
10
0
-10
-20

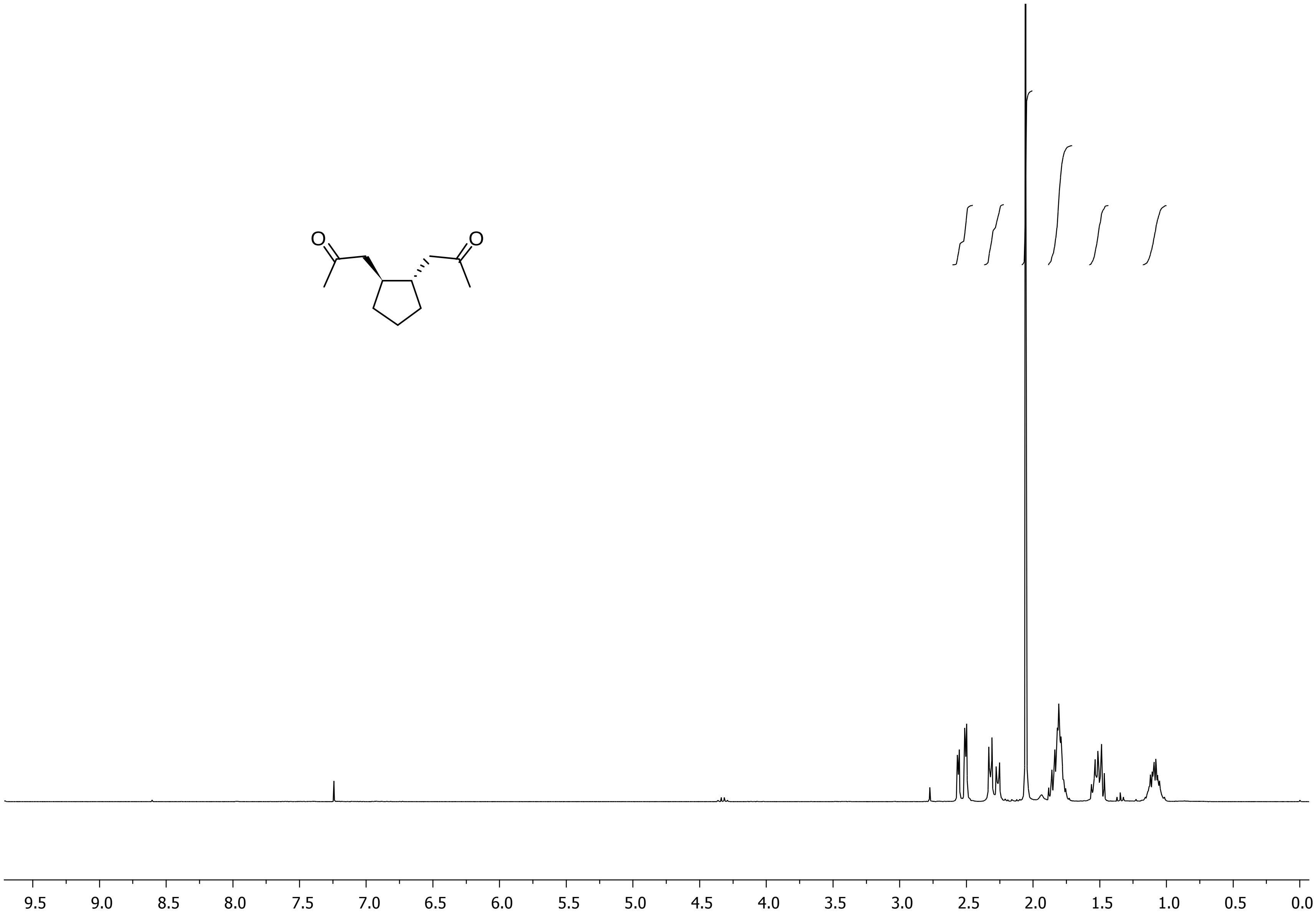

9.5
9.0
8.5
8.0
7.5
7.0
6.5
6.0
5.5
5.0
4.5
4.0
3.5
3.0
2.5
2.0
1.5
1.0
0.5
0.0
O
O

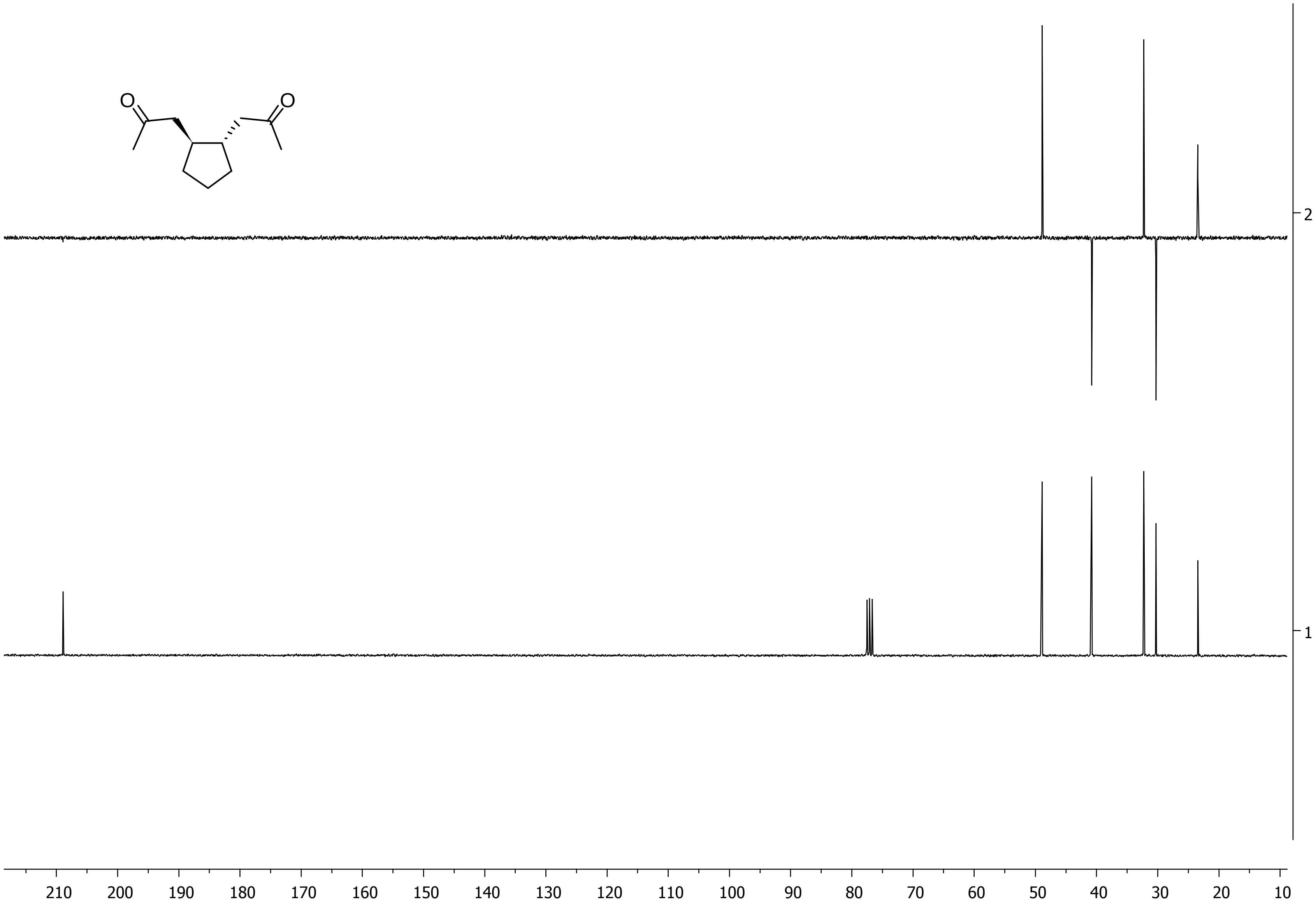
O
O
2
1
210
200
190
180
170
160
150
140
130
120
110
100
90
80
70
60
50
40
30
20
10

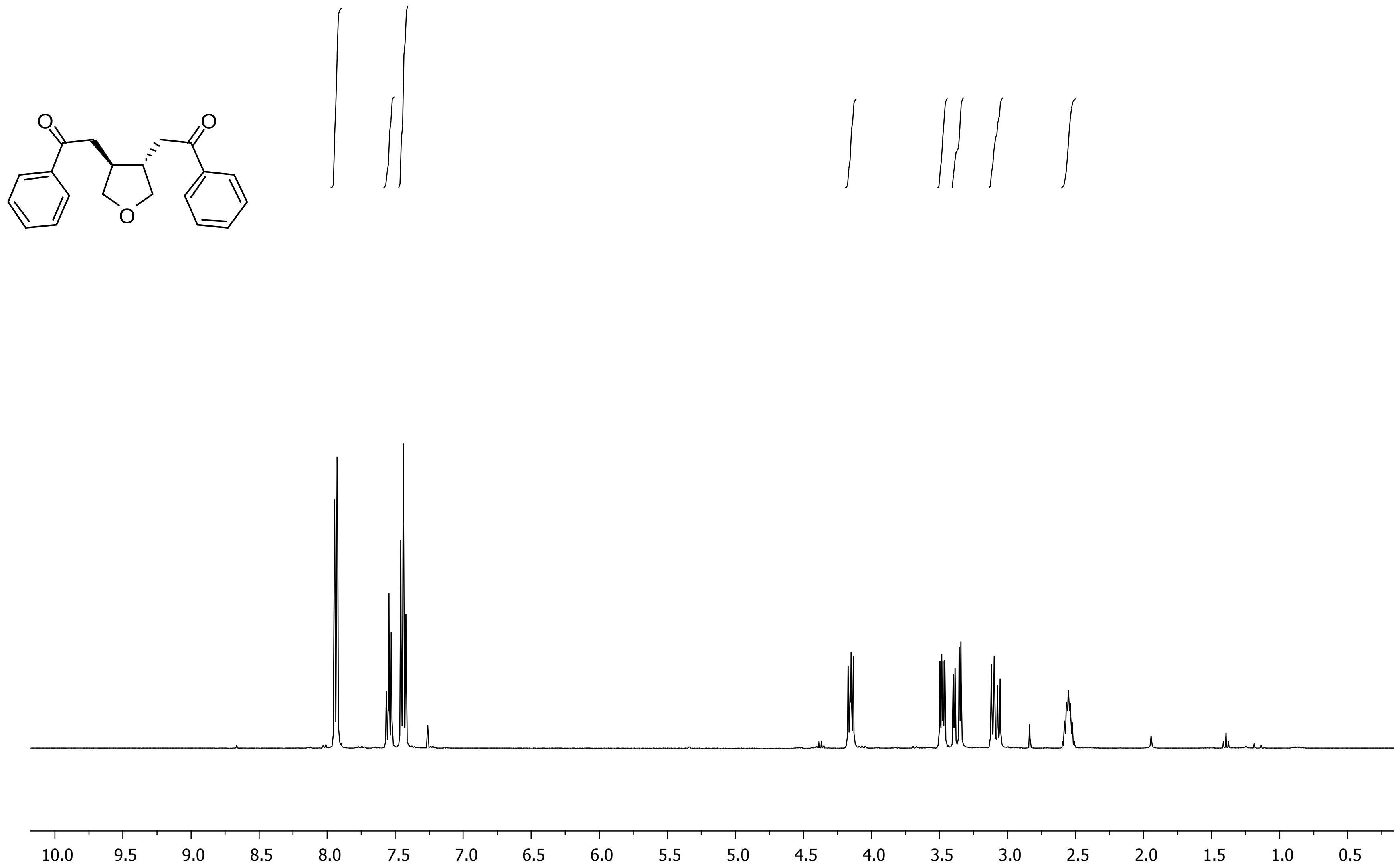

10.0
9.5
9.0
8.5
8.0
7.5
7.0
6.5
6.0
5.5
5.0
4.5
4.0
3.5
3.0
2.5
2.0
1.5
1.0
0.5

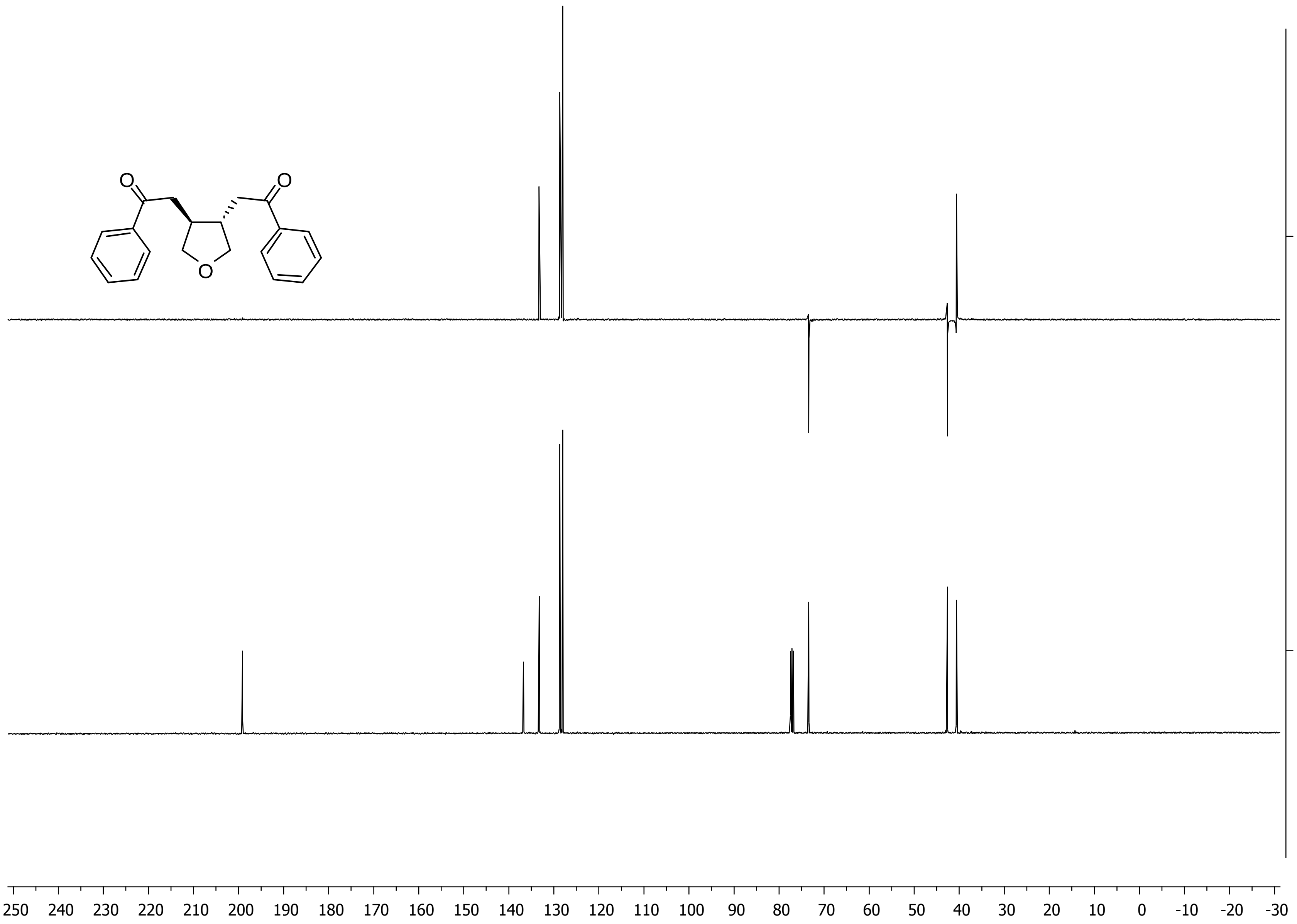
O
O
O
2
1
250 240 230 220 210 200 190 180 170 160 150 140 130 120 110 100 90 80 70 60 50 40 30 20 10 0 -10 -20 -30

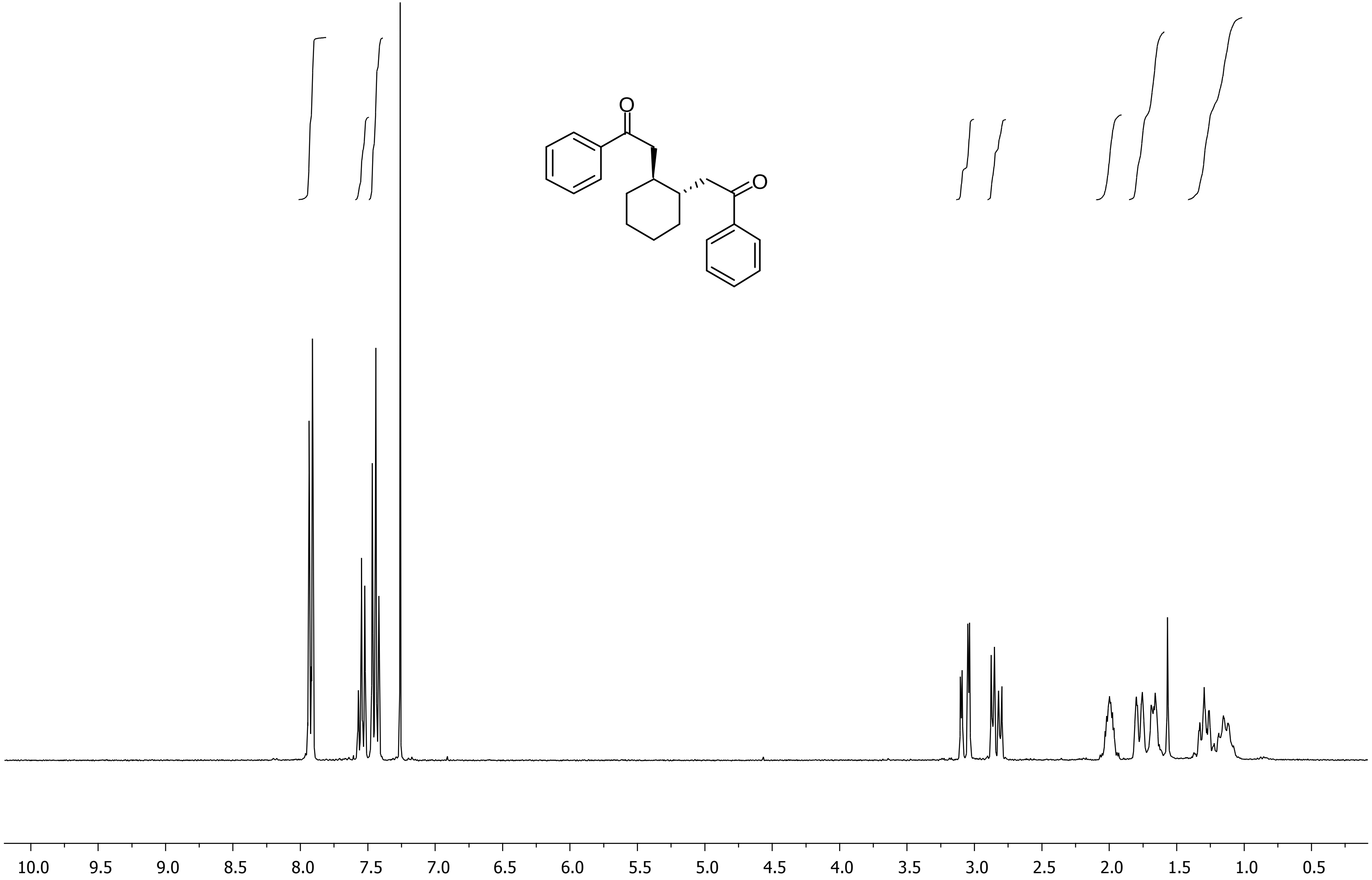
O
O
10.0
9.5
9.0
8.5
8.0
7.5
7.0
6.5
6.0
5.5
5.0
4.5
4.0
3.5
3.0
2.5
2.0
1.5
1.0
0.5

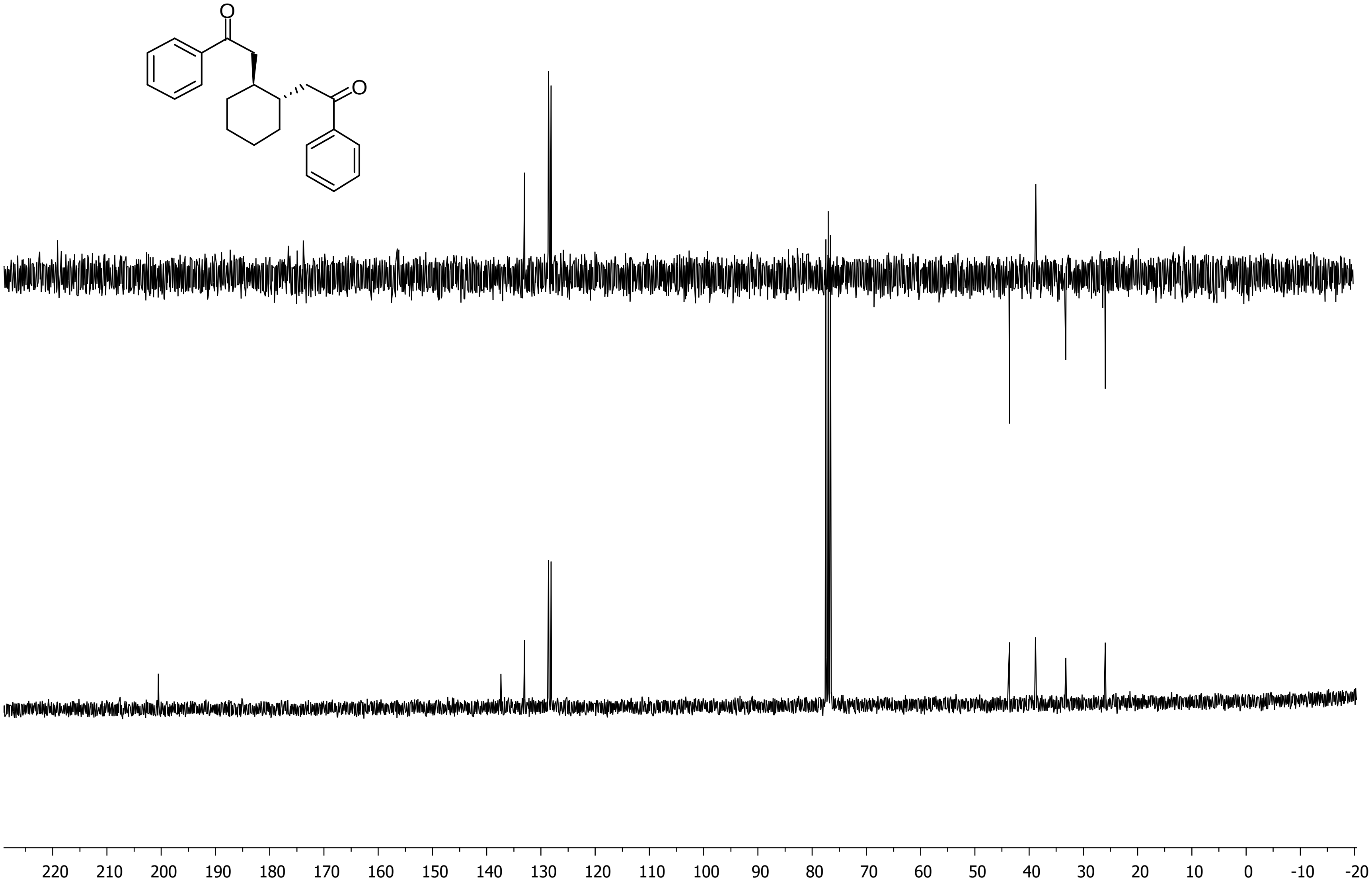
O
O
220
210
200
190
180
170
160
150
140
130
120
110
100
90
80
70
60
50
40
30
20
10
0
-10
-20

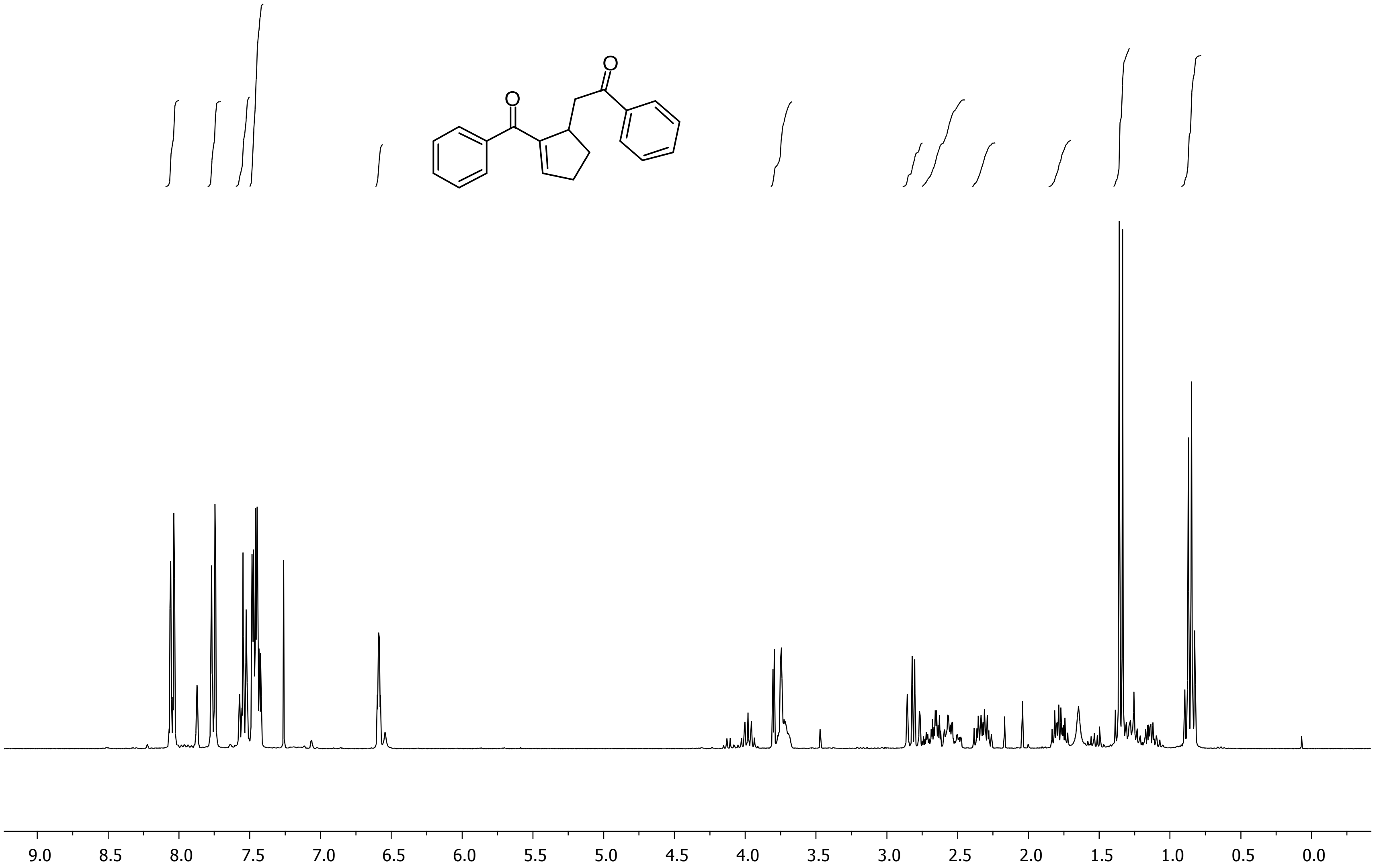
O
O
9.0
8.5
8.0
7.5
7.0
6.5
6.0
5.5
5.0
4.5
4.0
3.5
3.0
2.5
2.0
1.5
1.0
0.5
0.0

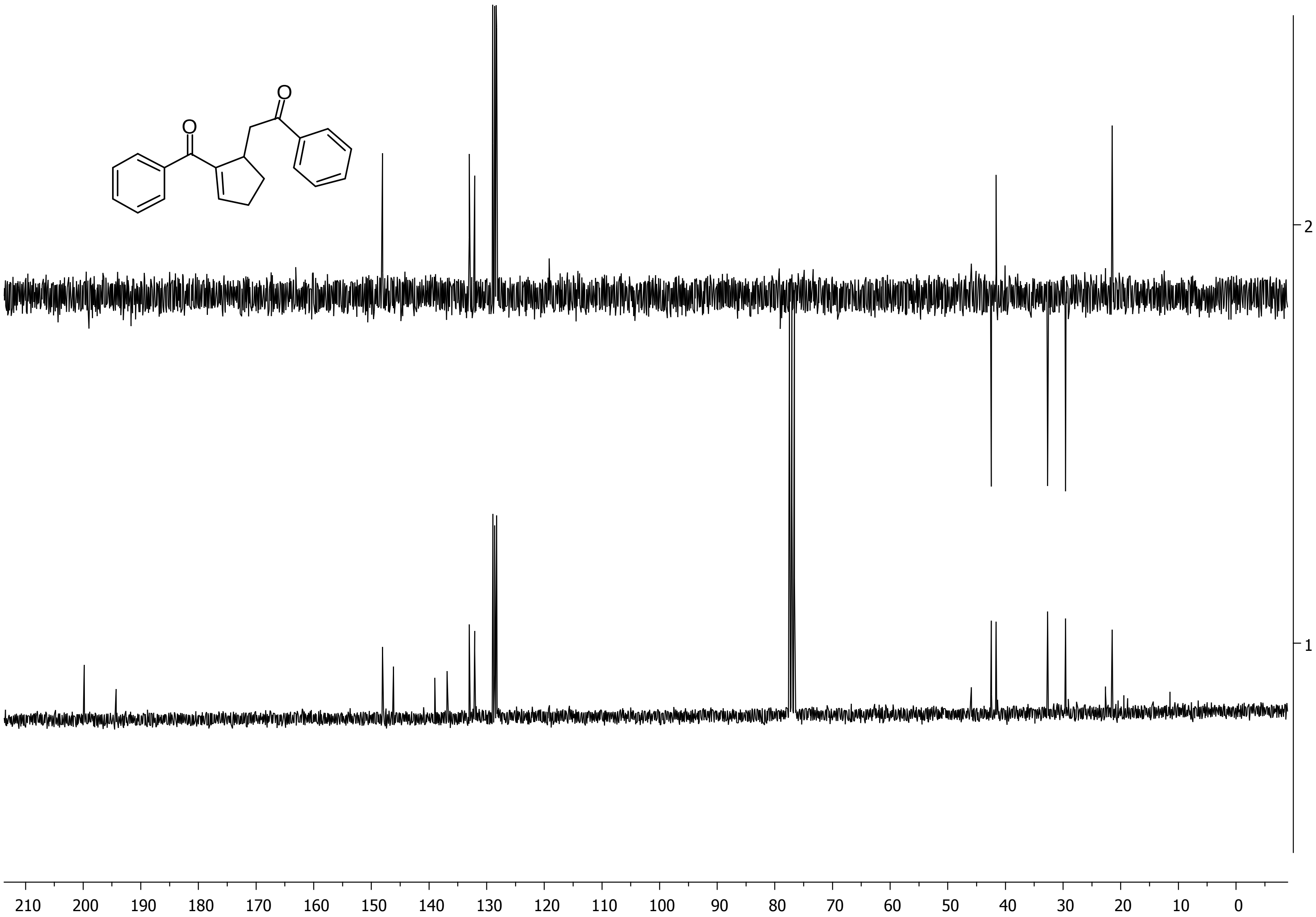
O
O
2
1
210
200
190
180
170
160
150
140
130
120
110
100
90
80
70
60
50
40
30
20
10
0

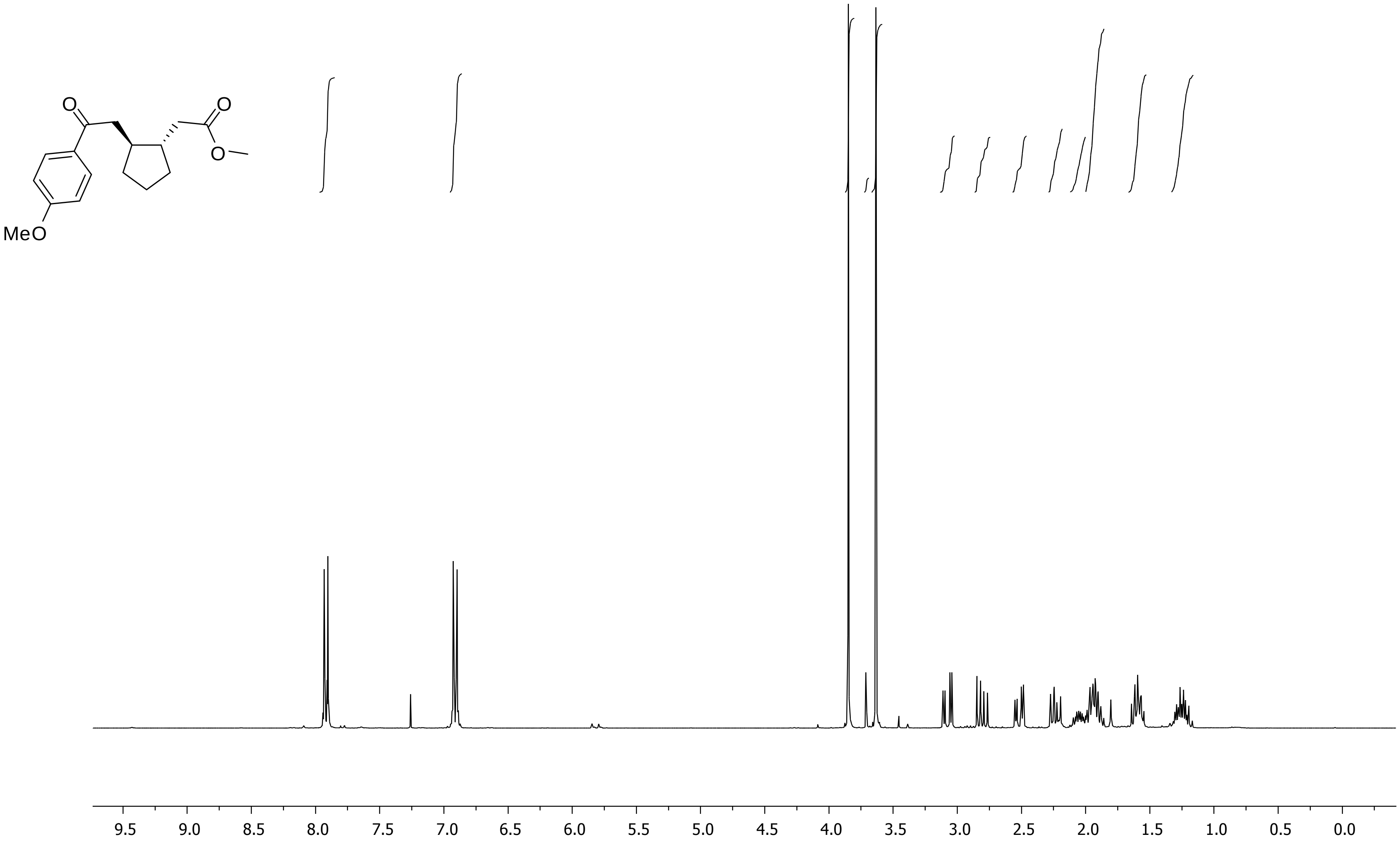
O
O
O
MeO
9.5
9.0
8.5
8.0
7.5
7.0
6.5
6.0
5.5
5.0
4.5
4.0
3.5
3.0
2.5
2.0
1.5
1.0
0.5
0.0

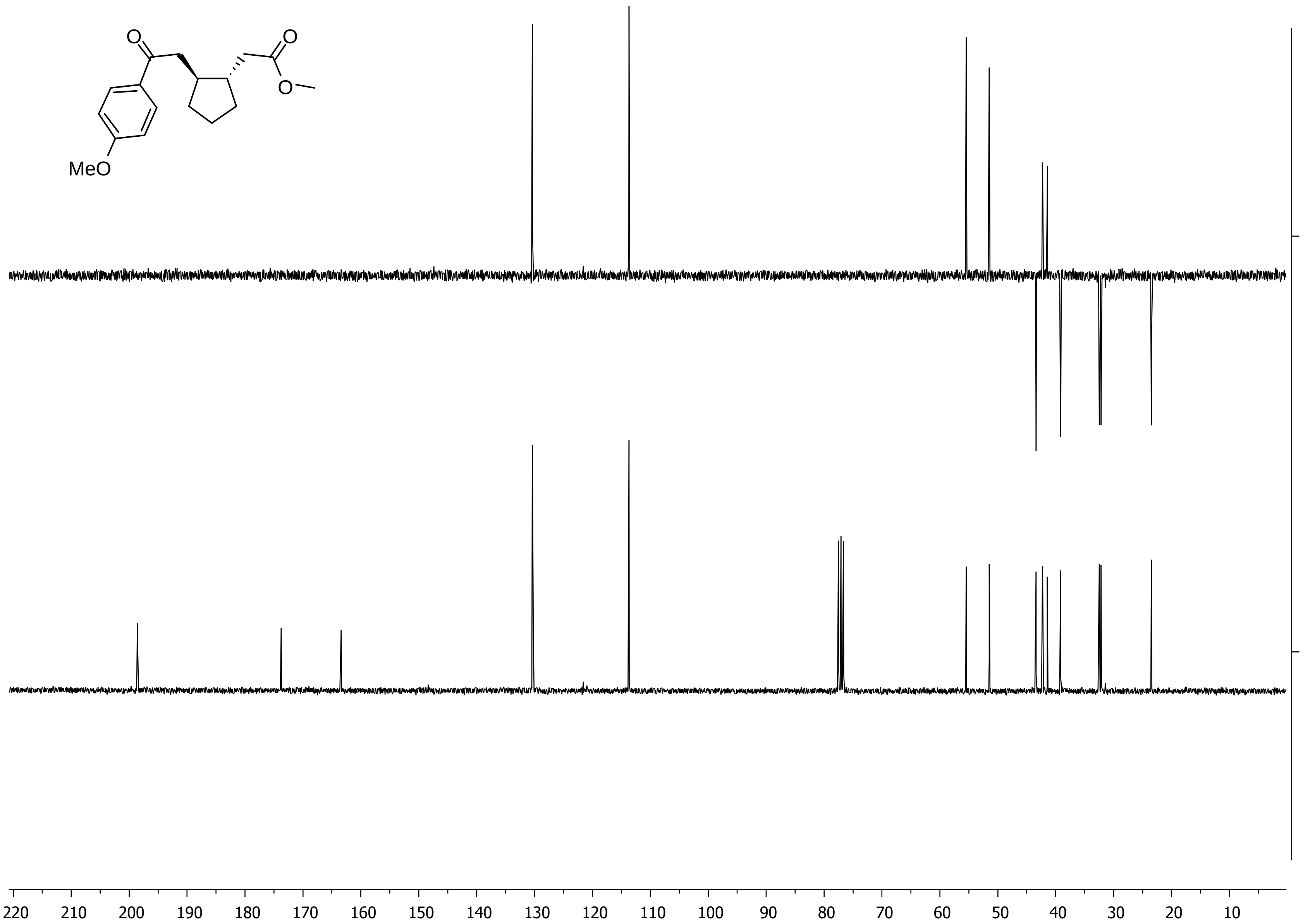
MeO
O
O
O
2
1
220
210
200
190
180
170
160
150
140
130
120
110
100
90
80
70
60
50
40
30
20
10

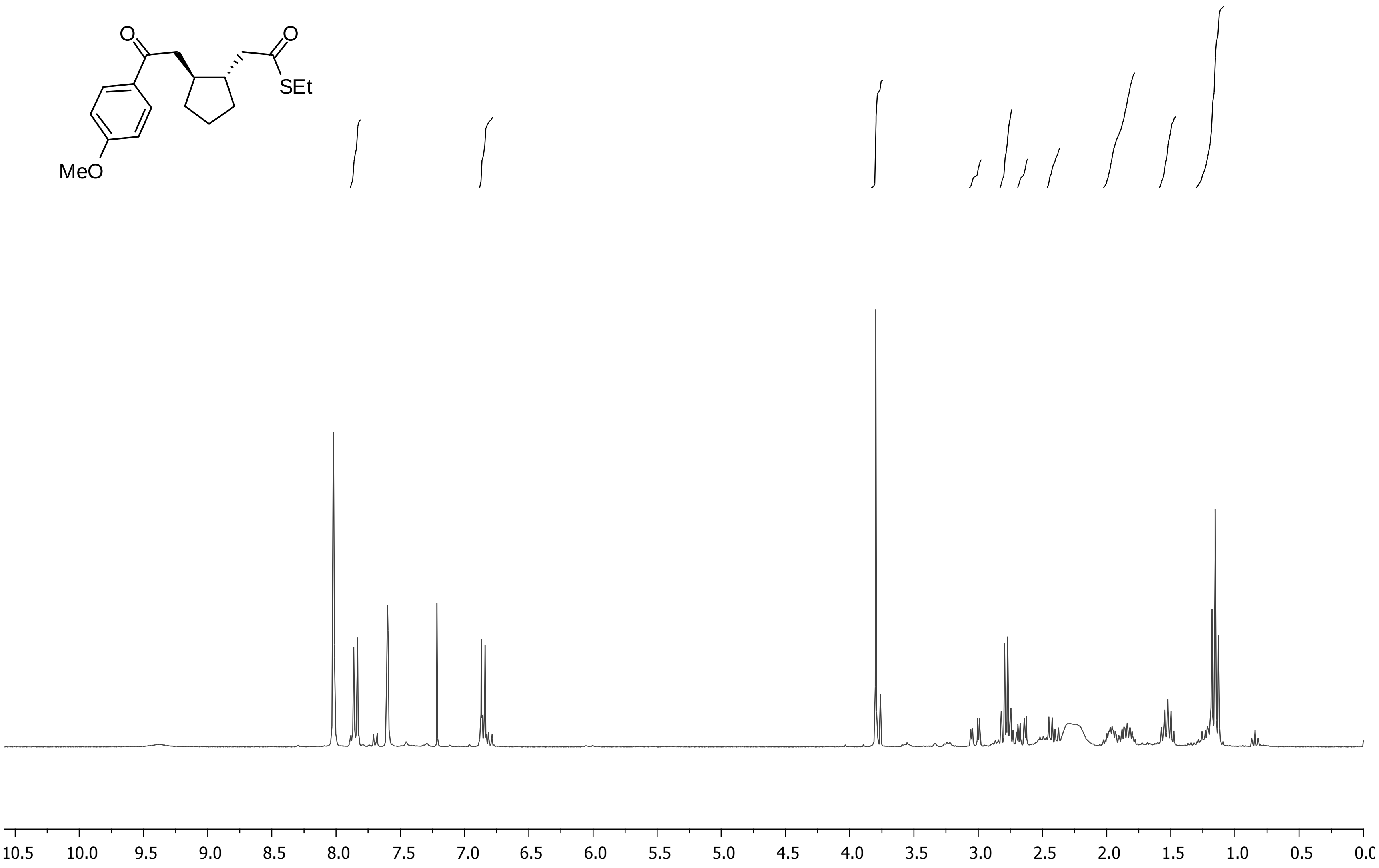
O
O
SEt
MeO
10.5
10.0
9.5
9.0
8.5
8.0
7.5
7.0
6.5
6.0
5.5
5.0
4.5
4.0
3.5
3.0
2.5
2.0
1.5
1.0
0.5
0.0

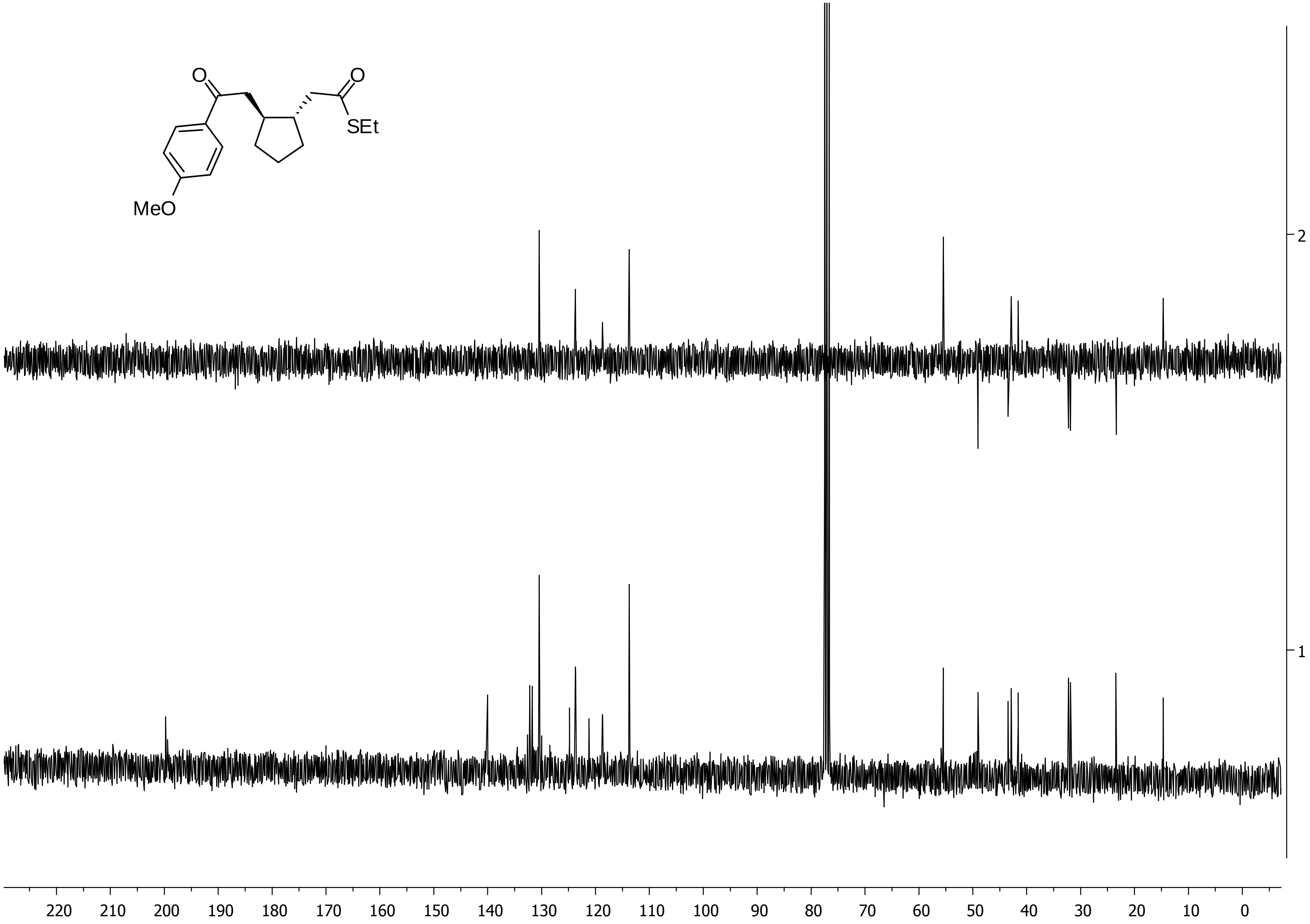
O
O
SEt
MeO
2
1
220
210
200
190
180
170
160
150
140
130
120
110
100
90
80
70
60
50
40
30
20
10
0

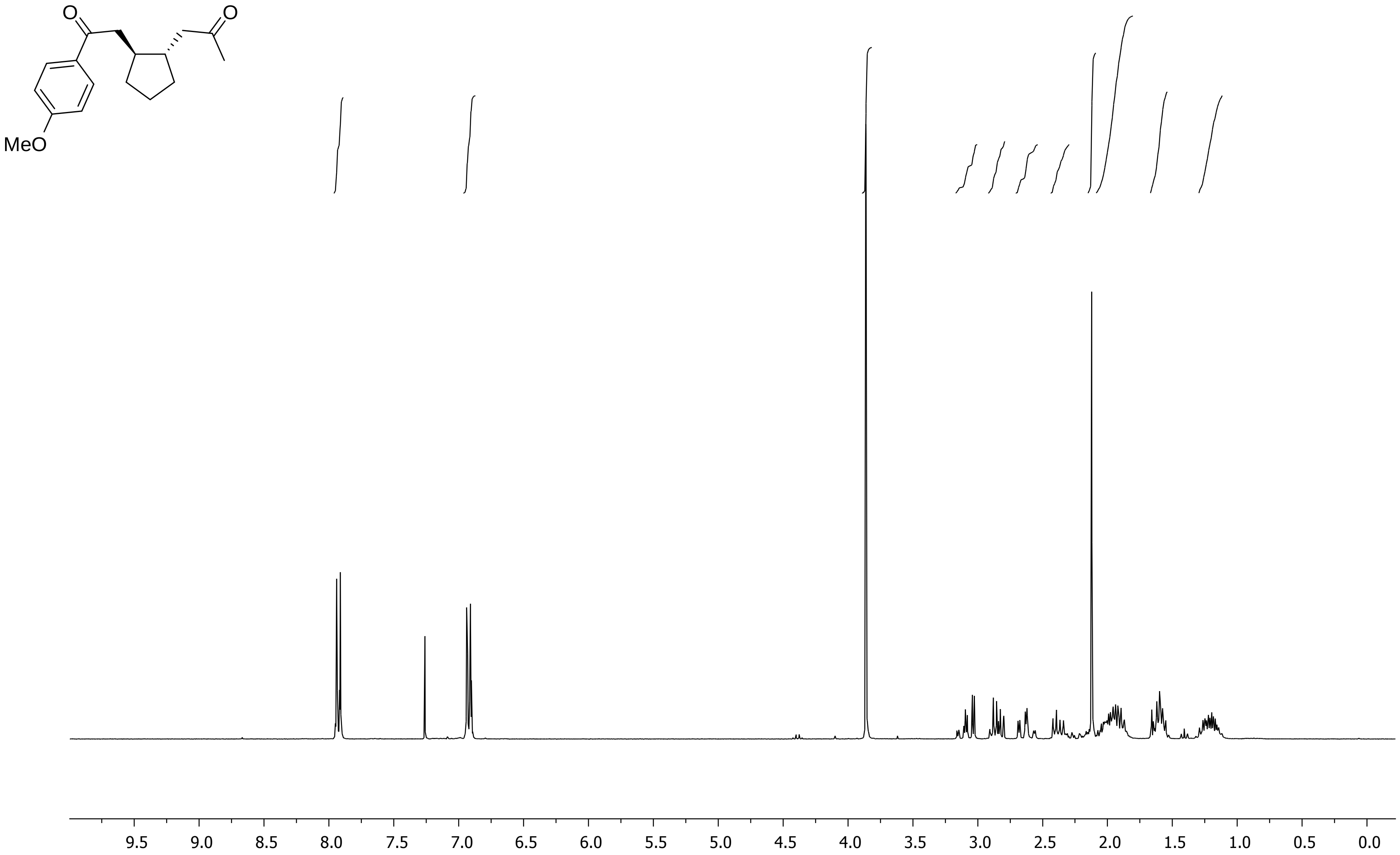
O
O
MeO
9.5
9.0
8.5
8.0
7.5
7.0
6.5
6.0
5.5
5.0
4.5
4.0
3.5
3.0
2.5
2.0
1.5
1.0
0.5
0.0

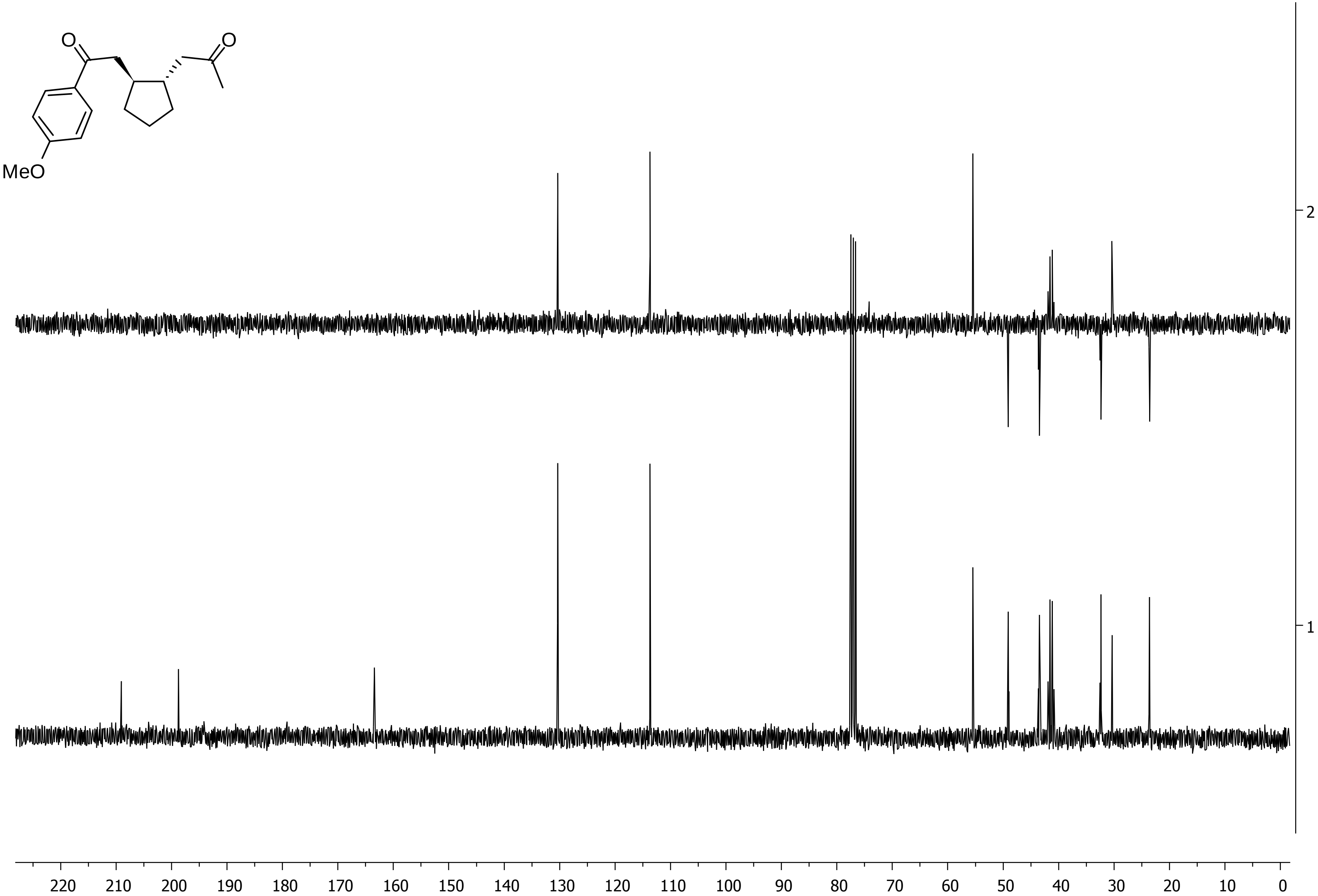
O
O
MeO
2
1
220
210
200
190
180
170
160
150
140
130
120
110
100
90
80
70
60
50
40
30
20
10
0

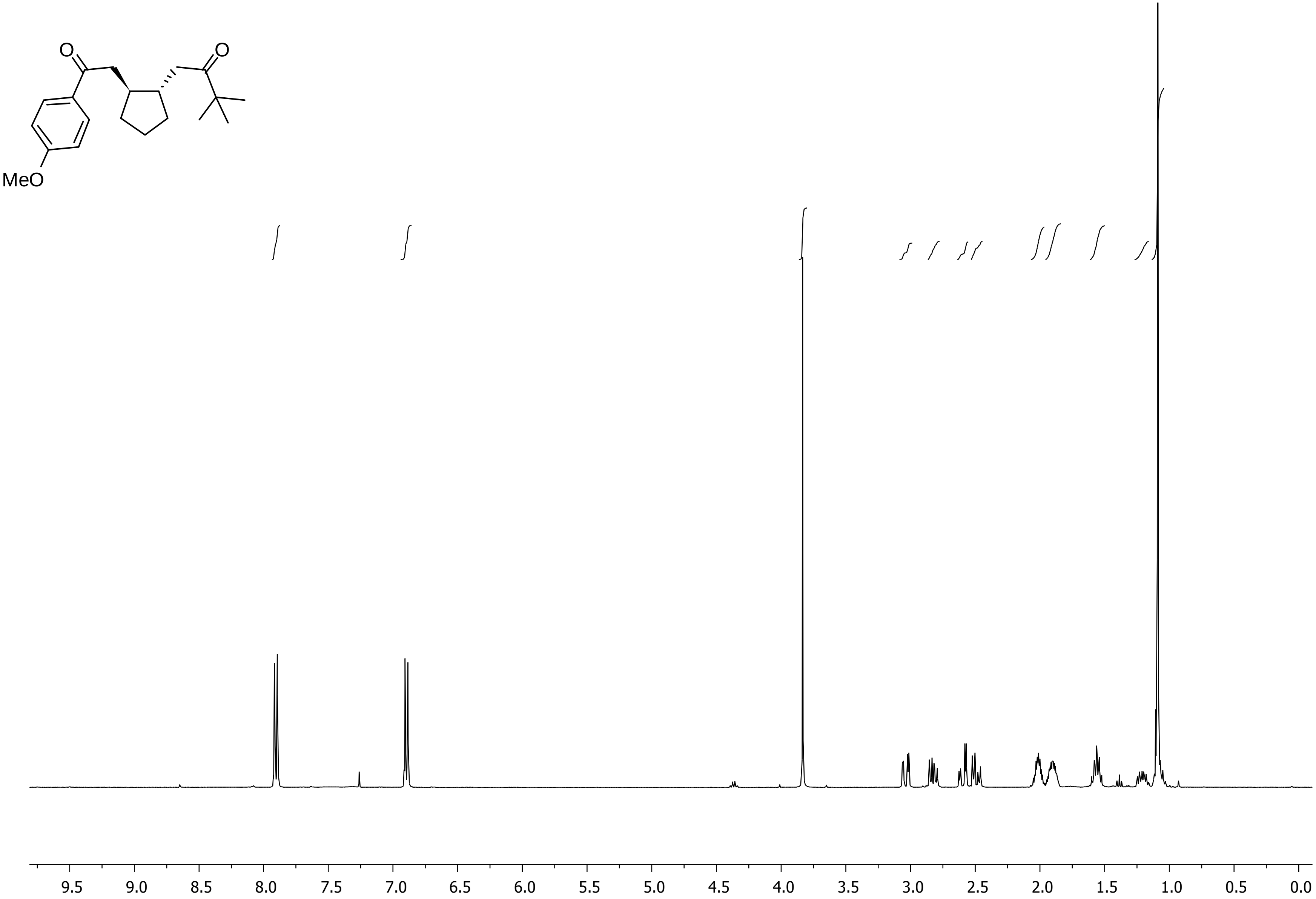
O
O
MeO
9.5
9.0
8.5
8.0
7.5
7.0
6.5
6.0
5.5
5.0
4.5
4.0
3.5
3.0
2.5
2.0
1.5
1.0
0.5
0.0

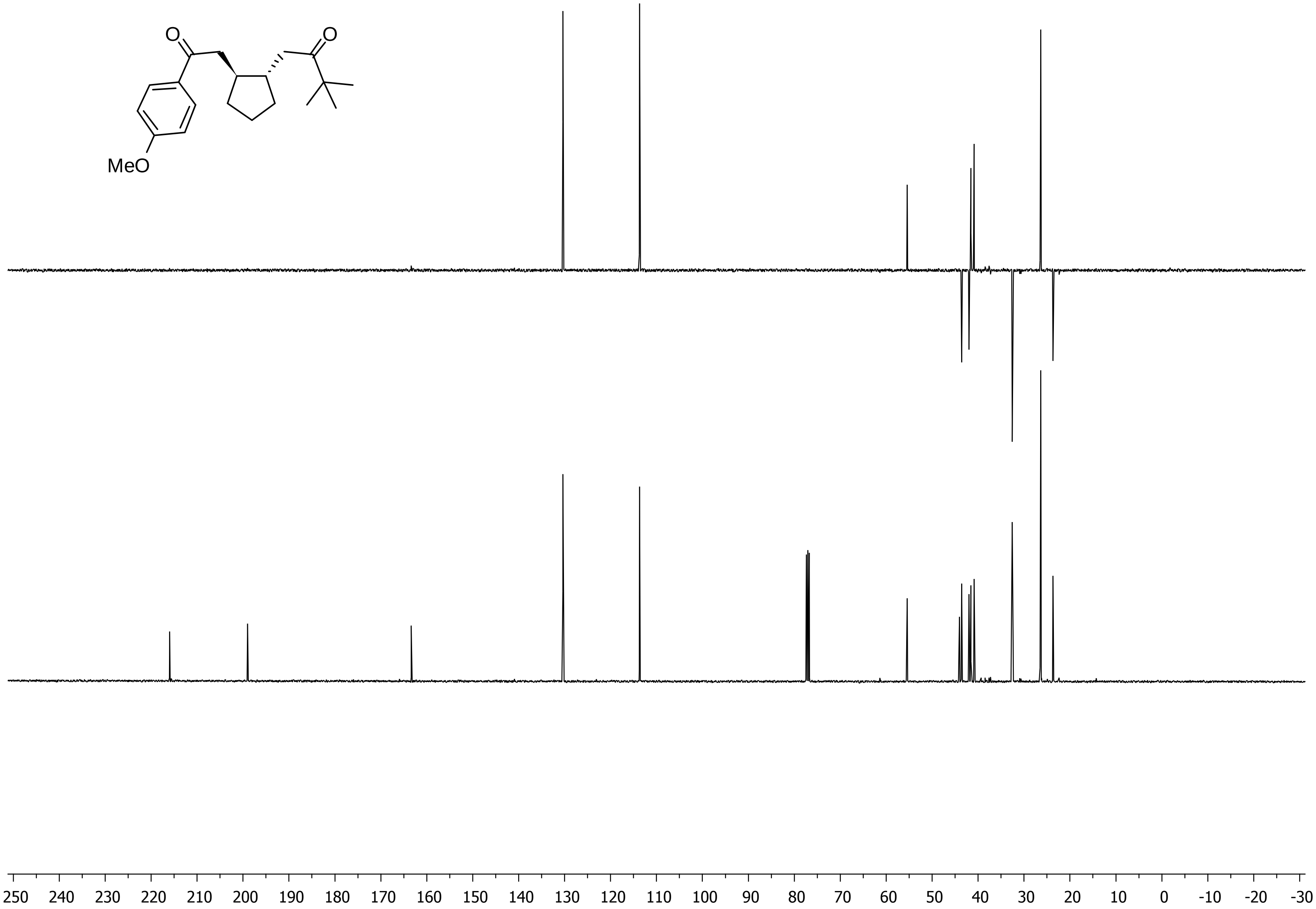
O
O
MeO
250
240
230
220
210
200
190
180
170
160
150
140
130
120
110
100
90
80
70
60
50
40
30
20
10
0
-10
-20
-30

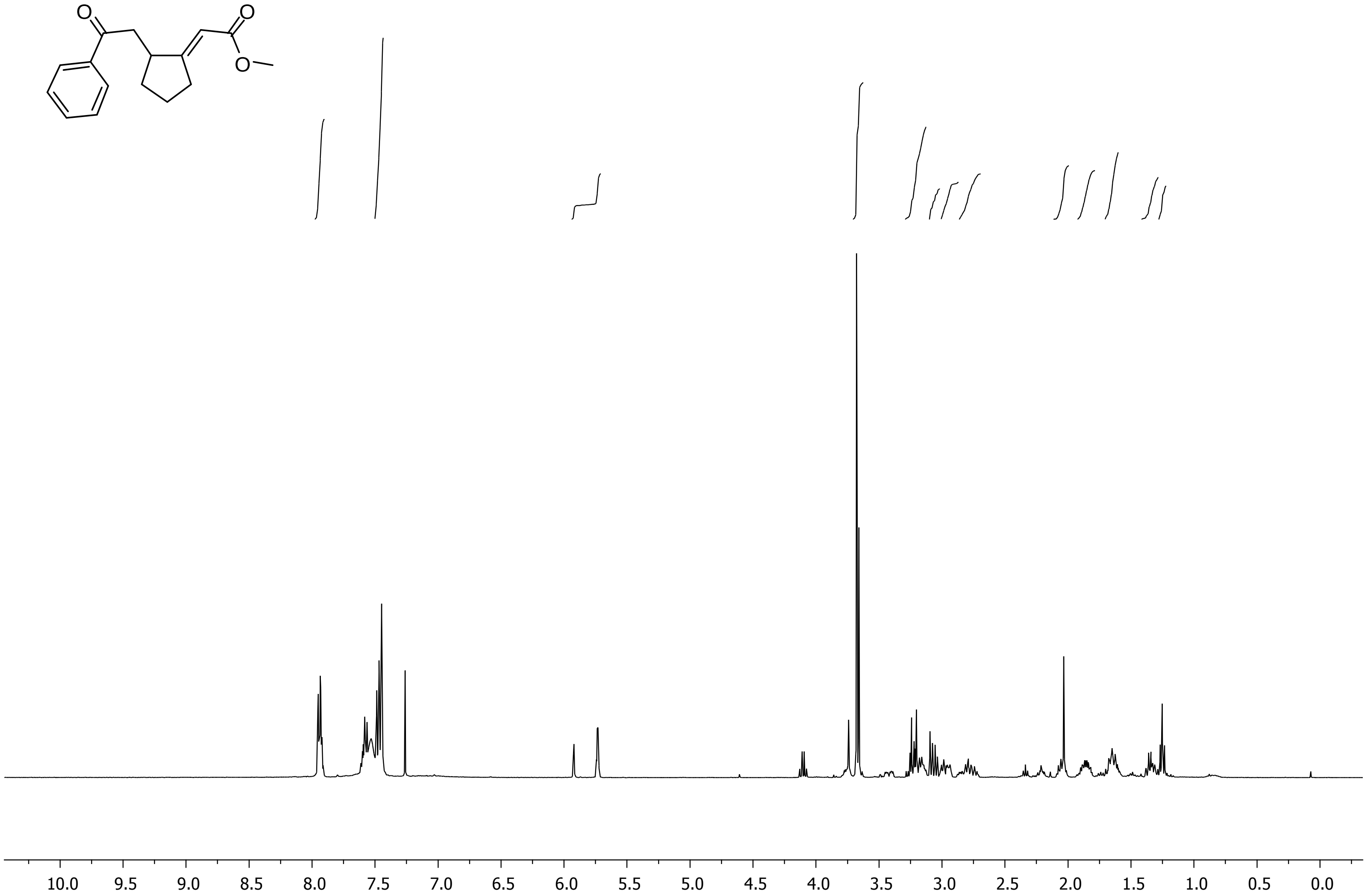
O
O
O
10.0
9.5
9.0
8.5
8.0
7.5
7.0
6.5
6.0
5.5
5.0
4.5
4.0
3.5
3.0
2.5
2.0
1.5
1.0
0.5
0.0

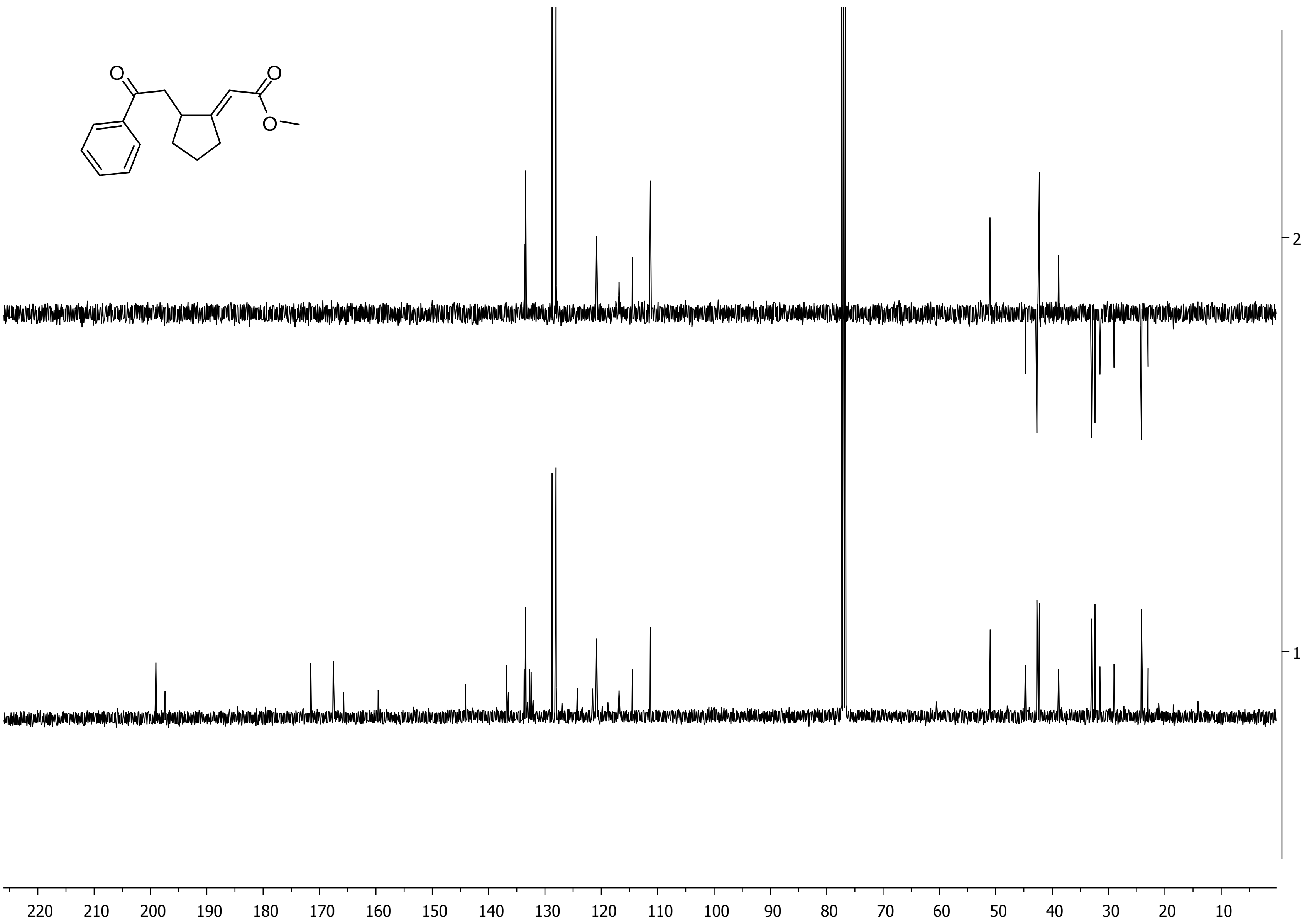
2
1
220
210
200
190
180
170
160
150
140
130
120
110
100
90
80
70
60
50
40
30
20
10

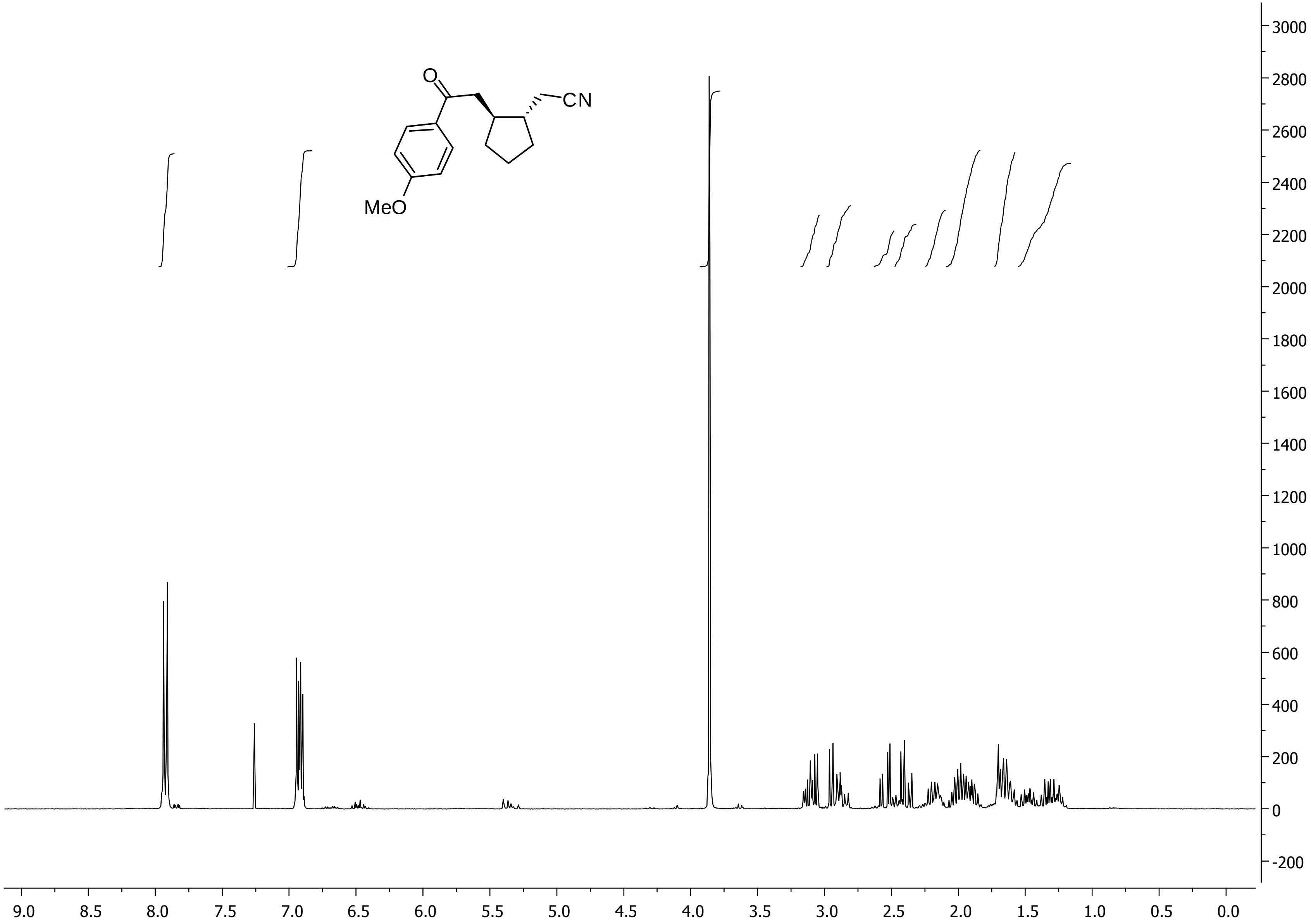
O
CN
MeO
3000
2800
2600
2400
2200
2000
1800
1600
1400
1200
1000
800
600
400
200
0
-200
9.0
8.5
8.0
7.5
7.0
6.5
6.0
5.5
5.0
4.5
4.0
3.5
3.0
2.5
2.0
1.5
1.0
0.5
0.0

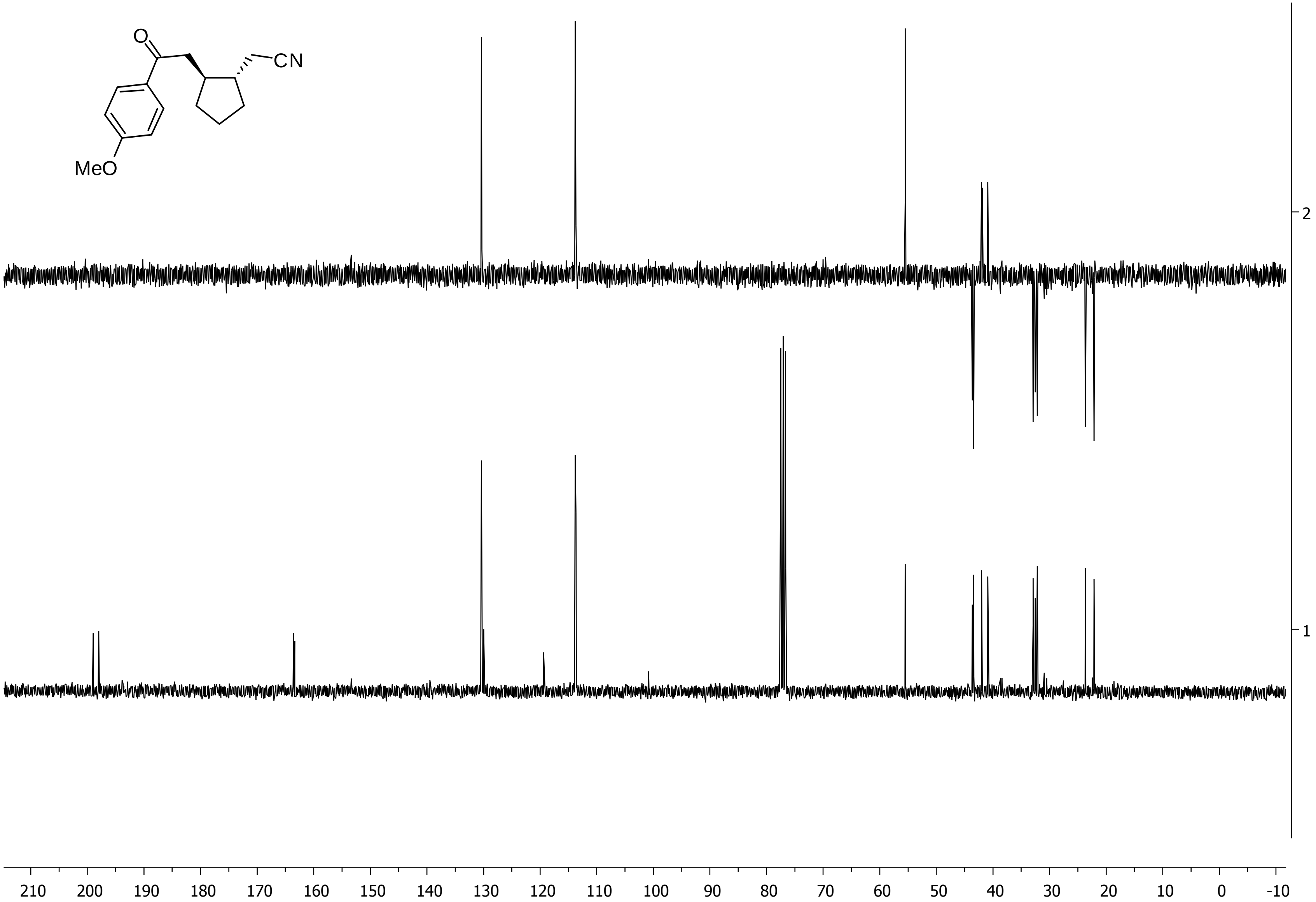
O
CN
MeO
2
1
210 200 190 180 170 160 150 140 130 120 110 100 90 80 70 60 50 40 30 20 10 0 -10

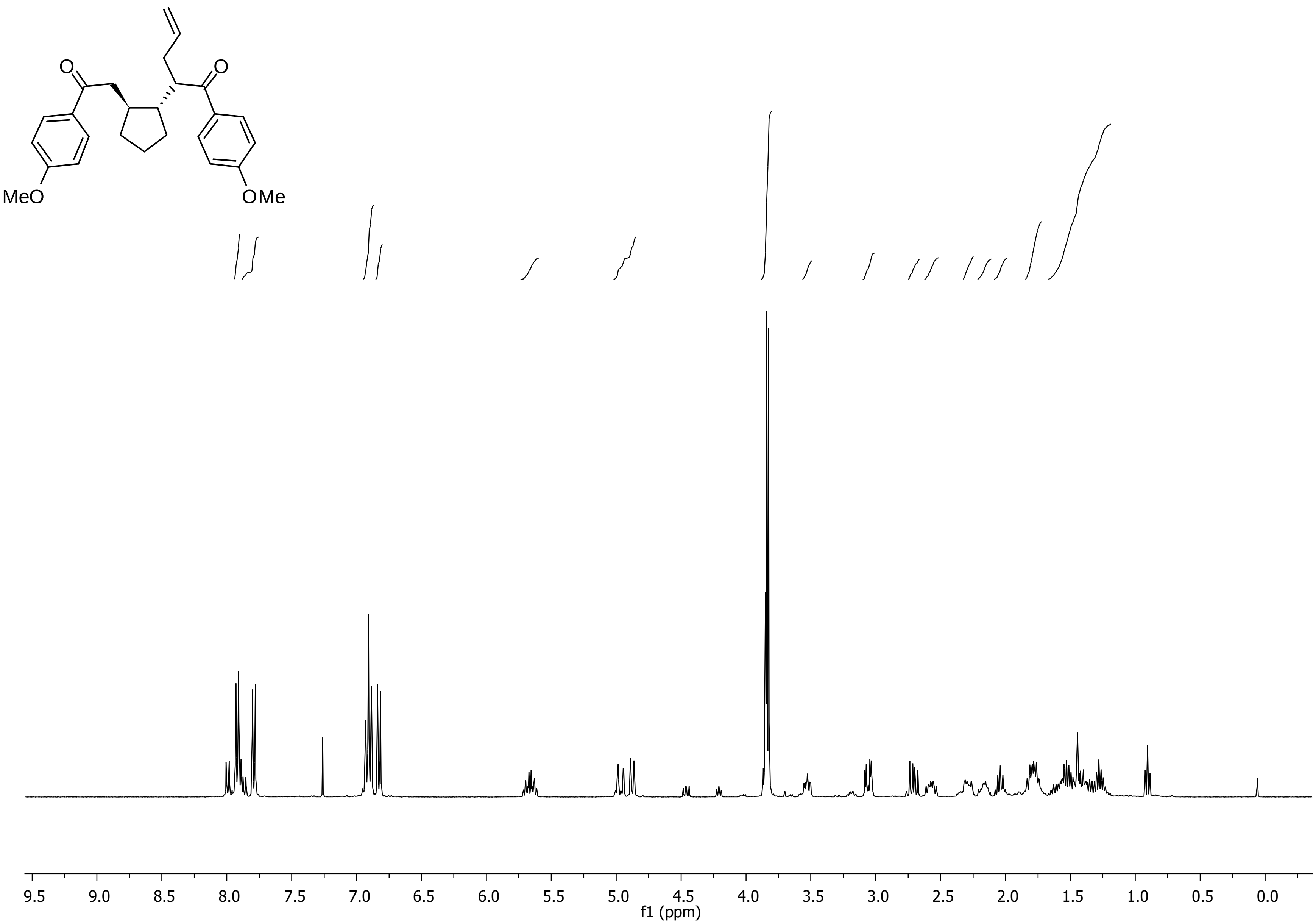
O
O
MeO
OMe
9.5
9.0
8.5
8.0
7.5
7.0
6.5
6.0
5.5
5.0
4.5
4.0
3.5
3.0
2.5
2.0
1.5
1.0
0.5
0.0
f1 (ppm)

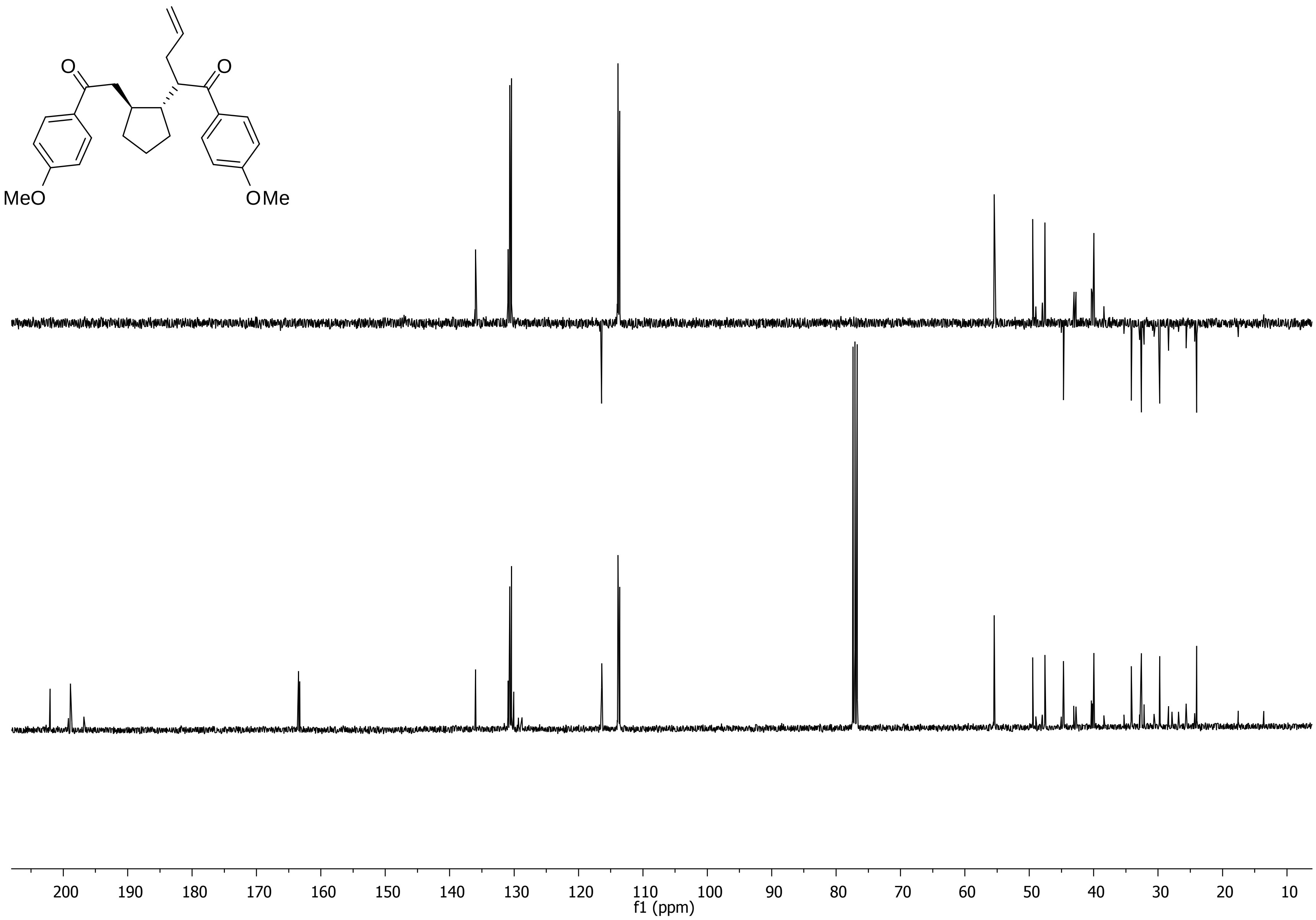
O
O
MeO
OMe
200
190
180
170
160
150
140
130
120
110
100
90
80
70
60
50
40
30
20
10
f1 (ppm)

1.5.5 References

[1] a) R. C. Wende, P. Schreiner, *Green Chem.* **2012**, *14*, 1821; b) A. E. Allen, D. W. C. MacMillan, *Chem. Sci* **2012**, *3*, 633; c) C. Grondal, M. Jeanty, D. Enders, *Nat. Chem.* **2010**, *2*, 167.

[2] a) S. B. Jones, B. Simmons, A. Mastracchio, D. W. C. MacMillan, *Nature* **2011**, *475*, 183; b) D. W. C. MacMillan, *Nature* **2008**, *455*, 304.

[3] For strategies of combining photoredox catalysis with transition metal catalysis, see: a) D. Kalyani, K. B. McMurtrey, S. R. Neufeldt, M. S. Sanford, *J. Am. Chem. Soc.* **2011**, *133*, 18566; b) M. Rueping, R. M. Koenigs, K. Poscharny, D. C. Fabry, D. Leonori, C. Vila, *Chem.- Eur. J.* **2012**, *18*, 5170; c) Y. Ye, M. S. Sanford, *J. Am. Chem. Soc.* **2012**, *134*, 9034.

[4] D. A. Nicewicz, D. W. C. MacMillan, *Science* **2008**, *322*, 77.

[5] M. Rueping, C. Vila, R. M. Koenigs, K. Poscharny, D. C. Fabry, *Chem. Commun.* **2011**, *47*, 2360.

[6] D. A. DiRocco, T. Rovis, *J. Am. Chem. Soc.* **2012**, *134*, 8094.

[7] For a recent application of Cu-based photoredox catalysts, see: M. Pirtsch, S. Paria, T. Matsuno, H. Isobe, O. Reiser, *Chem. Eur. J.* **2012**, *18*, 7336.

[8] a) M. Neumann, S. Füldner, B. König, K. Zeitler, *Angew. Chem., Int. Ed.* **2011**, *50*, 951; For an overview on other applications of metal-free photocatalysis, see: b) D. Ravelli, M. Fagnoni, A. Albini, *Chem. Soc. Rev.* **2012**; c) D. Ravelli, M. Fagnoni, *ChemCatChem* **2012**, *4*, 169; For selected recent examples, see: d) Y. Pan, C. W. Kee, L. Chen, C.-H. Tan, *Green Chem.* **2011**, *13*, 2682; e) Y. Pan, S. Wang, C. W. Kee, E. Dubuisson, Y. Yang, K. P. Loh, C.-H. Tan, *Green Chem.* **2011**, *13*, 3341; f) D. P. Hari, B. König, *Org. Lett.* **2011**, *13*, 3852; g) D. P. Hari, P. Schroll, B. König, *J. Am. Chem. Soc.* **2012**, *134*, 2958; h) P. Schroll, D. P. Hari, B. König, *ChemistryOpen* **2012**, *1*, 130; i) K. Fidaly, C. Ceballos, A. Falguieres, M. S.-I. Veitia, A. Guy, C. Ferroud, *Green Chem.* **2012**, *14*, 1293. j) D. P. Hari, T. Hering, B. König, *Org. Lett.* **2012**, DOI: 10.1021/ol302517n.

[9] a) A. G. Doyle, E. N. Jacobsen, *Chem. Rev.* **2007**, *107*, 5713; b) P. M. Pihko, *Angew. Chem., Int. Ed.* **2004**, *43*, 2062; c) P. R. Schreiner, *Chem. Soc. Rev.* **2003**, *32*, 289; d) M. S. Taylor, E. N. Jacobsen, *Angew. Chem., Int. Ed.* **2006**, *45*, 1520; e) A. N. Thadani, A. R. Stankovic, V. H. Rawal, *Proc. Natl. Acad. Sci.* **2004**, *101*, 5846.

[10] a) D. Seebach, *Angew. Chem. Int. Ed.* **1979**, *18*, 239; b) X. Bugaut, F. Glorius, *Chem. Soc. Rev.* **2012**, *41*, 3511.

[11] a) E. J. Enholm, K. S. Kinter, *J. Am. Chem. Soc.* **1991**, *113*, 7784; b) D. S. Hays, G. C. Fu, *J. Org. Chem* **1996**, *61*, 4.

[12] a) J. Montgomery, E. Oblinger, A. V. Savchenko, *J. Am. Chem. Soc.* **1997**, *119*, 4911; b) T.-G. Baik, A. L. Luis, L.-C. Wang, M. J. Krische, *J. Am. Chem. Soc.* **2001**, *123*, 6716; c) A. D. Jenkins, A. Herath, M. Song, J. Montgomery, *J. Am. Chem. Soc.* **2011**, *133*, 14460.

[13] J. Yang, G. A. N. Felton, N. L. Bauld, M. J. Krische, *J. Am. Chem. Soc.* **2004**, *126*, 1634.

[14] a) G. A. N. Felton, N. L. Bauld, *Tetrahedron* **2004**, *60*, 10999; b) Y. Roh, H.-Y. Jang, V. Lynch, N. L. Bauld, M. J. Krische, *Org. Lett.* **2002**, *4*, 611.

[15] a) G. Pandey, S. Hajra, *Angew. Chem., Int. Ed. Engl.* **1994**, *33*, 1169; b) G. Pandey, S. Hajra, M. K. Ghorai, *Tetrahedron Lett.* **1994**, *35*, 7837; c) G. Pandey, S. Hajra, M. K.

Ghorai, K. R. Kumar, *J. Am. Chem. Soc.* **1997**, *119*, 8777; d) E. L. Tyson, E. P. Farney, T. P. Yoon, *Org. Lett.* **2012**, *14*, 1110.

[16] A. E. Hurtley, M. A. Cismesia, M. A. Ischay, T. P. Yoon, *Tetrahedron* **2011**, *67*, 4442.

[17] a) J. Du, T. P. Yoon, *J. Am. Chem. Soc.* **2009**, *131*, 14604; b) M. A. Ischay, M. E. Anzovino, J. Du, T. P. Yoon, *J. Am. Chem. Soc.* **2008**, *130*, 12886.

[18] a) H. Du, D. Zhao, K. Ding, *Chem. Eur. J.* **2004**, *10*, 5964; b) Y. Huang, A. K. Unni, A. N. Thadani, V. H. Rawal, *Nature* **2003**, *424*, 146.

[19] a) M. Kotke, P. R. Schreiner, *Tetrahedron* **2006**, *62*, 434; b) M. Kotke, P. R. Schreiner, *Synthesis* **2007**, *2007*, 779; c) P. R. Schreiner, A. Wittkopp, *Org. Lett.* **2002**, *4*, 217; d) A. Wittkopp, P. R. Schreiner, *Chem. Eur. J.* **2003**, *9*, 407.

[20] L. Furst, B. S. Matsuura, J. M. R. Narayanam, J. W. Tucker, C. R. J. Stephenson, *Org. Lett.* **2010**, *12*, 3104.

[21] M.-H. Larraufie, R. Pellet, L. Fensterbank, J.-P. Goddard, E. Lacôte, M. Malacria, C. Ollivier, *Angew. Chem., Int. Ed.* **2011**, *50*, 4463.

[22] For details see supporting information.

[23] L. Flamigni, A. Barbieri, C. Sabatini, B. Ventura, F. Barigelletti, *Top. Curr. Chem.* **2007**, *281*, 143.

[24] J. E. Baldwin, *J. Chem. Soc., Chem. Commun.* **1976**, 734.

[25] a) P. M. Brown, N. Käppel, P. J. Murphy, S. J. Coles, M. B. Hursthouse, *Tetrahedron* **2007**, *63*, 1100; b) L.-C. Wang, A. L. Luis, K. Agapiou, H.-Y. Jang, M. J. Krische, *J. Am. Chem. Soc.* **2002**, *124*, 2402; c) P. S. Selig, S. J. Miller, *Tetrahedron Lett.* **2011**, *52*, 2148.

[26] Control experiments without photocatalyst (Eosin Y) did not show any conversion. Prolonged reaction times (5 d) only resulted in decomposition.

[27] a) H.-W. Shih, M. N. Vander Wal, R. L. Grange, D. W. C. MacMillan, *J. Am. Chem. Soc.* **2010**, *132*, 13600; b)A. Rausch, H. Homeier, H. Yersin, *Top. Organomet. Chem.* **2010**, *29*, 193.

2 List of Abbreviations

abs.	absolute
Ac	acetyl
aliph.	aliphatic
Ar	aryl
Bn	benzyl
bpy	bipyridine
br	broad
Bu	butyl
calcd.	calculated
CAN	cer ammonium nitrate
CB	conduction band
CDC	cross dehydrogenative coupling
CI	chemical ionization
d	doublet, day(s)
DCM	dichloromethane
DIPEA	di*iso*propylethylamine
DMF	*N,N*-dimethylformamide
DMSO	dimethylsulfoxide
DNB	dinitro-benzene
DSSC	dye sensitzes solar cell
dtb-bpy	di-*tert*-butly bipyridine
ee	enantiomeric excess
EI	electron impact
equiv	equivalents
ESI	electrospray ionization
Et	ethyl
EWG	electron withdrawing group
EY	Eosin Y
fac	facial
Fc	ferrocene
FEP	fluorinated ethylene proylene copolymer
FT	fourier-transform
h	hour
HOMO	highest occupied molecular orbital
HPLC	high performance liquid chromatography
HRMS	high-resolution mass spectroscopy
i-Pr	isopropyl
IR	infrared
LED	light emiting diode
LUMO	lowest occupied molecular orbital
m	multiplet

m.p.	melting point
Me	methyl
MeCN	acetonitrile
MeOH	methanol
min	minute
MOF	metal organic framework
MS	mass spectroscopy
MV	methylviologen
n.d.	not determined
NHC	*N*- heterocyclic carbene
NMR	nuclear magnetic resonance
Nu	arbitrary nucleophile
OAc	acetate
OLED	organic light emitiing diode
PET	photoelectron transfer
Ph	phenyl
ppm	parts per million
ppy	phenyl pyridine
q	quartet
QY	quantum yield
R	arbitrary residue
r.t.	room temperature
rac.	racemic
R_f	retention factor
s	singlet, seconds
SCE	saturated calomel electrode
SET	single electron transfer
SOMO	single occupied molecular orbital
t	triplet
t-Bu	*tert*-butyl
TEMPO	(2,2,6,6-Tetramethylpiperidin-1-yl)oxyl
tert	tertiary
Tf	trifluoromethanesulfonate
THF	tetrahydrofurane
THIQ	tetrahydroisoquinoline
TLC	thin layer chromatography
TMS	tetramethylsilane or trimethylsilyl
UV	ultraviolett
VB	valance band
VIS	visible

3 Summary

This dissertation deals with the multicatalytic combination of visible light photoredox catalysis and organocatalytic activation modes. Special focus lies on the development of metal free approaches for C-C bond formations in purely organophotoredox processes. In this regard five manuscripts are presented studying different aspects of organophotoredox chemistry.

The principles of multicatalytic visible light photoredox chemistry are summarized in a concept article (*chapter 1.1*) introducing the field by covering the state of the art and discussing challenges and opportunities accompanied.

Typically, photoredox catalysts are transition metal polypyridine complexes, mainly based on ruthenium and iridium. The limited future availability of these rare metals, high costs and potential toxicity curtails their attractiveness. The identification of inexpensive and broadly applicable surrogates to standard organometallic photocatalysts is the content of the first two chapters. Herein organic dyes (*chapter 1.2*) and inorganic semiconductors (*chapter 1.3*) are studied in the context of synergistic photoredox alkylation reactions covering both reductive halogen bond cleavage in synergistic aldehyde alkylations by Eosin Y as well as oxidative amine activation in nitro-Mannich alkylations of amines with inorganic semiconductor CdS.

For an efficient photoredox conversion high light intensity as well as light distribution within the reaction mixture is crucial. Due to the exponential decrease of light intensity along the path length through the absorbing media only the outer sphere of a reaction flask enjoys sufficient light intensity limiting the scalability of such processes. A possible approach to overcome this drawback is presented in *chapter 1.4*, where the beneficial effects of microflow conditions for photoredox reactions are studied with regard to rate acceleration, the feasibility of challenging batch transformations and scale up processes. In this context it was shown that for instance the reaction time of aza-Henry reactions can significantly be reduced from 20 hours to 40min if performed under microflow conditions; furthermore, the possibility to convert substrates, that only scarcely or even do not react at all under batch conditions, was demonstrated. By construction of a simple tube reactor from FEP-polymer tubing, a glass beaker and a household fluorescent bulb the scale up of enantioselective α-alkylations of aldehydes was examined resulting in an increase of productivity (mmol/h) of two orders of magnitude.

The third major aspect of this dissertation deals with the development of a new multicatalytic organophotoredox transformation. In *chapter 1.5* the first combination of Lewis acid like organocatalytic carbonyl activation with H-bond donors and metal-free photoredox catalysis is presented in the context of a cooperative diastereoselective cyclization reaction. A series of symmetrical and unsymmetrical bisenone systems as well as other Michael-type acceptor moieties are shown to undergo reductive intramolecular cyclizations triggered by Eosin Y photoredox catalysis.

4 Zusammenfassung

Die vorliegende Dissertation befasst sich mit der multikatalytischen Kombination von Photoredoxkatalyse mit sichtbarem Licht und Organokatalyse. Besonderer Fokus liegt auf der Entwicklung metallfreier Verfahren zur C-C Bindungsknüpfung in rein organophotoredox-katalytischen Prozessen. In diesem Zusammenhang werden fünf Manuskripte präsentiert, die sich mit verschiedenen Aspekten der Organophotoredox-Chemie beschäftigen.

Die Grundlagen der multikatalytischen Photoredoxkatalyse mit sichtbarem Licht sind in einem Übersichtsartikel (*Kapitel 1.1*) zusammengefasst, welcher den aktuellen Stand der Forschung aufzeigt und Herausforderungen und Möglichkeiten die daraus resultieren behandelt.

Photoredox-Katalysatoren sind üblicherweise Übergangsmetall-Polypyridinkomplexe, meist basierend auf Ruthenium oder Iridium. Deren zukünftig eingeschränkte Verfügbarkeit, ihr hoher Preis sowie die potentielle Toxizität schränkt ihre Attraktivität ein. Die Suche nach kostengünstigem, potentem Ersatz ist Inhalt der folgenden beiden Kapitel. Hier werden organische Farbstoffe (*Kapitel 1.2*) und anorganische Halbleiter (*Kapitel 1.3*) in synergistischen Photoredox-Alkylierungen untersucht. Neben reduktiven Halogen-Kohlenstoff-Bindungsspaltungen durch Eosin Y wird auch die oxidative Aminaktivierung in Nitro-Mannich-Alkylierungen mit CdS untersucht.

Für effiziente Photoredoxprozesse sind eine hohe Lichtintensität sowie gute Lichtverteilung ausschlaggebend. Aufgrund des exponentiellen Abfalls der Intensität entlang der durchstrahlten Strecke genießen nur die äußeren Bereiche eines Reaktionsgefäßes die volle Lichtintensität, was die Skalierbarkeit solcher Prozesse besonders nach oben einschränkt. Ein möglicher Ansatz diese Einschränkung aufzuheben wird in *Kapitel 1.4* durch den Einsatz von Mikroreaktoren untersucht. Ziel dabei ist es, Reaktionsraten zu beschleunigen, kritische Reaktionen und „Scale-up“ Prozesse zu ermöglichen. In diesem Zusammenhang wurde gezeigt, dass zum Beispiel die Reaktionszeit von photokatalytischen Aza-Henry Reaktionen von 20 Stunden auf 40 Minuten reduziert werden kann; darüberhinaus können in dieser Reaktion Substrate, die unter Batch-Bedingungen kaum oder gar nicht reagieren, unter Mikroreaktor-Bedingungen gut umgesetzt werden. Durch den Bau eines Photoreaktors aus FEP-Schlauch, einem Beherglas und einer haushaltsüblichen Eneergiesparlampe konnte die Produktivität (mmol/h) enantioselektiver α-Alkylierungen von Aldehyden um zwei Zehnerpotenzen gesteigert werden.

Der dritte Hauptaspekt dieser Dissertation liegt auf der Entwicklung neuartiger multikatalytischer organophotoredox-katalytischer Prozesse. In *Kapitel 1.5* wird die erste Kombination von organokatalytischer Carbonylaktivierung mit Wasserstoffbrücken-Donoren und metallfreier

Photoredoxkatalyse im Rahmen kooperativer diastereoselektiver Zyklisierungen vorgestellt. Hier wird gezeigt, dass eine Reihe von symmetrischen und unsymmetrischen Bisenonsystemen sowie anderweitige Michael-artige Akzeptoren durch Eosin Y und einem Thioharnstoff Derivat katalysiert eine reduktive hoch diastereoselektive intramolekulare Zyklisierung eingehen.

5 Curriculum Vitae

Matthias Neumann
Master of Science

Am Hang 26
93138 Lappersdorf

0176 / 96522553
matthias.neumann@chemie.uni-r.de

Personal data

Birthday, -place	26.08.1982, Jena
Nationality	German
Civil status	single

Education

since 02/2009	PhD Thesis in Organic Chemistry, in the group of Prof. Dr. Kirsten Zeitler at the University of Regensburg
01/2009	Master of Science Chemistry
04/2008 – 01/2009	Master thesis under supervision of Prof. Dr. Kirsten Zeitler *„Immobilisierung von chiralen Brønstedsäuren zur Organokatalyse“*
10-2003 – 03/2007	Bachelor of Science Chemistry
09/2006	Bachelor thesis under supervision of Prof. Dr. Oliver Reiser *„Katalyse der asymmetrischen Benzoylierung von Hydrobenzoin mit immobilisierten Azabisoxazolin-Kupferkomplexen“*

School and military service

07/2002 – 03/2003	Basic military service
06/2002	A-level, Gymnasium Neustadt an der Waldnaab

Professional experiences

Since 02/2009	Scientific co-worker at the Institute of Organic Chemistry of the University Regensburg tasks: - supervision of student practical courses - supervision of Bachelor and Master thesis

05/2010 – 10/2010 04/2011 – 10/2011	Spokesman of the graduates GRK 1626
11/2007 – 03/2008	Project work at agrostulln GmbH „*Downscale of sulphur grinding to laboratory scale and development of optimization approaches.“*
08/2007 – 9/2007	Working student at Kunststofftechnik Weiden/Oberpfalz

Publications

(1) “*Metal-Free, Cooperative Asymmetric Organophotoredox Catalysis with Visible Light*”
Matthias Neumann, Stefan Füldner, Burkhard König, Kirsten Zeitler
Angew. Chem. Int. Ed., **2011**, 50, 951
Angew. Chem., **2011**, 123, 981

Cover picture: *Angew. Chem. Int. Ed* 4/2011
Angew. Chem. 4/2011

Synfact of the month: *Synfacts*, **2010**, 1419

Angewandte
Chemie
International Edition
2011–50/4
WILEY-VCH

(2) “*Visible-Light-Promoted Stereoselective Alkylation by Combining Heterogeneous Photocatalysis with Organocatalysis*”
Maria Cherevatskaya, Matthias Neumann, Stefan Füldner, Christoph Harlander, Susanne Kümmel, Stephan Dankesreiter, Arno Pfitzner, Kirsten Zeitler, Burkhard König
Angew. Chem. Int. Ed., **2012**, 51, 4062
Angew. Chem., **2012**, 124, 4138

(3) “*Application of Microflow Conditions to Visible Light Photoredox Catalysis*”
Matthias Neumann, Kirsten Zeitler
Org. Lett., **2012**, 14, 2658

(4) “*Synergistic Visible Light Photoredox Catalysis”*
Matthias Neumann, Kirsten Zeitler
Bookchapter in *Chemical Photocatalysis* (de Gruyter) in print

(5) “*A Cooperative Hydrogen Bond Promoted Organophotoredox Catalysis Strategy for Highly Diastereoselective, Reductive Enone Cyclizations*”
Matthias Neumann, Kirsten Zeitler
(to be submitted)

Presentations and talks

(1) *“Organic Dyes in Photoredox Catalysis using visible light*”
Matthias Neumann, Stefan Füldner, Burkhard König, Kirsten Zeitler
Poster presentation: - BOSS XII (Namur, Belgium 07/2010)
- Isoμ (MPI Mühlheim, 07/2010)
- 22.Lecture conference of the Division Photochemistry GDCh

(2) *“Photochemistry in Microstructured Flow Reactors”*
Matthias Neumann
Tutorial: 3rd seminar day GRK 1626 (Regensburg 11/2010)

(3) *“Organocatalysis meets Photoredox Chemistry*“
Matthias Neumann, Kirsten Zeitler
Poster presentation: - CATAFLU.OR (Bologna, Italy 03/2011) citated in product flyer
Photomodul Future Chemistry BV and cited in:
“Recent Advances in Microflow Photochemistry”
Molecules, **2011**, 16, 7522
- ESOC 2011 (Crete, Greece 06/2011)
- Wissenschaftsforum 2011 (Bremen 09/2011)

6 Acknowledgments

Besonderer Dank gilt meiner Betreuerin Prof. Dr. Kirsten Zeitler für die überragende Betreuung während Masterarbeit und Promotion: Verfügbar rund um die Uhr, egal wie wenig Zeit, trotzdem immer ein offenes Ohr für Fragen und was man auch brauchte es wurde organisiert; bessere Arbeitsbedingungen hätte ich nicht bekommen können – und darüber hinaus eine gute Freundin im und außerhalb des Labors.

Desweiteren möchte ich mich bei Herrn Prof. Dr. Oliver Reiser für die finanzielle Unterstützung und für die Möglichkeit an dessen Gruppenseminar teilnehmen zu können bedanken.

Der Deutschen Forschungsgesellschaft (DFG) und dem Graduierten Kolleg 1626 – Chemische Photokatalyse möchte ich für die Finanzierung des Großteils meiner Forschungsarbeit und die Möglichkeit an zahlreichen Tagungen und Fortbildungen teilnehmen zu können danken.

Dr. Kaspar Koch von Future Chemistry Holdings BV möchte ich für die Leihgabe eines Mikroreaktorsystems und die fruchtbare Zusammenarbeit danken.

Ebenso gehört mein Dank den Mitarbeitern der Zentralen Analytik für die Aufnahme zahlreicher NMR- und Massenspektren und den Mitarbeitern der Werkstätten der Chemie für Reparaturen und den Bau einiger „Spezialanfertigungen“.

Allen Freunden und Kollegen besonders meinem Arbeitskreis mit allen jetzigen und früheren Mitgliedern sowie meinen Wegbegleitern durchs Studium Wolfi, Michl und Julian danke ich für eine tolle Zeit und die aufgebrachte Geduld mit mir.

Meinen Eltern möchte ich für die Finanzierung meines Studiums danken und für alles was sie mir mit auf den Weg gegeben haben.

Und zu guter Letzt: Danke Astrid für alles was wir in den letzten Jahren geteilt und erlebt haben.